University of Zurich[UZH]

Potentials and Challenges of Probabilistic Precipitation Data for Runoff Modelling: An Analysis of Spatio-Temporal Variability Patterns.

GEO 511 Master's Thesis

Author
Laura Markwalder
14-712-293

Supervised by
Prof. Dr. Jan Seibert

Faculty representative
Prof. Dr. Jan Seibert

28.01.2021
Department of Geography, University of Zurich

Abstract

Water is involved in almost all natural processes and is the element on which our life depends in many ways. Alpine catchments as a specific part of the hydrological cycle have attracted considerable attention as they serve both as water storage and as freshwater supply to its sphere of influence. The hydrological cycle of such catchments is influenced by meteorological and climatic processes, by topography and by human activities. In the Swiss Alps, the focus of investigating changes in the hydrological cycle and water resources lies traditionally on changes in precipitation amount and patterns in time and space. Among the most influential processes on runoff generation are changes in local precipitation, snow cover patterns, reduced glacier storage and soil storage capacity. Such natural processes show a high spatio-temporal variability. Due to the enormous impact of changing circumstances such as climate, forestry, and energy production on the runoff-precipitation-relationship, it is essential for our understanding of the local water resources to investigate and better comprehend how the water cycle is affected. Urban planning, water management and societal resilience are only a few affected applications depending to a large extent on hydrological data availability. A commonly used method to provide precipitation data on various scales is the interpolation of measurements from rain gauge networks. The problem that the resolution of the precipitation data set is often higher than the underlying rain gauge network is known as *problem of scaling*. To overcome this problem, Frei & Isotta (2019) provide a promising approach for Switzerland. Instead of single interpolation values, an ensemble of analyses in terms of possible precipitation estimations is provided. Like the single interpolation method (*deterministic*), the ensemble analysis (*probabilistic*) also depends on available measurement data but additionally displays the estimation uncertainty. The aim of this research is to analyse the uncertainty—measured by the variability of ensemble runs—from three different perspectives whereby spatio-temporal uncertainty patterns should be identified.

(1) The analysis of ensemble run variabilities within a subcatchment for different precipitation occurrences mainly enables to address the uncertainty to seasonality.
(2) By contrast, spatial patterns are recognized in comparing the variability measures between the subcatchments.
(3) Finally, the probabilistic data set mean is compared to the deterministic one to quantify the general performance of the probabilistic data set.

From the findings of these three research approaches, it can be concluded that the ensemble data on average differs slightly, if at all, from the deterministic data, resulting in neither a deterioration nor an improvement of the runoff simulations. However, if the additional information about the estimation uncertainty in the probabilistic data set is taken into account, the data identifies a spatio-temporal uncertainty cluster. The estimation of precipitation occurrence as well as the runoff is observed to be increasingly more uncertain in the summer months and at higher altitudes. This dependency can be attributed to various factors:

(a) local, spontaneous precipitation (*convective, difficult to interpolate*) occurs with higher intensity and more often during summer months compared to widespread precipitation (*stratiform, easier to interpolate*);
(b) the measurement station density is lower in high altitudes which leads to more uncertain interpolation values;
(c) the model accuracy decreases due to the difficult assessment of the soil storage capacity, dependent of seasonality and elevation. Furthermore, the variability of the runoff influence correlates with higher precipitation occurrences during summer months;
(d) the catchment size and the amount of discharge only plays a minor role in terms of estimation uncertainty;
(e) the data set variability increases with a higher precipitation sum (*heavy precipitation events*) but those events are not responsible for the highest measured variabilities.

This research provides an important basis to apply the new approach by Frei & Isotta (2019) for runoff simulations in Switzerland. However, further research is needed to determine how the above findings can be usefully transferred to runoff simulations and related applications.

Keywords: *probabilistic data, RhydchprobD, deterministic data, RhiresD, spatio-temporal patterns, runoff simulation, HBV, semi-distributed modelling, variability analysis, natural variability, methodological variability, coefficient of variation, ensemble data*

Acknowledgements

With the submission of this master's thesis my studies at the University of Zurich come to an end. I would like to thank everyone who inspired, motivated and supported me throughout this time and especially during this thesis. Without the inspiring network of people, it would have been much more laborious. I am particularly grateful for the support given by:

Prof. Dr. Jan Seibert; Thank you for supervising this master's thesis. I appreciate the time you took for discussions and for asking me the right question to keep my focus on the topic. Even though we were forced to meet and communicate in a digital way, I have always received prompt replies from you.

Marc Vis; Thank you for the technical support with running the HBV model and the help to improve my code. Without your knowledge, the simulations would probably still be running.

Christoph Frei; Thank you for supporting my master's topic and the initiation of the data release by MeteoSwiss. Without your work on the data set, this work would not have been possible.

Tobias Frey, Nathalie Herrmann, Corinne Jörg and *Simon Schudel;* Thank you for finding the right words while proof-reading and providing valuable feedback. Special thanks to Tobias, who shared his knowledge of data visualisation and programming with me.

My family and dear friends; Thank you for your loving support throughout my studies and taking my mind off this thesis every once in a while.

Table of Contents

List of Figures

List of Tables

List of Abbreviations

CV – Coefficient of variation
FOEN – Federal Office for the Environment
GIS – Geographic Information Science
MSC – Measurement station catchment (of *FOEN's* runoff measurement stations)
RhiresD – Deterministic precipitation data set
RhydchprobD – Probabilistic precipitation data set
TabsD – Deterministic temperature data set
TEZGNR40 – Hydrological terrain units of ~ 40 km^2
TEZGNR150 – Hydrological terrain units of ~ 150 km^2
TEZGNR1000 – Hydrological terrain units of ~ 1000 km^2

1 Introduction

Water is involved in almost all natural processes and is the element on which our life depends in many ways. Hydrology as an applied science deals with surface and underground water. A specific part of this science is concerned with water in alpine regions (Hendriks 2010). Alpine catchments have attracted considerable attention as they serve both as water storage and as freshwater supply to its sphere of influence. The hydrological cycle of such catchments is influenced by meteorological and climatic processes, by topography and by human activities (EEA 2009). Moreover, the water cycle is dependent on the catchment behaviour, i.e. the production and transfer function of precipitation (Kusumastuti & Jokowinarno 2012). Due to the enormous impact of changing circumstances such as climate changes, forestry, and energy production, it is essential for our understanding of the local water resources to investigate and better comprehend how the water cycle is affected. In the Swiss Alps, the focus of investigating changes in the hydrological cycle and water resources traditionally lies on changes in precipitation amount and patterns (EEA 2009; Brönnimann et al. 2018). Several studies, among others Brönnimann et al. (2018), forecast a decrease in summer precipitation and more intense perennial precipitation extremes in the Swiss Alps. Even moderately extreme events (e.g. 10-year return period events, maximum annual precipitation events) tend to be important for climate change adaptation of nature and creatures. Besides changes in precipitation in volume and pattern caused by climate change, the generation process of precipitation may be responsible for precipitation variability. The characteristics of precipitation events on a catchment scale differ between those of stratiform and convective origin in the Alps, with a wide range of intensities (Lobligeois et al. 2014). Convective precipitation events are typically responsible for larger peak values and smaller-scale variations in the hydrographs on summer days (Frei & Isotta 2019). Such intense, transient precipitation events can cause flash floods or floods (Huza et al. 2014). In comparison, stratiform and orographic precipitation show a more gradual distribution, especially in autumn (Frei & Isotta 2019). Climate change and human activities indirectly influence any kind of precipitation generation process which is why changes in the runoff-precipitation-relationship on a large scale as well as on catchment scale have been detected (Osborne et al. 2015). Due to these influences, Ternynck et al. (2016) supported the inclusion of hydrograph classification based on hydrograph characteristics (e.g. hydraulic structures, flood types characteristics) in extreme event modelling to ensure a better understanding of the underlying processes and flood behaviours.

The discharge in mountain-dominated regions such as the Swiss Alps depend on various processes. Among the most influential are changes in local precipitation, snow cover patterns, reduced glacier storage related to climate change and soil storage capacity that will presumably influence the runoff. The changes in the measures *time to peak*, *discharge volume* and *peak flow* will thus affect runoff characteristics in such drainage basins (EEA 2009). As Winchel et al. (1998) summarized in their early review, several studies show a high sensitivity of runoff-generation to spatial and temporal variability of precipitation. Large flow variations can occur caused by spatial-temporal variability. It is thus essential to broaden the knowledge of this variability to better understand the hydrological response (Ochao-Rodriguez et al. 2015). Even though precipitation and runoff are two closely related components of the water cycle, they have regularly been investigated separately (Xu et al.

2010). However, Osborne et al. (2015) suggested that runoff measurements can improve the prediction of observed precipitation and quantify changes in the hydrological cycle.
A commonly used method to provide precipitation data on various scales is the interpolation of rain gauge networks. The problem that the resolution of the precipitation data set is often higher than the underlying rain gauge network is commonly known as *problem of scaling*. To overcome this problem, Frei & Isotta (2019) provide a promising approach for Switzerland: instead of single interpolation values, an ensemble of analyses in terms of possible precipitation occurrence is provided. The ensemble members overcome the limited number of rain gauges by displaying more realistic spatial variance and peak values (Frei & Isotta 2019). Like the single interpolation method, the ensemble analysis also depends on available measurement data but additionally displays its uncertainty. The ensemble enables the allocation of the uncertainties in relation to weather situation (convective vs. stratiform; precipitation sum), density of observation network, and scale of spatial and temporal aggregation (size of catchment, climate indices) (Frei & Isotta 2019). Territories with a dense station spacing, as is the case in the Swiss Alps, tended to depend less on the scale of measurement network. The uncertainty is rather dependent on the spatial variance of precipitation occurrences within the observed catchment (Frei & Isotta 2019).

1.1 Motivation and Goal

This master's thesis will compare the precipitation occurrence and the discharge modelling of the various ensemble runs against each other, as well as examine the difference to the previously used deterministic data set *RhiresD* in the catchment *Andelfingen*. The aim is to assess the contribution of the new approach in the probabilistic data set *RhydchprobD* to discern precipitation patterns and to model discharge simulations in Swiss alpine catchments. For this purpose, the first step is the performance of analysis to investigate whether the precipitation occurrence shows significant patterns in time (e.g. months, seasons, years, study period) and space (different size classification of hydrological units). It should further be described how the intra-catchment and inter-catchment variability of the ensemble data behave compared to the single interpolation method. Second, the two data sets will be used for runoff modelling in the *Hydrologiska Byråns Vattenavdelning (HBV)* model. Those simulations will, like in the first part, be examined for spatial and temporal variations. To validate the simulations, the output will be compared to discharge data from the *Federal Office for the Environment's* (*FOEN*; *German: Bundesamt für Umwelt, BAFU*) measurement stations at the basin outlet and at various locations within the catchment *Andelfingen*. The findings of this thesis should give an indication of whether the probabilistic data set *RhydchprobD* increases the accuracy in terms of *time to peak* and *volume* of hydrograph modelling in *HBV*. More reliable forecasts provide a considerable resource potentially suitable for a better understanding of hydrological response and local water resources of scientific and public interests.

The comparison of probabilistic precipitation data with deterministic data relying on the same measurement network certainly provides valuable insights on the application of probabilistic precipitation data in hydrological simulations. With regards to the research objectives, several findings are expected. Spatial precipitation variability supposes to be dependent on scale and event characteristics. A large scale enhances the probability to capture spatial heterogeneity in a diverse topographical catchment. Differences related to precipitation origin, however, generally point to less spatial variability for stratiform events and higher values for convective events. Additionally,

the meteorological differences in space are closely related to the catchments' topography, e.g. elevation gradient. Urban and agricultural areas characterise the north of the catchment *Andelfingen*, while rugged areas predominate in the southern part. The generation of precipitation in the southern mountainous upstream area will most often be affected by orographic effect and strong altitudinal gradient, which causes convective precipitation. In contrast, stratiform events will predominate in the lowlands in the northern region. Previously published studies have identified trends showing strong spatial variability for shorter precipitation events and shorter but stronger precipitation events in summer due to convective storms with high spatial variability. Therefore, the intra-ensemble variability is expected to increase with convective precipitation events as well as with smaller scales. It is furthermore assumed that such high variability decreases slower with a coarser spatial and temporal resolution compared to ensemble variability of large-scale stratiform events. However, the similar computational methods for the data set *RhiresD* and the data set mean of all ensemble runs from *RhydchprobD* indicate that merely no differences in meteorology or hydrology can be expected. Finally, streamflow modelling in catchments with high spatial heterogeneity is expected to benefit from precipitation input in a higher spatial resolution. This dependency will most likely be strongest for small and short precipitation events. Due to the additional information of uncertainty, the ensemble approach is less likely to support conditional biases, unrealistic spatial smoothing, underestimation of extremes and overestimation of wet-day frequencies.

1.2 Research Objectives

With the following research objectives, this thesis intends to contribute to the outlined research gaps, whereas the questions in the meteorological and hydrological part follow the same structure.

Meteorological part

RO.1.1 What are measurable spatio-temporal differences in meteorological variability within the probabilistic precipitation data set (*RhydchprobD*)?

RO.1.2 What is the influence of heavy precipitation events on meteorological variability?

RO.1.3 To what extent do the daily precipitation sums per subcatchment of the deterministic (*RhiresD*) and probabilistic data sets (*RhydchprobD ensemble mean*) coincide?

Modelling part

RO.2 To what extent does the probabilistic data set (*RhydchprobD*) influence the accuracy of hydrological simulations?

Hydrological part

RO.3.1 What are measurable spatio-temporal differences in hydrological variability within the probabilistic precipitation data set (*RhydchprobD*)?

RO.3.2 What is the influence of heavy precipitation events on hydrological variability?

RO.3.3 To what extent do the daily runoffs per subcatchment of the deterministic (*RhiresD*) and probabilistic data sets (*RhydchprobD ensemble mean*) coincide?

1.3 Structure

Chapter 2 introduces the scientific background of this master's thesis. The importance of meteorological data for hydrological modelling as well as current and past application of runoff modelling are elucidated. Furthermore, the knowledge of natural precipitation and runoff cycle in alpine catchments is indispensable in order to analyse and discuss the results of meteorological and hydrological variability in the catchment *Andelfingen*. Subsequently, *chapter 3* introduces the study site. Given that every model is subject to several structural uncertainties and the uniqueness of model and catchment, the research is limited to an alpine catchment without glaciological influence. The data sets used in this study are presented in *chapter 4* and cover a large time period of more than 50 years, a promising duration for detailed statements on variability and hydrological processes. *Chapter 5* explains the basic methodology from the analysis of the meteorological variability to the runoff modelling using *HBV* and the measurements of the runoff variability. All ensemble analyses are compared to the *RhiresD* data set. *Chapter 6* presents the results that are subsequently discussed in *chapter 7*. Both chapters are structured into the three parts meteorology, modelling and hydrology, analogous to the research objectives. Finally, *chapter 8* concludes the findings and points out future research opportunities.

2 Scientific Background

The presence of water is decisive for hydrological processes. Beside snow and ice melt water, it mainly enters the water balance in the form of precipitation. This chapter will give an overview of the natural cycle of precipitation and runoff in the Swiss Alps as well as its driving factors. Precipitation and runoff are strongly interlinked natural phenomena of which many mechanisms and influencing factors remain unknown. Therefore, it is even more important to lay out the current knowledge of such processes in order to analyse and discuss the results later on and identify possible new relationships. Observed precipitation and runoff data enable several hydrological applications, including runoff simulations. The importance of meteorological and hydrological data for runoff modelling and particularly the use of probabilistic data will thus be explained.

2.1 Use of Technical Terms

Before introducing the scientific background, several terms used throughout the thesis are clarified. First, it should be noted that the term «variability» is used in two different ways. On the one hand, variability describes spatial and temporal differences in precipitation and runoff occurrence. The use of the term in this sense is mainly used to describe the inter-subcatchment patterns. On the other hand, the term is used later in this work to characterise the intra- and inter-ensemble variability and with it the uncertainty of precipitation values in the probabilistic data, measured as *standard deviation* and *coefficient of variation*. Intra-variability refers to the differences of the ensemble runs during a defined time-space unit (e.g. how different do the ensemble runs perform on one day in specific subcatchments *TEZGNR40)*, whereas inter-variability refers to the differences of location and time unequal units (e.g. ensemble run variability in various subcatchments *TEZGNR40* during one precipitation period) (Figure 1). In this context, the term «variability» is always complemented by the term «ensemble run» or described as «ensemble spread».

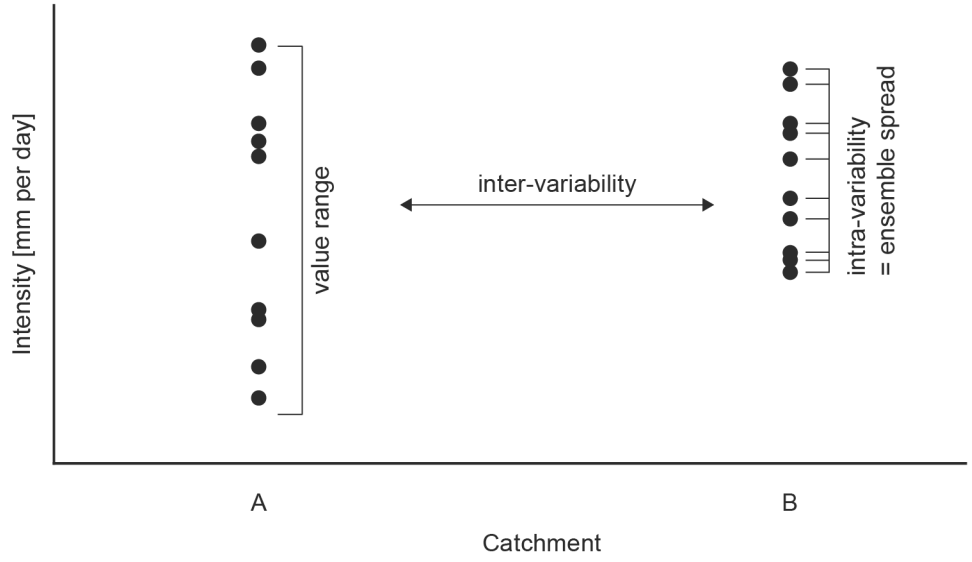

***Figure 1: Definition of terms «value range», «intra-variability», «ensemble spread» and «inter-variability»**. «Value range» is used for the spread of the catchment's ensemble run values, «intra-variability» and «ensemble spread» as synonyms for the variability measure within the ensemble and «inter-variability» as the term for the variability comparison of different catchments.*

Second, if not pointed out specifically, «precipitation» is understood to be the process by which water particles fall from the atmosphere to the earth's surface in both liquid (rain, drizzle) and solid form (snow, graupel, hail, ice pellets). The *HBV* model uses a degree-day method that allows to consider precipitation either as snow or rain. Lastly, the term «deterministic data set» is synonymously used for the data set *RhiresD*, while «probabilistic data set» is used for *RhydchprobD*. For the sake of clarity, Figure 2 shows the terms used in relation to the precipitation data sets. From the measured values at the stations, precipitation is interpolated for the entire entity. The result is a deterministic grid, *RhiresD*. This data set is contrasted with the data set *RhydchprobD*, where measured values of the same stations are also interpolated for the entire entity. However, compared to *RhiresD,* the data set *RhydchprobD* is composed of different interpolation realisations, the ensemble runs. A single run can be equated with the deterministic grid. The 50 ensemble runs together form the ensemble. Further information on the data sets will be given in *Chapter 4*.

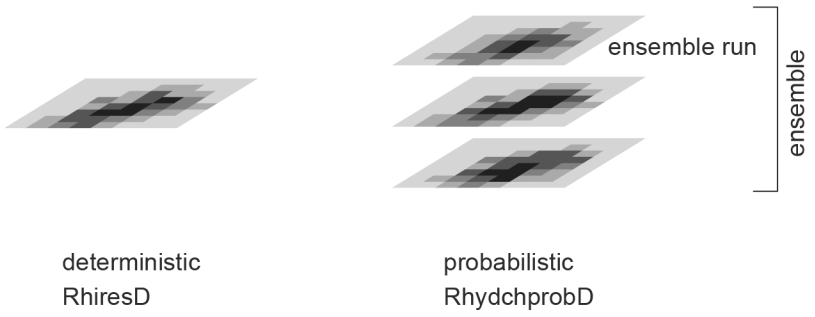

***Figure 2: Data types**. Interpolated precipitation estimations are provided as one realisation in the deterministic data set «RhiresD» whereas the probabilistic data set «RhydchprobD» consists of a 50-member ensemble. The term «ensemble run» is used for one of those ensemble members.*

2.2 Precipitation and Runoff Generation

Precipitation is understood as any falling liquid (drizzle or rain) or solid (snow, graupel, hail, ice pellets) water as a result of gravity that originates from atmospheric water vapor condensation in clouds and fog (Häckel 2016). Depending on the processes leading to the air uplift and its process scale, three main forms of precipitation generation can be distinguished.

(1) *Convective precipitation* results from local lifting and cooling of air particles due to thermal convection that causes strong vertical air current with high condensation if the ascending air mass has a high degree of humidity. This process mainly occurs in the interior of continents and is typical of strong summer precipitation in cold front areas. The time series of precipitation in Figure 3 shows that the more frequent convective precipitation in the alpine catchment *Andelfingen* is mainly responsible for the increase of annual precipitation cycle during summer months.

(2) On the windward side of mountains, *orographic precipitation* results from horizontal air currents that are forced to rise over natural barriers (Hendriks 2010). These circumstances are responsible for the increase of the precipitation rates with elevation (Sikorska & Seibert 2018). Both convective and orographic precipitation are local, often short and intense, typical of thunderstorms and occur in mountainous basins (Hendriks 2010; Yu et al. 2015). Both types of precipitation are caused by strong vertical air currents, which is why many studies do not distinguish between these types of precipitation (e.g. Frei & Isotta 2019; Gobiet et al. 2014; Lobligeois et al. 2014; Thurai et al. 2016). For this reason, the term *convective precipitation* is used in the following for local precipitation occurrences.

(3) The last type of precipitation generation is the *stratiform precipitation*. These cyclonic precipitations are formed by a large-scale updraft mostly at a warm front. When gradually lifted and cooled air masses condensate, moderate precipitation over a long duration arises (Hendriks 2010).

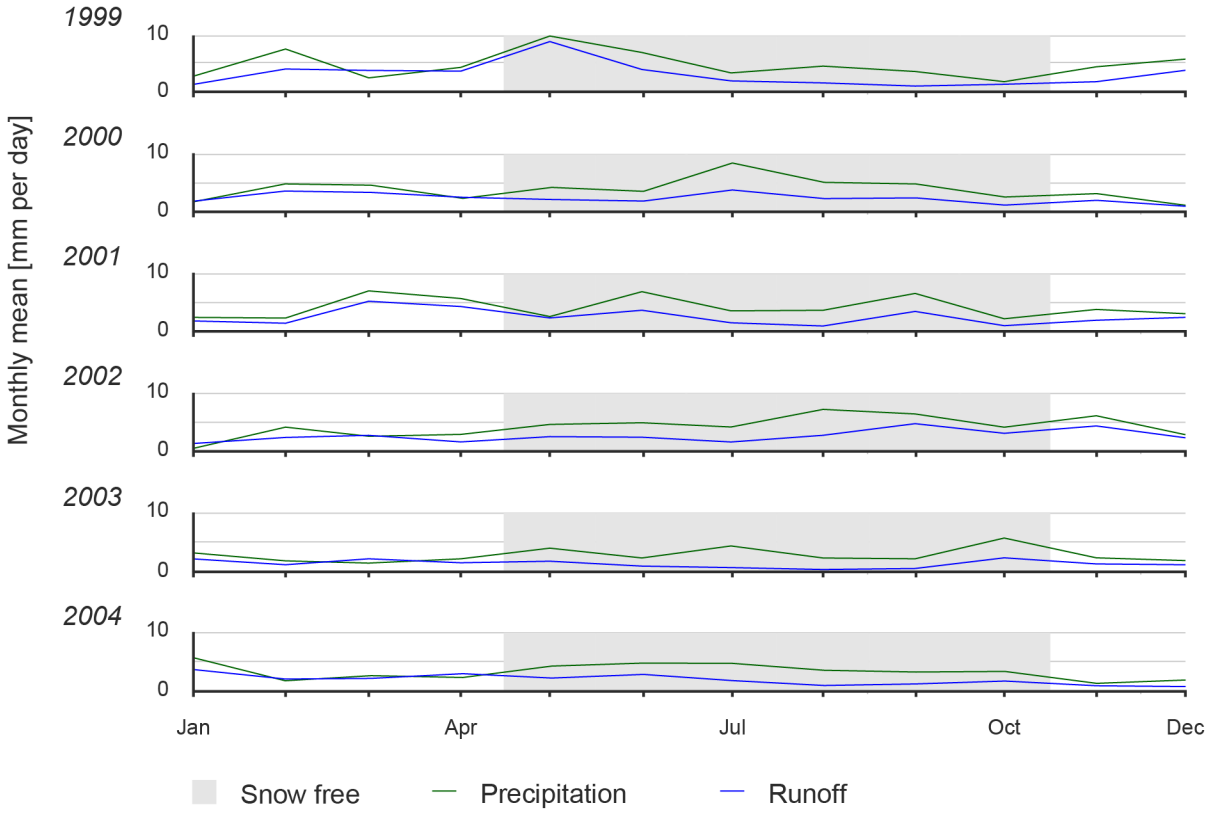

Figure 3: Time series of monthly mean precipitation and runoff in the catchment Andelfingen for the hydrological years 1999–2004 (RhydchprobD monthly ensemble mean). *The seasonal patterns of precipitation (green) and runoff (blue) is illustrated for exemplary years. The months May to October are assumed to be snow free.*

When precipitation falls onto the surface, it begins to move either into the groundwater or to a large proportion as surface runoff due to gravity. The volume of water that flows through a stream on the surface in a particular time interval is defined as runoff (Q) in this thesis. It is the result of precipitation (P), evaporation (E) and change in storage (ΔS), i.e. $Q = P - S - \Delta S$ (Hendriks 2010). During the colder months November until April, almost all precipitation is discharged by the river —as long it does not settle as snow. Low soil storage capacity as well as high field capacity and frozen surface make it difficult for the precipitation to be absorbed by the soil. Furthermore, due to the low temperatures and small angle of incidence of the sun's radiation, there is only little evaporation. These circumstances can be seen in Figure 4 by the parallel lines during the winter months. In March, the evaporation rates rise because of increasing temperature and thus bind an increasing part of the precipitation. As a result, the runoff rate becomes smaller than the precipitation, i.e. decreasing runoff curve despite increasing precipitation. Until April the evaporation rate strongly increases so the water stored in the soil is gradually dissolved. The soil moisture content decreases continuously. Although a decrease in runoff can thus be expected in the months of March to May, the runoff reaches the annual peak due to the snowmelt and the associated decrease in the snow reservoir in May (Häckel 2016). These correlations show that soil moisture conditions are of particular importance for hydrological processes, as they have a significant influence on the relative proportion of precipitation input to the surface and subsurface pathways (Massari et al. 2013). The increasing precipitation towards the end of the summer gradually replenishes the soil reservoir. The rising soil moisture together with the decreasing

evaporation ultimately leads to an increase in the runoff rate at the end of the summer. Finally, in December, when the field capacity is reached, the entire precipitation is again discharged by the runoff (Häckel 2016).

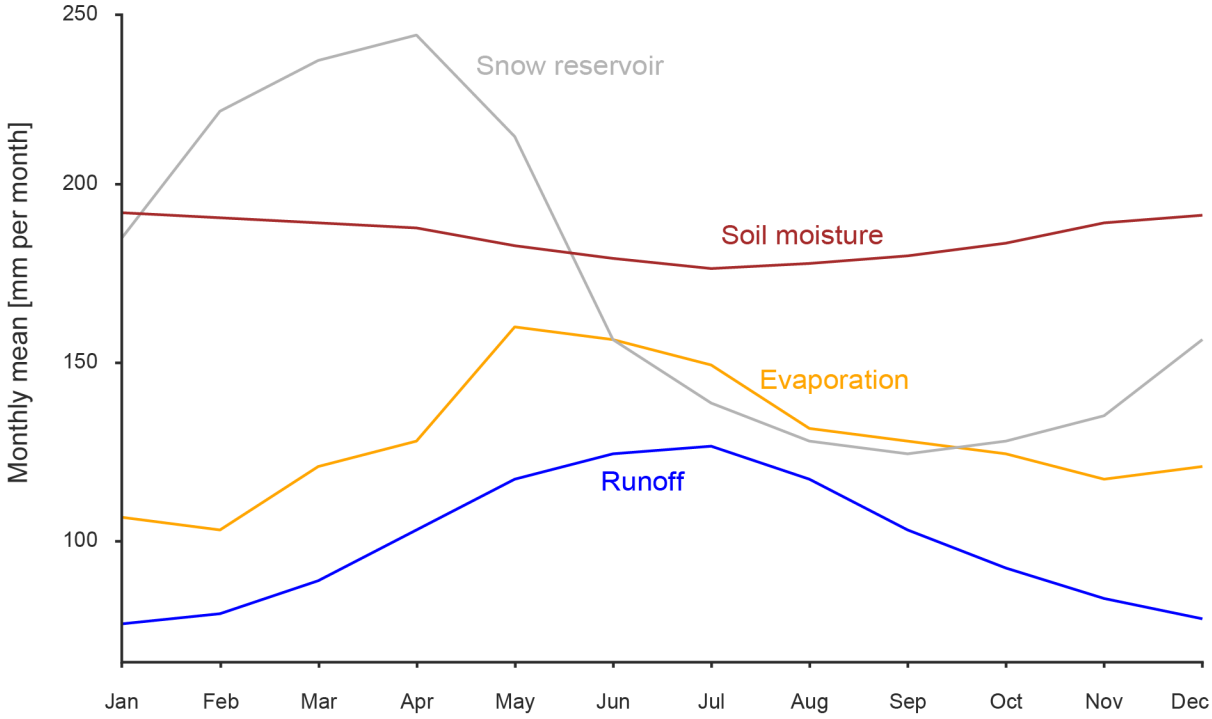

***Figure 4: Water balance of Switzerland**. The seasonal behaviour of evaporation (yellow), soil moisture (brown) and snow reservoir (grey) give indication of the processes generating runoff (blue). Figure modified from Liechti et al. (2020).*

2.2.1 Alpine Regions

With the focus on the catchment *Andelfingen*, alpine regions are very important for the hydrological cycle in three different ways. First, the orographic effect in mountains is responsible for a higher accumulation of precipitation occurrence. Second, colder temperatures due to the higher altitudes cause precipitation from exceeding evapotranspiration and therefore implicate a positive water balance. Lastly, water is temporarily stored in form of snow and ice before it is released to the runoff with a delay. All those conditions influence the amount and time of runoff that originate from mountainous areas, whereby the water availability in the lowlands is controlled. The dependency of the lowlands on water supply from the mountains is highest during summer season when comparatively low precipitation occurrence coincides with high evapotranspiration and irrigation demand (Zierl & Bugmann 2005). Compared to precipitation, which is a spatially heterogeneous phenomenon and thus a measurement on catchment scale is not trivial (Sikorska & Seibert 2018), runoff describes an aggregated response to the precipitation in a catchment that can be measured at its outlet only (Vaze et al. 2011).

2.2.2 Climate Change in Alpine Regions

The hydrological cycle in alpine catchment depends on local precipitation, snow coverage and glacier ice melting. Although natural fluctuations occur interannually (Bartolini et al. 2009) and the precipitation-runoff relationship shows a strong seasonal cycle dependency (Gourley & Vieux 2006), the water resources in mountainous regions are subject to climatic change and thus drive changes in the seasonal cycle (Hock 2005). Temperature changes affecting snow as well as ice accumulation and melt are the main processes controlling the runoff and peak discharge. Beside the temperature influence, changes in spatial patterns, seasonality and amount of precipitation are expected to be the key subject of changed hydrological cycles (Nakicenovic & Swart 2000). Heavy precipitation events are likely to occur more frequently (Sikorska & Seibert 2018), whereas precipitation trends show an increase in winter and a decrease in summer months (Zierl & Bugmann 2005). In many alpine streams, a short-term increase of discharge has been monitored due to glacier melt in the last few years. Nevertheless, the long-term annual runoff is expected to decrease with the disappearance of glaciers (Stahl & Moore 2006; Huss et al. 2008; Huss 2011). The similar patterns and trends of hydrological and meteorological changes imply a close relation of the two process chains (Burn & Hag Elnur 2002). These expectations will affect the water availability and flood control, wherefore better process understanding is required and adaptation strategies for example in terms of water management measures have to be elaborated carefully (Xu & Singh 2004).

2.3 Hydrological Modelling

Hydrological models contribute to the quantification of hydrological interactions and a better understanding of its variables. These models rely on measured precipitation and runoff values in order to learn from realistic values (*calibration*) and obtain simulation values that are as accurate as possible (*validation*) (Seibert & Vis 2012). For this reason, several questions arise: (1) what should the accuracy of observed data be as model input; (2) what will improve the resolution; and (3) which application possibilities are enabled by simulated runoff.

2.3.1 Data Accuracy and Improvement

The key factor affecting the hydrological processes is precipitation. Streamflow simulations are thus strongly depending on the way precipitation is described by the simplified representations of the reality in a hydrological model (Rafieeinasab et al. 2015). Several studies conclude that spatial information on precipitation is indispensable, and its importance increases with decreasing catchment sizes (e.g. Beven 2000; Gourley & Vieux 2006; Rafieeinasab et al. 2015). On the one hand, higher spatial resolution in precipitation inputs results in significantly improved streamflow simulations for catchments featuring diverse topography. This term refers to the different characteristics of the earth's surface (Girons Lopez & Seibert 2016). The spatial variation of terrain elevation is responsible for convective precipitation events because the humid air mass rises at topographical obstacles resulting in heavy precipitation (Isotta et al. 2014; Sikorska & Seibert 2018; Thurai et al. 2016). On the other hand, several authors conclude that the precipitation volume is more important than its spatial pattern (e.g. Lobligeois et al. 2014; Winchell et al. 1998). The precipitation amount also depends on the surface characteristics. In flat catchments with low

topographical variability, precipitation is dominated by stratiform origin from a weather front, which leads to a dependency on the precipitation volume (Lobligeois et al. 2014).

To improve the quality of streamflow simulations, various technologies can be consulted to gather precipitation information. First, *Geographic Information Science (GIS)* and analysis of time series allow to visualise and evaluate spatio-temporal patterns of precipitation and runoff (Amiri & Mesgari 2016). This work benefits from these possibilities of *GIS-technologies*. Second, remote sensing data from satellites and radar can help to improve the spatial resolution of input data for simulation models, conditional on the data resolution. This improvement can, as a result, increase the information content of the predicted precipitation amount (Girons Lopez et al. 2015).

2.3.2 Probabilistic Data

Not only different data systems such as *GIS* and remote sensing but also alternatives of data processing can improve the data accuracy. Precipitation data from spatial interpolation of underlying measurement stations are an important basis for meteorological and hydrological applications. Such data are commonly available in a regular, deterministic grid (Frei & Isotta 2019) and are the result of a single, optimal realization (e.g. Georgakakos et al. 2004; Huizman et al. 2009). Deterministic data find application in hydrological modelling, climate model evaluations and calibration of satellite retrievals (e.g. Fantini et al. 2018; Isotta et al. 2015; Viviroli et al. 2009). Because the grid resolution is most likely higher than the rain gauge network, values in the data sets are subjects to uncertainties in precipitation estimates which are only partially captured by the conventionally used cross-validation approach (Frei & Isotta 2019; Antolini et al. 2015; Hijmans et al. 2005). For the high spatio-temporal variability in precipitation occurrence, however, this uncertainty can be of great importance for application and its performance validation (Frei & Isotta 2019; Huizman et al. 2009). In contrast to deterministic data, the application of a probabilistic ensemble data set enables addressing various sources of uncertainty (Strauch et al. 2012). Explicitly allocating the uncertainties derived from the limited spatial distribution is a main advantage of the probabilistic estimates over single estimates (Frei & Isotta 2019). This alternative concept of precipitation estimation provides a probabilistic likelihood measure constituting several, although not equally likely, representative realizations of the system response for each time unit (Duan et al. 2007; Huizman et al. 2009). The widely used approach of equiprobable realizations in form of ensemble data benefits a range of research activities in three ways: (1) probabilistic data is found to provide the benefit of more reliable weather forecasts in terms of precipitation and temperature (Wu et al. 2011; Buizza et al. 1999; Yu et al. 2015); (2) the implementation of greater uncertainty knowledge improves reservoir managements and early warning systems (Georgakakos et al. 2004; Yu et al. 2015); and (3) the application of such a data set contributes to a generally more realistic spatial knowledge on precipitation variability (Frei & Isotta 2019). This more realistic knowledge is a crucial improvement over the deterministic interpolation due to the fact that it reduces the exaggerated smoothing and the biased extremes depending on the spatial rain gauge distribution (Schroeer et al. 2018; Chappell et al. 2012). The European Centre for Medium-Range Weather Forecasts (ECMWF) and National Centres for Environmental Prediction (NCEP) have been producing probabilistic precipitation data sets since 1992. This illustrates the widespread application of this concept and its implementation. Although the use of probabilistic data also

retains uncertainties and inaccuracies, such data seem to outperform the deterministic approach in various ways (Frei & Isotta 2019).

2.3.3 Significance and Application

Various value-added applications of simulation data exist. Because precipitation has a decisive influence on runoff generation, the spatial and temporal distribution and the amount of precipitation are of great interest for various applications (Girons Lopez et al. 2015). Urban planning, water management and societal resilience are only a few affected sectors depending to a large extent upon hydrological data availability (Girons & Seibert 2016). While coarse spatial and temporal data resolution and the resulting low forecast quality are suitable for some hydrologically related applications, more detailed spatial and temporal knowledge of precipitation occurrence is necessary for (semi-)distributed hydrological modelling and forecasting (Girons Lopez et al. 2015). The accuracy of spatial and temporal changes in precipitation patterns relies on the characteristics of precipitation data inputs (measurement and estimation accuracy, network density, reliability...). A number of studies have shown that the neglection of precipitation variability frequently causes inaccurate model predictions (e.g. Dawdy & Bergmann 1969; Troutman 1983; Duncan et al. 1993; Faures et al. 1995; Lopes 1996; Andréassian et al. 2001; Bárdossy & Das 2008). Such hydrological predictions should, however, provide a convenient data basis for climate change or land use change evaluations, economic incentives or flood management (Beven 2000; Falkenmark & Rockström 2004). Moreover, early warning systems and emergency management — especially in mountainous catchments — heavily depend on observed and forecasted precipitation data with a high spatiotemporal resolution (Rafieeinasab et al. 2015).

Alpine catchments with their special characteristics of steep terrain and rapid discharge generation are strongly affected by heavy precipitation events (Girons & Seibert 2016). Such rapid discharge generation in the regions of headwaters can lead to severe natural hazards (Girons & Seibert 2016; Girons et al. 2017). Unfortunately, estimating precipitation in these mountainous areas is difficult and uncertain because of the high spatial as well as the elevation-dependent variability in combination with high intensities and large amounts of precipitation events. Prediction of such heavy events should nevertheless be as accurate as possible. Early warning systems benefit from more accurate knowledge of precipitation and runoff generation which in turn can minimise the risks of such hazardous events (Sikorska & Seibert 2018). Girons et al. (2015) have shown that areas with large precipitation variability positively correlated with precipitation amounts. The application of ensemble weather data for forecasts in mountainous catchments can thus help to capture this uncertainty in quantifying the variations of ensemble runs and enhance the reliability of hydrological variability-based forecasts (Yu et al. 2015).

3 Study Site

The expression «water tower of Europe» gives indications for the significance of the Alps for regional and supraregional water cycles (EEA 2009). The Rhine, one of the major European rivers originate in the Swiss Alps. With only 20% of the total catchment area, the headwaters of the Swiss Alps contribute almost 50% of the mean discharge of the Rhine in Switzerland (Viviroli et al. 2003). The topography largely influences the generation and flow characteristics of discharge. The Swiss Alpine area is characterized by a wide range of topography, containing flatlands, mountain massifs, deep valleys and several small-scale hill ranges in the foreland (Isotta et al. 2014). This chapter describes the topography and hydrology of the catchment *Andelfingen* with the main river *Thur* (Figure 5), which forms part of the large-scale catchment Rhine. The former is divided into hydrologically similar subcatchments on different spatial aggregation levels by *FOEN* (2019), whereas the numbers in the abbreviations give indication of the average size of a subcatchment. *TEZGNR1000* is the denotation of the entire catchment *Andelfingen*, divided into subcatchments of on average 150 km^2 (*TEZGNR150*), which in turn are further subdivided into areas with an average size of 40 km^2 (*TEZGNR40*).

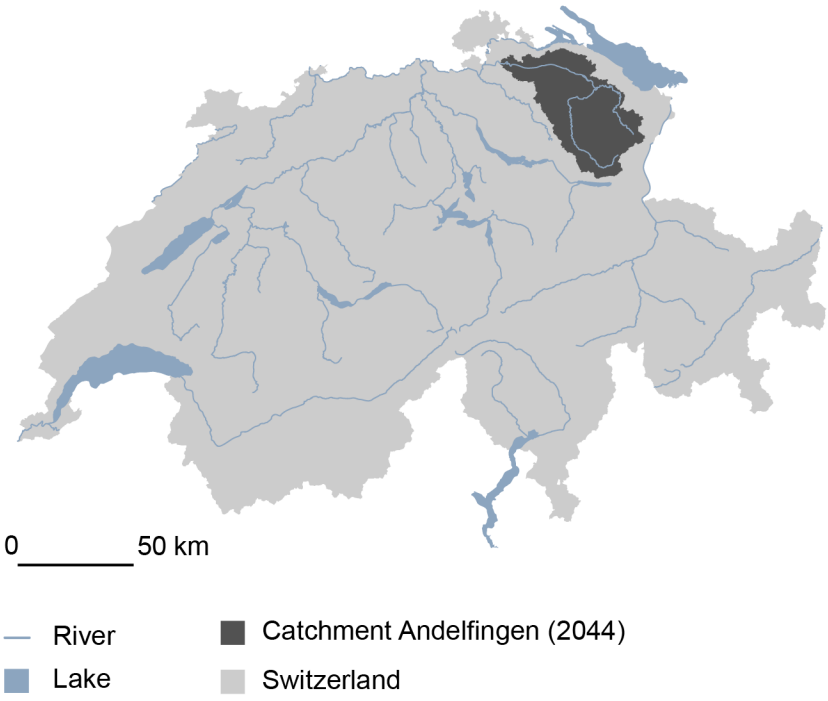

Figure 5: Map of Switzerland with the catchment Andelfingen highlighted (Data by swisstopo 2020).

3.1 Catchment *Andelfingen* (*TEZGNR1000*)

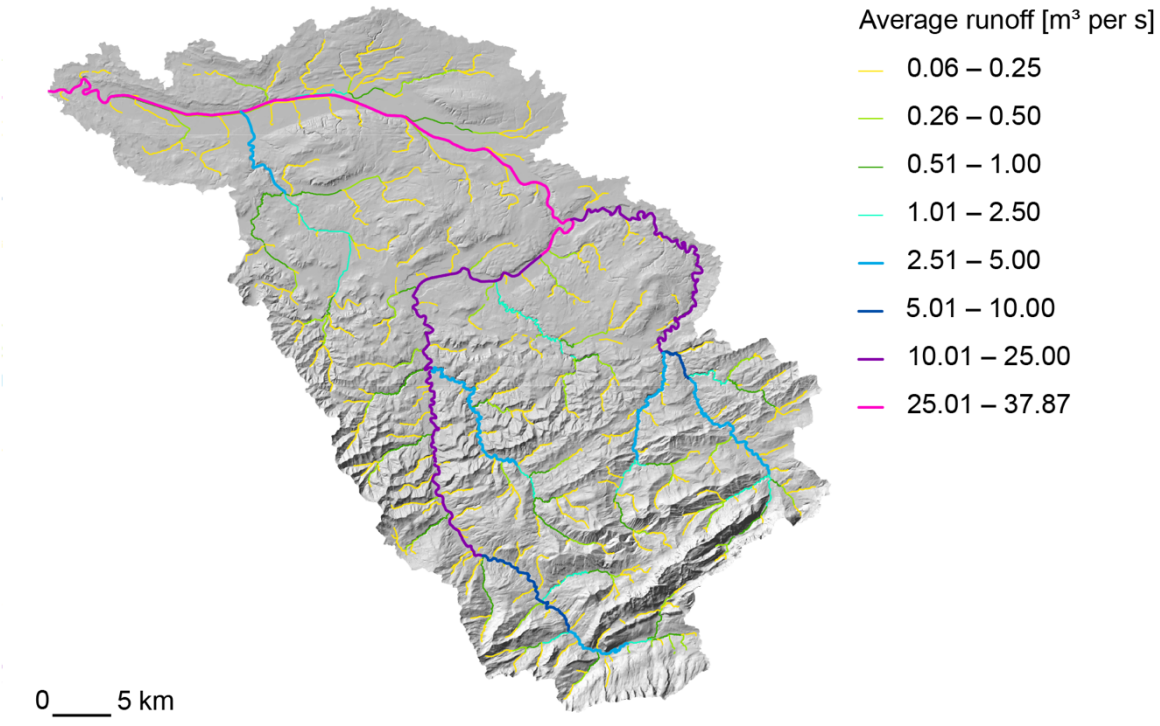

Figure 6: The river system in the catchment Andelfingen*. The rivers are coloured according to their average runoff (Data by swisstopo 2020).*

Table 1: Characteristics of catchment Andelfingen (HYDROmaps 2020).

Area	1712 km^2
Affiliation to large-scale catchment	Rhine
Catchment length and width	56.2 km/62.5 km
Catchment shape factor (width/length)	1.11
Minimum altitude	358 m a.s.l.
Maximum altitude	2 500 m a.s.l.
Mean altitude	768 m a.s.l.
Measurement station	356 m a.s.l.
Slope	10° (difference in ground elevation between upstream most point and outlet/catchment length)
Flow regime type	Nivo-pluvial
Landcover	Grassy and herbaceous vegetation (31%), agriculture (30%), forest (28%), urban area (8%), wetlands (1%), loose rock (1%), bush vegetation (1%) → no glaciation and lake/artificial water constructions
IMP (sealed surface)	8%

The catchment *Thur-Andelfingen* (in the following *Andelfingen* or *TEZGNR1000*) in the north east of Switzerland, #2044 in the national inventory of hydrological stations of *FOEN*, has been chosen as a data base for the present study due to its appropriate characteristics (Table 1). These characteristics are outlined in the following. The 1 712 km^2 large catchment is to a large extent covered by grassy vegetation and forest (59 %). The southern, more mountainous part extends to 2 431 m a.s.l. and features smaller mountain streams, whereas the rivers in the northern lowlands

(~350 m a.s.l.) carry more water and are dominated by agricultural and urban areas (Figure 6). The detailed land cover classification is attached in the appendix *A.1 Additional Illustrations* Figure 66. The main river in this catchment *Thur* with its inlets is the largest non-regulated river in Switzerland and is part of the northern front ranges of the Swiss Alps (PEER 2010). Apart from the two larger agglomerations St. Gallen and Frauenfeld within the examined area, the population is mainly concentrated in scattered settlements of rural character (HYDROmaps 2020; CLC 2018; swisstopo 2005; FOEN 2019; Girons & Seibert 2016). To minimize uncertainty outside the data sets, methodology and technical processing, the study examines an area not affected by glaciers, lakes and regulated rivers (Woosley et al. 2007).

In order to be able to interpret the results and place them in the context of natural events, it is important to describe the characteristics of the catchment *Andelfingen*. The prevailing combination of a (pre-)alpine climate is characterized by moderate winters in the lowlands, cold winters in mountainous areas, and summer months with relatively large deviations from the annual mean temperatures (Yang et al. 2007). Figure 7 represents the annual mean precipitation. The highlighted hydrological years 1999 (above average annual precipitation), 2003 (below average annual precipitation) and 2013 (average annual precipitation) are used as examples for the different annual precipitation in this work. The average precipitation is approximately 1 300 mm per year (MeteoSwiss 2020d), whereas the monthly mean temperatures fluctuate between 10 and 25° C in summer months and −15 and 7° C during winter months (Yang et al. 2007). Clear trends can be observed during the summer. Whereas both the precipitation and the temperature show a peak during this time, a positive elevation gradient for precipitation and a negative one for temperature is determined (Girons & Seibert 2016). Dominated by snowmelt input (nivo-pluvial), the annual average of the runoff at the *Andelfingen* station is about 2.39 mm per day, the 100-year high flow is 53.80 mm per day and the 100-year low flow 0.16 mm per day (FOEN 2020). The steep terrain and short concentration times support a rapid discharge build-up at the basin outlet during heavy precipitation events in the headwaters (Girons & Seibert 2016). The meteorological and hydrological data used in this research have been measured by 21 weather stations and ten runoff measurement stations within the catchment and five temperature gauges within and close to the catchment (MeteoSwiss 2020a).

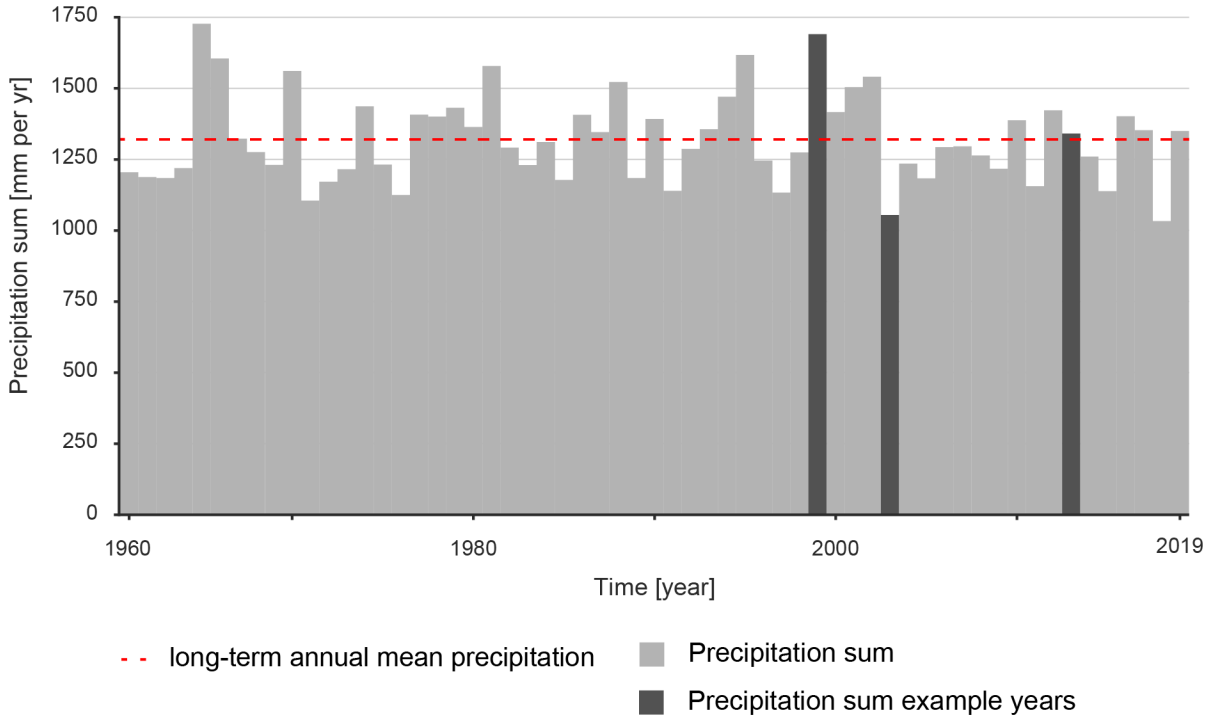

Figure 7: Annual precipitation sum in the catchment Andelfingen. *The highlighted years 1999 (very high precipitation sum), 2003 (very low precipitation sum) and 2013 (average precipitation sum) are used as examples to illustrate several patterns and behaviours in the following.*

3.2 Subcatchments *TEZGNR150*

As described above, the catchment *Andelfingen* is very heterogeneous in terms of topography, precipitation and runoff. For this reason, a finer subdivision into eleven subcatchments *TEZGNR150*, which present an average area size of 150 km^2, is useful. These eleven subcatchments are based on natural phenomena (catchment areas) according to the classification of *FOEN* (2019). Therefore, all spatially aggregated meteorological analyses, where the natural properties are mainly responsible for precipitation patterns and non-overlapping areas are required, are calculated for the subcatchments *TEZGNR150*.

3.3 Subcatchments *TEZGNR40*

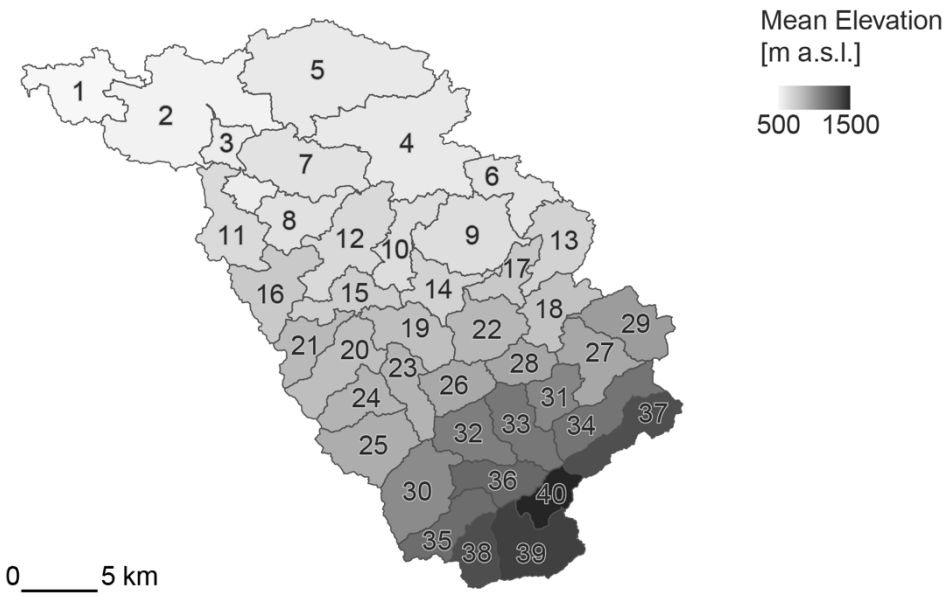

Figure 8: Subcatchments TEZGNR40 in the catchment Andelfingen*. The subcatchments are coloured and numbered by ascending average elevation* (Data by FOEN 2019).

The catchment *Andelfingen* is, according to the classification of *FOEN* (2019), divided into 40 subcatchments for hydrological terrain units (also referred to as «*Basisgebiete*» or «*Teileinzugsgebiete 40 km²*»), which are henceforth named by ascending mean elevation—starting with 1 for the subcatchment with the lowest mean elevation and going up to 40 referring to the highest subcatchment (Figure 8). The highlighted subcatchments #5 (lowlands), #14 (average catchment elevation), #29 (above average elevation) and #36 (high elevation) are used as examples for differently characterised subcatchments in further analysis. Because the probabilistic precipitation data set *RhydchprobD* provided by *MeteoSwiss* is limited to the resolution of subcatchments with an average size of 40 km², all the present study analyses are carried out at this level of spatial aggregation. The subcatchments *TEZGNR40* with one assignable outlet are based on the topographical classification for hydrological terrain units of *FOEN* (FOEN 2019). In general, the long-term annual precipitation sum of the subcatchments positively correlates with the elevation gradient because of precipitation generation processes, shown in Figure 9. The relationship between precipitation volume and elevation will later be important in distinguishing between natural precipitation variability and estimation uncertainty. The lowest monthly precipitation mean is recorded in February for all 40 subcatchments, whereas the peaks vary between June and August with a tendency for an earlier peak in lower regions (Figure 10).

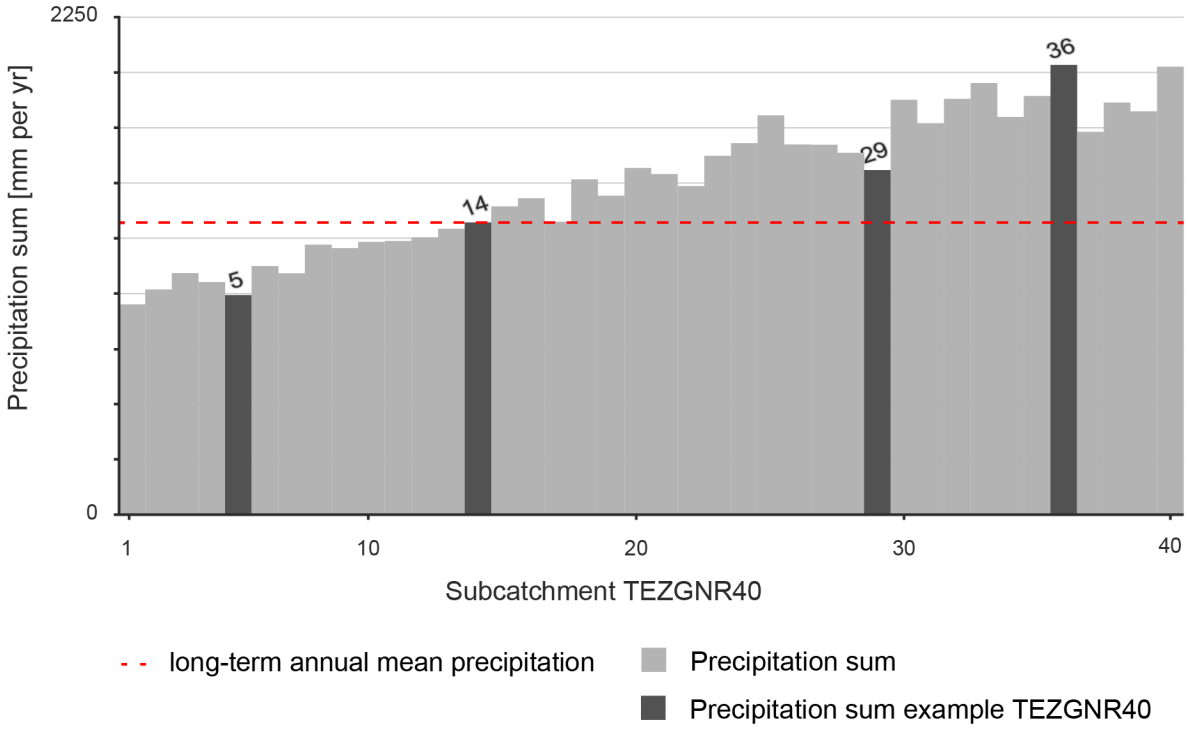

Figure 9: Annual mean precipitation sum of the subcatchments TEZGNR40. *The highlighted subcatchments TEZGNR40 #5 (lowlands), #14 (subcatchments average), #29 (slightly above the long-term average precipitation sum) and #36 (highlands) are used as examples to illustrate several patterns and behaviours in the following.*

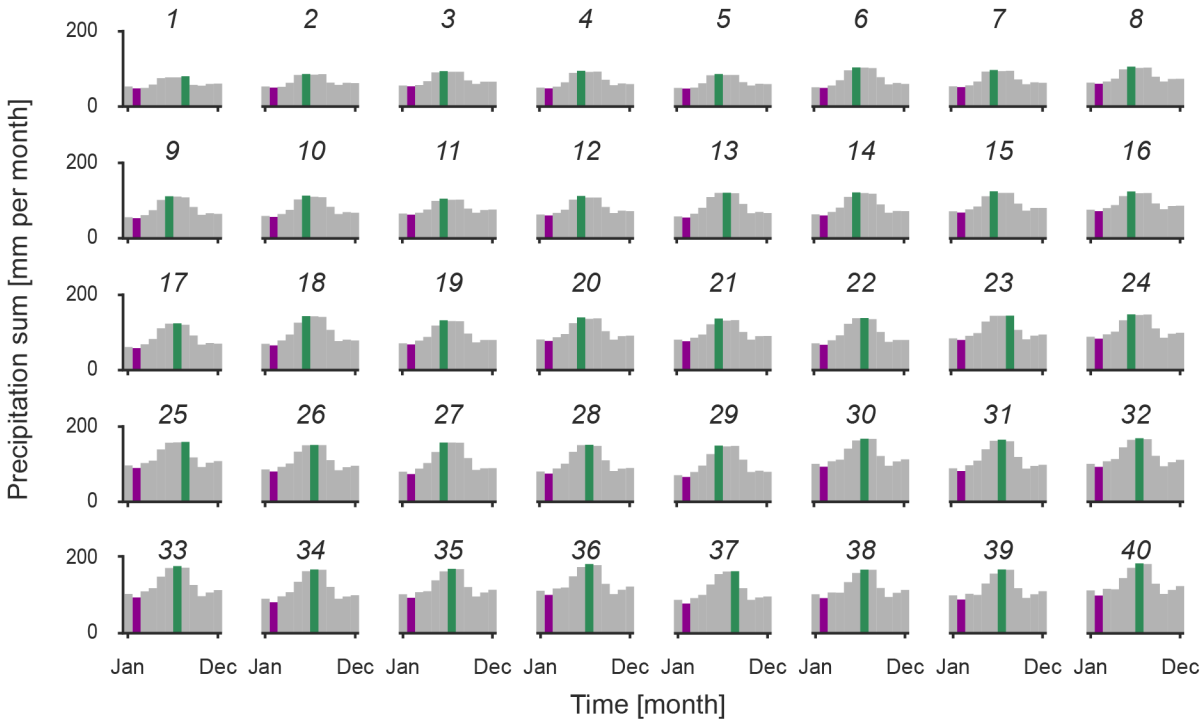

Figure 10: Monthly mean precipitation sum of subcatchments TEZGNR40. *The lowest and highest monthly precipitation sums are coloured in purple and green respectively.*

3.4 Measurement Stations

This work is based on measured values from two different measurement networks. The precipitation measurement data come from meteorological stations of *MeteoSwiss*, the runoff measurement data from *FOEN*. The weather measurement station network of *MeteoSwiss*, visualized in Figure 11 (black), comprises over 400 high-resolution manual and automatic gauges of which 27 lie within the study catchment (MeteoSwiss 2019; MeteoSwiss 2020a). All interpolations for precipitation and temperature data are based on this subset of stations.

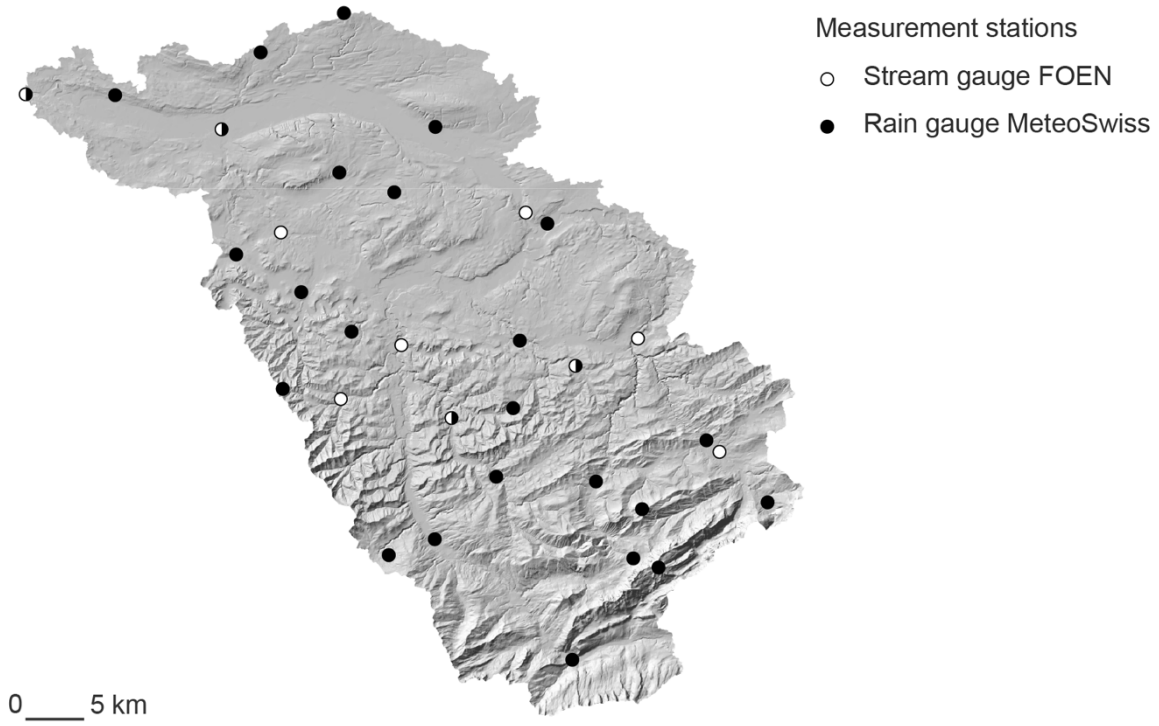

Figure 11: Stream (white) and rain gauges (black) in the catchment Andelfingen (Data by MeteoSwiss 2019; MeteoSwiss 2020a; HYDROmaps 2020).

The measurements from eight *FOEN* stream gauging stations used for hydrological simulations are mapped in Figure 11 (white) and their characteristics (corresponding river, catchment name, *FOEN* code as well as area and elevation) are listed in Figure 12 and Table 2. It is important to note that the size-dependent hydrological classification of *FOEN's* subcatchments differs from the runoff measurement station catchments of *FOEN* (further named *MSC* in combination with the station number of *FOEN*, e.g. *MSC 2044* for the catchment *Andelfingen*) in terms of classification. Instead of being divided into areas of similar size, the *MSC* are determined by the location of the measuring stations. Each of these *FOEN* measurement stations is located at the outlet of an *MSC*. The discharge measured at these stations can be allocated to a defined drainage basin. Therefore, it happens that especially *MSC*, with the measuring stations in the lowlands, also include mountainous *MSC*, where smaller mountain streams flow into larger rivers. Because of the dependencies of observed runoff at these stations, the hydrological analysis and simulations are based on eight subcatchments of runoff measurement stations within the catchment *Andelfingen* to verify the simulated with the observed runoff. Some of the *MSC* overlap or are composed of several subcatchments. Because the catchment area of two measurement stations, i.e. 2305 Zellersmühle and 2414 Mosnang, are smaller than the spatial resolution of the underlying subcatchments

TEZGNR40, these measurement stations will not be used in this thesis. Even though the measurement stations of both networks (*MeteoSwiss* and *FOEN*) are evenly distributed from a spatial perspective, altitudes above 1 200 m a.s.l. remain underrepresented. Meteorological as well as hydrological stations are predominantly installed at low elevations with higher population density and correspondingly higher hazard risk (Frei & Schär 1998). A systematic underestimation of precipitation in high altitude areas is the result of the spatial representation bias (Girons et al. 2015), although the general mean precipitation increasing with altitude should be observed carefully (Peck & Brown 1962).

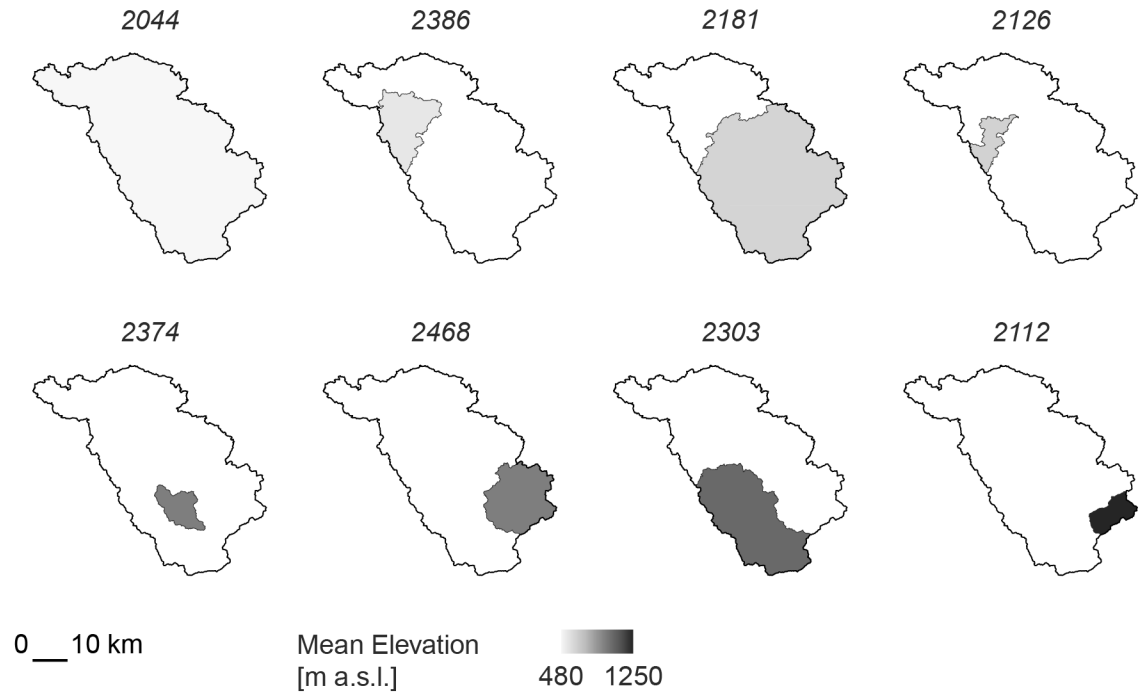

Figure 12: Measurement station catchments (MSC). *The catchments are defined by the location of FOEN's stream gauges. The MSC are listed and coloured according to their average elevation (Data by HYDROmaps 2020; swisstopo 2005).*

Table 2: List of FOEN's stream gauges with their corresponding identification code, location name, main river, catchment area and elevation of station (HYDROmaps 2020).

FOEN code	Location name	Main river	Area [km^2]	Station elevation [m a.s.l.]
2044	Andelfingen	Thur	1712	356
2386	Frauenfeld	Murg	213	390
2181	Halden	Thur	1085	456
2126	Wängi	Murg	80.2	466
2414	Mosnang	Rietholzbach	3.2	682
2468	St.Gallen	Sitter	261	527
2303	Jonschwil	Thur	493	534
2374	Mogelsberg	Necker	88.1	606
2305	Herisau, Zellersmühle	Glatt	16.7	679
2112	Appenzell	Sitter	74.4	769

4 Data

This chapter describes all data sets used in this research concerning precipitation and runoff variability. A brief overview of these data sets is given in Table 3. Two different daily precipitation interpolations of the same underlaying rain-gauge network of Switzerland, namely *RhiresD* and *RhydchprobD*, form the data base for the following meteorological and hydrological analysis. The measurement stations provide data covering the time period from 1961 until present. While the spatial distribution of rain-gauge stations within the catchment *Andelfingen* is fairly homogenous in the west-east directions, a clear heterogeneity in the north-south directions emerge. Particularly, areas above 1 200 m a.s.l. are underrepresented (Frei & Schär 1998). Additionally, ten runoff measurement stations within the catchment *Andelfingen* by *FOEN* provide hourly data and will be used to benchmark the runoff simulations. To generate these simulated values, air temperatures found in the *TabsD* (MeteoSwiss 2020b) data set are included as well.

Table 3: Overview of included data sets. (MeteoSwiss 2020b/c/d; HYDROmaps 2020; FOEN 2020)

	Precipitation (*RhiresD*)	**Precipitation (*RhydchprobD*)**	**Runoff**	**Air temperature (*TabsD*)**
Data type	Interpolation fields	Interpolation fields	Measurement entity	Interpolation fields
Interpolation method	Climatological mean precipitation (local weighted linear regression)	Probabilistic analysis of mean precipitation (ensemble with 50 members by trans-Gaussian random fields)	–	Climatological mean air temperature (local weighted linear regression)
Number of measurement stations included	25 (of total 420 to 520 in CH)	25 (of total 420 to 520 in CH)	10 (of total 251 in CH)	8 (of total 84 to 93 in CH)
Period	1961 to 2020	1961 to 2020	1980 to 2019 (partly from 1974/1975)	1961 to 2020
Temporal resolution	Daily D; 06:00 UTC of day D to 06:00 UTC of day D+1	Daily D; 06:00 UTC of day D to 06:00 UTC of day D+1	Hourly mean	Daily D; 06:00 UTC of day D to 06:00 UTC of day D+1
Spatial resolution	2.3 km^2 (N–S) x 1.6 km^2 (W–E)	40 subcatchments with average size of 40 km^2	Variable (depending on catchment size)	2.3 km^2 (N–S) x 1.6 km^2 (W–E)
Unit	mm (=l/m^2)	mm (=l/m^2)	m^3 per s	°C
Data source	Swiss rain-gauge network, *MeteoSwiss*	Swiss rain-gauge network, *MeteoSwiss*	Measurement stations, *FOEN*	Swiss rain-gauge network, *MeteoSwiss*

4.1 Deterministic Grid Data *RhiresD* and *TabsD*

The deterministic data set *RhiresD* for daily precipitation (*ch02.lonlat*) and *TabsD* (*TabsD v1.2 in ch02.lonlat*) for daily air temperature are two of the data sources provided by *MeteoSwiss*. *RhiresD* is the result of a distance and angular weighting interpolation technique. In this technique, measurements of the weather stations are interpolated considering the local precipitation-topography relationships at the climatological time scale for the entire territory of Switzerland. Relative anomalies of observed daily precipitation totals are derived from climatological reference fields by Schwarb et al. (2001), similar to the method of Widmann & Bretherton (2000). With the use of climatological reference fields for the interpolation of daily precipitation, systematic errors in high elevation regions are expected to be reduced. Measurement stations are often underrepresented in such areas (Widmann & Bretherton 2000). Nevertheless, an underestimation of the measured precipitation is expected at high elevations, during winter days with snowfall and at wind-exposed locations (e.g. Sevruk 1985; Isotta et al. 2014; Fantini et al. 2018).

As it is the case for the precipitation data, spatial differences are also taken into account for the interpolation of air temperatures within *TabsD*. The data set *TabsD* is based on the digital elevation models USGS GTOPO30 (2 km grid) and SRTM (1 km grid) as well as on near-surface, mostly automated air temperature measurement stations of the operational station network SwissMetNet by *MeteoSwiss* (2 m above ground level). To reproduce the spatially different temperatures, a supra-regional vertical temperature dependence is estimated with a non-linear parametric profile independently for each day. This procedure allows to reproduce temperature inversion and warm boundary layers based on the measured temperatures at the weather stations. The deviations of measurements from the vertical profile are then interpolated by a non-Euclidean distance weighting function (Deng & Stull 2005). The resulting raster data set is assumed to represent the spatially heterogeneous temperature more realistically (MeteoSwiss 2020b).

Both products feature a spatial resolution of approximately 2 km^2, although the distance between the measuring stations is greater. The distance between the stations vary from 10 km in densely covered areas in the north-west of the catchment up to 25 km in remote areas in the south (Isotta et al. 2014). Frei & Isotta (2019) argue that a consistent station network is an inevitable precondition for various reasons: (1) the estimations are more reliable; (2) inhomogeneities in reconstruction are avoided; and (3) observed data are needed for interpolation. The statistical results thus rely on the measurement station density and its estimation accuracy. Even though rain-gauges only provide exact measurements for limited locations, they are a widely used data base to record precipitation (Frei & Isotta 2019). Such data have the advantage that the precipitation is measured above the surface and thus provides ground-level precipitation observations with limited errors (Song et al. 2015). However, these point measurements are vulnerable to wind drifts and shading effect from slopes (Frei et al. 2006). Such disturbances can reduce the increasing precipitation rate with elevation (Viviroli et al. 2011; Xie et al. 2007) and ignore spatially restricted precipitation events (Sikorska & Seibert 2018). The above-named effects often result in an underestimation of true precipitation values (Neff 1977; Yang et al. 1999). Thus, in combination with the limited spatial resolution, it is pointed out that the data set is unsuitable for the analysis of local heavy weather events (MeteoSwiss 2019; MeteoSwiss 2020a). A finer spatial interpolated grid can thus only improve the estimations if the measurement station availability in high elevations is simultaneously increased (Sikorska & Seibert 2018).

The data provided by *MeteoSwiss* are originally stored in multidimensional NetCDF-files. The daily mean air temperature and precipitation values for each hydrological subcatchment *TEZGNR40* are extracted and aggregated from the data stacks in RStudio.

4.2 Probabilistic Grid Data *RhydchprobD*

The second data source provided by *MeteoSwiss* is the probabilistic grid data set *RhydchprobD* (*ch01h.swisscors*), which features daily precipitation data as a 50-member ensemble (*ensemble runs*) of possible spatial precipitation occurrence. The probabilistic data set has some similarities with the deterministic *RhiresD*: the data are based on the same high-resolution rain-gauge network, covers the same time period and the interpolation method follows the concept of local stationarity or local likelihood (Kuusela & Stein 2018; Frei & Isotta 2019). These circumstances enable a comparison of the precipitation estimation. Nevertheless, the probabilistic approach differs from conventional, deterministic spatial interpolations in two fundamental aspects: the precipitation estimations are provided (1) as daily area-means over hydrological units *TEZGNR40* rather than in points on a regular grid and (2) represent an ensemble of possible realizations. The concept of equifinality—which describes the possible existence of equally likely representations of natural phenomena—concerning precipitation realisations is common and well adopted in scientific studies (e.g. Germann et al. 2009; Schleiss et al. 2012; Ahrens & Jaun 2007). The advantage over conventional single, deterministic estimates is the provision of daily variation within the ensemble, which is a measure of interpolation uncertainty. Such uncertainties can arise from the limited availability of measurement stations. Furthermore, the probabilistic interpolation reproduces characteristics of extremes more accurately (Frei & Isotta 2019). However, estimation error uncertainties (systematic and random) remain disregarded which results in an underestimation of the effective uncertainty given by the ensemble spread. Further details on the interpolation method, stochastic model and parameter set ensembles are described in Frei & Isotta (2019).

A disadvantage shared with the deterministic approach is the fact that the model does not include a component for topographic features (e.g. elevation, slope, wind exposition). As a consequence, the data sets do not reflect precipitation-topography relationships smaller than the station network resolution. The producers thus discourage from using the product for applications focussing on long-term precipitation sums. They rather support the data application for the analysis of precipitation occurrence and statements about the precipitation estimation uncertainties at daily or event time scale purposes (MeteoSwiss 2020d).

4.3 Runoff Measurements

Most of the water produced by precipitation is discharged by rivers. Not only the amount of precipitation but also the runoff is measured regularly. The basic monitoring network of *FOEN* currently encompasses about 250 measurement stations in surface waters. About 200 of these stations automatically measure the runoff as hourly mean in m^3 per second, which enables fast data availability. Ten out of the 250 measurement stations are located in the catchment *Andelfingen*, eight of which are used for hydrological simulations and considered as ground truth for runoff analysis. Because the catchment area of the measurement stations *2305 Zellersmühle* and *2414 Mosnang* are smaller than the spatial resolution of the underlying subcatchments *TEZGNR40*, the runoff data

of these stations will not be used in this thesis. The historical data measured at the various stations are aggregated into daily averages from 06:00 UTC of day D to 06:00 UTC of day D+1 equivalent to the precipitation data of *MeteoSwiss*. According to the Hydrological Atlas of Switzerland (HADES), all studied rivers are categorised as members of the nivo-pluvial flow regime type (HADES 2015).

Although the rivers belong to the same flow regime type, their runoffs differ. How different the runoff behaviour in the various subcatchments is, is visualized with the daily long-term mean runoff in Figure 13. While the lower-lying areas have a relatively small seasonal amplitude with the runoff peak in the winter months, the seasonal differences are greater in the alpine areas due to snow melt. Their maximum runoff is recorded in the spring months April and May. By taking a closer look at the runoff data and their metadata (e.g. size, elevation, terrain), it becomes clear that the size of the catchment area has a marginal effect on the runoff amount compared to the topography. As an example, the magnitude and pattern of seasonal variability in the runoff of subcatchments *2374 Mogelsberg* and *2181 Halden* are relatively similar, although the catchment size of *Halden* is twelve times larger than *Mogelsberg* (1 085 km^2 vs. 88 km^2).

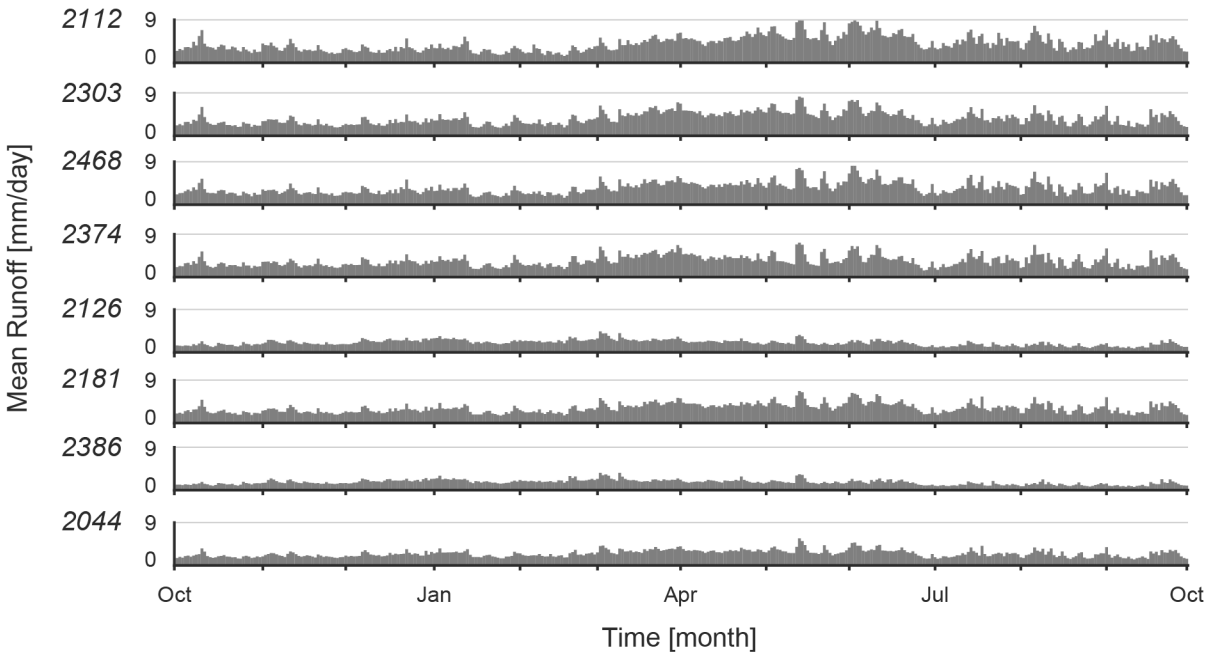

Figure 13: Daily long-term runoff for each MSC.

5 Methods

The main methodological procedure is visualised in Figure 14. The methodological steps are divided into the two pre-processing sections *5.1 Data processing* and *5.2 Measures of variability* followed by the three main sections *5.3 Meteorological data analysis*, *5.4 Hydrological simulations* and *5.5 Hydrological data analysis* with six analysis steps. While section *5.3* investigates meteorological data and processes, the parts *5.4* and *5.5* process these data and focus on hydrological simulations. Each of these processes involve several sub-processes which are explained in detail in the following sections.

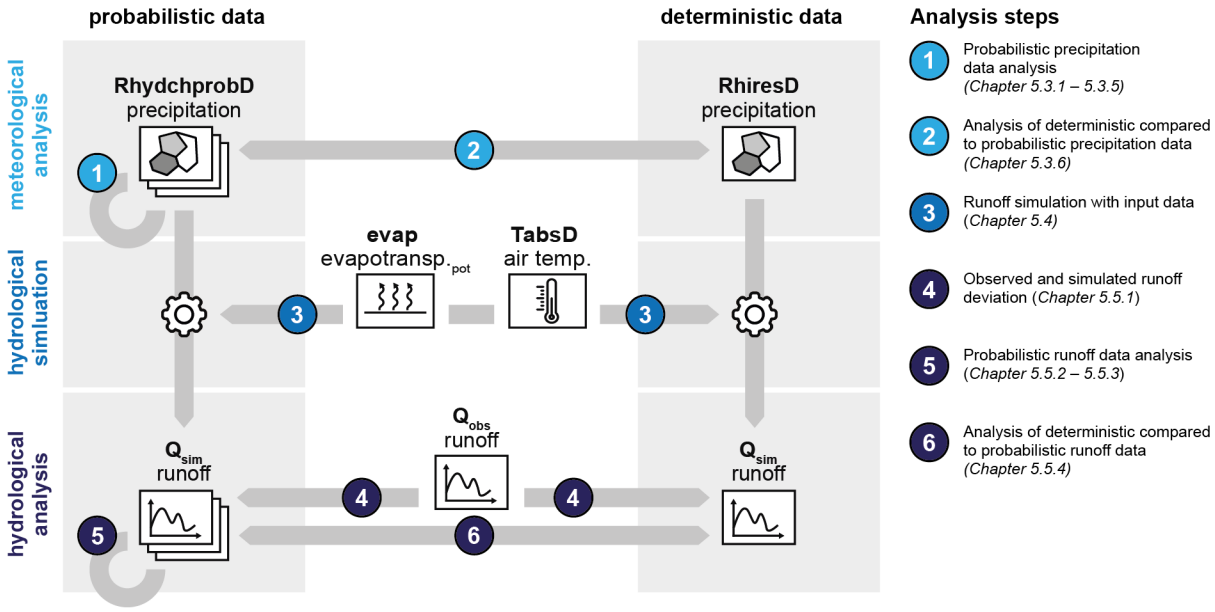

Figure 14: Flow chart illustrating the different aspects of the applied methodology and the data sources included. *The five methodological steps (listed in blue) and the corresponding analysis steps (number in circles) are shown (Icon sources are listed in A.4 Icons).*

Software

For all processes and visualisations of the precipitation and runoff data except for the hydrological simulations, RStudio is used. The appendix *A.3 Software* gives an overview of the software applied, including all packages extending the base functionalities. The runoff simulations are outputs of the semi-distributed model *HBV* in the *HBV Light* version.

5.1 Data Processing

Some data sets in their original form did not correspond to the desired spatial extent. For this reason, they are pre-processed before being used for further analysis.

5.1.1 Processing Geometry of Subcatchments *TEZGNR40*

Based on the definition by *FOEN*, catchments and subcatchments are derived from topography. Every subcatchment is allocated to a single catchment which by definition has exactly one outlet.

This research work focuses on the catchment *Andelfingen* which consists of 44 (*TEZGNR40*) and 10 (*TEZGNR150*) hydrological subcatchments, depending on the spatial aggregation. The geometry used by *MeteoSwiss* to interpolate the precipitation on a subcatchment scale is not congruent with the hydrological division as used by *FOEN* (MeteoSwiss 2020d; HYDROmaps 2020). Even though the *FOEN's* hydrological classification is more accurate, four *TEZGNR40* subcatchments are manually merged to their larger hydrological unit used by *MeteoSwiss*. This step is enforced by the lower spatial resolution of the precipitation data by *MeteoSwiss*. With this step, the geometrical inconsistency is overcome. *MeteoSwiss* plans to recalculate the spatial interpolation based on the subcatchments provided by *FOEN* in the near future (Frei 2020).

5.1.2 Spatial Aggregation of *RhiresD* and *TabsD*

Before the two data sets *RhiresD* and *RhydchprobD* can be used and compared, they need to be aggregated into the same spatial entities (*TEZGNR40*). For this purpose, the mean value of the grid data *RhiresD* is extracted for each subcatchment *TEZGNR40*. Even though the median value would in fact provide a more robust value against outliers, spatially averaged precipitation is common in the literature (e.g. Brown et al. 2012; Martin et al. 2010) and subsequently used statistical coefficients also include mean values. The difference between the aggregated mean and median value ranges between −7.70 and 8.43 mm per day for the entire data period and between −4.24 and 5.55 mm per day for the exemplary year 1999, respectively.

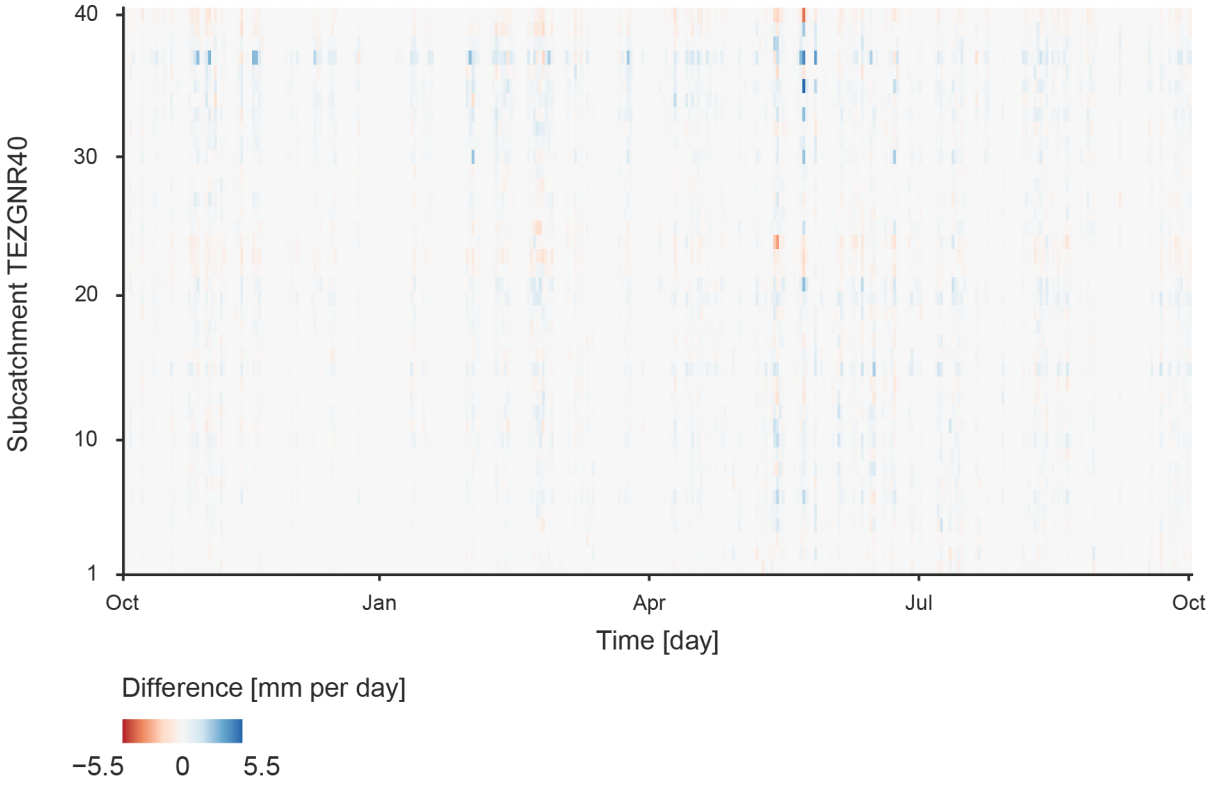

Figure 15: Precipitation difference of Rhydchprob ensemble mean and Rhydchprob ensemble median per subcatchment TEZGNR40. *Negative values indicate a higher median value compared to the mean and positive values a higher mean value than the median.*

The hydrological simulations are run for the subcatchments of eight measurement stations which sometimes adjoin but can also contain each other. Therefore, all subcatchments *TEZGNR40* are

assigned to one or multiple measurement station subcatchments. For all data sets, i.e. *RhiresD, TabsD* and *RhydchprobD,* the spatial resolution is adjusted to the measurement station subcatchments by the calculation of mean values.

5.2 Measures of Variability

The application of a variability measure is based on the assumption that a high variability within the ensemble can be equated with a high interpolation uncertainty. The *standard deviation* is a common descriptive measure of such variability and is used to describe ensemble spreads, i.e. the variability within the ensemble (Martin et al. 2010). Compared to other measures of dispersion such as the variance, this measure is recorded in the same unit as the underlying measured values, which simplifies the interpretation. Because the standard deviation is based on the squared deviation of all measurements from their arithmetic mean, it includes all measurements and can be defined as the *absolute ensemble spread* (Benninghaus 2007). But this total inclusion has the consequence that the standard deviation is highly susceptible to outliers; it is not a robust measure (Stahel 2009). A high absolute ensemble spread implies that the precipitation or runoff values are on average far from the arithmetic mean. Conversely, a small absolute ensemble spread means that all ensemble run values are close to the arithmetic mean. However, the deviation for smaller values does not have the same weight as the same deviation for large precipitation and runoff occurrences. For example, given the samples [4, 2, 6, 5] and [200, 198, 202, 201]: even though they have the same absolute ensemble spread (= 1.48), the weight of the interpolation uncertainty is higher for the first sample with lower values. In certain cases, however, such as in the analysis of heavy precipitation events, the application of the absolute ensemble spread is justified and reasonable.

In order to deal with the above-mentioned bias of the standard deviation, the absolute ensemble spread is commonly normalised with its mean value (e.g. Girons Lopez et al. 2015; Kling et al. 2012; Rakovec et al. 2012). This relative standard deviation is known as the *coefficient of variation* (*CV*). The ratio of the values standard deviation to their mean express the interpolation uncertainty within the ensemble. The *relative ensemble spread* thus allows a comparison of the ensemble variability during different precipitation and runoff periods—regardless of their intensity—and with focus on the model accuracy (Rakovec et al. 2012). Although different precipitation and runoff intensities lead to different mean values, the standard deviation is often approximately proportional to the mean value, which is why the coefficient of variation remains roughly the same (Stahel 2009). While the standard deviation for the above introduced example results in the same value, the *CV* for the samples is 0.34 and 0.007, respectively.

A calculation of this relative ensemble spread for all values would result in a large number of very high relative variability caused by the division of a small precipitation amount. Therefore, the definition introduces a minimum precipitation threshold of 1 mm per day for a wet day (Rivoire et al. 2019). For all ensemble with a daily mean precipitation below this threshold, the *CV* is considered 0. A $CV > 1$ implies that the standard deviation is higher than the mean precipitation. The threshold value for a wet day is certainly at the lower limit and could be increased if reasoned. It can be assumed that the proportion of high relative variability for weak precipitation events will decrease with a higher threshold. In order to give importance to such weak events and to test the performance of the probabilistic data set with as few conditions as possible, the value 1 mm per

day is retained in this work. The variability analysis shows that this threshold could actually have been set higher. For the majority of precipitation occurrences (95% = 820 040 entries) the probabilistic ensemble data features a precipitation uncertainty measured by the ensemble spread of less than 3.15 mm per day (absolute) and 2.35 mm per day (relative). These occurrences have an average precipitation sum of 3.08 mm per day. Furthermore, these observations show that a combined analysis of absolute and relative ensemble spread provides the most explicit statements. A high absolute variability does not always imply a high degree of estimation uncertainty in the amount of precipitation, as the absolute variability is strongly depending. Conversely, a high relative variability does also not necessarily imply a high degree of uncertainty. However, if the absolute and relative variability both show high spread values for an average precipitation amount of more than 3.08 mm per day, it can be assumed that the precipitation estimation on that day for the concerning subcatchment *TEZGNR40* is subject to uncertainty.

5.3 Meteorological Data Analysis

Research objectives 1.1, 1.2, 3.1 and 3.2 intend to verify the spatial and temporal precipitation variabilities in comparing various statistical values. The analysis distinguishes between intra- and inter-ensemble variability as well as variabilities between the probabilistic data set mean of *RhydchprobD* and the deterministic data *RhiresD*. Standard deviation, median and mean values give a first impression of the precipitation occurrence at different spatio-temporal levels (e.g. daily, monthly, seasonal, yearly, study period in combination with *TEZGNR40*, *TEZGNR150* as well as the entire catchment *TEZGNR1000*). Because topographical barriers—information on obstacle function is derived from the elevation—influence the precipitation generation, the subcatchments are classified based on their mean elevation from 1 to 40. This classification allows the comparison of subcatchments with similar characteristics regarding precipitation formation (see *2.2 Precipitation and Runoff Generation*).

5.3.1 Precipitation Event and Period

The static definition of Rivoire et al. (2019) for a wet day does not consider natural preconditions for precipitation formation such as elevation. To extend the definition from literature, the long-term precipitation mean for each subcatchment *TEZGNR40* is included in this research. A precipitation event is registered if 80% of all ensemble runs for a *TEZGNR40* subcatchment on a single day are above the threshold of long-term precipitation mean. With this extended definition, very small precipitation values are excluded. Furthermore, the precipitation occurrence can be differentiated according to its type of formation (convective and stratiform). Based on the definition of precipitation in chapter *2.2 Precipitation and Runoff Generation,* the threshold for a stratiform precipitation event is set to a coverage of at least 80% of the catchment area. If precipitation is classified on a day but covers a smaller area, it is defined as convective precipitation.

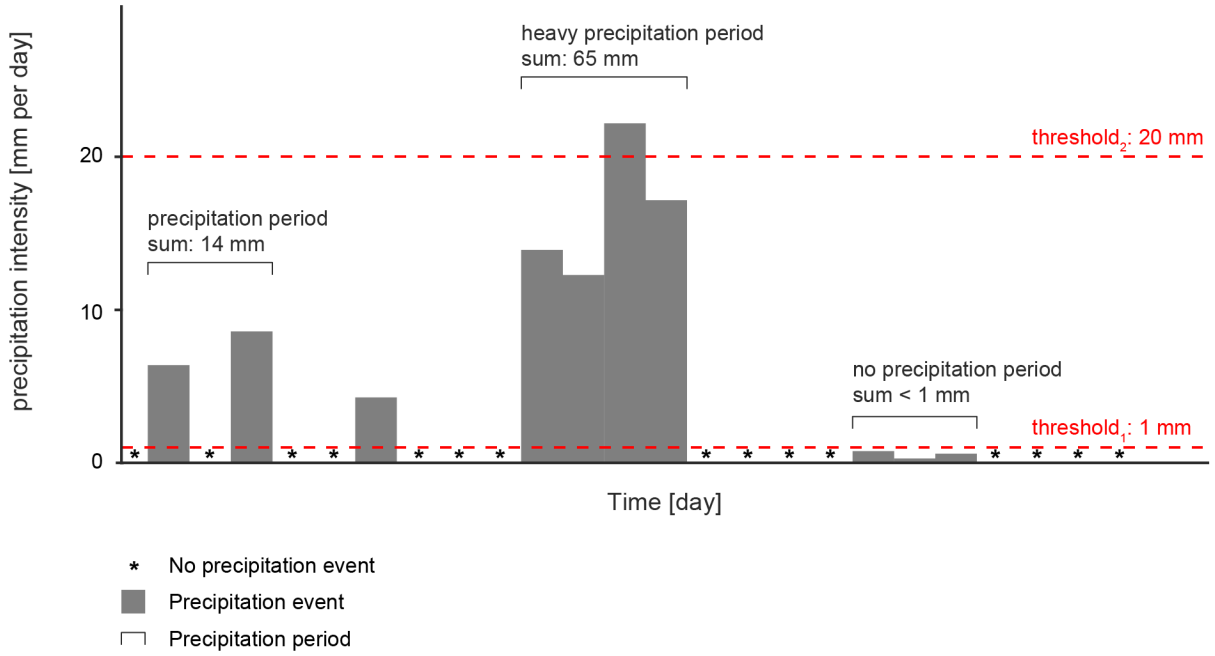

***Figure 16: Terms related to precipitation occurrences**. A precipitation period consists of at least two precipitation events (= daily precipitation occurrences). The threshold$_1$ of 1 mm is included to filter out small, irrelevant precipitation estimations from the analysis. A precipitation period with a precipitation event more intense than 95 % of all precipitation estimations (= threshold$_2$ of 20 mm) during the study period is defined as a heavy precipitation period.*

While the previous definition considers precipitation types on a daily scale, it is important to include longer lasting precipitation periods as well. Especially because the reaction of the runoff to precipitation occurrence is delayed, it is of great interest to analyse the characteristics of precipitation and runoff over several days. Therefore, for each ensemble run and year in the various *MSC*, precipitation periods are defined with regards to the preceding and following day. A day is considered relevant for a precipitation period if the precipitation value is above 1 mm or the preceding and following day meet this condition. With this assumption, a day with less or no precipitation is still accounted to the on-going precipitation period in a larger weather system. After at least two days with no precipitation, a new precipitation period is defined. The inclusion of a dry day has a major influence on the number of precipitation periods. If this parameter is excluded from the definition, the number of precipitation periods increases. At the same time, their duration and their precipitation sums would decrease. In combination with the previously explained spatial relationships of precipitation generation types, it can be assumed that this pattern of change is not the same throughout the catchment: for the lowlands, where stratiform, longer-lasting precipitation periods are more frequently detected (Hendriks 2010), the number of precipitation periods should change less with an adapted definition. For the higher elevation areas, where short-lasting, heavy precipitation events are recurring (Hendriks 2010; Yu et al. 2015), the number of individual precipitation periods is expected to be greater. Because of the temporal accumulation of such convective precipitation occurrence in spring and summer months, the change in the number of precipitation periods will be intensified during this time. Without an adjustment of the threshold parameter, however, short-term, local precipitation events are aggregated into longer precipitation periods. The higher variability in temporal patterns, i.e. number and duration of precipitation periods, compared to the spatial patterns can be explained with the used definition of a

precipitation period. The findings suggest that, despite topographic differences, the catchment *Andelfingen* is not large enough for major, natural spatial differences in precipitation period occurrences. Nevertheless, the estimated total precipitation sum and with it the risk potential during the summer months is not affected by the definition of precipitation periods.

On the one hand, the introduction of precipitation periods makes it possible to compare the performance of the individual ensemble runs (Figure 17). The periods defined with this method per year and ensemble run are characterized by their *duration*, *maximum precipitation sum* and *time to peak*. On the other hand, generating such periods enables the verification of the dependence of runoff on precipitation and the examination of the behaviour of the runoff in the different precipitation periods at a later stage.

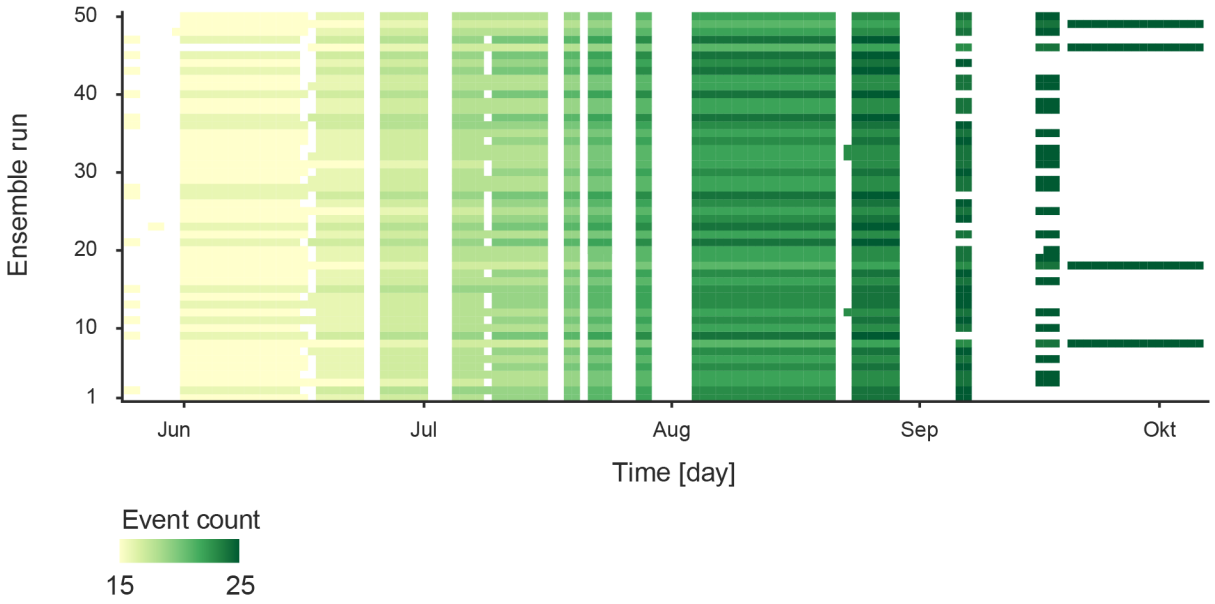

Figure 17: Exemplary excerpt of precipitation period definition for the various ensemble runs. *The precipitation periods #15 to #25 in the year 1999 are illustrated. Differences in the precipitation estimations within the ensemble runs lead to different precipitation period classification and numbering.*

5.3.2 Natural Precipitation Variability

Regardless of the individual ensemble runs, it is interesting to analyse the natural fluctuations and annual cycle of precipitation occurrence (e.g. Bartolini et al. 2009; Gourley & Vieux 2006). Mean precipitation as well as precipitation sum in combination with the absolute and relative variability give an indication of temporal and spatial patterns. While the consideration on distinct monthly, seasonal and yearly time scale reveal inter- and intra-annual patterns, long-term patterns become apparent from combined analysis on the same scales.

As precipitation formation is elevation-dependent (Sikorska & Seibert 2018), the mean elevation of each subcatchment *TEZGNR40* is added to analyse the temporal variations. One of the basic concepts in geographical processes, Tobler's First Law of Geography, describes that «everything is related to everything else, but near things are more related than distant things» (Tobler 1970).

Transferred to precipitation formation, this concept indicates similar patterns of closer subcatchments.

5.3.3 Precipitation Variability within Ensemble Runs

So far, naturally occurring precipitation variabilities have been identified. As a next step, this thesis focus on the examination of intra- and inter-variability and with it on the uncertainty of precipitation values in the probabilistic data. How variabilities or uncertainties are classified is described in the following chapters. Although the data set *RhydchprobD* is provided and validated by *MeteoSwiss* and the applied methodology should return independently distributed results, a general independency verification is carried out before working with the data. To check for independent predictability performance of the ensemble runs, the ensemble run values are compared with the daily probabilistic data set mean value for each subcatchment *TEZGNR40*. A uniform distribution of values below and above the mean value is assumed in case of run-independency.

With the independent distribution of ensemble run values, the pre-condition for meaningful variability analysis is fulfilled. An initial overview of data behaviour is provided by the daily ensemble spread. The standard deviation and coefficient of variation as measures for absolute and relative ensemble spread are used to characterise the intra-ensemble-variability. On the one hand, the precipitation value range can be compared to the ensemble spread. Higher values for the absolute as well as the relative spread are expected in combination with large ranges, whereby the coefficient of the absolute ensemble spread will almost always be higher than the relative because it is not standardised with the amount of precipitation. On the other hand, the comparison of ensemble spread and the ensemble mean precipitation sum per subcatchment *TEZGNR40* enables to find dependencies between variability and precipitation amount. Regarding the spatial location, the variabilities of more intense, large-scale precipitation events are, according to Tobler's First Law of Geography, based on a cost distance (Tobler 1970). Translated into reality, this implies similar variabilities for closer and comparable subcatchments and similarly behaving precipitation events.

5.3.4 Heavy Precipitation Events

Heavy precipitation events are difficult to record due to changeable characteristics and often short generation times, wherefore their estimation accuracy is usually overestimated (Brown et al. 2012). This is why a closer look at the behaviour of the data sets during such events can help to improve an interpretation of such events and to locate spatial variabilities in precipitation occurrences. In this study, heavy precipitation is defined as precipitation events with an intensity above the 95th percentile of all ensemble runs over the entire study period and subcatchments. By including all precipitation estimations, the ensemble spread as well as the interpolation uncertainty is maintained. Topography is a main driver for the occurrence of heavy precipitation events, but the above introduced threshold is a constant for the entire catchment. For this reason, no specific threshold is given for the subcatchments. If 80% of the ensemble runs (40 out of 50) per day and subcatchments *TEZGNR40* are above the 95th percentile, the precipitation occurrence is characterized as a heavy precipitation event.

As described in chapter *2.2.1 Precipitation and Runoff Generation in Alpine Regions,* the type of precipitation event is important for the hydrological response, i.e. the streamflow reaction to precipitation. For large-scale, stratiform events, the precipitation and runoff are accumulated within the catchment and reach the area outlet in large quantities. Based on the definition of precipitation in chapter *5.3.1 Precipitation Event and Period*, a *stratiform heavy precipitation event* is described with a coverage of at least 80% of the catchment area. If heavy precipitation events are classified on a day but extend over a smaller area, they are defined as *convective heavy precipitation events*. In the following, the potential correlation between event type and precipitation sum is analysed specifically for heavy precipitation events.

5.3.5 Aggregation of Meteorological Data

Up to this point, the data have been used in the highest possible resolution across all data sets provided by *MeteoSwiss*. Due to the high variability of precipitation (Lobligeois et al. 2014), an expected approach in hydrological studies would be to always use the best available spatio-temporal resolution (Rauthe et al. 2013). However, with the data accuracy constantly increasing, this assumption is no longer expected and the added value of overly accurate data might become negligible (Girons Lopez & Seibert 2016). With regards to precipitation estimations and meteorological variability, many studies conclude that the quality of the data benefits from a high temporal and spatial resolution of the precipitation occurrence information (e.g. Winchell et al. 1998; Lobligeois et al. 2014; Sikorska & Seibert 2018). To what extent the ensemble data are sensitive to temporal and spatial variabilities will be investigated by aggregation in the sections below. Intrinsically, under idealized conditions of perfect models and precipitation input, an increase of spatio-temporal specificity and accuracy is expected with higher resolution (Rafieeinasab et al. 2015). However, the benefit of improved resolution of precipitation estimates is often limited by errors in precipitation input and hydrological applications, e.g. model parameterization and imprecise initial conditions (Rafieeinasab et al. 2015; Craig et al. 2012; Biggs & Atkinson 2011).

Temporal Aggregation

An important variable for the resolution is the time unit in which the data is available. The precipitation data sets provided by *MeteoSwiss* come with a maximum temporal resolution of one day. On a daily temporal resolution, it is assumed that the effect of short-lasting precipitation on the interpolation uncertainty will be recorded. For a larger time window, however, the ensemble spread is expected to decrease and short but strong precipitation events mitigated. To confirm this assumption and to show the time span over which estimation uncertainties of individual precipitation events are significant, a rolling mean is calculated for different aggregation windows. 2, 3, 7, 14 and 30 days are defined as aggregation windows. Initially, smaller aggregation steps are chosen to observe the reaction time before the time windows are doubled. With the rolling mean approach, the same number of data points is retained, but the values are smoothed over time. The absolute and relative ensemble spread of the aggregated precipitation values are calculated using the approach described in chapter *5.2 Measures of Variability*. In a further step, the additional information of precipitation sum per aggregation window might indicate a dependency between ensemble spread and precipitation sum. One method to quantify the differences of temporal aggregation is the empirical cumulative density function. The *empirical cumulative density function* (*ECDF*) gives for each value x the proportion of the values of the sample that are smaller than or

equal to x (Stahel 2009). Cumulative relative frequency with values between 0 and 1 are represented on the y-axis, whereas the x-axis displays the corresponding ensemble spread. The advantage of using the *ECDF* approach is mainly the ease to interpret results and that it is nonparametric, which makes it independent of normality assumptions (Hoffman et al. 2017). The character is given by the steepness of the density function and the point on the x-axis at which the relative frequency of 1 is reached. Because smaller variability of the precipitation values for smoothed data are assumed, the steepness should increase for a larger aggregation window. In detail this means: (1) the curve should reach the level of 1 faster in the case of larger aggregation values but (2) less values close to an ensemble spread of 0 exist due to the ensemble spread calculation method (number of days with less than 1 mm precipitation that are classified with $CV = 1$ correlates negatively with the aggregation window). (3) Assuming that the *CV* at a cumulative relative frequency of 50% is 0.2, half of the relative ensemble spreads of the examined time period are less or equal to 0.2.

Spatial Aggregation

In addition to the temporal resolution, the spatial extent in which the data are available is important. The accuracy of a precipitation data set not only depends on the temporal but also on the spatial resolution. Precipitation estimations strongly interact between the two variables (Ochoa-Rodriguez et al. 2015). Varying the size of subdivision in the newly calculated data sets illustrates the spatial dependency of precipitation variability and the quality of its analysis. The maximum size of the basin in this research is limited to the catchment area, which is divided into the finer subcatchments *TEZGNR150* and *TREZGNR40*. Reduced to the measurement station density, a small-scale interpolation would assume to estimate and capture precipitation-topography relationships more reliable. However, residual inhomogeneities and sampling limitations by the station network can distort the variability analysis and small scale precipitation trends (Hiebl & Frei 2018). With the spatial aggregation of precipitation values to the various subcatchments, the ensemble spreads increase because of spatial precipitation heterogeneity, whereas the precipitation sums itself are smoothed in using the mean precipitation for each spatial unit. The precipitation sum (in mm per day) is divided by the subcatchment areas of the aggregation level to keep the relative spatial reference. Based on the new spatially aggregated data sets, the same temporal aggregation approach as for the subcatchments *TEZGNR40* is applied. The *ECDF* as a measure for difference again allows to compare the various behaviours. The coarser spatial resolution suggests that the absolute and relative ensemble variability is larger for the aggregation on *TEZGNR150* as well as on catchment scale compared to the original spatial resolution *TEZGNR40*. These assumptions speak for a flatter empirical cumulative density function curve. However, if the spatial and the temporal resolution are combined, it can be assumed that the increased variability with spatial aggregation declines in combination with a temporal aggregation.

Meteorological Data Aggregation for Model Input

Finally, a further spatial aggregation of the meteorological data sets is necessary. The meteorological input data for simulations in the *Hydrologiska Byråns Vattenavdelning (HBV)* model must have the same resolution as the *measurement station subcatchments* (*MSC*) (see chapter *3 Study Site*). For the eight partially overlapping areas as defined by the various stream gauge subcatchments, the daily mean precipitation values are calculated for the *RhiresD* and the *RhydchprobD* data set. The process of calculating the probabilistic data set is distinguished within the individual ensemble runs and the ensemble mean.

5.3.6 Precipitation Variability between Deterministic Data Set and Probabilistic Data Set Mean

Since the deterministic and probabilistic data sets are based on the same precipitation measurements, it is expected that the precipitation values will be relatively similar in their entirety. The main advantage of the probabilistic data set *RhydchprobD* is that it facilitates the analysis of the uncertainty due to the limited sampling of the spatial distribution by the station network. This information is eliminated when calculating the daily ensemble mean per subcatchment *TEZGNR40*. It is therefore assumed that the mean values of the probabilistic data are similar to those of the conventional deterministic approach (hypothesis on RO.1.3). The histogram should correspond to a Gaussian Normal Distribution. The difference between the two data sets is related to the mean precipitation and the ensemble spread to allocate possible relationships. As will be discussed in the following sections, past studies have shown that a conditional bias may exist. Ensemble precipitation forecasts seem to systematically overestimate low observed precipitation and underestimate high precipitation, respectively (Brown et al. 2012). On et al. (2018) additionally specify for a study area in Japan that ensemble data set means underestimate the observed precipitation amount by averaging ensemble members. If these results can be transferred to the comparison between deterministic and probabilistic data based on the same measurement network, it is expected that the deterministic data set outperform the probabilistic data set mean when applied to heavy precipitation events.

5.4 Hydrological Simulations in *HBV*

The research objectives focus on the uncertainties in interpolated precipitation and simulated runoff values. The runoff simulations are based on the meteorological input data. Because of this, chapter *5.4 Hydrological Simulations* describes how the two data sets *RhiresD* and *RhydchprobD* are used as inputs in *HBV* to model runoff and thus creates the possibility to investigate the meteorological-hydrological response relation. In the first part, the semi-distributed model *HBV* with its functionality and parameters is explained. A semi-distributed model allows to divide simulations into different elevation and vegetation zones as well as into different subcatchments (Seibert & Vis 2012). On the one hand, this semi-distributed approach allows for better improvements in model performance, which is dependent on spatial precipitation estimation in the input data and the model parameters (Lobligeois et al. 2014). On the other hand, variability of precipitation patterns and magnitudes can be identified and allocated to different origins of precipitation generation (i.e. convective and stratiform precipitation generation). This advantage of semi-distributed simulations is used in the following chapter *5.5 Hydrological Data Analysis* for hydrological variability analysis, after the discussion of the different calibration and validation alternatives applied in this research (section *5.4.2*).

5.4.1 *HBV model*

The semi-distributed precipitation-runoff model *HBV*, introduced by Bergström in 1976, has been continuously developed and is an internationally established application for runoff modelling (Bergström 1976; Bergström 1990; Bergström 1992). The model in the version *HBV Light* with its twenty parameters builds on the original version and is adapted for research and educational usage (Seibert & Vis 2012). Runoff simulations, usually on daily time steps, are calculated using time

series of precipitation, temperature, observed runoff and the monthly long-term potential evaporation as input (Seibert & Vis 2012).

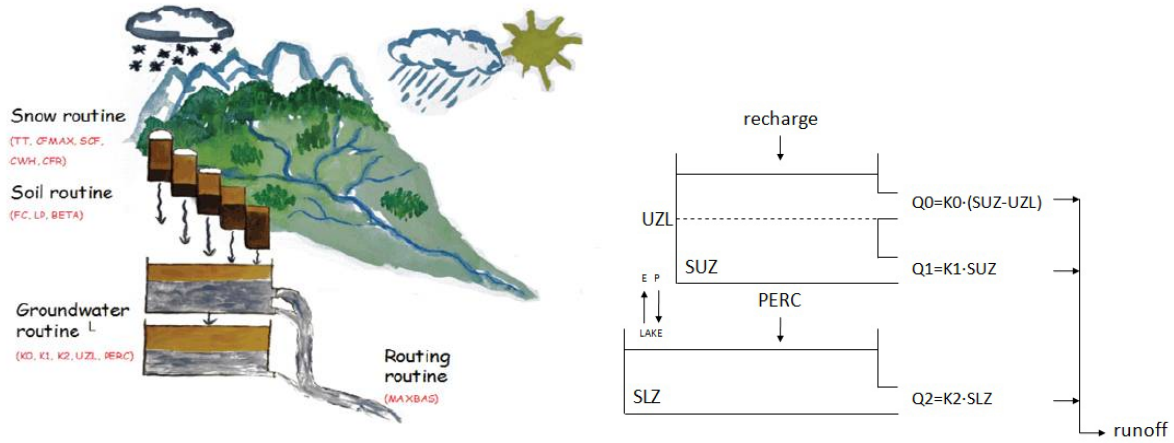

Figure 18: Modules of HBV model. *The abbreviations of the parameters are explained below in Table 4 (Illustration by Seibert & Vis 2012).*

The model is made up of different modules. The modules are as follows: the *snow routine* (snow accumulation, snow melt and melt water retention), the *soil moisture routine* (groundwater recharge and actual evaporation), the *response or groundwater routine* (runoff as a function of catchment storage) and the *routing routine* (runoff routing depending on triangular weighting function). The model structure allows different model types, which differ in the computation method of the routines. As there are no glaciers in the area *Andelfingen*, the standard version is used, in which the snow and soil routines are performed separately for each elevation zone (Seibert & Vis 2012). The above-mentioned modules are connected by the runoff which is composed of three contributions: (1) *additional runoff (Q0)*, which is generated when the *water hold capacity (UZL)* in the *upper soil zone (SUZ)* is exceeded; (2) a *steady runoff (Q1)* partially released and transferred into the lower soil zones by the *SUZ*; and *runoff (Q3)* which is the released and evaporated water in the lower soil zones. Several control values influence the runoff processes within the modules. With a defined *threshold temperature (TT)*, precipitation is distinguished in either rain or snow during simulation. Because temperature and precipitation are elevation-dependent, different elevation zones are implemented for which the values are adjusted with the two parameters *PCALT* [percentage decrease of precipitation per 100 m] and *TCALT* [temperature decrease per 100 m]. For further information on model structure and parameters, see Seibert & Vis (2012) and *HBV*-Help (Version 4.0.0.23; access in 2020). The *HBV* model requires additional inputs, namely daily air temperature, evaporation rate and elevation classes. These inputs and their processing are described in the following.

Daily Air Temperature

In order to distinguish precipitation between rain and snow, the mean daily air temperature provided in the data set *TabsD* by *MeteoSwiss* is used (MeteoSwiss 2020b). Analogue to the preparation of the precipitation data set, the air temperature data are pre-processed so that the data set has the same spatial resolution as the measurement station catchments. Together with the precipitation and observed runoff information, the thus compiled environmental variable data set (ptq-data set) is completed.

Evaporation Rate

Evaporation reduces the amount of water, which is why the information about the potential evapotranspiration (*PET*) in each measurement station subcatchment is considered in the simulations. A simple and efficient method for calculating the *PET* is provided by Oudin et al. (2005). Within their study, they identified that the atmospheric variables temperature and radiation tend to be the most relevant to compute an accurate potential evapotranspiration estimation for precipitation-runoff modelling. The biggest advantage of this method is that it requires only an average air temperature and the latitude as inputs. The average air temperature can be derived from the long-term, monthly averages. With this approach, the following calculation is implemented:

$$PET = \frac{Re}{\lambda\rho} * \frac{Ta+5}{100} \text{ if } T_a + 5 > 0, \text{ otherwise } PET = 0$$

PET = potential evpotransporation [mm per day]
R_e = extraterrestrial radiation [MJ per m^2 per day]
λ = latent heat flux [MJ per kg]
ρ = density of water [kg per m^3]
T_a = mean daily air temperature [° C], derived from long-term average

The result is the long-term, monthly potential evapotranspiration for each measurement station subcatchment. Compared to the values used in Girons & Seibert (2016), only small differences in decimal places can be identified and are therefore negligible. These differences are most likely due to different time periods (here 1961–2019; Girons & Seibert (2016) 2003–2010) and calculation methods for average temperatures.

Elevation Classes

The model supports the classification of the catchment area into different elevation bands for a more realistic representation of hydrological processes. Such a differentiation is recommended if elevation differences are expected to affect temperatures within in the catchment. Based on the *dhm25* from swisstopo (2005), the elevation bands of the equal percentile distribution are used to define ten elevation zones per measurement station subcatchment. The mean elevations of these bands are used as the input variables. Vegetation zones were not taken into account in this study for simplicity reasons (recommended by Seibert & Vis 2012).

5.4.2 HBV Model Calibration

Based on the processed data and the functionalities of the above discussed model modules (see *5.4.1 HBV Model*), the HBV model has been calibrated. Grouley & Vieux (2005) emphasize that it is important to address sensitive model parameters and to reduce the value range to an appropriate extent. Since the deterministic approach is the more established precipitation data type, the *genetic calibration algorithm* (*GAP*) is run for the *RhiresD* data set with a warm-up period of three years (1974-10-01 to 1977-09-30) followed by a 17-year-long calibration period (1977-10-01 to 1995-09-30). The warm-up period is needed to get appropriate initial values of the different state variables at the beginning of the simulation period. This calibration step results in ten equally likely parameter sets which will later be used for the model validation. It is an important prerequisite that the warm-up as well as the calibration period covers at least one annual hydrological cycle. Otherwise, the state variables cannot appropriately develop from standard initial values to their appropriate values

according to meteorological conditions and parameter values (Seibert & Vis 2012) and neither can the model acquire the knowledge of altering flow regime behaviours (Sikorska & Seibert 2018). According to Wu et al. (2011) and Hamill et al. (2008), an extended calibration time improves the forecast skill. The calibration and validation period of equal length enables the time periods to be reversed, i.e. calibration period 1998-10-01 to 2016-09-30 and validation period 1977-10-01 to 1995-09-30. If this inversion returns a more or less identical result as in the original simulation, the model is not dependent on the time period of the input data and is therefore well calibrated. The ideas of this approach are further explained in section *5.4.8 Model Calibration and Validation Alternatives*.

HBV offers various possibilities for (automatic) model calibration. In this work, the *GAP* method is used. The *GAP* searches for optimized parameter sets through an evolution of parameter sets. During the evolution progress, the parameters are selected and recombined resulting in the optimized parameter sets selected on its model efficiency (R_{eff}). The initial, random parameter set lies within the user defined parameter boundaries listed in Table 4. Even though parameter uncertainty can be reduced, better results in parameter sets might lead to equifinality (Bormann & Diekkrüger 2003). This problem is counteracted by calculating ten independent calibration rounds. From the initial parameter set population, 3 500 times two parameter sets are used to generate a new one. The selection of the parameter sets is random, although the likelihood increases for sets with a better fitness (i.e. R_{eff}). The evolutionary process results in ten equally reliable parameter sets whose parameters are used for the validation (Seibert & Vis 2012). Using the same initial parameterization for model calibration for all subcatchments and simulation alternatives, the result of the semi-distributed precipitation-runoff simulations are comparable with measures such as *peak flow*, *time to peak* and *runoff volume*.

The following input files and parameterisation are used for the *GAP*-optimization:

- **ptq**: daily precipitation, temperature and observed runoff from *RhiresD*
- **simulation.xml** (model settings): start of warming up period 1974-10-01, start of simulation period 1977-10-01, end of simulation period 1995-09-30
- **clarea.xml**: mean elevation of elevation zones for each measurement station subcatchment
- **EVAP.txt**: monthly long-term potential evapotranspiration for each measurement station subcatchment
- **GAP_parameters.xml** (model parameters):

Table 4: Parameters of the HBV model. *A parameter range (minimum and maximum) is defined for the model calibration.*

Parameter	Explanation	Minimum	Maximum	Unit
Vegetation Zone parameters: snow and soil routine				
TT	Threshold temperature	−1.5	2.5	°C
CFMAX	Degree-day factor	1	10	$mm°C^{-1}d^{-1}$
SP	Seasonal variability in degree-Δt factor	1	1	–
SCF / SFCF	Snowfall correction factor	0.4	1	–
CWH	Water holding capacity	0	0.2	–
CFR	Refreezing coefficient	0	0.1	–
FC	Maximum of SM (storage in soil box)	50	500	mm
LP	Threshold for reduction of evaporation (SM/FC)	0.3	1	–
BETA	Shape coefficient	1	6	–
CET	Correction factor for potential evaporation		0.03	–
Catchment parameters: Response routine				
K0	Recession coefficient 0	0.1	0.5	d^{-1}
K1	Recession coefficient (1; upper box)	0.01	0.4	d^{-1}
K2	Recession coefficient (2; lower box)	0.001	0.15	d^{-1}
PERC	Maximal flow from upper to lower box	0	3	$mm\ d^{-1}$
MAXBAS	Routing, length of weighting function	1	7	d
UZL	Threshold parameter	0	70	mm
PCALT	Change of precipitation with elevation	10	10	%/100m
TCALT	Change of temperature with elevation	0.6	0.6	%/100m
Pelev	Elevation of precipitation data in ptq file	Dep. on catchment	Dep. on catchment	m
Telev	Elevation of temperature data in ptq file	Dep. on catchment	Dep. on catchment	m

Table 5: HBV Model settings for the calibration process.

Model settings	**Number**
Number of Runs	3500
Number of Powell Runs	0
Number of Parameter Sets	50
Number of Populations	1
Number of Calibrations	10

5.4.3 HBV Model Validation

Because of equifinality, the model is validated with ten equally likely parameter sets as a result of the model calibration for all probabilistic ensemble runs as well as the deterministic data set within the period between 1998-10-01 and 2016-09-30 (17 years validation = 50 % of the used data). The average of each of the ten single runs per input data set is used as a simulation result. The goodness of fit (= performance of each validation) is represented by various performance measures, among others the *model efficiency*, the *Kling-Gupta efficiency* (parametric and non-parametric), the *volume error* and the *Spearman Rank correlation coefficient* (Table 6).

Table 6: Model performance for each MSC. *The mean accuracy of the simulated runoff values is determined using the following performance measures: Model efficiency, Kling-Gupta efficiency (parametric) Kling-Gupta efficiency (non-parametric), Volume error and Spearman Rank.*

Measurement station subcatchment (FOEN code and name)	Mean Model efficiency	Mean Kling-Gupta efficiency (parametric)	Mean Kling-Gupta efficiency (non-parametric)	Mean volume error	Mean Spearman Rank
2044; *Andelfingen*	0.67	0.56	0.62	0.67	0.82
2112; Appenzell	0.34	0.24	0.37	0.44	0.73
2126; Wängi	0.79	0.82	0.84	0.93	0.85
2181; Halden	0.53	0.38	0.48	0.54	0.78
2303; Jonschwil	0.45	0.31	0.42	0.49	0.75
2374; Mogelsberg	0.67	0.56	0.64	0.71	0.79
2386; Frauenfeld	0.78	0.84	0.85	0.99	0.85
2468; St.Gallen	0.57	0.42	0.51	0.58	0.77

5.4.4 HBV Model Calibration and Validation Alternatives

Some of the results from the standard simulation do not fully meet expectations. This led to the calculation of two further alternatives of runoff simulations: (1) *Version B* the swapping of the time periods for calibration and validation allows a statement about the model independence on the used input data. Consequently, the time period 1998-10-01 to 2016-09-30 is used for calibration and 1977-10-01 to 1995-09-30 for validation. All other model parameters remain unchanged. (2) *Version C* So far, the model has been calibrated with the deterministic data set before the runoff has been simulated for the probabilistic data set. Contrary to expectations, relatively small runoff variability can be identified in the resulting ensemble realisations. Whether this smoothing of the ensemble spread is a (direct) result of the model calibration has to be verified by a modified calibration. In this alternative, the model is calibrated for all ensemble runs. As with the regular method, the ten best parameter sets per ensemble run are determined. For each ensemble run, ten parameter sets result in a total of 500 parameter sets, which can ultimately be used for the validation of the deterministic precipitation values.

5.5 Hydrological Data Analysis

The results of the semi-distributed precipitation-runoff simulations not only enable the identification of variability of precipitation patterns and magnitudes but also the allocation to different origins of precipitation generation (i.e. convective and stratiform precipitation generation). For this reason, three aspects in connection with simulations and runoff are considered in this section, namely (1) the validation of model simulations with runoff measurements (observed runoff) at each subcatchment outlet, (2) the examination of temporal, spatial and scale variability in runoff as in the precipitation pattern analysis, and (3) the analysis of the 50 ensemble simulations compared to the ensemble mean simulations and the deterministic simulation. In particular, the uncertainty of precipitation and runoff simulations during the five days preceding a runoff peak event is examined. The comparisons drawn in (3) enable statements about a possible accuracy increase of model simulations with ensemble data. Special attention must be paid to precipitation in the form of snow and how it influences the model performance.

5.5.1 Runoff Deviation

To start the hydrological analysis, the deviation of observed and simulated runoff values is quantified. The performance measures listed in chapter *5.4.3 Model Validation*, which are all smaller than one (one is equal to 100% model accuracy), already indicate that the simulated runoff differs from the observed measurements. In calculating the difference between observed and simulated runoff values, the differences can be quantified more precisely.

The analysis on a daily granularity enables the determination of short-term, major changes in runoff. However, it is possible that the precipitation values averaged for a catchment area are too imprecise for this temporal resolution, and thus imprecision in the runoff simulation should be expected. An event-based consideration of the differences between observed and simulated runoff values intercepts outliers and enables the description of the interplay of processes over several days. Therefore, four different event measures are used to compare observed and simulated runoff data: (1) *precipitation event duration* is defined by the time span between the first and last day of a precipitation period; (2) *time to peak* describes the time of the first precipitation day to the runoff peak which is (3) the maximum runoff (*runoff* peak) of a precipitation period; (4) the last parameter is the *precipitation sum* of a precipitation period. The comparison of these parameters is expected to show the extent to which the model is able to capture longer lasting processes in relation to daily runoff values.

5.5.2 Variability of Daily Ensemble Run Simulations

A major research objective in this thesis deals with the performance of the various ensemble runs in hydrological simulations in *HBV*. To answer this question, the *standard deviation* (absolute variability) and *coefficient of variation* (relative variability) of the simulated runoff values per day and measurement station subcatchment are calculated. Whether the precipitation and runoff variability coincide over time and space is both in numbers and visually verified. As the days prior to a runoff peak event are mainly responsible for the different runoff behaviour, the variability analysis focuses on the characteristics of the five days prior to a runoff peak and the runoff peak day itself. Further details on this event detection are explained in the following chapter *5.5.3 Variability of Ensemble Runs within 5 Days prior to Runoff Peak*. For all those peak events, the absolute precipitation as well as runoff ensemble spread per day and measurement station subcatchment (*MSC)* are assumed to increase with higher precipitation sum. This assumption is based on the mathematical calculation of the standard deviation which does not standardise the spread value by the precipitation sum. To overcome this bias, the relative ensemble spread is also provided.

5.5.3 Variability of *Ensemble Runs* within 5 Days prior to Runoff Peak

The previous analysis focused on differences and variability including all ensemble runs and the entire validation period of about 17 years. However, the ability to capture uncertainties in model simulation over such a large data amount—one of the main advantages of probabilistic data—is quite low. These interesting but infrequent events are likely to be masked out by the large amount of data and the calculation of various averages. Therefore, and because large amounts of runoff accumulated prior to such events pose great risks, the five days prior to a runoff peak and the peak day itself are examined more closely. A special focus is given to the runoff during heavy

precipitation events. For this objective, runoff peaks must be identified. The runoff peaks are, for comparative purposes, defined in the probabilistic data set mean, to which the ensemble run data are attached in a later step. A simulated runoff value is classified as a peak if it meets all of the three following conditions: (1) the value is the highest runoff value in a time window of six days; (2) the precipitation three days prior to the considered day exceeds 1 mm per day; and (3) the simulated runoff is higher than the third percentile of all simulated runoff values (= 2.1725 mm per day). The first and second condition are set to find noticeable changes in the runoff because of precipitation. To ignore very small runoff fluctuations for peak classification which are less important for minimising flood risks, environmental planning, etc., the last condition is introduced. For each measurement station catchment, the five days prior to a runoff peak in the ensemble data set mean are extracted. Because the day of a runoff peak in the individual ensemble runs does not always coincide with the dates in the ensemble data set mean, a moving window of three days (one day prior/after the runoff peak in ensemble mean) is used to select the corresponding runoff peak within each ensemble run. The resulting data includes precipitation and simulated runoff values for each ensemble run and the ensemble mean five days prior as well as on the runoff peak days.

The data set is used to derive a number of indicators, namely (1) *the absolute and relative precipitation and runoff ensemble spread,* (2) *the runoff peak*, (3) *the precipitation sum*, (4) *the ratio of runoff peak to precipitation sum* and (5) *the runoff range*. All of them quantify the different behaviour of precipitation and runoff prior to a (2) *runoff peak* event. First, the respective performances of the ensemble runs are described with the (1) absolute ensemble spread (*standard deviation*) and relative ensemble spread (*coefficient of variation*). It is expected that the absolute spread of *(3) precipitation sum* and runoff peak positively correlate with the increasing precipitation sum per runoff peak event. The effect of large numbers is mainly responsible for this trend, which is why—in the same way as before—the relative ensemble spread is used to eliminate this bias in the analysis. The difference between the ensemble spreads for either precipitation and runoff give indication to the uncertainty and variability of the computed values. In order to consider not only the differences on the day of the runoff peak and the precipitation sum responsible for this, the range of precipitation and runoff values in the 5 days prior to a runoff peak event are calculated for each ensemble run and examined as a function of the precipitation sum. Second, (4) *the ratio of runoff peak to precipitation sum* is calculated as an approximation of the *runoff coefficient* to describe the character of runoff peak events. This simplified calculation is based on the runoff coefficient defined by Hendriks (2010). It uses the runoff coefficient on a storm basis defined as quickflow volume [mm] as a percentage of the precipitation volume [mm]. The runoff coefficient is expected to be higher for runoff peak events with very small precipitation sums and runoff peaks. Such observations are most likely accompanied by the occurrence of snow fall during the winter months rather than by heavy precipitation events which go with an increase in runoff volume. This expectation contrasts with to those of the runoff peak flows and precipitation sum. To emphasise the observation, the behaviour of the runoff peak and (5) *runoff range* depending on the precipitation sum during the runoff peak events illustrate the relationships between meteorological and hydrological processes. With this detailed analysis, the variability of the ensemble runs is quantified. The 10th and 90th percentiles show how many events are responsible for this very small and large variability, respectively.

The indicators introduced above represent the behaviour of the runoff peak events in its entirety. As outlined in chapter *5.3.4 Heavy Precipitation Events*, heavy precipitation events are particularly noteworthy. With an interest in the impact of such heavy precipitation events on runoff, for

example from the perspective of natural hazard management, the behaviour of runoff during these days is examined more closely. This approach builds on the definition of Rafieeinasab et al. (2015), which also determines the runoff peak events depending on precipitation thresholds per subcatchment and focuses on the response of runoff peaks to precipitation event. The heavy precipitation definition in chapter *5.3.4 Heavy Precipitation Events* distinguishes between regional, convective and large-scale, stratiform events. Since the spatial resolution in runoff modelling is lower and features a higher variability than in the prior meteorological analysis, the evaluation of runoff during heavy precipitation events is limited to stratiform events. The runoff data of all ensemble runs as well as for the ensemble mean within a timeframe of two days prior to and three days after the heavy precipitation record are selected for further analysis. If the time lag from a precipitation event to the change in runoff is measured, a time lag of two days on average can be determined. In order to also monitor the reaction of the runoff after the peak flow, three days after the peak are included. The analysis can either focus on a single event or the different behaviour of several events in terms of precipitation and runoff simulation. On an event basis, the performance of the ensemble runs during one event are considered. It becomes apparent how great the simulation uncertainty is and how the uncertainty differs within the days investigated. In contrast, the different characters of runoff peak events are described, showing their course in the probabilistic data set mean.

5.5.4 Differences of *RhiresD* and *RhydchprobD* Simulations

So far, the research work mostly focuses on the performance of the probabilistic data set. As a last aspect in this thesis (RO.3.3), however, the difference of the established deterministic and the probabilistic data set mean with regard to simulations of hydrological processes are examined. According to the expectations in chapter *5.3.6 Precipitation Variability between Deterministic Data Set and Probabilistic Data Set Mean*, the difference between the runoff simulations based on the deterministic (*RhiresD)* and the probabilistic data set (*RhydchprobD probabilistic data set mean)* should be negligible. Nevertheless, the simulated runoff difference of the two data sets is quantified. This comparison gives a first impression of the simulation performance. Nevertheless, the absolute difference between the two data sets gives no indication of how well simulations approximate the observed values. For this reason, two further indicators for the data set comparison are calculated, namely (1) the deviation of either simulated values to the observed runoff and (2) the quantification of the frequencies each data type perform better. The deviation from observed runoff is used as a measure for simulation performance, i.e. the larger the deviation of a simulated value from the observed value, the worse the model performs. Combined with the information of precipitation sum—the precipitation is mainly responsible for runoff changes—the visual analysis of runoff time series indicates whether the performance of the data types depends on the amount of precipitation.

6 Results

As outlined in the methodology (chapter *5 Methods*), the first main section «meteorology» (*6.1 Meteorological Data Analysis*) is followed by a minor section featuring the description of the model performance (*6.2 Hydrological Simulations in HVB*) leading into the second main section «hydrology» (*6.3 Hydrological Data Analysis*). In both main sections, the intra-ensemble variability (RO.1.1 and RO.3.1) within the probabilistic data set are quantified by the measures described in the previous chapter. As events of great interest, the behaviour of the variability during heavy precipitation events will be examined more closely (RO.1.2 and RO.3.2). The RO.1.3 and RO.3.3 aim to describe the coincidence of the deterministic and probabilistic data sets. Based on all these results, statements on the influence of the new data set on hydrological simulations in *HBV* can later be formulated (RO.2).

6.1 Meteorological Data Analysis

The first main section focuses on the natural fluctuation of precipitation patterns, as well as on the uncertainty involved in estimating precipitation. Chapter *6.1.1* gives an overview of the natural precipitation occurrence in the catchment *Andelfingen*. Based on the knowledge of the natural variability, the following chapters *6.1.2–6.1.5* deal with the variability in the form of methdological uncertainties. A distinction is made between daily precipitation uncertainties, the behaviour during heavy precipitation events, the dependence of interpolation accuracy on spatio-temporal resolution (scale), and the data set variabilities between the *RhiresD* and *RhydchprobD*.

6.1.1 Natural Precipitation Variability

At the beginning of this thesis, it was pointed out that variability in relation to precipitation can be understood either as the natural pattern of precipitation occurrence or the uncertainty of precipitation sum estimation. To later distinguish between natural and methodological variability in the results, the natural meteorological variations of the study area *Andelfingen* are described. For this purpose, the variability of precipitation is considered on different temporal units: (1) daily, (2) precipitation period, (3) longer timeframes such as months, seasons and years. The variability analysis is related to different influencing factors and parameters, namely the *type of precipitation generation*, the *duration* of a precipitation period, the *precipitation sum* or the *long-term variability* quantified using the standard deviation.

(1) The topography of the catchment combined with the type of precipitation generation (convective or stratiform) explains the main pattern precipitation occurrence. While convective precipitation occurs with a moderate intensity but at shorter intervals in higher altitudes (long-term mean ~4.9 mm per day in subcatchment *TEZGNR40* #19 to #40), such spontaneous precipitation caused by raising humid air is less frequent and intense in lowlands (long-term mean ~3.7 mm per day in subcatchment *TEZGNR40* #1 to #18). Such spatial differences are also visible for stratiform precipitation with an average precipitation sum of 9.3 mm per day for the lowlands and

13 mm per day for mountainous areas, respectively (Figure 19). Those results clearly reflect a strong spatial correlation for natural precipitation occurrence and intensity.

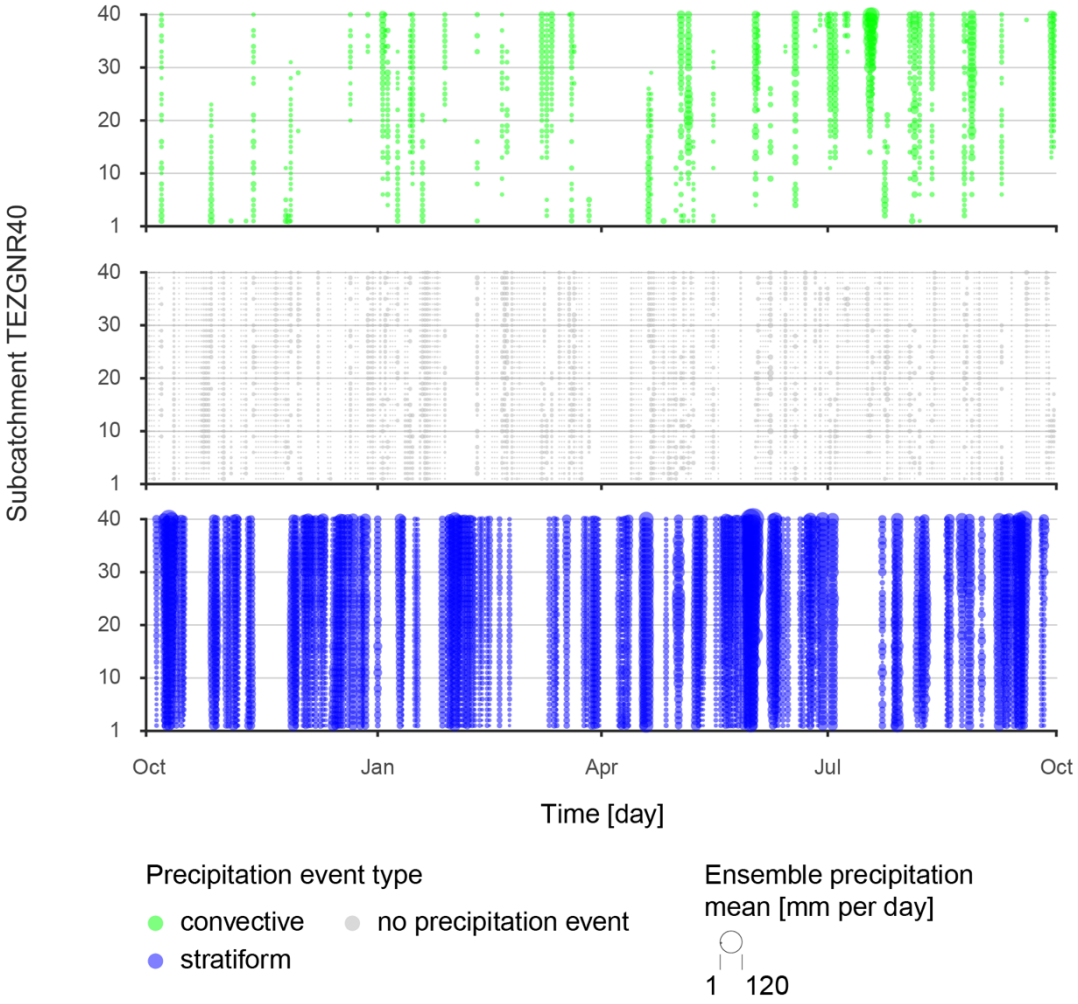

Figure 19: Precipitation events divided according to their type of origin: «convective» or «stratiform». *Precipitation events with a precipitation sum less than 1 mm are defined as «no precipitation event». The symbol size of a precipitation events is depending on the precipitation sum found in the data set mean.*

Beside the location, the season is an important driver for precipitation generation types. These findings result in the following spatio-temporal patterns: Stratiform precipitation appears more frequently and with a higher intensity in the summer months May to August in all subcatchments *TEZGNR40* (Figure 20). For convective precipitation, a more variable spatio-temporal correlation can be determined. The clear seasonal difference in intensity and occurrence for convective precipitation is most noticeable in the high mountainous subcatchments *TEZGNR40* (#30 to #40 with average elevation > 1 000 m a.s.l.) during July and August.

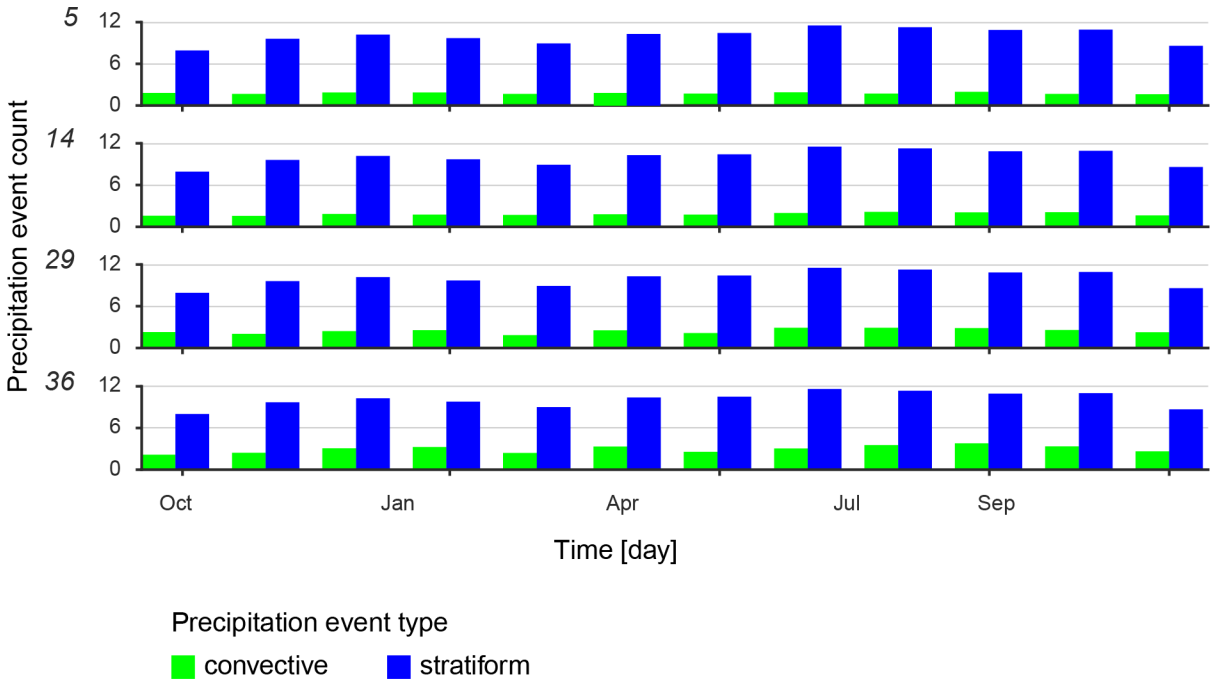

Figure 20: Average number of precipitation events per month divided according to their type of origin: «convective» or «stratiform». *With the exemplary subcatchments TEZGNR40 #5, #14, #29 and #36 the seasonal patterns of precipitation events are illustrated.*

(2) Precipitation occurrences, which constitute a natural phenomenon, are not linked to the classification of a day. It is therefore important to look at the precipitation pattern over a longer time period. According to the methodology described in chapter *5.3.1 Precipitation Event and Period*, precipitation periods are defined as precipitation events lasting several days with an intensity of more than 1 mm per day. As seen in Figure 21, exemplary for the entire catchment *Andelfingen* in summer 1999, the definition of individual precipitation periods differs between ensemble runs. The differences are attributed to the distinct ensemble run values and the threshold value for a precipitation-relevant day. Over a hydrological year, however, neither the period count of precipitation periods of the individual ensemble runs nor the average period count of such events in the different measurement station catchments (*MSC)* differ significantly (Figure 21). Because the precipitation periods are later used in the runoff analysis, the precipitation variability is shown for the *MSCs* and not the subcatchments *TEZGNR40*.

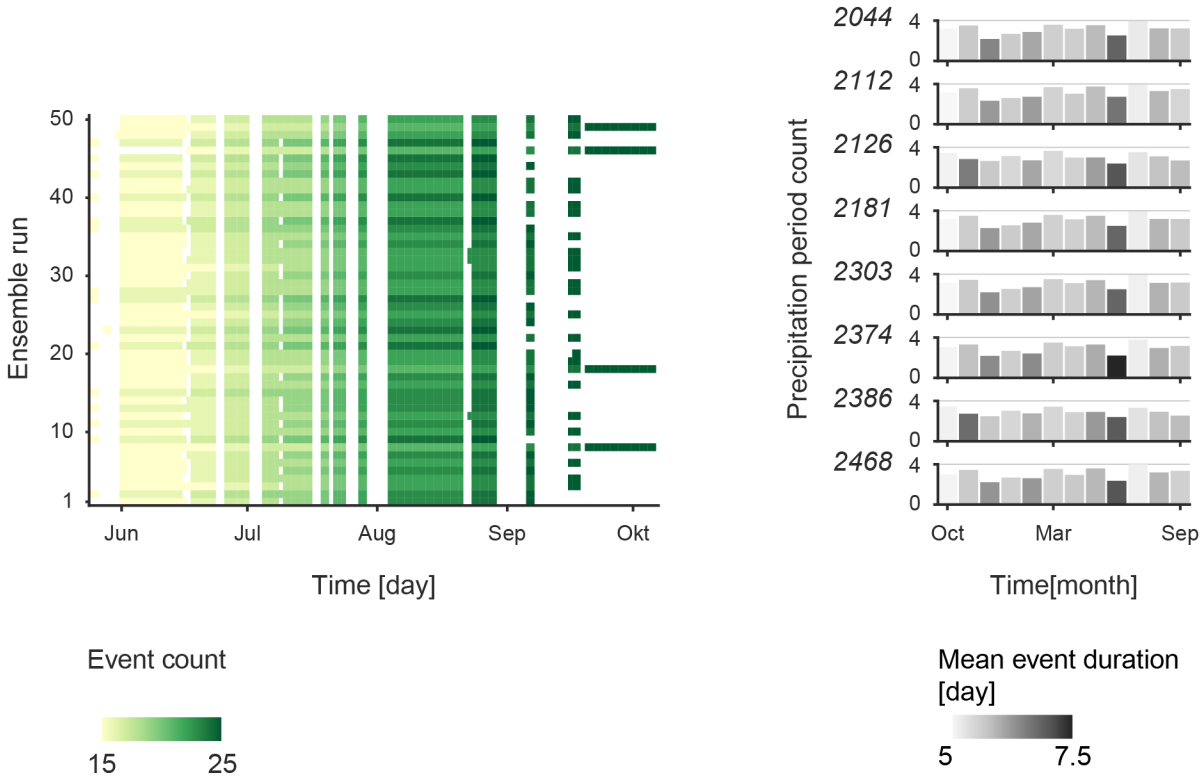

Figure 21: Precipitation period definition per ensemble run (left) and the precipitation period count per month and MSC (right). *The average period count and mean duration of precipitation periods depends on the seasonality.*

Contrary to the weak period count dependency on ensemble runs and space, clear seasonal patterns can be seen in the period count of precipitation periods. The increased occurrence of stratiform precipitation in summer months leads to longer precipitation periods, especially in June (Figure 21). The long-term average in June is 2.56 periods per month, with an average event duration of 10.4 days. The precipitation periods last longest in the *MSC 2374*. This spatial occurrence is certainly linked to the topography. The steep flanks of the *Säntis* mountain begin in this area which force the humid air mass to rise. In contrast, August is the month with the highest average period count of 4.06 periods in all *MSC*, but these are clearly of shorter duration (average 3.77 days). Figure 21 shows that in the long-term average, the natural variability of precipitation periods is more significant for temporal than for spatial differences.

Based on the periods of precipitation, it is determined whether intra-annual patterns emerge and how the ensemble runs vary. Therefore, the natural, annual variability in precipitation periods is shown for the ensemble runs (Figure 22) as well as depending on the duration and mean precipitation sum per period (Figure 23). Differentiating the precipitation periods per hydrological year makes it possible to visualise natural fluctuations in precipitation occurrence. Although the annual precipitation sum of the example years 1999, 2003 and 2013 differ considerably (1 691, 1 055 and 1 341 mm per year, respectively), only small differences in the period count of precipitation periods (between 30 to 40 periods per *MSC* and year) can be detected. From this observation it can be concluded that the number of rain events is relatively constant over the years, but their duration and intensity vary greatly. These irregularities are responsible for the annual

precipitation sums. The data indicates that the amount of precipitation per event depends on the duration of the event. In 1999, one of the wettest years in the study period (1691 mm per year), precipitation periods are above average in duration and intensity. In the extraordinary dry year 2003 (1055 mm per year), however, these precipitation periods are characterised by short durations and low intensities. A trend analysis of the change in precipitation is deliberately omitted, as this is not the focus of this thesis and requires further research (reference to studies on climate change e.g. EEA 2009). Inter-annual patterns regarding the event duration and intensity within the ensemble runs or various *MSC* cannot be observed. Only the small-size *MSC 2374* shows, as already in the long-term monthly average, a weak conspicuousness. Although not in the period count, most years record the highest values in terms of duration and intensity in this area (Figure 22 and 23). This annual balance supports the previous assumption that the precipitation periods for the ensemble runs are not the same, but that there are no major inter-annually differences.

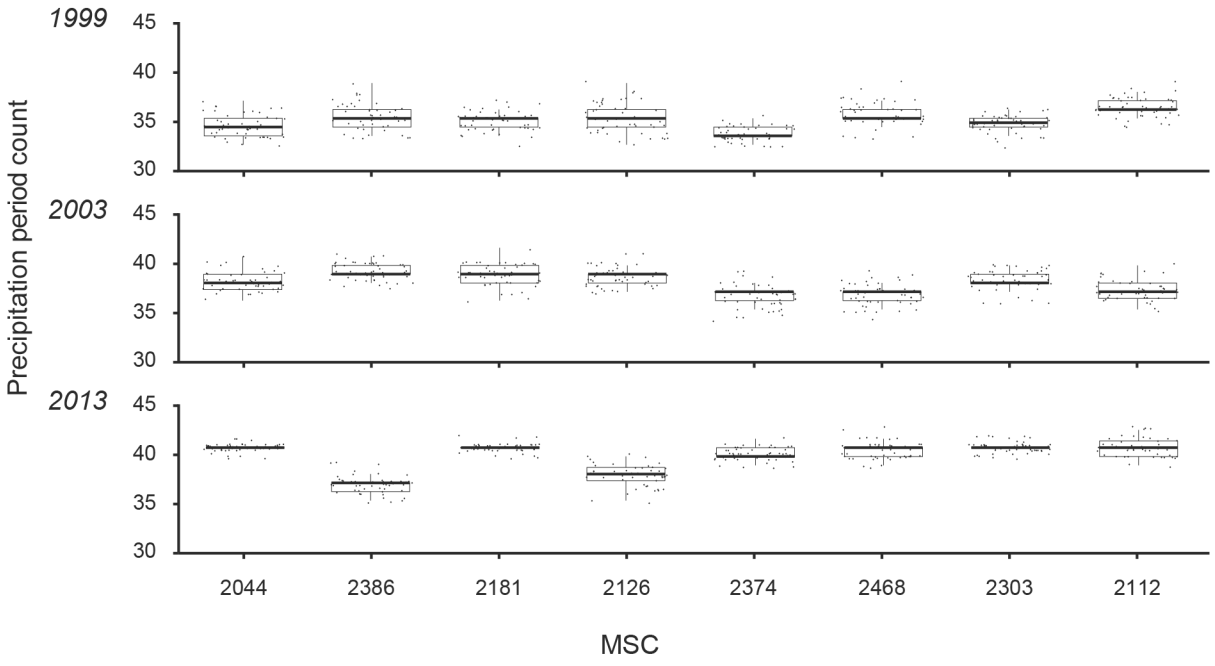

Figure 22: Precipitation period count of each ensemble run per MSC for the hydrological years 1999, 2003 and 2013. *Because of the precipitation period definition, the count of such periods varies across the ensemble runs.*

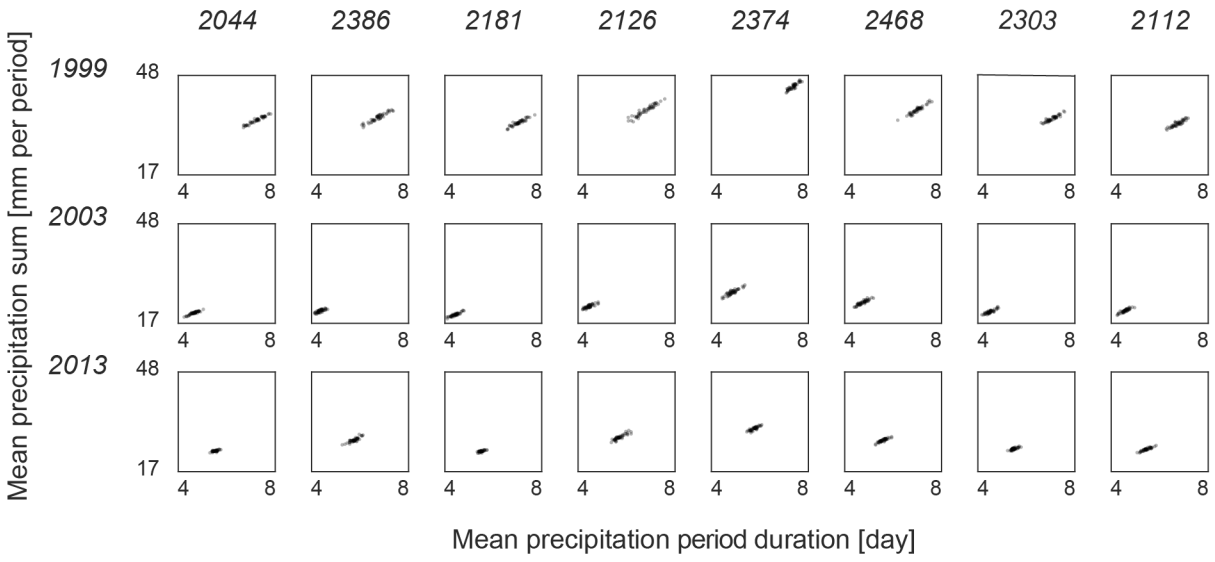

Figure 23: Precipitation periods per MSC depending on their duration and precipitation sum for the hydrological years 1999, 2003 and 2013. *The figure illustrates the positive correlation of precipitation sum and duration of precipitation periods.*

(3) Finally, on the subject of precipitation occurrences in the study area, the natural variability on larger timeframe is analysed. The standard deviation of the precipitation values of the individual ensemble runs is considered as a measure of variability for the subcatchments *TEZGNR40*. It is assumed that larger weather differences are reflected in a larger interpolation uncertainty and consequently in a larger standard deviation within the considered time-space unit. In the annual overview, the more saturated colours of the subcatchments *TEZGNR40* #1 to #18 show that the interpolated ensemble values vary slightly less in the lowlands than in the mountainous areas (Figure 24). Over the years, the variability fluctuates in an irregular pattern (from 2.4 to 12.3 mm per day). On the monthly and seasonal scale, the spatial and temporal differences become more clearly visible: the variability of the ensemble runs increases with the higher precipitation volume in the summer months. The positive correlation between variability and altitude is also strengthened. The extent to which the probabilistic precipitation uncertainty follows a spatial or temporal pattern will be discussed in the next sections.

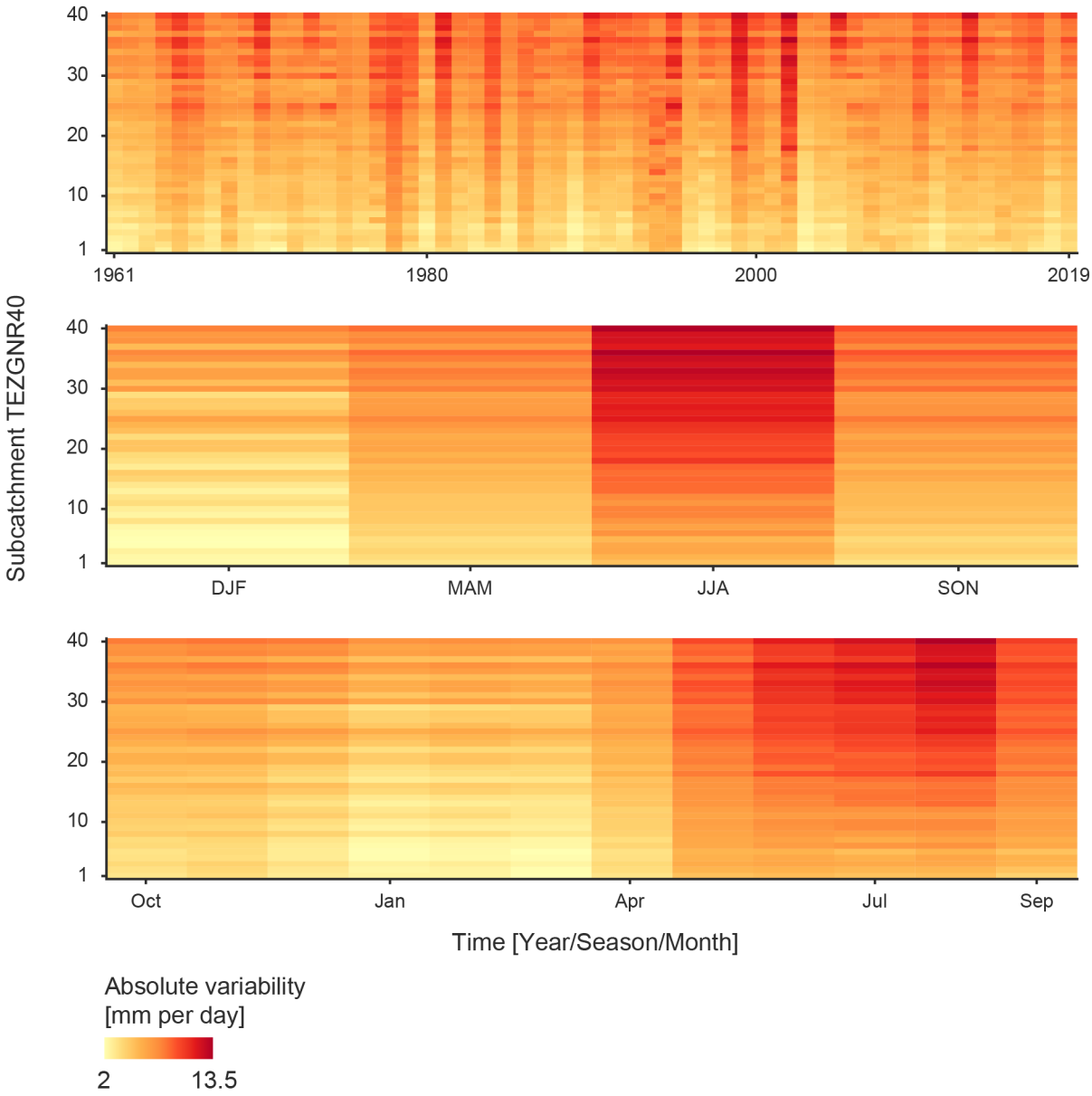

Figure 24: Natural variability of precipitation. *The natural variability is characterised by the absolute variability (standard deviation) within the probabilistic data set RhydchprobD for the time scales year, season and month.*

6.1.2 Precipitation Variability within Ensemble Runs

After having pointed out the natural variations of the precipitation occurrence in the catchment *Andelfingen* in the previous part, the analysis on ensemble run variability builds on these results. This section focuses on the intra-ensemble and inter-ensemble differences of the data set *RhydchprobD* from several perspectives. These are (a) the precondition of normal distribution, (b) the overall variability behaviour, (c) the annually variability behaviour, and (d) variability dependency on precipitation sum.

(a) Precondition of normal distribution

The evaluation of the ensemble runs spread yields the expected normal distribution. This random distribution of the deviations from the probabilistic data set mean value in the individual runs can be seen in Figure 25 exemplarily for the subcatchments *TEZGNR40 #5, #14, #29 and #36*. For all ensemble runs, the values are randomly distributed around zero, independent of time and space. Therefore, the ensemble runs are considered independent.

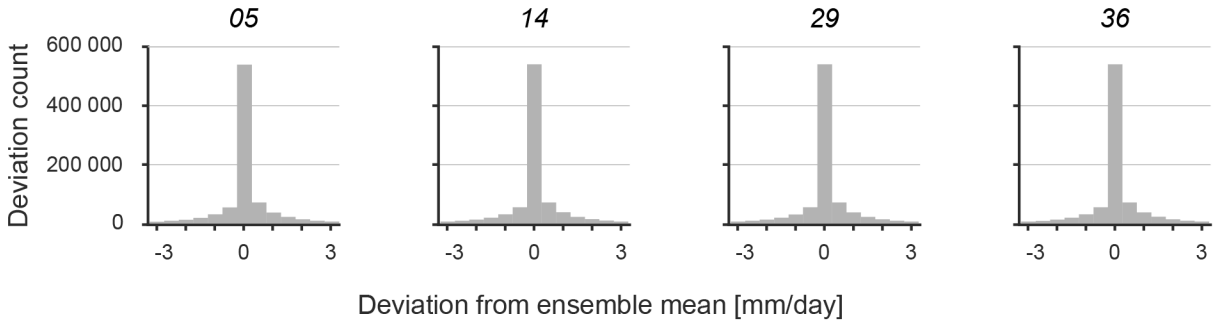

Figure 25: Deviation of ensemble run values from probabilistic data set means for the ensemble runs #05, #14, #29 and #36. *Negative deviations indicate higher ensemble run values compared to the probabilistic data set means whereas positive deviations illustrate smaller ensemble run values.*

(b) Overall variability behaviour

As the data set *RhydchprobD* fulfils the precondition of being normally distributed, the ensemble can be used for uncertainty examinations. The normal distribution is important for the uncertainty analysis insofar as the results are not biased by the ensemble run number, i.e. a certain parameter set does not always lead to an overestimating/underestimating ensemble run. One of the major advantages of the probabilistic data set is the provision of an equally likely ensemble of precipitation realisations per time and space unit. It is therefore of great interest how these realizations differ. As described in the methodology (chapter *5.2 Measures of Variability*), the absolute ensemble spread (*standard deviation*) and the relative ensemble spread (*coefficient of variation*) are used as measures of dispersion. Not surprisingly, the absolute ensemble spread increases with higher precipitation values due to the effect of large numbers. This absolute ensemble spread is shown in Figure 26 as a grey band around the probabilistic data set mean curve. In order to standardise the mentioned bias between precipitation volume and variability, the relative ensemble spread is applied. In Figure 26 it is clearly evident that the relative variability measure changes on a different scale, almost no variability of the relative ensemble spread is visible. The maximum difference of precipitation realisations in absolute terms is more than twice as large as in relative terms (59 mm per day and 26 mm per day, respectively).

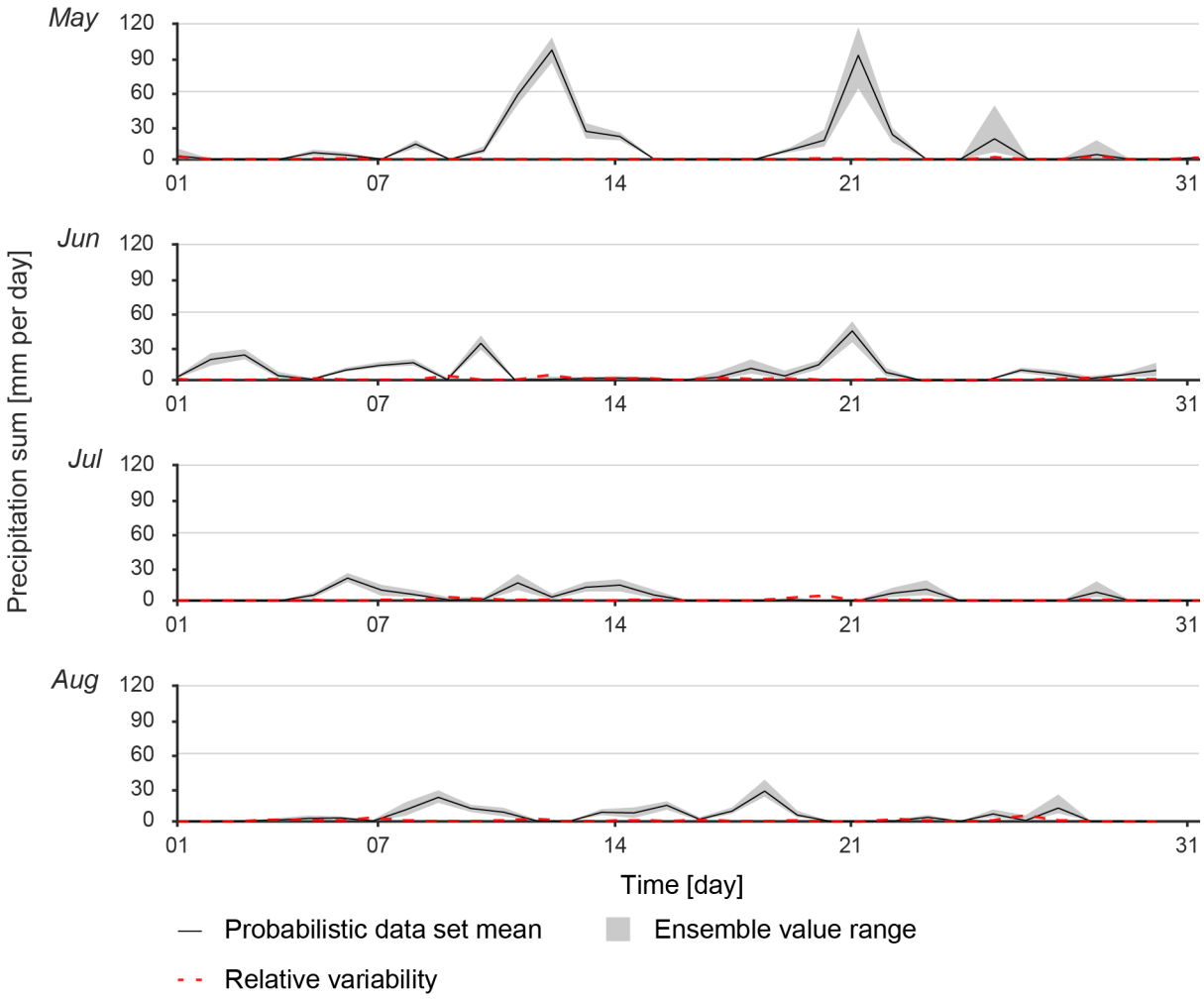

Figure 26: Methodological variability. *The value range of the ensemble runs (grey) together with the probabilistic data set mean (black) and the resulting relative variability (red) for the exemplary subcatchment TEZGNR40 #29 for the months May to August in the hydrological year 1999. The figure illustrates the relationship of a higher value range and relative variability in combination with an increasing precipitation sum.*

These maximum spread values should, however, be considered in relation to the 5/95th percentiles: for both absolute and relative variability, the lowest 5% of the data points show a variability of 0 mm per day whereas 95% of the data are below a spread of 3.15 mm per day for the absolute variability and 2.35 mm per day for the relative variability, respectively. Especially the spread values for the 95th percentile clarify that only less than 5% of the data—but which nevertheless still covers 43 160 entries (i.e. ensemble spread in one of the subcatchments *TEZGNR40* on one day)—are responsible for the large variability range. A closer inspection of the highest 5% relative spreads shows that the high values are attributable to the calculation definition of the relative ensemble spread. In order for a relative variability to be calculated on a day and subcatchment *TEZGNR40*, the assumed threshold value must exceed a minimum precipitation amount of 1 mm per day. If the relative spread for a subcatchment *TEZGNR40* with an average precipitation slightly above 1 mm per day is calculated, this computation will almost certainly give a large relative variability measure. This assumption is supported by the fact that 95% of the precipitation values of these 5% very high relative spread entries are less than 5.1 mm per day.

(c) Annually variability behaviour

The analysis of natural precipitation variability has already shown that even in a catchment area of about 1 000 km^2, large temporal and spatial differences in precipitation occurrences are recognised. In order to enable the detection of such spatio-temporal patterns in terms of interpolation uncertainty, the ensemble spreads as a function of the probabilistic data set mean precipitation is examined in greater detail for a single year. Taking the average meteorological year 2013 as an example, the relative ensemble spread shows higher values more frequently in the months of May to September. In addition, these variabilities occur more often in the higher elevation subcatchments *TEZGNR40* #19 to #40. This temporal and spatial clustering of the variability is also unambiguously visible in the dry year 2003. In order to illustrate the spatio-temporal patterns, only precipitation events with an intensity greater than the long-term mean per subcatchment *TEZGNR40* is shown in Figure 27. Small precipitation events can be found about the same frequency all year round and in the entire catchment (see Figure 19 in chapter *6.1.1 Precipitation events*).

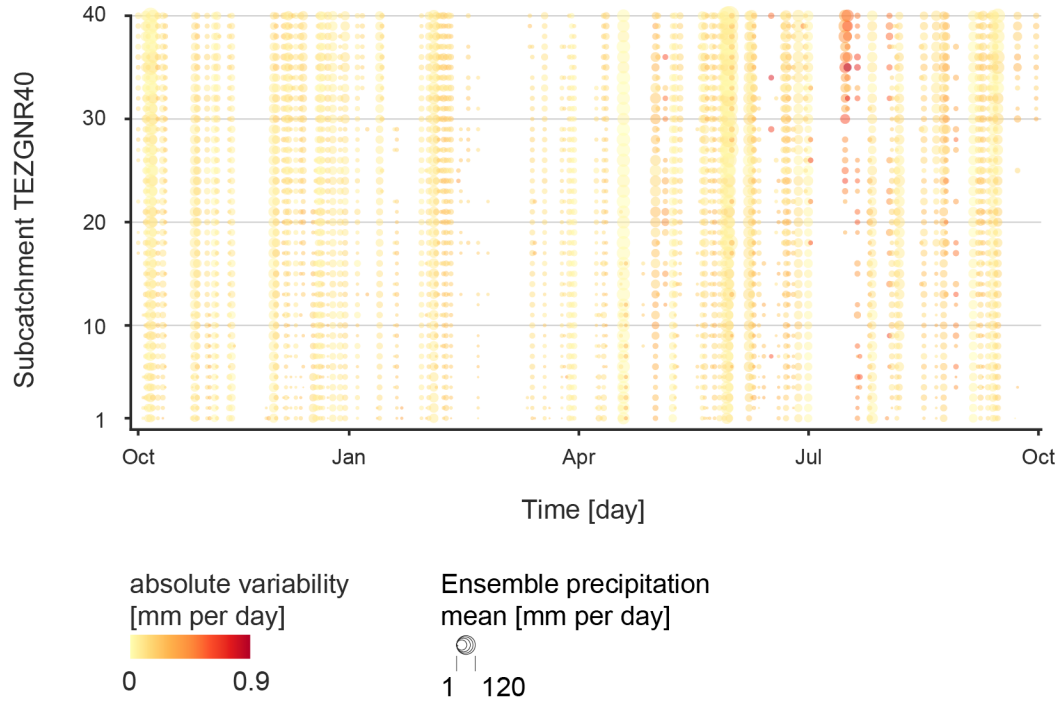

Figure 27: Precipitation events with an intensity greater than the long-term mean per subcatchment TEZGNR40 in the hydrological year 2013. *Each precipitation event is symbolised with the corresponding precipitation sum of the probabilistic data set mean (size) and the absolute variability within the probabilistic data set (colour). A spatio-temporal increase of precipitation sum and absolute variability for high elevation areas during the summer months is recognisable.*

(d) Variability dependency on precipitation sum

It appears that there is a certain correlation between ensemble spread and precipitation sum. To highlight this, Figure 28 shows the absolute and the relative ensemble spread as a function of the mean precipitation sum per day and subcatchment *TEZGNR40*. The distributions support the statement that the ensemble spread depends more on the seasonality rather than on the spatial situation. While the absolute ensemble spread enlarges with increasing precipitation, the relative ensemble spread decreases. Except for February, when sporadic, more intense precipitation events occur, the data points of the absolute and relative dispersion of the lowlands (subcatchment

TEZGNR40 #1 to #18) and the high elevations (subcatchment *TEZGNR40* #19 to #40) are similar. From this observation it can be concluded that within the ensemble runs no large daily spatial differences in precipitation variability are observed over the 58-year study period. While the dispersion of the ensemble spreads and the mean precipitation sum are comparatively low in the months of October to April, the gap is growing wider in summer. Both for low precipitation occurrences as well as for heavy precipitation, the higher measures of dispersion become visible in the summer months.

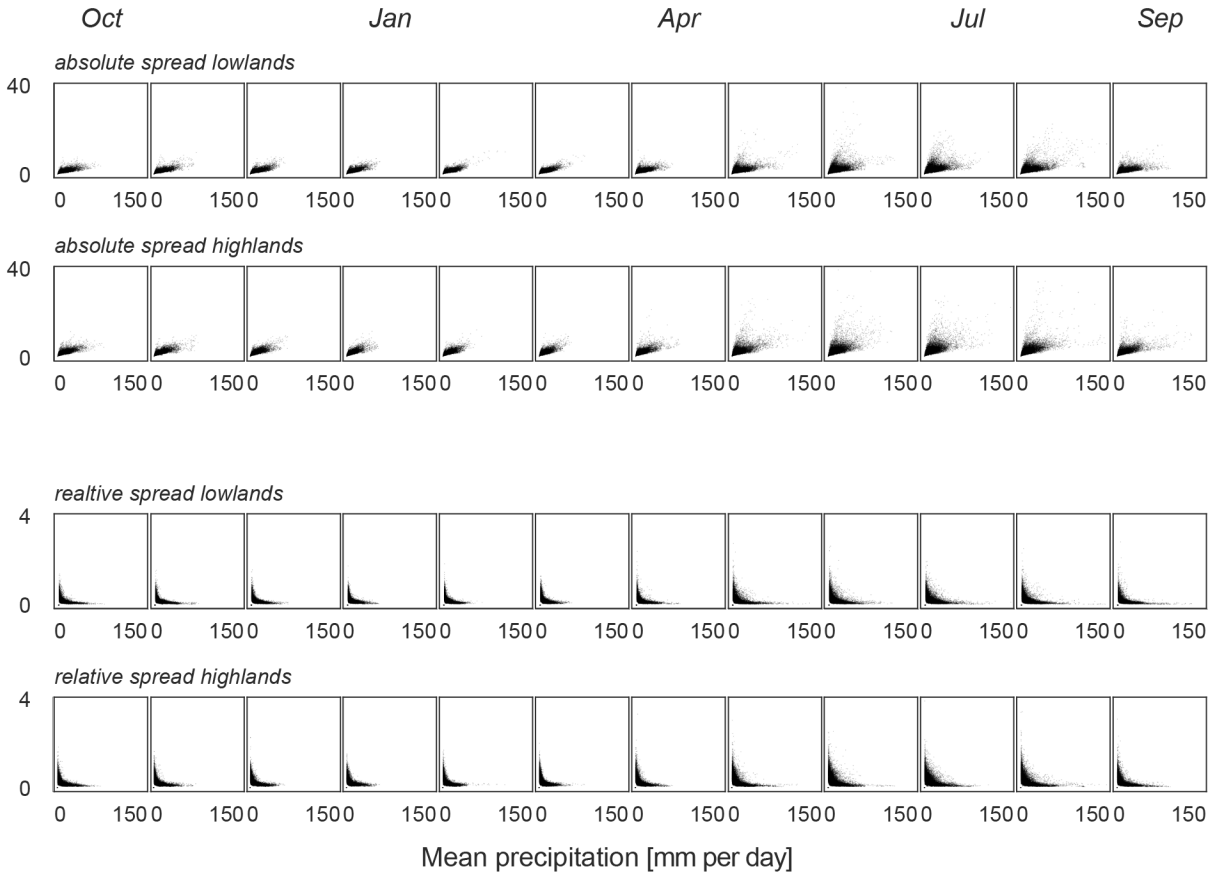

Figure 28: Precipitation events over the entire study period as a function of the absolute and the relative variability and the daily precipitation sum of the probabilistic data set mean. *The analysis is divided in subcatchments TEZGNR40 in the lowlands (#1 to #18) and highlands (#19 to #40).*

6.1.3 Heavy Precipitation Events

The results of all precipitation events show that the heavy precipitation values are smoothed out in the large amount of data because they occur less frequently. For the period 1. October 1961 to 30. September 2019 (58 years; 21 447 days), 1 571 days of heavy precipitation events are recorded, according to the definition in chapter *5.3.4 Heavy Precipitation Events*. Conversely to the general precipitation analysis, heavy precipitation events occur more frequently in the form of convective precipitation. Of all heavy precipitation events, 221 extend over the entire basin, which is equivalent to stratiform precipitation. The remaining 1 350 events occur only in certain subcatchments *TEZGNR40*. The results of heavy precipitation occurrence analysis can be divided into (a) spatial and (b) temporal patterns.

(a) With regards to spatial patterns, the occurrences of this particular type of precipitation event correlates positively with the average elevation of the subcatchments *TEZGNR40* (Figure 29). The number of heavy precipitation events in the ten highest subcatchments *TEZGNR40* is on average about six times higher (~600 events) than in the ten lowest areas (~100 events). This comparison is only valid because the catchments TEZGNR40 are about the same size. The spatial distribution thus resembles the natural pattern of precipitation in the catchment *Andelfingen* as outlined in chapter *6.1.1 Natural Precipitation Variability*.

(b) From a temporal perspective, convective events occur throughout the year, with higher frequency in the summer months than in winter. However, apart from few exceptions, heavy stratiform precipitation does not occur during the summer months. In more detail very few heavy stratiform precipitation events occur in the summer months of June, July and August. By far the most frequent heavy precipitation events occur in May, and occasionally in September to December as well as in February and April.

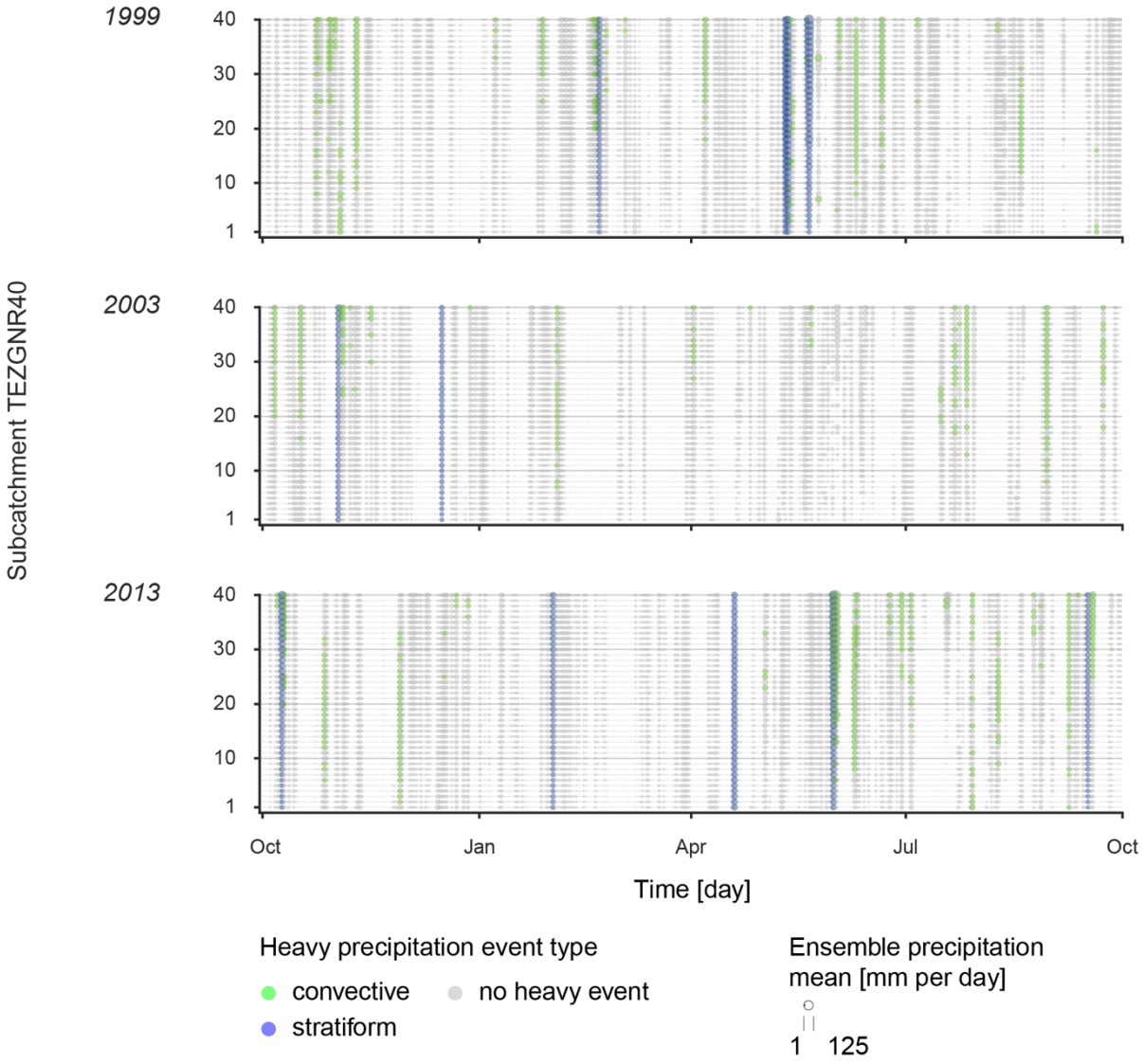

Figure 29: Heavy precipitation events during the hydrological years 1999, 2003 and 2013. *Events with a precipitation sum above the long-term 95th percentile of the ensemble runs over the entire study period and subcatchments TEZGNR40 are defined as heavy precipitation events (> 20 mm). The colour indicates the precipitation generation type, green for convective and blue for stratiform precipitation, whereas the size of an event shows the precipitation sum.*

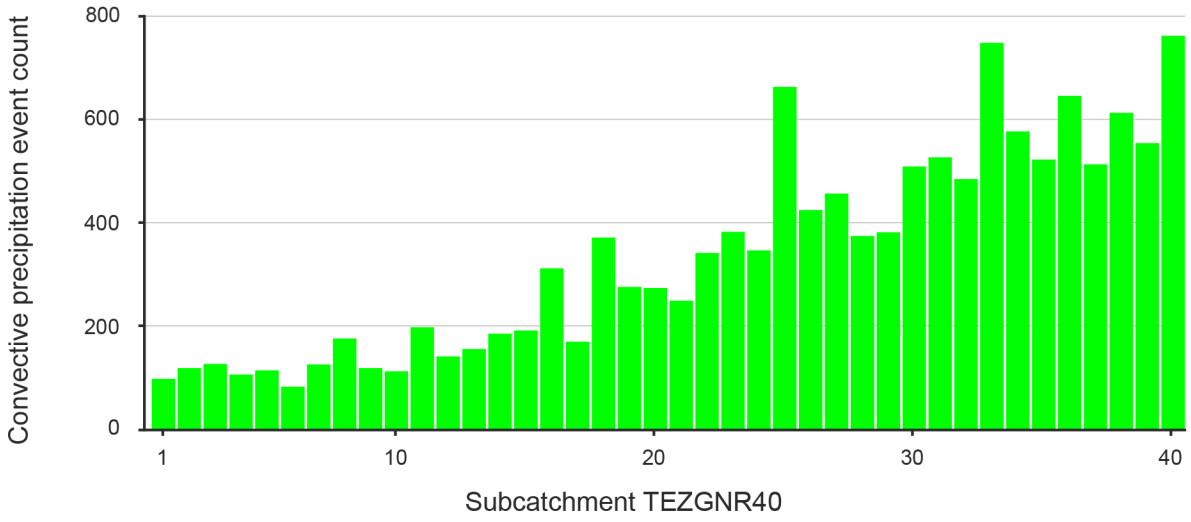

Figure 30: Convective precipitation event count per subcatchment TEZGNR40. *The number of convective precipitation events positively corelates with the subcatchment's mean elevation.*

Now spatial and temporal patterns of heavy precipitation occurrences have been explained, the interpolation uncertainty of such events is appended. The values of the ensemble variability indicate that the highest interpolation uncertainties are attributable to very strong heavy precipitation events. Since the heavy precipitation event definition already excludes very low precipitation values and thus very high, precipitation-dependent ensemble variability, only the absolute ensemble spread is used as a measure in the extreme event analysis. If this weren't the case, the variability would be considered twice as a function of the precipitation sum. The maximum absolute variability of 23.5 mm per day for heavy precipitation events—which corresponds to a precipitation range of 113 mm per day—is over three times larger than the 95th percentile value (approximately 7.04 mm per day). Since the study period of about 58 years is relatively long, the 5% with the highest variability still correspond to 59 occurrences. This is equal to one very strong heavy event featuring very high interpolation uncertainty per year and thus should not be neglected. Furthermore, the uncertainty in heavy precipitation estimation shows a high spatio-temporal correlation with the type of precipitation generation. As Figure 31 shows, the ensemble variabilities for less frequent, stratiform heavy precipitation events are considerably higher than for convective events, which is emphasised by the average absolute ensemble spreads of 4.42 and 3.68 mm per day, respectively. The majority of the data (within the 5/95th percentiles) are estimated with an uncertainty of 1.85 to 6.37 mm per day for convective precipitation and 2.10 to 9.81 mm per day for stratiform events. This relationship is well illustrated by the two stratiform heavy precipitation events in June 1999 and the one event in June 2013 by the darker coloured points compared to other heavy precipitation events (Figure 31). In summary, the results show that the ensemble variability is dependent on the generation type of precipitation. Due to the natural seasonal dependence of precipitation formation, variability also fluctuates inter-annually.

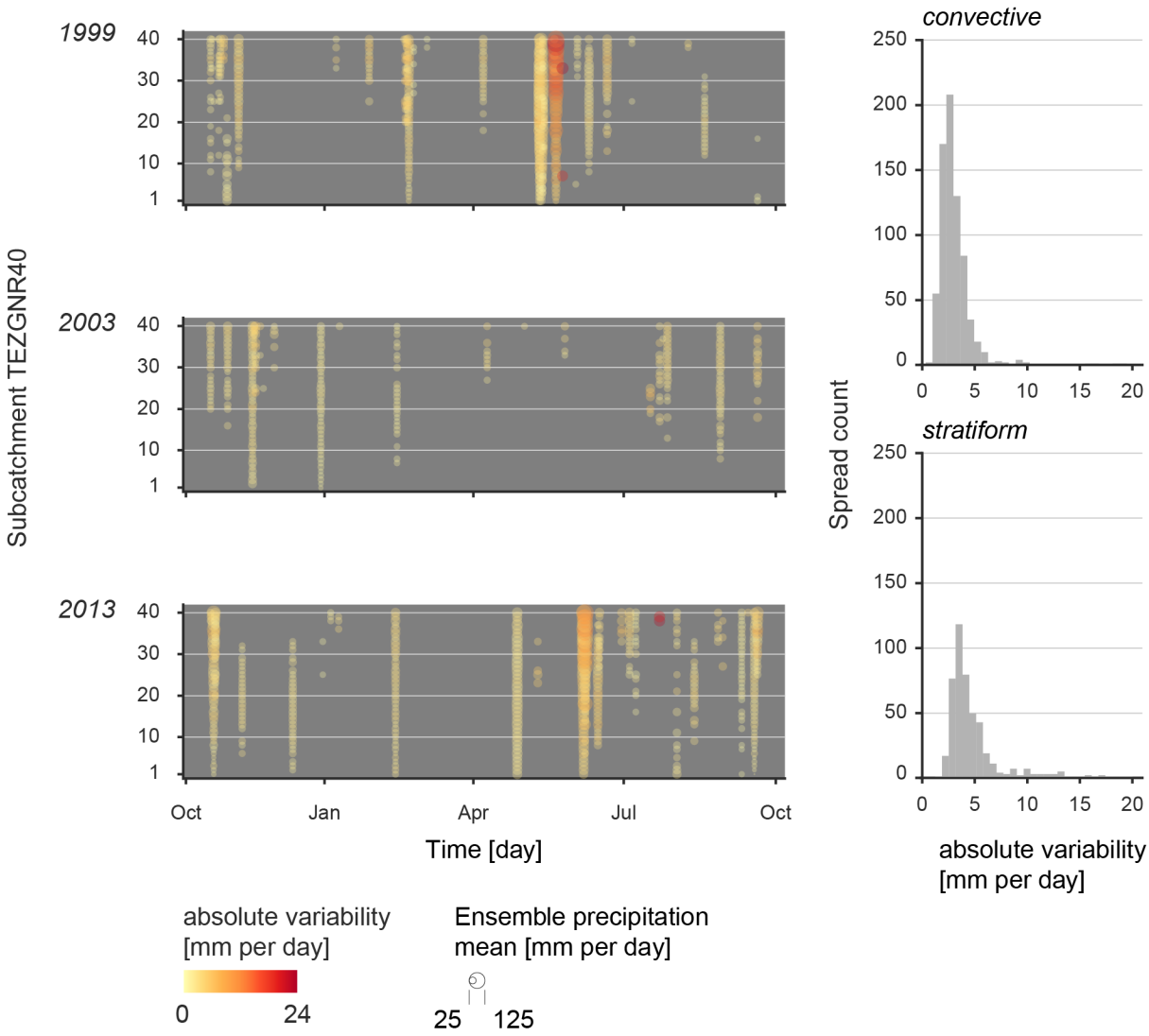

Figure 31: Absolute variability of heavy precipitation events during the hydrological years 1999, 2003 and 2013. *The illustration on the left shows all extracted heavy precipitation events (see Figure 29) with the corresponding absolute variability (colour) and precipitation sum (size). How the number of events are distributed across the generation types «convective» and «stratiform» and the absolute variability can be seen in the graphs on the right.*

6.1.4 Aggregation of Meteorological Data

The results in the previous chapters showed that precipitation occurrences feature a high spatial and temporal variability due to natural and mathematical processes. Whether such variabilities are significant over a longer time period and over a larger area is to be found out by applying three different aggregations. More precisely, it is first examined separately for (a) the temporal aggregation and (b) the spatial aggregation followed by (c) the combined spatio-temporal aggregation over which time/space the uncertainties remain recognisable or whether they are smoothed out over time. The analysis should provide indications of desirable spatio-temporal resolution for precipitation data.

(a) Temporal Aggregation

The first aggregation analysis is on the persistence of the ensemble variability over time. Figure 32 shows the relative ensemble spread values aggregated over time with different moving windows (1, 2, 3, 7, 14 and 30 days) for the exemplary years 1999, 2003 and 2013. Up to the aggregation window of 7 days, only small differences are discernible, regardless of the seasonality. The temporal aggregation of less than a week is not sufficient to noticeably smooth out even small local variability, which can be seen in the remaining variable events (darker coloured tiles) for the aggregation levels of 1, 2, 3, 7 days. The same pattern can be seen for the precipitation sum (Figure 32). This auxiliary information allows to link the relative ensemble spread with the amount of precipitation. Even the shorter but heavier precipitation events remain visible up to an aggregation window of one week. Only after two weeks does a more homogeneous, less variable pattern become apparent. With an aggregation window of 30 days, 95% of the precipitation events show a relative ensemble spread of less than 0.11 mm per day with a precipitation sum less than 14.5 mm per day. This is a 76% decrease in relative variability (0.47 mm per day) and a 58% decrease in intensity from the time resolution of 1 to 30 days. Despite the temporal aggregation, the spatio-temporal variability patterns found in the previous sections remain visible. In other words, precipitation events in the higher-lying areas and in late spring or early autumn days are estimated with a higher uncertainty even with an aggregation window of one week.

The empirical cumulative density function (*ECDF*) represents the distribution of the relative ensemble spread values equivalent to the percentile in a graphical, descriptive way (Figure 33 and 34). Independent of the year and the corresponding precipitation amount, the number of very low relative ensemble spreads decreases with increasing number of aggregation days. While initially, more than 50% of the values have a relative ensemble spread of 0 mm per day, this extent drops to less than 10% for 30 days. The range of spread values, in which a large part of the data varies, is also decreasing, i.e. the curve of the *ECDF* is becoming increasingly steeper. Whereas a large part of the data variability originally had reached a relative ensemble spread of less than 0.75 mm per day (red curve), this probability reaches only about 0.3 mm per day with an aggregation window of 30 days (yellow curve). Overall, as can be seen in Figure 33, the *ECDF* curves differ only minimally in their course between the study years. For the above-average wet year 1999 and the average wet year 2013, the curves are almost identical, while for the very dry year 2003, the values are on average somewhat higher at the beginning. This leads to less steep and slightly closer curves, especially the 30-day curve is closer to the 14-days-curve than in the other two years.

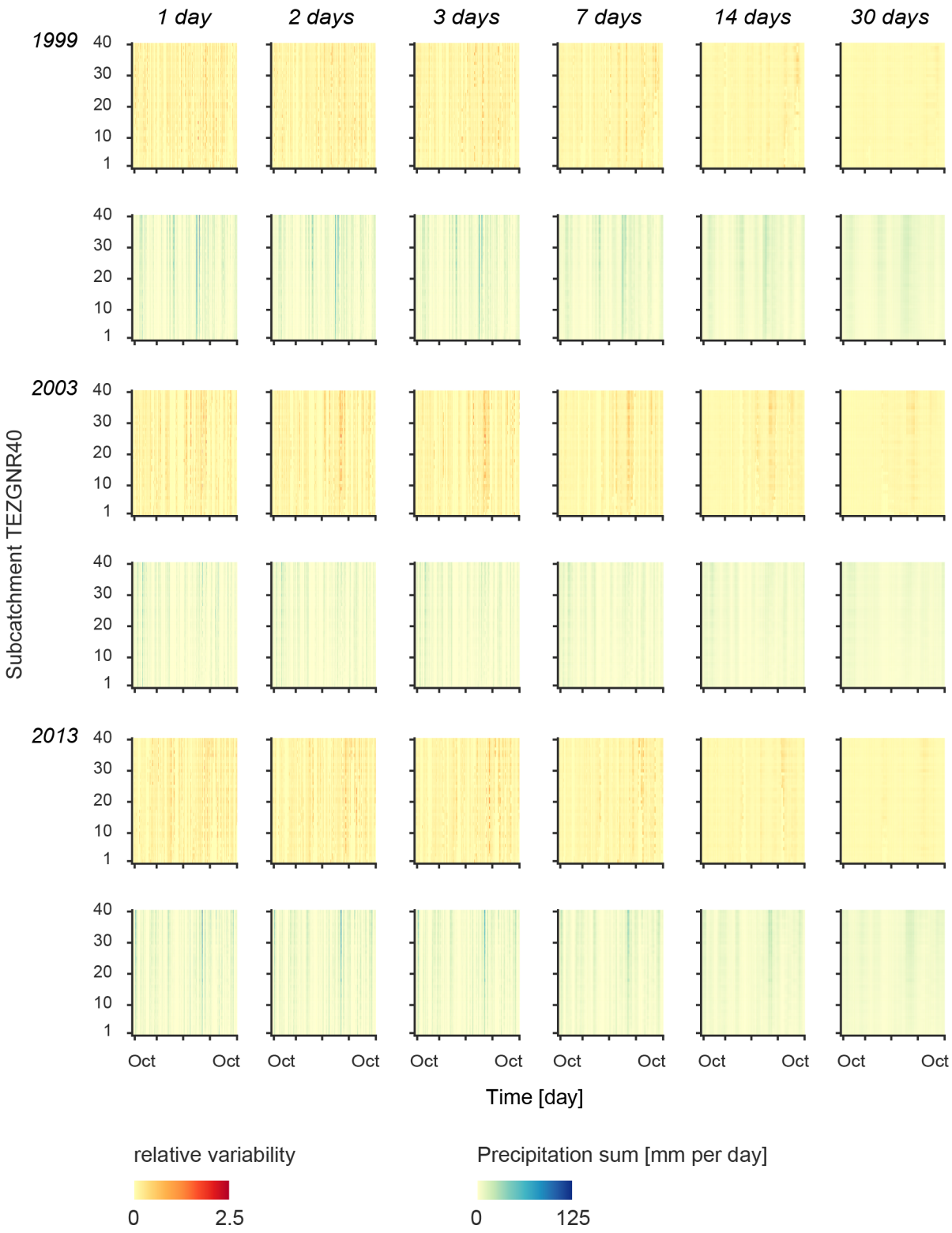

Figure 32: Temporal data aggregation for the hydrological years 1999, 2003 and 2013. *The probabilistic data set is temporally aggregated with a rolling window of 1, 2, 3, 7, 14 and 30 days per subcatchment TEZGNR40. The relative variability in the data set (first lines) as well as the precipitation sum (second line) per day and subcatchment are illustrated.*

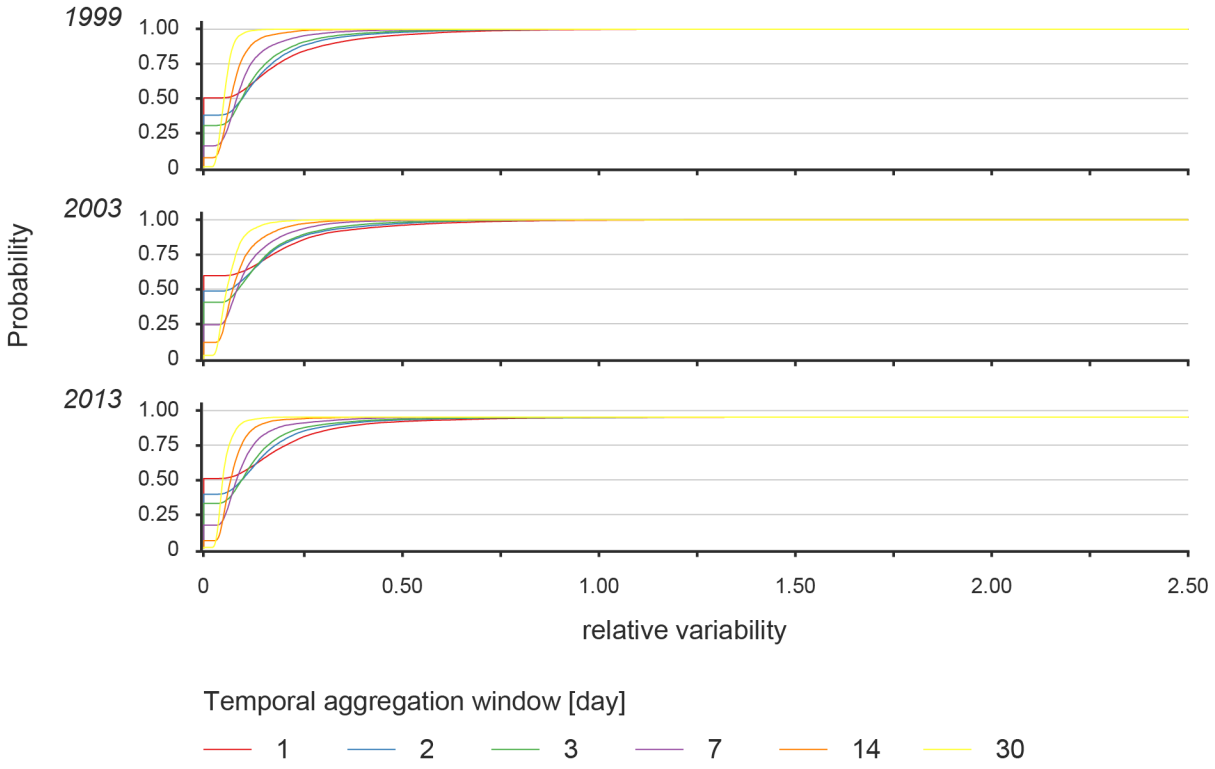

Figure 33: Empirical cumulative density function for the temporal aggregated data during the hydrological years 1999, 2003 and 2013. *The functions show the probability of an event to have a certain relative variability for the aggregation windows 1, 2, 3, 7, 14 and 30 days.*

In contrast to the observation level «year», on which only very slight differences become visible, differences are recognisable in the spatio-temporal analysis. In all example subcatchments *TEZGNR40*, the number of events for the initial ensemble spread of 0 mm per day decreases with increasing mountainous character. Furthermore, the curves for all aggregation windows in areas with a larger mean elevation increase less rapidly due to the higher precipitation variability. In the same way as in other analysis, the largest ensemble run variability is still measured for the month of June.

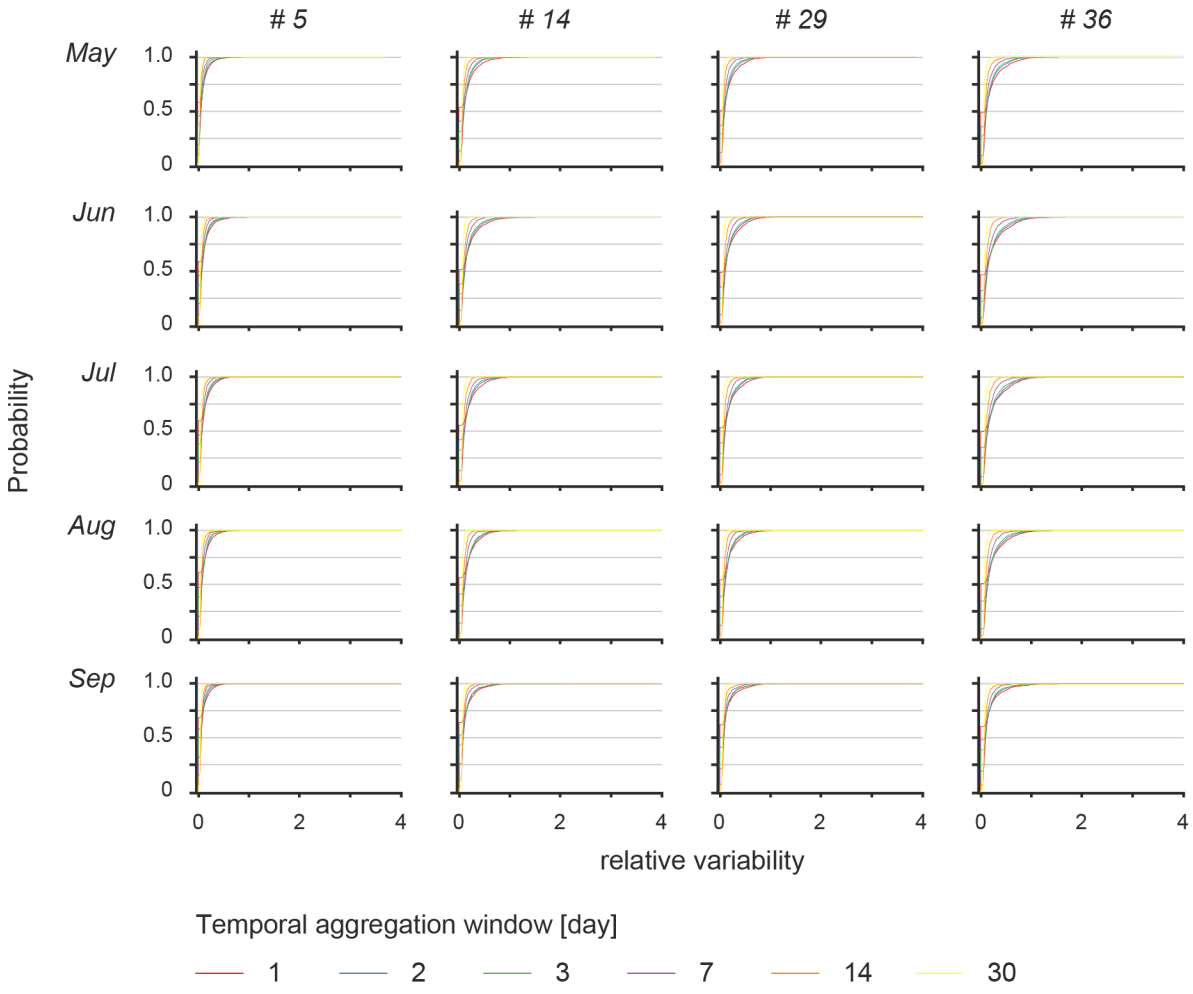

Figure 34: Empirical Cumulative Density Function for the temporal aggregated data for subcatchments TEZGNR40 #5, #14, #29 and #36. *The functions show the probability of an event to have a certain relative variability for the aggregation windows 1, 2, 3, 7, 14 and 30 days.*

(b) Spatial Aggregation

The second aggregation analysis focusses on the persistence of the ensemble variability in space. The *Andelfingen* catchment area *TEZGNR1000* can be divided into the hydrological subcatchments *TEZGNR150* (see chapter *3 Study Site*) in addition to the finer resolved subcatchments *TEZGNR40*. As can be seen in Figure 35, the relative ensemble spread increases with a larger spatial aggregation. This visual observation is also reflected in the statistical key figure: the value of the 95th percentile increases for both the absolute and relative ensemble spread (the 5th percentile remains close to 0 mm per day and is therefore not further considered). While 95% of the absolute ensemble spreads are below 3.12 mm per day in the finest resolution, the value increases to 4.04 mm per day for the subcatchments *TEZGNR150* and to 7.49 mm per day for the entire catchment area *TEZGNR1000*. The picture is similar for the relative ensemble spreads, where the 95th percentile increases from 0.47 mm per day to 0.6 mm per day and 1.02 mm per day, respectively. However, because the local precipitation is distributed over a larger area during spatial aggregation, the precipitation sum per area decreases proportionately (Figure 35).

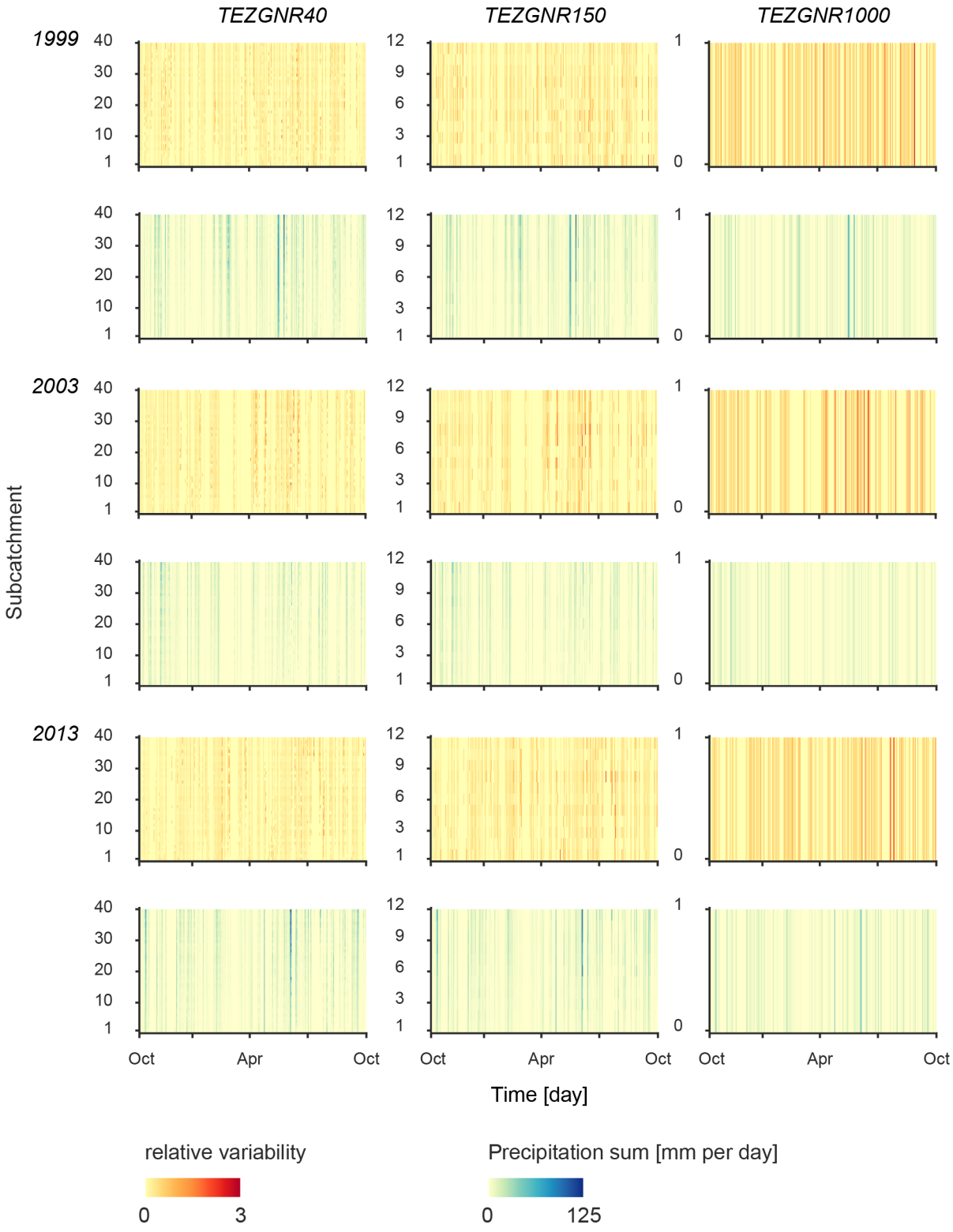

Figure 35: Spatial data aggregation for the hydrological years 1999, 2003 and 2013. *The probabilistic data set is spatially aggregated with the expansion of the hydrological units TEZGNR150 and TEZGNR1000. The relative variability in the data set (first lines) as well as the precipitation sum (second line) per day and subcatchment are illustrated.*

(c) Spatio-temporal aggregation

So far, the temporal and spatial scales have been investigated separately. But the moving window as well as the *ECDF* allow to combine those levels. While the spatial aggregation by itself causes an increase of the ensemble spreads, in combination with the temporal aggregation it strongly decreases. How the statistical key figures, namely 50th percentile, 95th percentile and maximum relative ensemble spread (100th percentile), decrease with spatio-temporal aggregation is shown in Table 7 as well as in Figure 36. The visual consideration clearly shows the decrease of the relative ensemble spread with lower spatio-temporal resolution. Half of the precipitation events on all spatial aggregation levels show no ensemble spread (0 mm per day), most of them correlate short-lasting events (1 day) with small to moderate precipitation sums. If the temporal resolution is decreased, this ensemble spread increases because of the higher variability up to the aggregation of 3 days. This development is visible in all spatial aggregation levels. With a temporal aggregation of more than 3 days, the variability of the less variable half of the data set (below 50th percentile) also follows the general development of the variability decrease.

Table 7: Relative variability values for the various spatio-temporal aggregation levels. *The values for the 50th, 95th and 100th percentiles are given for the temporal aggregation windows of 1, 2, 3, 7, 14 and 30 days as well as for the spatial extensions TEZGNR40, TEZGNR150 and TEZGNR1000.*

	50th percentile			95th percentile			100th percentile		
TEZGNR	**40**	**150**	**1000**	**40**	**150**	**1000**	**40**	**150**	**1000**
1 day	0	0	0	0.47	0.35	0.20	3.95	1.72	0.52
2 days	0.08	0.06	0.03	0.39	0.28	0.14	3.46	1.27	0.50
3 days	0.09	0.07	0.03	0.34	0.24	0.12	3.35	1.04	0.47
7 days	0.08	0.06	0.03	0.25	0.17	0.08	1.64	0.86	0.26
14 days	0.07	0.05	0.03	0.18	0.12	0.06	1.10	0.66	0.19
30 days	0.06	0.04	0.02	0.11	0.08	0.03	0.44	0.23	0.07

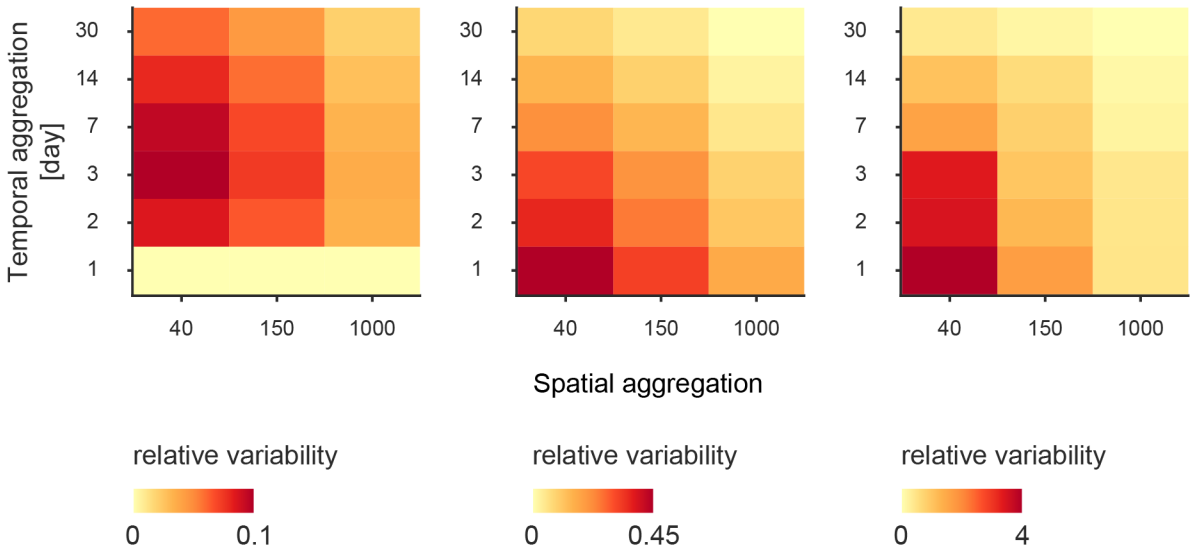

Figure 36: Relative variability values for the various spatio-temporal aggregation levels. *The values for the 50th, 95th and 100th percentiles are given for the temporal aggregation windows of 1, 2, 3, 7, 14 and 30 days as well as for the spatial extensions TEZGNR40, TEZGNR150 and TEZGNR1000.*

Transferred to the *ECDFs*, the curves of *TEZGNR150* and *TEZGNR1000* consequently rise steeper than for the subcatchments *TEZGNR40*. Precipitation events are below 0.5 mm per day with almost 100% certainty in all spatio-temporal aggregations with only small differences between *TEZGNR150* and *TEZGNR1000*. The uncertainty level of 0.5 mm per day is half that of *TEZGNR40* subcatchments, for which a 100% certainty is only achieved at a level of 1 mm per day. However, and independent of temporal aggregation, spatial aggregation implies that initially fewer values show a variability of 0 mm per day. Apart from these two differences, the course of the curves, especially the change with temporal aggregation, is similar to that of the *ECDFs* in the previous section.

6.1.5 Precipitation Variability between Deterministic and Probabilistic Data Sets

Before the probabilistic data set has been realised for Switzerland, the deterministic data set was used as a basis in various application fields. It is therefore interesting to find out how the novel data set differs from the established one. For this purpose, the probabilistic data set means of precipitation sums are compared to the deterministic data. If the individual runs rather than the probabilistic data set mean had been compared with the deterministic data, this would mean 50 times more comparisons and thus a much more complex analysis. The deviation is defined as the difference from the *RhiresD* data set to the *RhydchprobD*. Whereas half of the entries (approximately 420 000) have a deviation close to zero (~0.1 mm per day; 50th percentile), the range of 90% of the values is equally represented between −1.04 and 1.09 mm per day (5th and 95th percentile, respectively) within the total study period. Nevertheless, if the data set is reduced to the three sample years 1999, 2003 and 2013 and four sample subcatchments *TEZGNR40* #5, #14, #29 and #36, small differences can be observed. In the same way as before, the reduction of data points enables to discover irregularities. First, it is noticeable that in the lowlands (subcatchment *TEZGNR40* #5) there are conspicuously more deviations close to 0. With increasing altitude, the values show a slightly larger distribution, even if in a very narrow range. Second, the distribution of the values shifts from the lowlands to the mountains somewhat more from negative range into the positive, i.e. the probabilistic data set mean often records lower values than the deterministic data set values (Figure 37).

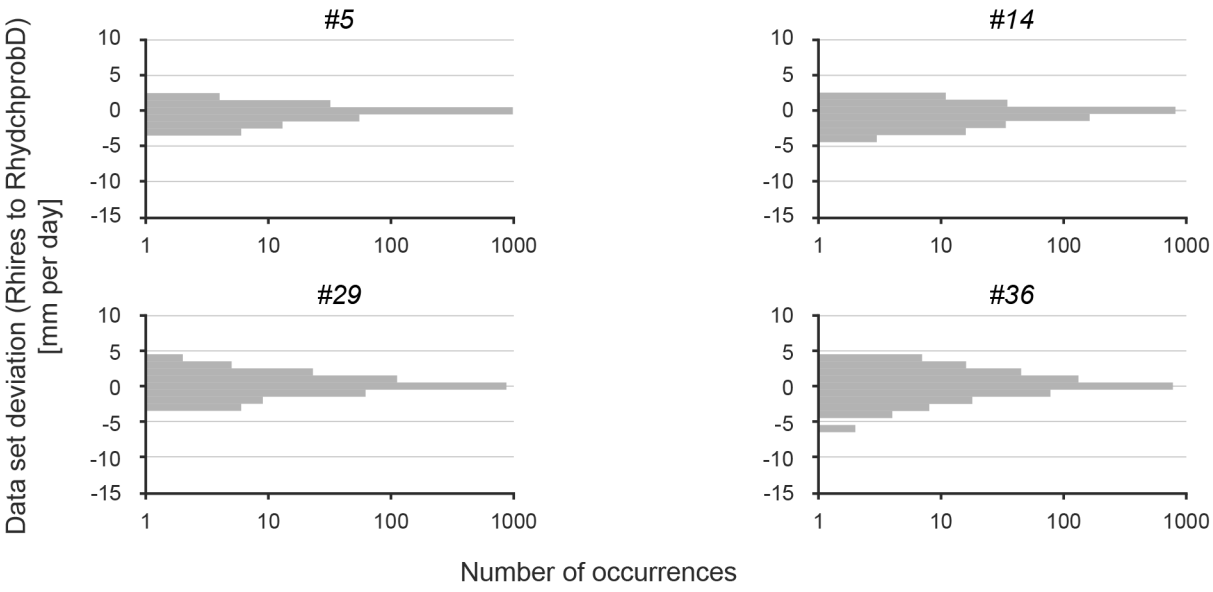

Figure 37: Data set deviation of RhiresD and RhydchprobD. *Negative deviations indicate a higher precipitation estimation of the probabilistic data set mean compared to the deterministic data set while positive deviations illustrate a higher precipitation estimation of the deterministic data set.*

Based on the spatio-temporal variabilities explained previously, the question arises whether these variabilities have an influence on the deviation of the data records. For this purpose, the deviations are analysed in combination with the (a) precipitation sum and (b) the seasonality. (a) For 90% of the precipitation values (between the 5th and 95th percentile) no dependence of the deviation of the two data sets on precipitation sum can be established. The deviation varies between −1.04 and 1.09 mm per day for both small and strong precipitation occurrences. (b) On the temporal scale, it is noticeable that the probabilistic data set mean tends to show higher values than the deterministic data set in the winter months November to February for values within the 90th confidence interval. Conversely, the deviations in the summer months are more positive, which are caused by higher deterministic than mean probabilistic precipitation values. Nevertheless, it becomes clear that the differences between the two data sets are very small and therefore negligible.

Since a majority of the data do not show any significant observations, the outliers are examined more closely. The outliers outside the 90th confidence interval show three conspicuousness: (1) the outliers occur mainly during the summer months; (2) they indicate that the averaged probabilistic approach estimates higher precipitation values for stronger precipitation events. These coherences result in more frequent negative deviations during the summer months (more in red saturated points in Figure 38); (3) the subset also highlights the previous statement that higher deviations do not only occur more frequently in the summer months, but also from a spatial perspective more frequently in the mountainous areas. As with the findings within the 90th confidence interval, however, it is pointed out that the deviations of the outliers are also very small.

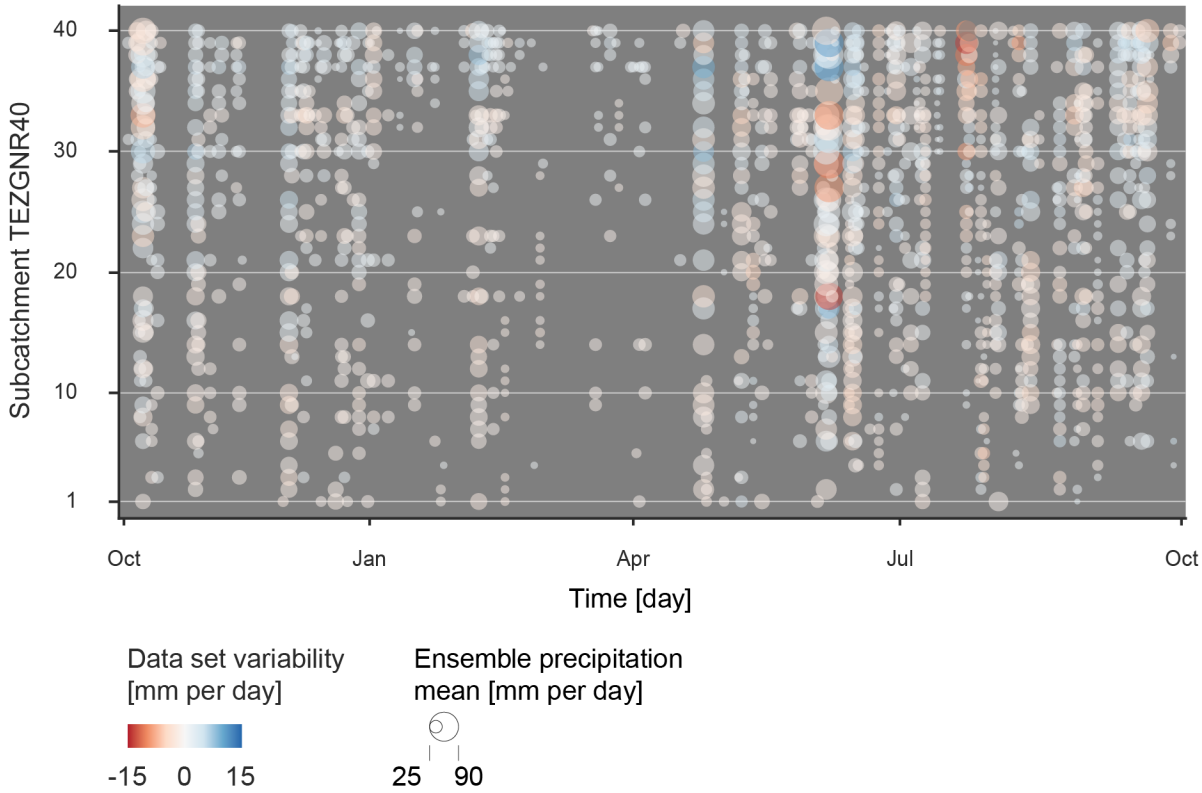

Figure 38: Data set deviation of RhiresD and RhydchprobD outside the value range -1.1 to 1.1 mm per day for the hydrological year 2013. *The precipitation events are illustrated with the corresponding data set variability and precipitation sum.*

6.2 Hydrological Simulations in *HBV*

The precipitation data analysed so far is used as an input to the *HBV* model which results in predictions of the amount of water in rivers. This section summarises the results of these simulations compared to observed values for the various calibration-validation versions (A) the deterministic-probabilistic approach where the model is calibrated with the *RhiresD* data and validated with the *RhiresD* and *RhydchprobD* ensemble runs in the recent 17 years; (B) the inverted deterministic-probabilistic approach where the same data as in *Version A* is used but the time periods of calibration and validation is inverted; and (C) the probabilistic-deterministic approach where the calibration is done with the *RhydchprobD* ensemble runs, which are then used in the validation with *RhiresD* for the same period as *Version A*.

6.2.1 HBV Model Calibration and Validation Version A

The standard *Version A* of the model calibration-validation uses the *RhiresD* data from 1st October 1977 to 30th September 1995 for calibration and the *RhiresD* and *RhydchprobD* data both from 1st October 1998 to 30th September 2016 for validation. The *HBV* model calibration step using the *GAP* for the *RhiresD* data sets results in ten equally reliable parameter sets for each measurement station catchment. The best achieved results of model calibration for the individual measurement station catchments are listed in Table 8. In general, the validation with the probabilistic data set (*RhydchprobD*) compared to the one with the deterministic data set (*RhiresD*)

does not increase the model accuracy. The resulting accuracy depends on the size in combination with the elevation of the catchment, whereby the most precise calibration is achieved for *MSC 2386* (mean elevation 648 m a.s.l. and area 80.2 km^2) and the most inaccurate for *MSC 2112* (mean elevation 1 250 m a.s.l. and area 74.4 km^2). A large catchment area has a higher variability of processes affecting the runoff generation and thus an increased difficulty in simulating. In contrast, precipitation in mountainous areas results almost one to one as runoff due to steeper flanks and less deep soils which simplifies the runoff simulation.

Table 8: Model efficiency for the calibration and validation processes per MSC. *The model efficiency is characterised with the measures R_{eff} and Volume Error. The validation values are given for the data sets RhiresD and RhydchprobD whereas the model is only calibrated with the data set RhiresD.*

	RhiresD				RhydchprobD	
	Calibration		Validation		Validation	
Measurement station subcatchment	**min**	**max**	**min**	**min**	**min**	**max**
2044; *Andelfingen*						
R_{eff} for top ten GAP results/Model efficiency	0.61	0.66	0.67	0.69	0.65	0.65
Volume Error	0.67	0.70	0.67	0.70	0.65	0.65
2386; Frauenfeld						
R_{eff} for top ten GAP results/Model efficiency	0.81	0.83	0.78	0.79	0.77	0.77
Volume Error	0.96	0.99	0.95	0.99	0.97	0.97
2181; Halden						
R_{eff} for top ten GAP results/Model efficiency	0.49	0.53	0.51	0.54	0.50	0.50
Volume Error	0.54	0.57	0.53	0.55	0.53	0.53
2126; Wängi						
R_{eff} for top ten GAP results/Model efficiency	0.80	0.81	0.78	0.79	0.78	0.78
Volume Error	0.90	0.94	0.89	0.94	0.91	0.91
2374; Mogelsberg						
R_{eff} for top ten GAP results/Model efficiency	0.69	0.71	0.66	0.69	0.65	0.65
Volume Error	0.74	0.78	0.70	0.73	0.70	0.70
2468; St.Gallen						
R_{eff} for top ten GAP results/Model efficiency	0.55	0.58	0.56	0.59	0.54	0.54
Volume Error	0.58	0.61	0.57	0.6	0.56	0.56
2303; Jonschwil						
R_{eff} for top ten GAP results/Model efficiency	0.42	0.45	0.44	0.47	0.42	0.42
Volume Error	0.49	0.51	0.49	0.50	0.47	0.47
2112; Appenzell						
R_{eff} for top ten GAP results/Model efficiency	0.28	0.30	0.32	0.37	0.30	0.30
Volume Error	0.43	0.44	0.44	0.46	0.43	0.43

The aim of the automatic model parameter calibration using *GAP* is to minimize total prediction uncertainty. The evaluation of the 80 best performance *GAP* parameter sets from all catchments

with the *RhiresD* data show the parameters PERC (maximal flow from upper to lower box), CFR (refreezing coefficient) and CWH (water holding capacity) to be the most volatile. As in previous results, the higher altitudes show more uncertain parameters within the possible parameter range, for example *MSC 2374* with the PERC range of 1.23 mm per day (defined range is 0 to 3 mm per day), *MSC 2468* with the CFR range of 0.09 (defined range is 0 to 0.1) and *MSC 2303* with the CWH range of 0.1 (defined range is 0 to 0.2). Nevertheless, a significant correlation between the catchment size and the parameter uncertainty cannot be identified. The parameter ranges are chosen so that none of the best performances exceed the defined limits (see Table 4 in chapter *5.4.2 HBV Model Calibration*).

From the model efficiency measures in Table 8, it can be concluded that except for the *MSC 2112* the model performance is sufficient. The change in performance between calibration and validation is twofold: while for the *MSC 2044* and *2112* a slight increase of the model efficiency and volume error can be noticed, for all other catchments the performance remains the same or even decreases. However, the transitions are marginal.

6.2.2 HBV Model Calibration and Validation Versions B and C

It has already been pointed out in the methodology that the results from the standard deterministic-probabilistic approach used (*Version A*) do not fully meet the expectations. In contrast to the meteorological analysis, relatively small ensemble spreads are present in the hydrographs. For this reason, two further simulation approaches are applied: *Version B* is calibrated and validated with swapped time period whereas *Version C* is calibrated with the ensemble data set *RhydchprobD* and validated with the *RhiresD* data set. The accuracy of these simulation alternatives for each *MSC* is compared to each other using three different approaches. The first approach analyses the model efficiency measure. Figure 39 shows these measures for the different simulation versions. From the scattered points on the y-dimension it can be seen that the runoff for the individual *MSCs* is generally simulated with very different accuracy. However, the results differ only minimally between the simulation *Versions A, B* and *C*, visible in the slightly different values on the x-dimension. It should be noted in particular that the efficiency of *Version A* and *C* does not differ in all *MSC*. In some cases, the results in the *Version B* are slightly lower (*MSC 2386, 2126, 2112*) or higher (*MSC 2374*) than *A* and *C*. Overall, the simulation results of the different approaches lead, however, to very similar results. The second approach focuses on the comparison of the parameter sets. The analysis of the parameter sets resulting from the *GAP*-calibrations and used for the simulations leads to the conclusion that no significant patterns can be found both between the *MSC* and between the approaches A, B and C (see appendix *A.1 Additional Illustrations* Figure 67). All parameters spread over the predefined range. Finally, several measures such as the average observed and simulated runoff, observed and simulated time to peak or number of runoff peak events are compared. All this analysis shows very similar behaviour which underlines the similarity of the simulation results.

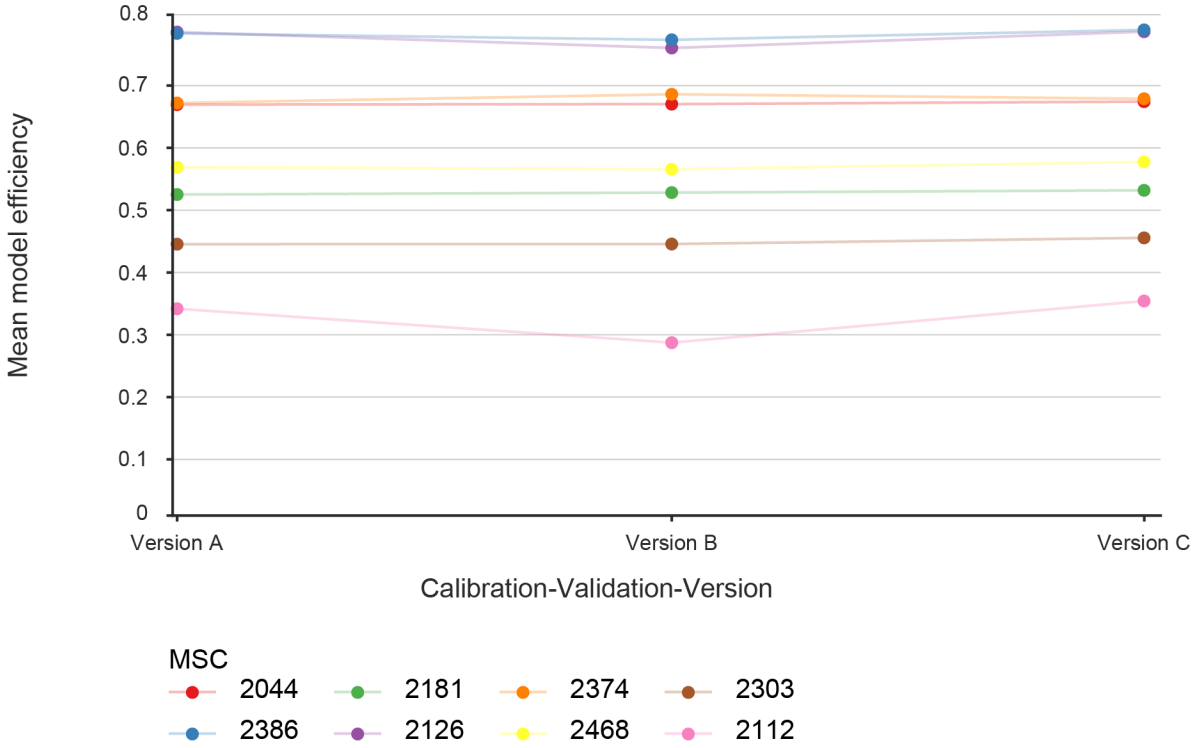

Figure 39: Model efficiencies for the various calibration-validation-versions per MSC.

6.3 Hydrological Data Analysis

The results of *HBV* simulations are runoff estimates for all *MSCs* for 17 hydrological years (1999 to 2016). The following sections focus on the variability analysis of these outputs. In a first step (*6.3.1*), the deviation of simulated and observed values is described. The absolute deviation is complemented by two descriptive measures for runoff events, namely t*ime to peak* and *event duration*. Both are used to characterise the performance of the probabilistic data set in hydrological simulations compared to observed values. The accuracy quantification is followed by the inter- and intra-ensemble variability analysis of the runoff data using the measures absolute and relative ensemble spread. This second part (*6.3.2*) puts the runoff simulation uncertainties in the context of space (*MSC*) and time (seasons). In a third part (*6.3.3* and *6.3.4*), it is investigated whether the precipitation variability correlates with the runoff variability. The focus thereby lies on two special subsets: the runoff behaviour is specifically observed on the five days prior to a runoff peak and during heavy precipitation events. In the final part (*6.3.5*), the coincidence of the deterministic (*RhiresD*) and the probabilistic data set (*RhydchprobD ensemble mean*) are identified analogue to the meteorological analysis.

6.3.1 Runoff Deviation

The consistent model performances <1.0 listed in chapter *6.2.1 HBV Model Calibration and Validation Version A* already give evidence of deviating simulation values (Q_{sim}) from the observed runoff values (Q_{obs}). On average the simulations underestimate the runoff by 1.05 mm per day (5^{th} percentile = −0.91 mm per day, 95^{th} percentile = 4.40 mm per day; negative values indicate

higher simulation than observed values). Only in 20% of the simulations the runoff is overestimated (20th percentile = 0.08 mm per day). The model efficiency in the previous section showed a weak size-dependent performance, which is why such a dependency is questioned also for the deviation. Although a dependency of the deviation on *MSC* size could be expected, the analysis contradicts this assumption. The comparably equally-sized *MSC 2126, 2374* and *2112* show very different mean deviations (Figure 40): (a) the simulated runoff values in *MSC 2126* differ only slightly from the observed runoff with the highest deviation in winter (0.39 mm per day), while (b) the simulations in *MSC 2374/2112* deviate up to 1.11/3.18 mm per day from the observations in spring/fall. The deviation in the entire catchment *MSC 2044* with an annual average of less than 1 mm per day is comparably small. Still, there remain some noteworthy correlations. On the one hand, from a spatial perspective the runoff in mountainous catchments is, according to the deviation results, more uncertain to simulate. Even though the mean elevation of *MSC 2181* is not that high, it extends over the *MSC 2374, 2468, 2303* and *2112* and thus it remains more complex to simulate the runoff. On the other hand, from a temporal perspective, the simulated values are generally higher underestimated in spring and summer months, when the majority of snowmelt flows down the streams and overlaps with an accumulation of precipitation occurrence.

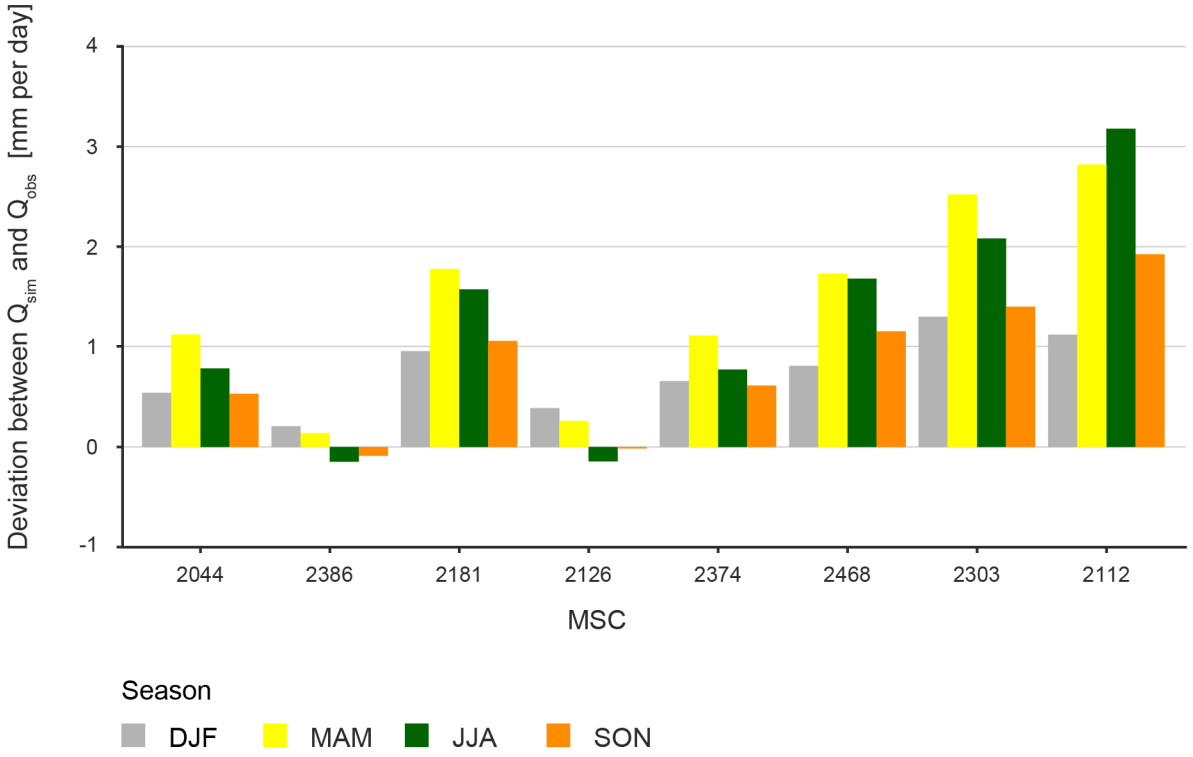

Figure 40: Average deviation between simulated to observed runoff per season and MSC. *A positive deviation illustrates higher observed runoff values compared to simulated values whereas a negative deviation indicates on average higher simulated runoff values compared to observed values.*

Runoff Peak Event Characteristics

The previous sections have analysed the difference of Q_{sim} and Q_{obs} on a daily basis. Since the runoff is a complex system (e.g. Gobiet et al. 2014) and often has a reaction time of several days (EEA 2009), the differences between the simulated and observed values are examined on a larger temporal scale. Based on the same precipitation period classification as in the meteorological analysis (see chapter *5.3.1 Precipitation Event and Period*), the difference between the simulated (probabilistic data set mean) and observed runoff peak event characteristics are examined.

Figure 41 and Table 9 show that the simulation and observation do not significantly distinguish in terms of *time to peak*.

Table 9: Time to runoff peak simulated and observed. *The 5th, 50th and 95th percentile values are listed for the observed as well as the simulated data.*

	observed	**simulated**
5th percentile	1 day	1 day
50th percentile	2 days	3 days
95th percentile	9 days	10 days

The range of *time to peak* is slightly higher during the above average wet year 1999 compared to the other exemplary years 2003 and 2013. Nevertheless, the median value of *time to peak* does neither differ between observed and simulated runoff nor between the individual years. Additionally, no differences in the median *time to peak* values between the *MSCs* can be detected although several outliers exist for example in the *MSC 2044* and *2374*.

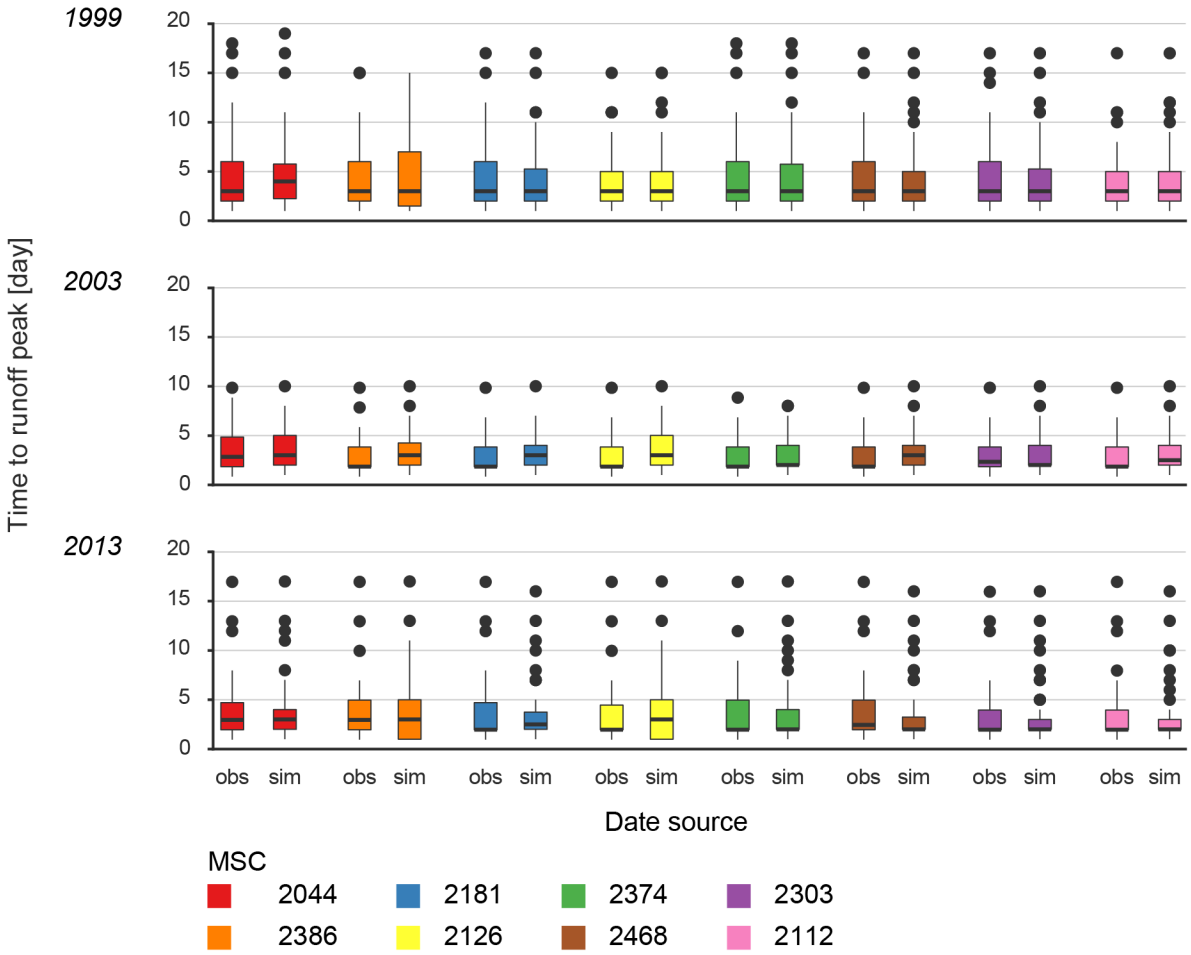

Figure 41: Time to runoff peak observed and simulated during the hydrological years 1999, 2003 and 2013 per MSC.

The previous results have shown that there are no significant differences in observed and simulated *time to peak* intra-annually and within the *MSCs*. In contrast, temporal patterns become visible in the values on a monthly consideration. For the monthly differentiation, the day of precipitation

start per event is decisive. Figure 42 illustrates the negligible difference of Q_{sim} and Q_{obs} on a runoff peak event scale. The inclination of the lines is independent of seasonality very close to 1. But the perspective reveals a dependency of *time to peak* on the *duration of precipitation period* and the *precipitation sum*. Runoff events with a *time to peak* less than five days (which cover 83% of all runoff events) last on average for three days (95th percentile = 13 days) with an intensity of 13.5 mm per day (95th percentile = 43.3 mm per day). Those events are visualised in small, light green points in the lower left corner in Figure 42. The remaining 17 % of the runoff events are characterised by an average precipitation amount of 46.6 mm (95th percentile = 132.5 mm) over a period of eight days (95th percentile = 19 days). By far the highest values are recorded in June, illustrated in dark green, larger bubbles. In summary, this means that a prolonged precipitation period is linked to a larger *precipitation sum* and causes a delay in the *runoff peak*.

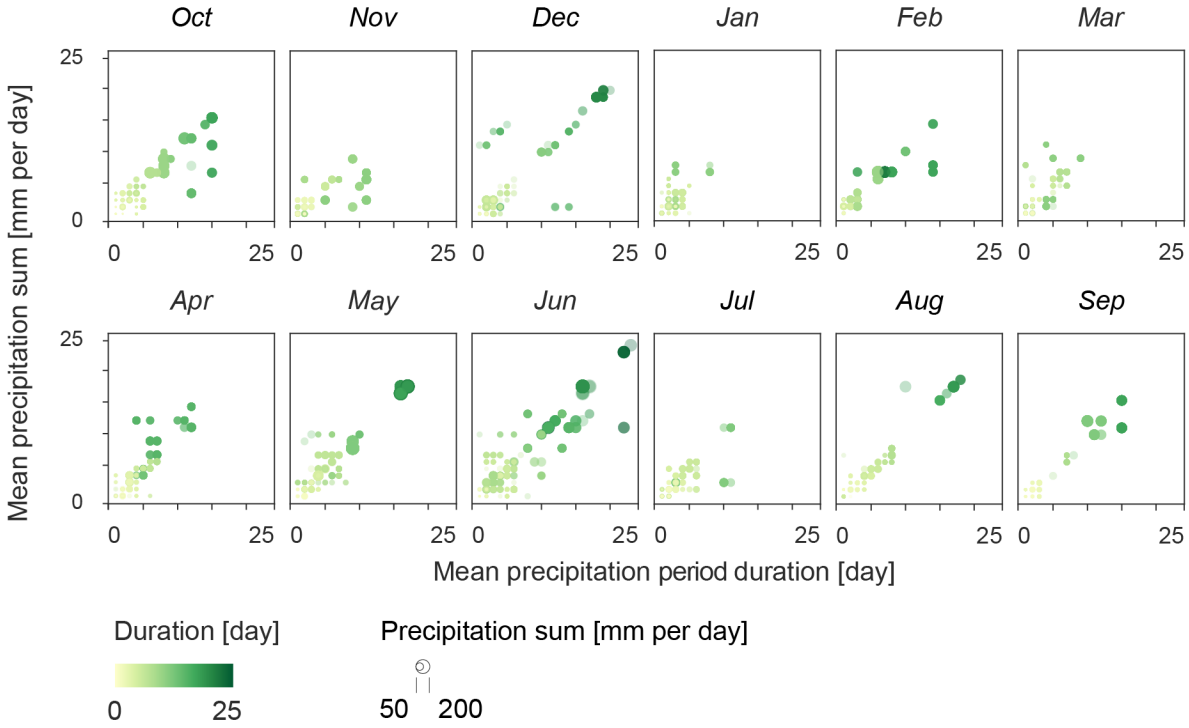

Figure 42: Precipitation periods during the hydrological years 1999, 2003 and 2013 as a function of precipitation sum and duration. *The precipitation periods are illustrated with the corresponding probabilistic data set mean of precipitation sum (size) and duration (colour).*

The statistical differentiation of the *time to peak* analysis on monthly basis looks consequently slightly more variable (Figure 43). In January 90% of all runoff peaks (between 5th and 95th percentile) are reached on average within two days (value range of one to six days), whereas in August it takes on average three days to reach the *runoff peak*. However, this period is increasingly delayed by up to 17 days (95th percentile in *MSC 2044*). The similar temporal pattern within the *MSC*—although with slightly different value ranges—suggests that the variability of *time to peak* depends heavily on seasonality rather than on catchment size and topography. This observation is similar to the difference found between Q_{sim} and Q_{obs}.

Figure 43: Simulated time to runoff peak per MSC and month. *The figure shows the spatio-temporal patterns of the time between the first precipitation and the following runoff peak.*

While the time span from first precipitation record to the *runoff peak* has been analysed previously, the relationship between the day of the *precipitation peak* and *runoff peak* is analysed in the following part. This relationship is graphically shown in Figure 44, in which the entire precipitation period is visualised as a black line and the moment of the *runoff peak* as a point. In addition, the *runoff peak* is marked depending on the *duration of precipitation* (colour) and the *runoff peak flow* (size).

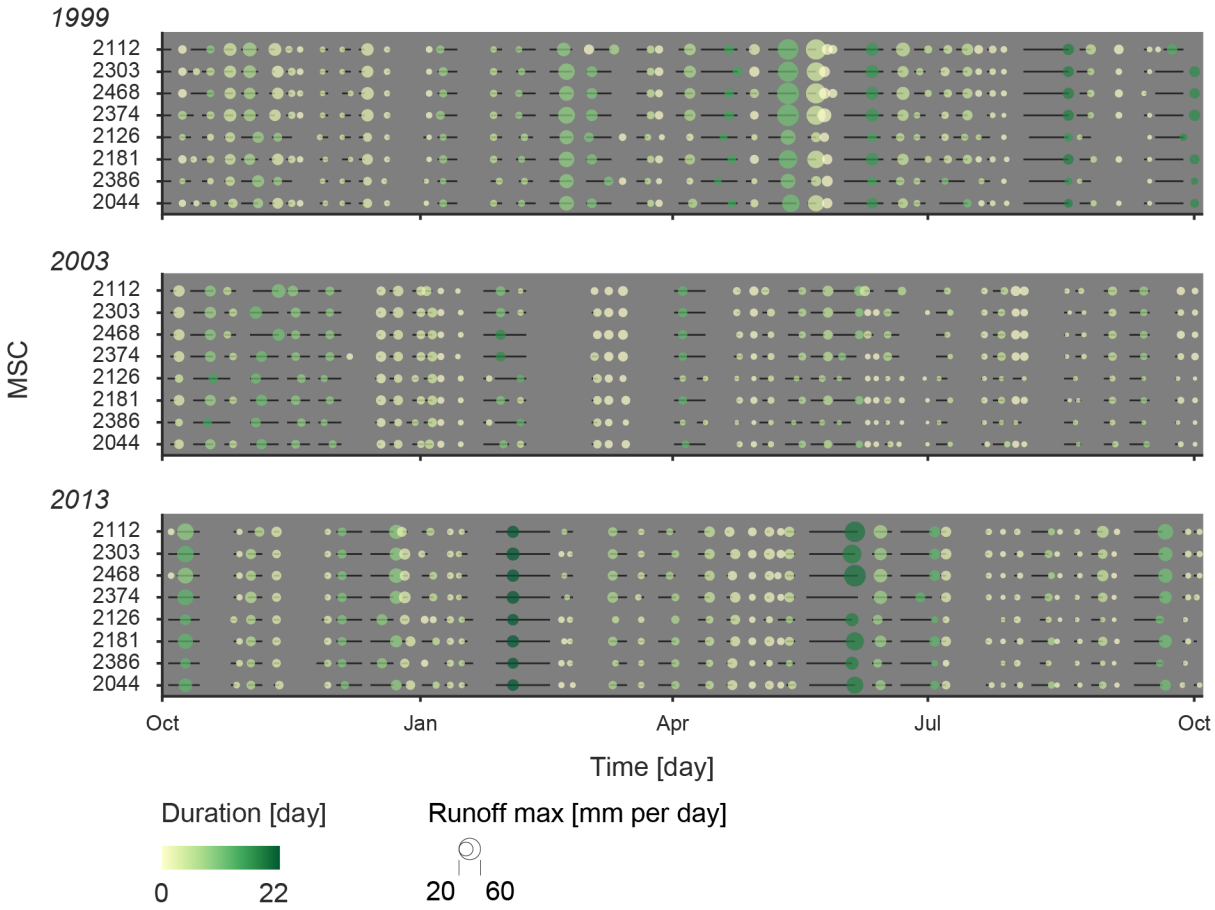

Figure 44: The influence of precipitation periods on runoff. *The entire precipitation period is visualised as a black line and the moment of the runoff peak as a point. In addition, the runoff peak is altered depending on the duration of precipitation (colour) and the runoff peak flow (size).*

The character of precipitation periods is highly variable and can be described with several parameters. Aside from the *duration* of an event and the *time to runoff peak*, the time at which a large amount of precipitation is discharged into the runoff is of great importance for risk mitigation. For this reason, the *time lag of precipitation to runoff peak* is calculated. Figure 45 illustrates the distributions for observed and simulated values. The simulations do not distinctively differ from the observation. In both analyses, the median time lag value is two days, i.e. in half of the precipitation periods the runoff peak is delayed by two days to the precipitation peak. Nevertheless, the observed time lag values are often 1 day longer. The higher value for the observed values in almost all *MSCs* indicates that the simulation predicts the runoff peak somewhat earlier. This finding is underlined by the distribution of values in Figure 46. Unlike the *time to peak*, the Figure 46 also illustrates that the *time lag* is not significantly dependent on seasonality, nor on the sum of precipitation per precipitation period. Only a slight tendency towards longer events for larger *time lags* is observable for the months March, June, July, August, September and December. It is further noticeable that 5% of the events have a negative *time lag* of two days on average. This case occurs when the runoff peak is recorded on average two days prior to the precipitation peak. On closer inspection, it is apparent that such a relationship exists especially in the combination of long-lasting events (on average 7 days) and low precipitation sum (on average with 22 mm per period).

Figure 45: Time lag between precipitation and runoff peak during the hydrological years 1999, 2003 and 2013 calculated with the simulated and observed data per MSC.

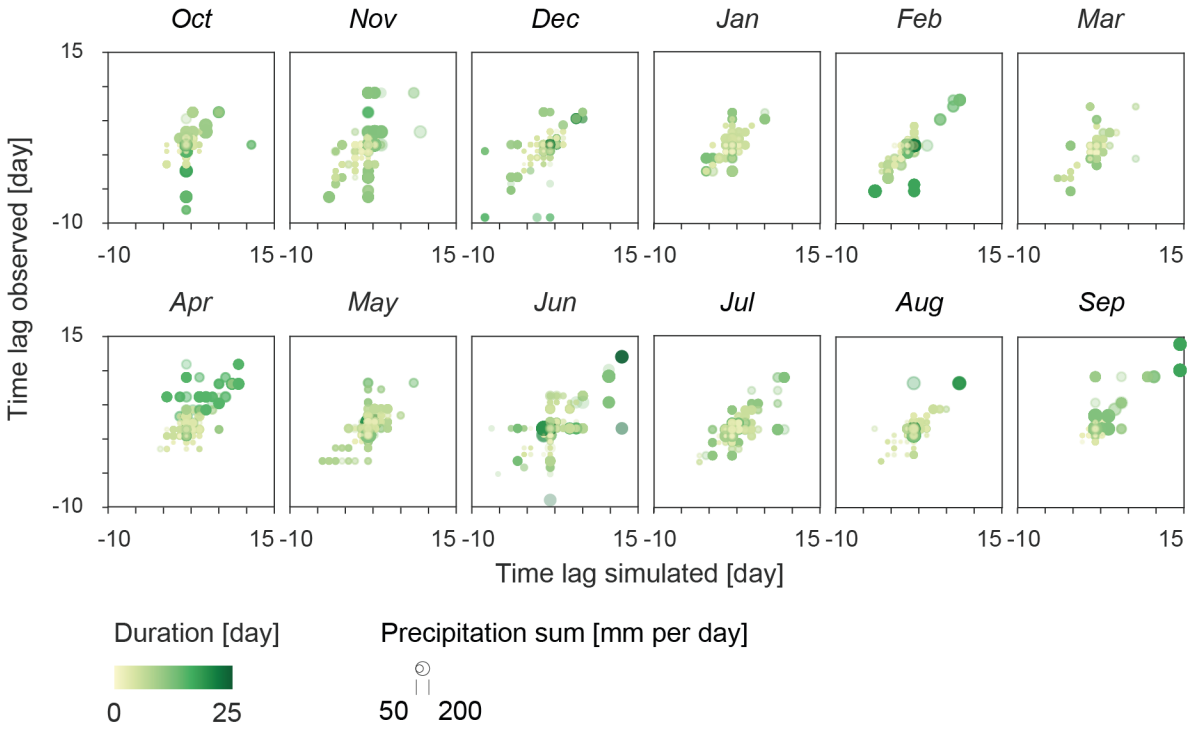

Figure 46: Precipitation periods as a function of the time lag between precipitation and runoff peak observed and simulated. *The precipitation periods are illustrated with the corresponding duration (colour) and precipitation sum (size).*

From the parameters presented, it can be concluded that the simulations underestimate the runoff values in general and particularly often in the summer months. Considering the runoff behaviour during the precipitation periods, it becomes apparent that the *time to runoff peak* is delayed with increasing *duration* of a precipitation period. This dependency also increases during the summer months. However, the *time lag of the precipitation and the runoff peak* is not strongly influenced by seasonality and precipitation sum.

6.3.2 Variability of Daily Ensemble Run Simulations

Only minor differences between the observed and simulated runoff characteristics exist. The ensemble run variability in simulations has been excluded in the analysis until now. In this section, one of the major advantages of the probabilistic data set, namely several equally realistic interpolations, will be used to characterise the uncertainty of the runoff simulation. For this purpose, the general course of absolute and relative spread of the ensemble realisations is examined. From the statistical key figures (Table 10) and visual inspections (Figure 47), it becomes apparent that both absolute and relative ensemble spread yield very low values. While the median and the corresponding 95th percentile minimum/maximum values for the absolute spread are in the same *MSCs*, the respective values for the relative ensemble spread differ.

Table 10: Minimum and maximum variability within the simulated runoff values. *The variability values of the 50th and 95th percentile are given as absolute and relative ensemble spread.*

	absolute spread min	**absolute spread max**	**relative spread min**	**relative spread max**
50th percentile	0.03 mm per day (*MSC 2044*)	0.07 mm per day (*MSC 2374*)	0.02 mm per day (*MSC 2112*)	0.04 mm per day (*MSC 2126*)
95th percentile	0.22 mm per day (*MSC 2044*)	0.58 mm per day (*MSC 2374*).	0.07 mm per day (*MSC 2044*)	0.18 mm per day (*MSC 2374*)

Although the ensemble variability is very small and thus less clear patterns could be assumed, several patterns in the simulated runoff can be observed. On the one hand, seasonal and spatial patterns are identifiable. As in other analysis, the absolute and relative ensemble variabilities are above average during the summer months July and August as well as in areas at higher elevations (*MSC 2374, 2468* and *2112*). On the other hand, the runoff variability does not show, identical to precipitation period analysis, a clear dependency on *MSC* size. For example, the *MSC 2386* and *2468* are of almost equal size but the *MSC 2386* is at the lower limit and the *MSC 2468* at the upper limit of variability range. Nevertheless, their variabilities do not clearly differ from the characteristics of other *MSCs*.

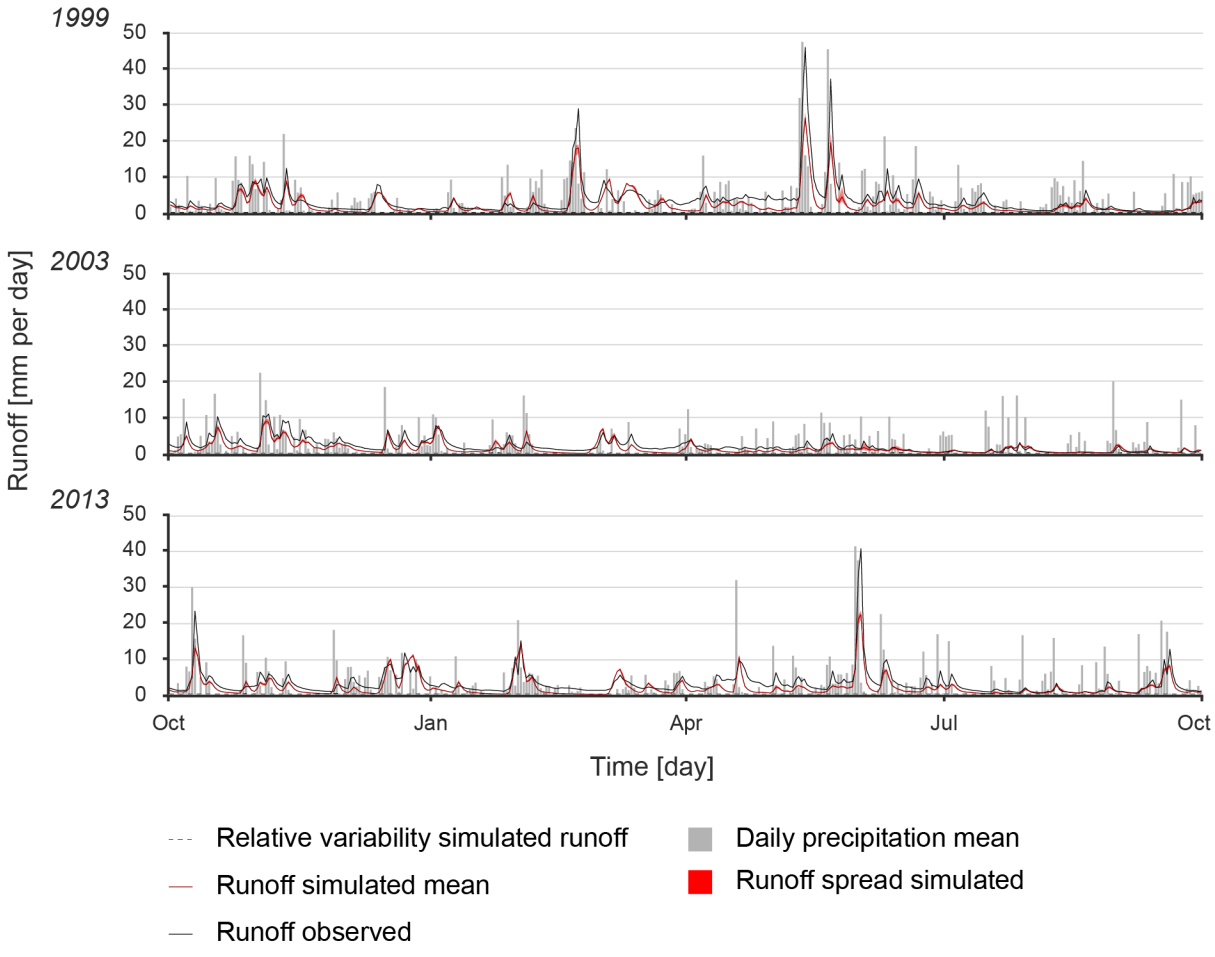

Figure 47: Daily precipitation and runoff during the hydrological years 1999, 2003 and 2013 for the MSC 2044 (Andelfingen). *The figure shows the reaction of the runoff to precipitation occurrences. The observed runoff (black) is on average higher than the mean simulated runoff (red). The red band gives indication to the value range of the simulated runoff values. The corresponding relative variability is shown as a black dashed line.*

In the following the focus lies on the spatio-temporal correlation of runoff variability. That the majority of spread values lies below 0.5 mm per day can divert from the fact that spatio-temporal trends exist (Figure 48). If the runoff volume is combined with the absolute runoff spread, it is possible to show correlations to (a) the mean elevation and thus from a spatial perspective; (b) seasonality as well as (c) spatio-temporal relationships.

(a) The ensemble spread shows values above 0.5 mm per day more frequently in the four catchments with higher mean elevation (*MSC 2374, 2468, 2303, 2112*).

(b) In winter months, the dispersion of runoff values in relation with ensemble spread is more diverse, whereas less runoff events of moderate intensity with a low absolute ensemble spread are discerned during summer months.

(c) Generally, the absolute (relative) variability increases (decreases) with higher runoff volume, independently of seasonality and elevation. The highest absolute variabilities almost always arise with a comparatively high runoff volume of above 10 mm per day. Very intense runoff events, however, are not the responsible events for these high absolute variability values. The relative ensemble spread, for which the absolute ensemble spread is normalised by its mean runoff, illustrate this relationship (Figure 48). The curves exponentially decrease from high relative variability at events with low runoff towards low relative variabilities at intense runoff events. The majority of relative ensemble spreads behave almost the same for all months. One exception occurs in July, where the same spatio-temporal differentiation from lowlands and mountainous areas as in the absolute ensemble spread is identifiable. However, if the spatio-temporal patterns are differentiated between lower-lying and alpine areas, differences become apparent. While from December to April the cluster of absolute ensemble spreads in higher elevation areas is considerably below 0.5 mm per day with a mean runoff of below 10 mm per day, the majority of runoff events show an average absolute ensemble spread of 0.5 mm per day with the same average runoff intensity. The maximum absolute ensemble spread of approximately 1.5 mm per day is recorded in August. In comparison to the higher-lying areas, the small absolute variability in July stands out in the lowlands. The average variability value is only 0.25 mm per day and reaches at maximum a value of 0.7 mm per day, which is about half as much as the value in higher elevations.

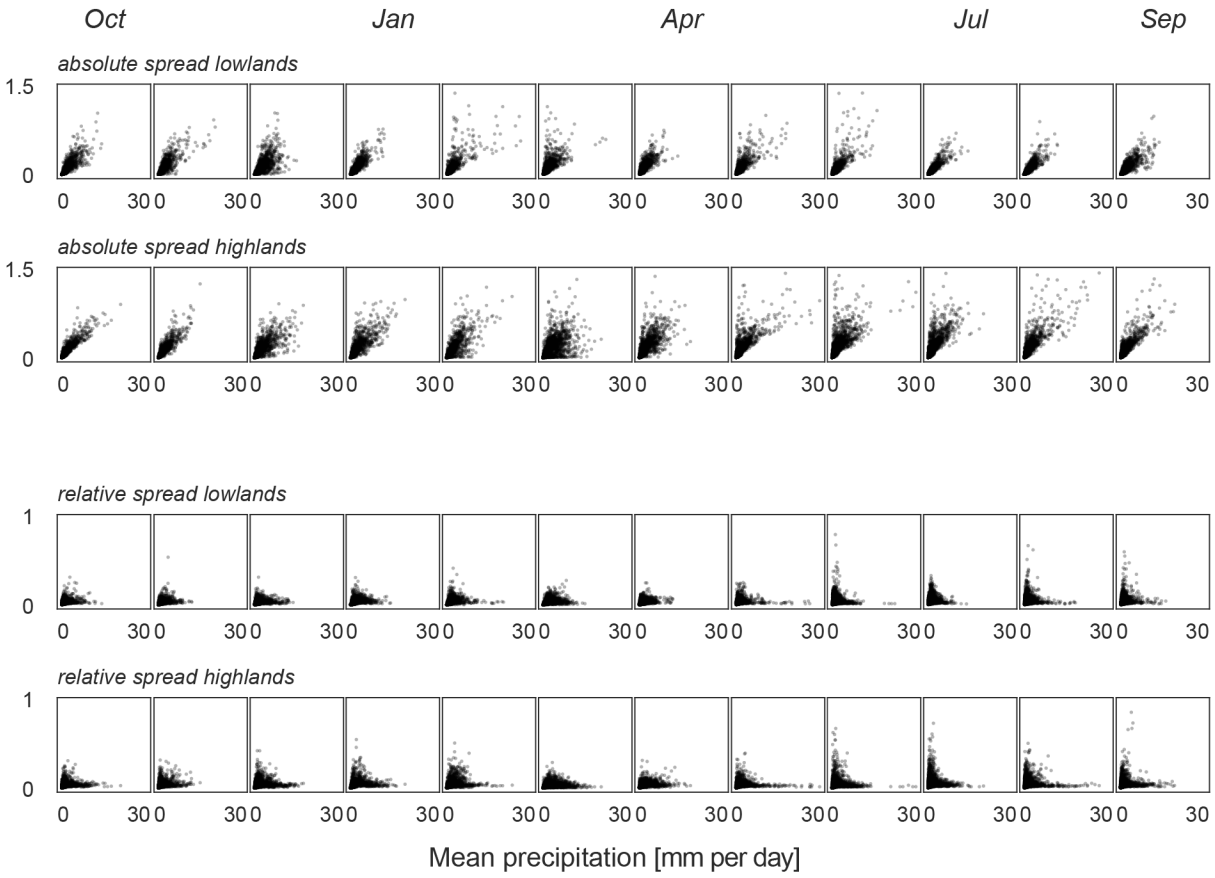

Figure 48: Daily runoff as a function of precipitation sum and variability over the entire study period. *The absolute and relative variability values per month for the lowlands (MSC 2004, 2386, 2181, 2126) and highlands (MSC 2374, 2468, 2303, 2112).*

Precipitation vs. Runoff Spread

The precipitation spread in chapter *6.1.2 Precipitation Variability within Ensemble Runs* and the runoff spread in the previous section have been analysed separately. The combined analysis substantially contributes to the question of advantages from probabilistic data in hydrological modelling. The applied precipitation-runoff-data show an average *time lag* between precipitation occurrence and increasing runoff of three days. Because of this dependence, a *time lag* of three days is applied to the precipitation data to analyse the impact of precipitation change on runoff. The temporally shifted curves resulting from this modification are illustrated in Figure 49. The comparison of the related values shows three main findings:

(1) the relative uncertainty of the runoff is almost always smaller than the relative precipitation uncertainty; (2) a noticeably high runoff simulation uncertainty occurs mostly in correlation with a high precipitation estimation uncertainty; (3) conversely, a high precipitation ensemble spread is not necessarily accompanied by a high runoff ensemble spread.

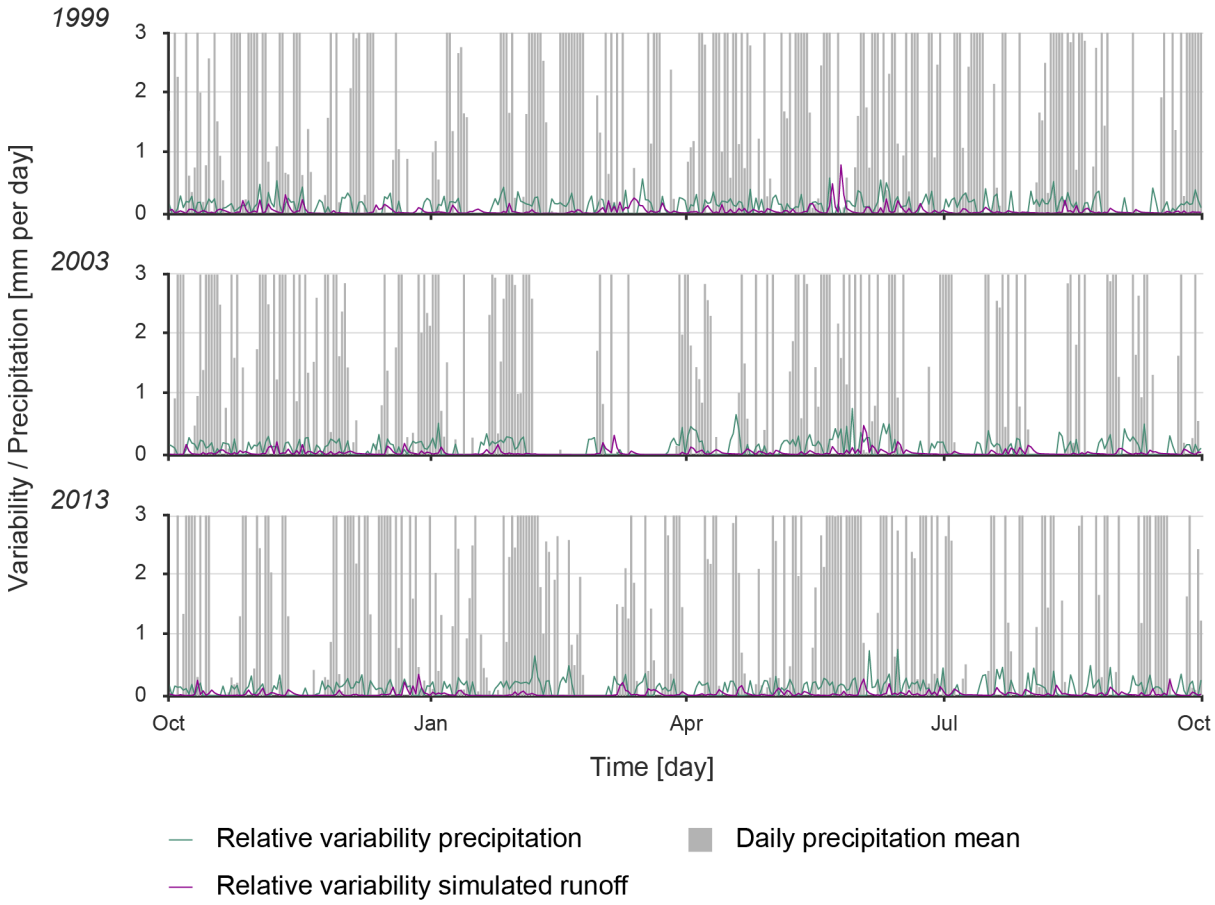

Figure 49: Relative variability of precipitation and simulated runoff during the hydrological years 1999, 2003 and 2013 in the MSC 2044 (Andelfingen). *For a better comparison of the impact of precipitation on runoff changes, the precipitation data has been moved forward by three days. Because the value range for precipitation sum is a lot larger than for the variability, the visualisation zooms in to a range of 0 to 3 mm per day to show the behaviour of the relative variabilities.*

Figure 49 unveils a problem of long data time series for very irregular occurrences: the quantity of runoff events with on average low to moderate ensemble variabilities distract from the fewer events with large variabilities. Low to moderate ensemble variabilities often go along with days without precipitation, whereas the variability usually increases with the presence of precipitation. However, since it is precisely the events with high variabilities that are of great interest and often entail great risk, a differentiated analysis of the spread behaviour prior to and during the runoff peak day is apposite. The classification of such runoff peaks, according to the methodology described in chapter *5.5.3 Variability of Ensemble Runs within 5 Days prior to Runoff Peak*, is exemplified in Figure 50.

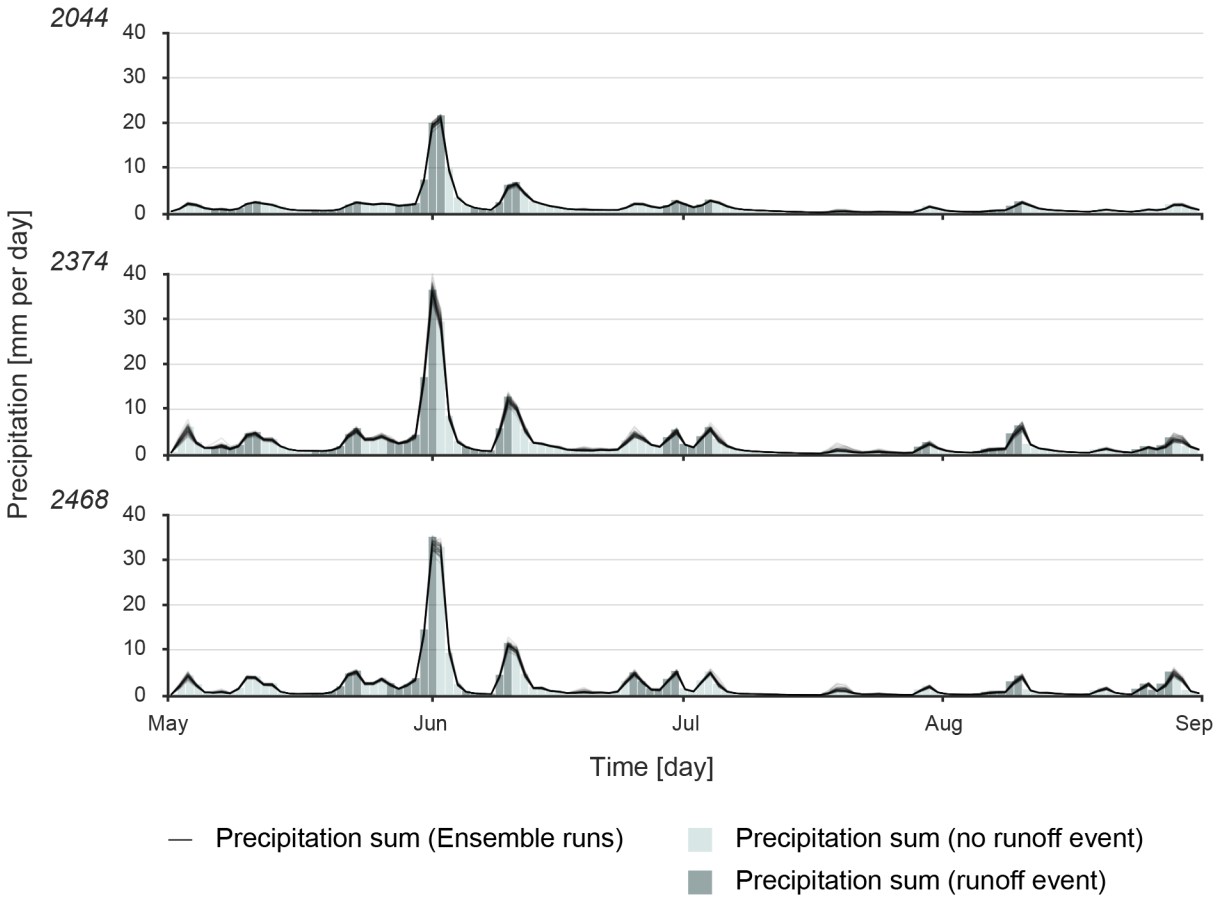

Figure 50: Exemplary visualisation of runoff peak events in the MSC 2044, 2374 and 2468 during the summer months of 2013*. Five days prior to a runoff peak are considered to display the behaviour of the simulated runoffs.*

The interaction of runoff and precipitation within five days prior to a runoff peak can be described as a function of ensemble variability and precipitation sum or range (Figure 51 and 52). The development of the ensemble spreads depending on precipitation sum and precipitation range does almost only differ in the level of ensemble spread. The amplitude of the precipitation spreads shown in dependence on precipitation sum is twice as large as the depending on precipitation range. Due to the similar patterns, only the development of the spread values that depend on precipitation sum will be discussed in the following. In the same way as the results of daily precipitation variability, the absolute precipitation and runoff spread increase with a higher precipitation sum whereas the relative spread decreases. The following patterns, subdivided (a) in terms of measure and course as well as (b) in terms of space, can be observed.

(a) On the one hand, the general behaviour of the spread values differ depending on measure (absolute/relative spread) and process (precipitation/runoff). The absolute ensemble spread of the precipitation is always higher than the one of the runoff, whereas the relative regression lines cross each other at a precipitation rate of approximately 25 mm per day in all *MSCs*. The regression curves of the absolute variability analysis exceed its maximum of 5 mm per day with a precipitation of about 150 mm per day in the *MSC 2374*. This value is not corresponding to the highest measured precipitation value. For very high precipitation sum (>150 mm), the absolute spreads slightly decline in all *MSCs*. In contrast to the absolute precipitation regression lines, the regression lines of the relative precipitation spread exponentially decrease from 0.25 to 0.05 mm per day below a

precipitation of 50 mm before decreasing at a constant level towards 0 mm per day. Even though a clear increasing and decreasing pattern of variability for precipitation is noticeable in both measures, these uncertainties are not directly transferred to the runoff values. The absolute runoff ensemble spreads steadily increase up to only 1 mm per day, while the relative runoff ensemble spreads do not peak as a function of the lowest precipitation levels comparable to the relative precipitation spread. The relative runoff ensemble spreads rather increase to a maximum of 0.1 mm per day on average with moderate precipitation (approximately 50 mm per day) before they slowly diminish towards 0 mm per day. Finally, it should be noted that with precipitation higher than 25 mm the relative runoff spread is larger than for the relative precipitation spread in contrast to the absolute values.

(b) On the other hand, spatial differences exist. There are almost no spatial differences in absolute variability of precipitation and runoff as a function of the precipitation sum, whereas the relative variability differs. With lower precipitation values (<25 mm), the relative runoff spreads are generally smaller than the relative precipitation spread and are comparatively very small for the *MSC 2044, 2181* and *2303*. For the *MSC* 2386, however, the relative runoff spread is the same as the precipitation spread.

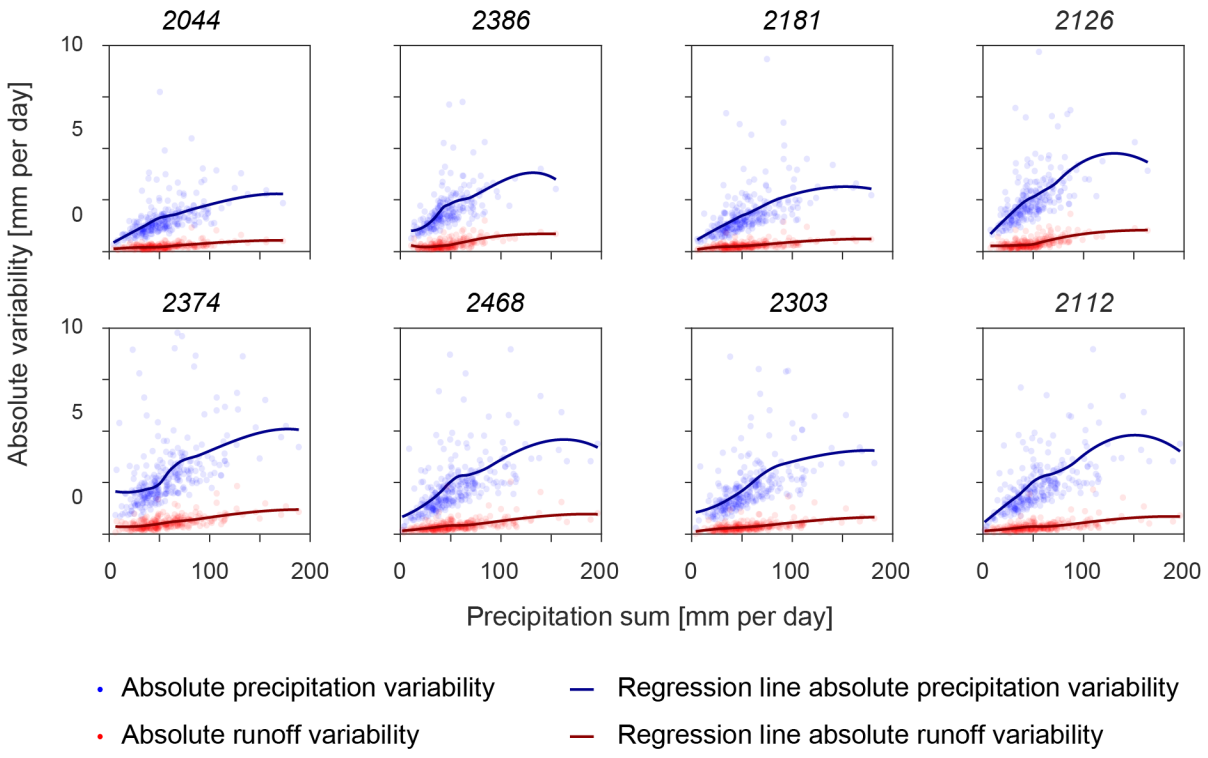

Figure 51: Precipitation and runoff values five days prior to a runoff peak as a function of absolute variability and precipitation sum per MSC. *The regression lines of the precipitation (blue) and runoff (red) values summarise the development depending on the absolute variability and the precipitation sum. In general, both lines show a positive correlation.*

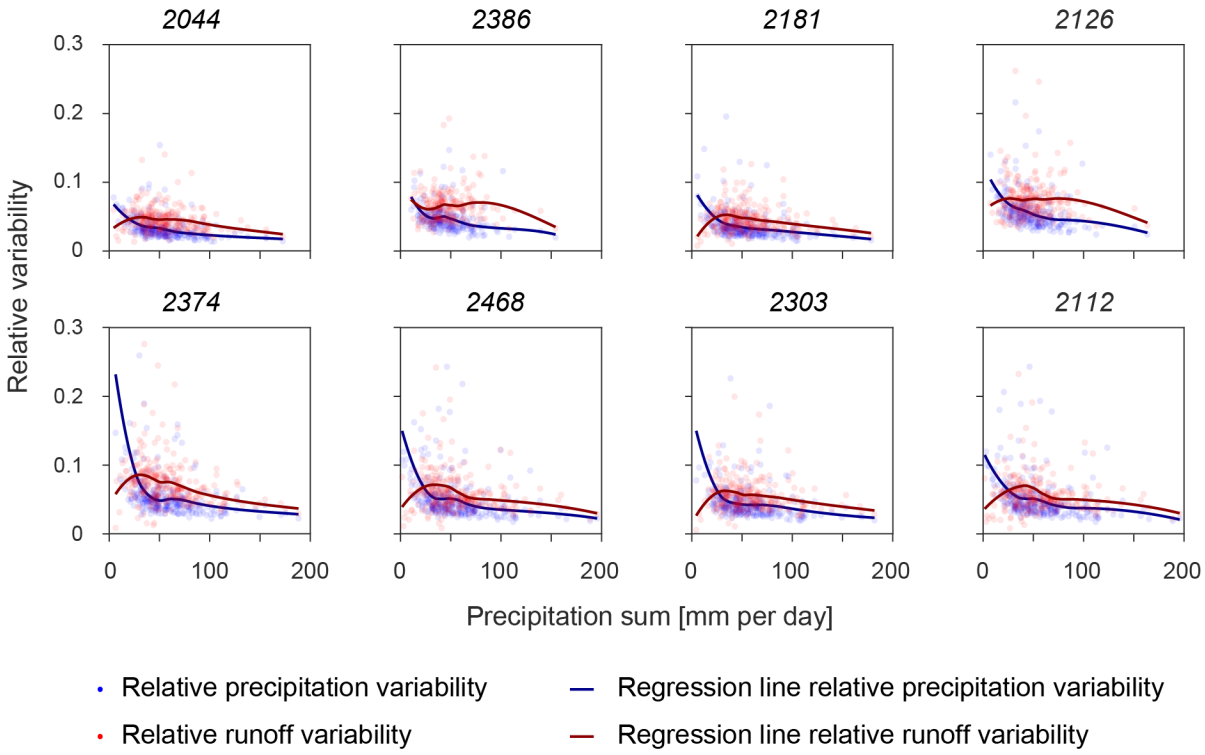

Figure 52: Precipitation and runoff values five days prior to a runoff peak as a function of relative variability and precipitation sum per MSC. *The regression lines of the precipitation (blue) and runoff (red) values summarise the development depending on the relative variability and the precipitation sum. In general, both lines show a negative correlation.*

Because a detailed knowledge of the runoff peak behaviour as a consequence of precipitation occurrence helps to interpret the runoff uncertainties, the relationship of the runoff (y-axis), runoff range (colour, line) and precipitation (x-axis) within the same five pre-peak days is pointed out in Figures 53 and 54. The runoff range is visualized with a fine line and a dot coloured in the corresponding range colour at the level of the simulated runoff. The runoff simulations give no indication of the presence of snow, which is why the following results are limited to the months May to October. Over the validation period of 17 years, between 102 (*MSC 2386*) and 155 (*MSC 2374*), runoff peaks are addressed during these months. The highest peak levels are thereby simulated for *MSC* with higher mean elevation (*MSC 2374, 2468, 2112*). It can be observed that a larger runoff peak range over all correlates on the one hand with a higher runoff and on the other hand with a higher precipitation amount.

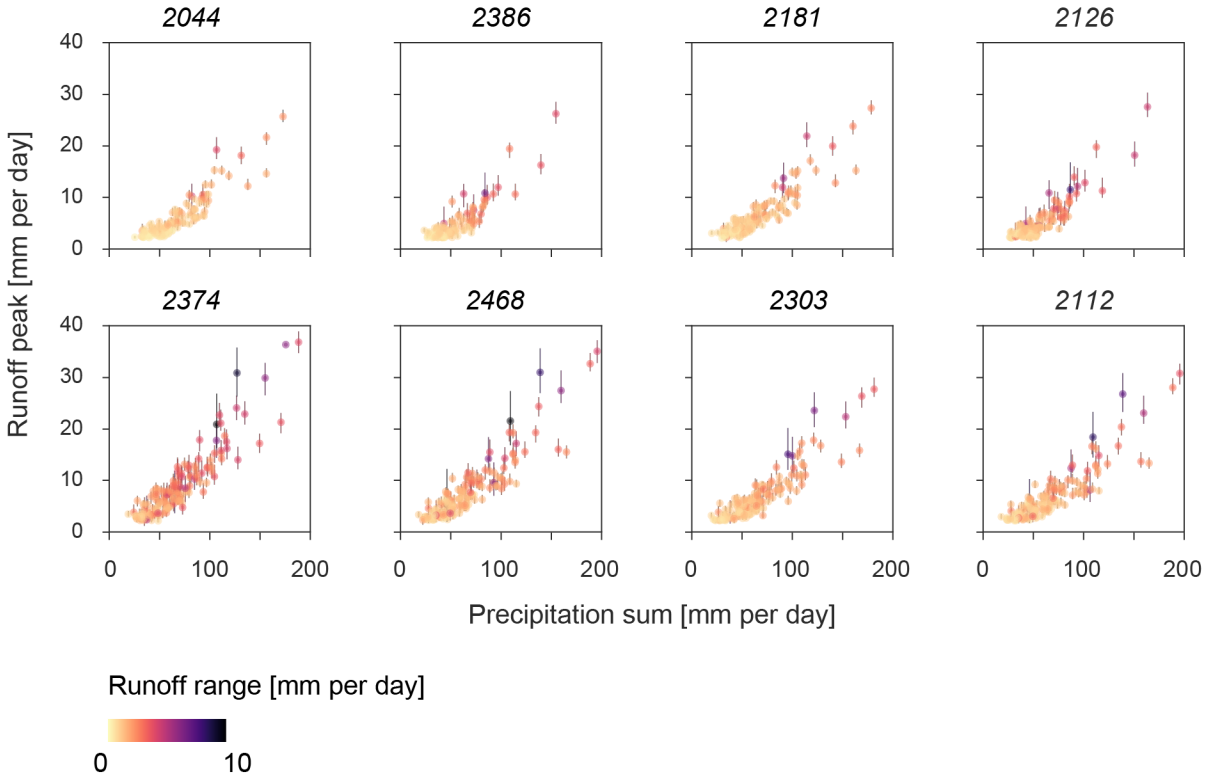

Figure 53: Runoff events five days prior to a runoff peak as a function of runoff peak and precipitation sum per MSC. *The vertical line and the colour of the runoff peak indicate the value range of the runoffs during the consideration period of six days (five days prior to runoff peak and runoff peak itself). The data is limited to the months May to October.*

To take these plots into differentiated consideration, the events with the lowest and highest ensemble run variability (10^{th}/90^{th} percentile) are analysed individually. The low runoff ranges go along with small precipitation intensities (lower left corner). There are clear spatial differences between the *MSCs* in the number of detected runoff values corresponding to low ensemble run variability. While up to 35 runoff values in the areas with a lower mean elevation (*MSC 2044, 2386, 3281*) are below the 10^{th} runoff range percentile, only a few runoffs with a low range are recorded in the higher elevation areas (*MSC 2126, 2468, 2303, 2112*). The slightly increased number of runoff values in *MSC 2303* is certainly due to the size of the subcatchment area, as it includes *MSC 2374, 2468* and *2112*. The reverse observation can be made for the distribution of runoff values with the highest runoff ranges: the number of runoff values above the 90^{th} percentile is generally increasing in the mountains (*MSC 2126, 2374, 2468, 2303* and *2112*). In contrast to the low runoff range distribution, the largest runoff ranges occur both at small runoff values and low precipitation as well as at high runoff values and high precipitation.

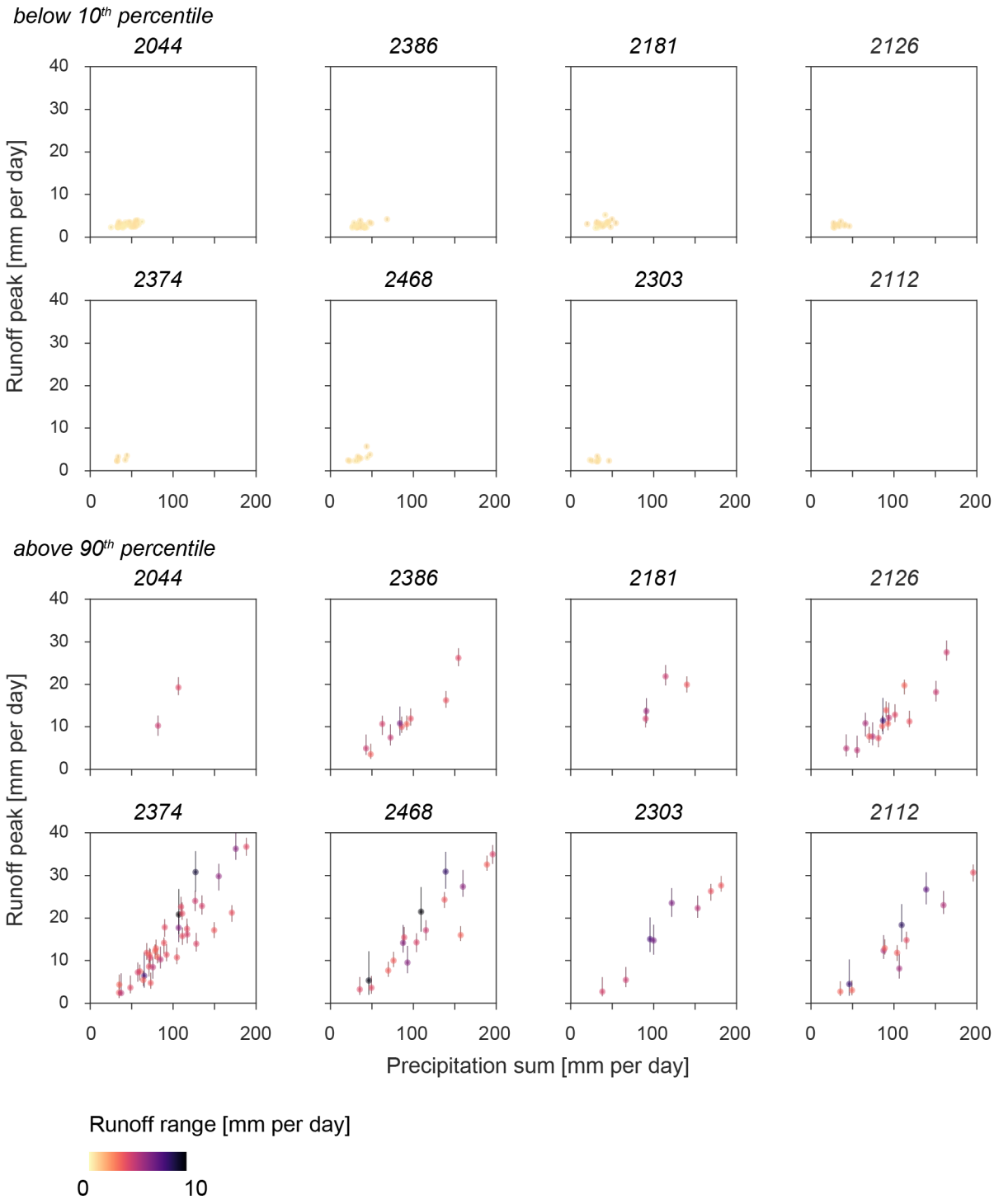

Figure 54: Runoff events five days prior to a runoff peak as a function of runoff peak and precipitation sum per MSC with a runoff range below the 10th percentile and above the 90th percentile respectively. *The vertical line and the colour of the runoff peak indicate the value range of the runoffs during the consideration period of six days (five days prior to runoff peak and runoff peak itself). The data is limited to the months May to October.*

6.3.3 Variability of *Ensemble Runs* within 5 Days prior to Runoff Peak

The timely restricted precipitation and runoff data to the 5 days prior to a runoff peak enabled statements about the interaction of the parameters *precipitation sum*, *runoff intensity range* and *ensemble variability*. Because of this relation, the subset of days within a time window of five days prior to a

runoff peak already used in the previous section is further investigated. In previous sections, the influence of the storage capacity of soils on the runoff has been shown. One of the indications to storage capacity in the different *MSCs* is the *runoff coefficient*. To simplify the analysis, the coefficient is only shown for the probabilistic data set mean. Therefore, in this case, the term «variability» is related to the temporal and spatial differences of runoff events and not to the inter-ensemble uncertainty. A *runoff coefficient* equal to 1 implies that the total precipitation amount is converted into runoff and 0 that none of the precipitation volume is transferred to runoff. The majority of the *runoff coefficients* is smaller than 0.5. Figure 55 illustrates the seasonal as well as spatial differences of the coefficient. In terms of seasonality, the *runoff coefficients* are comparably higher in all *MSCs* during winter months. Occasionally values above 1 can be observed where the precipitation sum is larger than the runoff. Such events occur mainly in the higher areas of *MSC 2374, 2468, 2303* and *2112* in January to March. In contrast, the lowest mean *runoff coefficient* is calculated for July. From a spatial perspective, it is noticeable that the *MSC 2374* and *2468* have in principle slightly higher average values than the other *MSCs*, a fact that will be taken up at a later stage.

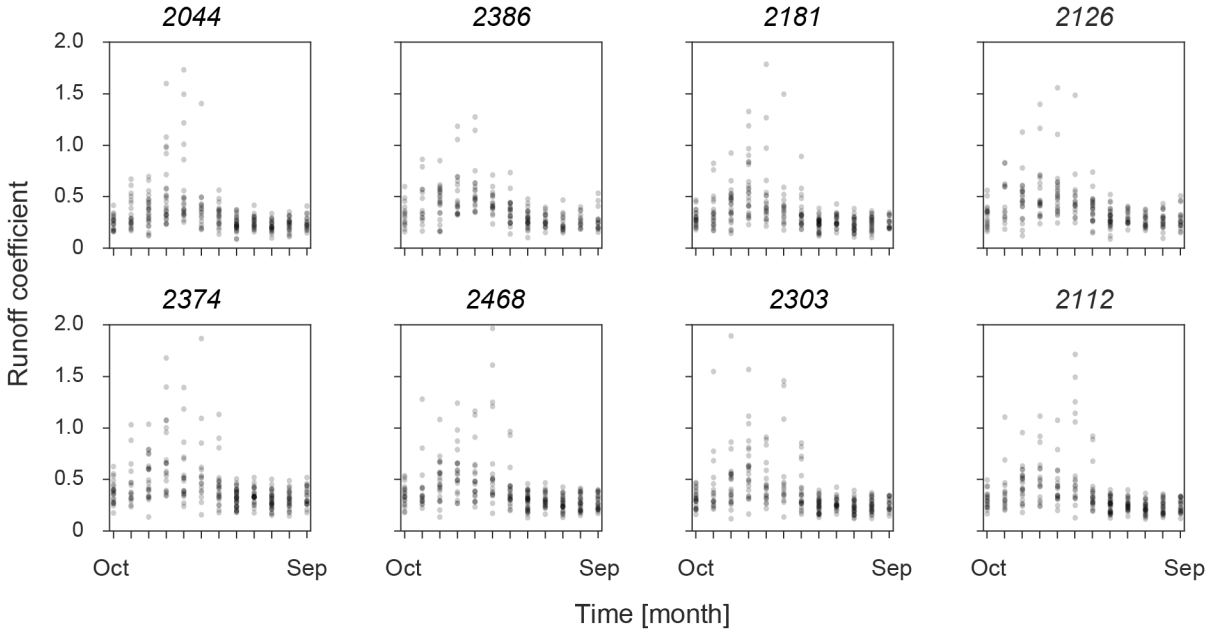

Figure 55: Runoff coefficient per month and MSC. *The ratio of runoff volume to precipitation sum during the considered runoff peak events. The highest value ranges are registered for the months December to April.*

To better relate the *runoff coefficient* to meteorological and hydrological processes, the *runoff coefficients* as a function of simulated runoff and precipitation sum are illustrated in Figure 56. The data points are differentiated in colours depending on the possibility of snow influence (assumed from November to April; the probability increases with higher elevation), which allows a better allocation of the processes. The seasonal variability of the *runoff coefficient* mentioned above are also visible in dependence of the runoff and the precipitation sum. Despite higher precipitation and runoff in the summer months, most events occur with a runoff below 10 mm per day and an intensity of around 50 mm per day. In contrast, most high *runoff coefficients* in winter are the result of a combination of low runoff and moderate precipitation. The change in runoff remains absent despite precipitation occurrence.

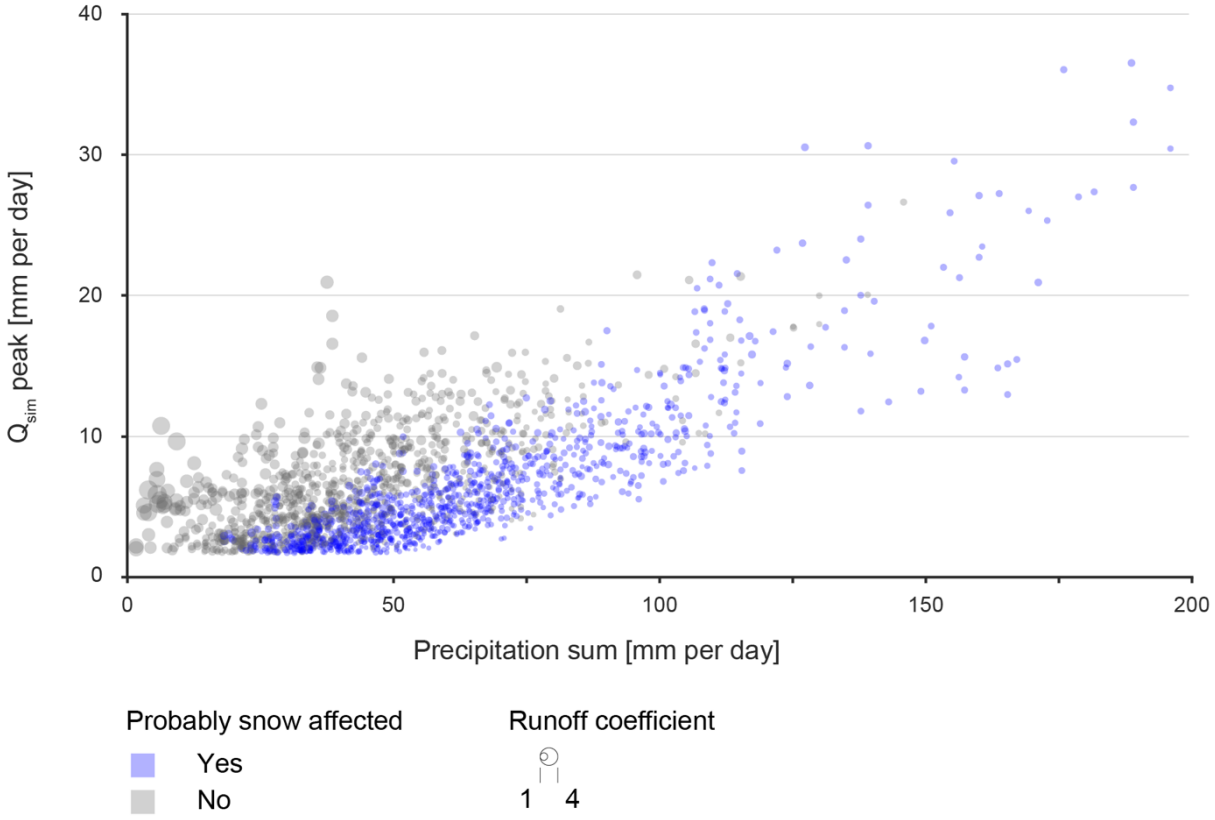

Figure 56: Runoff coefficient as a function of simulated runoff peak and the precipitation sum. *The ratio of runoff volume to precipitation sum during the considered runoff peak events. The highest runoff coefficients (size) are listed for small precipitation sum and a moderate runoff peak during the months May to October. The runoff events are coloured into the probability to be snow affected. It is assumed that the MSC are not affected by snow lying on the ground from May to October.*

6.3.4 Runoff Behaviour during Heavy Precipitation Events

As mentioned at various points, heavy precipitation leads to high changes in runoff and therefore represents greater human and natural risks. In the following, the runoff variabilities during the heavy precipitation events which have been identified in chapter *6.1.3 Heavy Precipitation Events* are examined. For this purpose, the ensemble run values are used from two days prior up to three days after a heavy precipitation peak, defined by previously determined reaction times (chapter *6.3.1 Runoff Deviation*). The absolute variability of simulated runoff and precipitation of each ensemble run is illustrated exemplarily for one heavy precipitation event (Figure 57). Three conditions should be considered: (1) To compare the behaviour during events between the *MSCs*, the visual results are limited to stratiform events even though heavy precipitation events more often occur as a convective, local event. (2) As for the precipitation spread analysis during heavy precipitation events, only the absolute spread is considered because the events are determined already depending on the precipitation event and thus do not have to be normalised. (3) In contrast to previous comparisons between runoff and precipitation spread, the *time lag* in runoff generation is not adjusted for the analysis. This allows to compare the runoff reaction time during heavy precipitation events to the general reaction time analysis. The following three connections can be recognised in the exemplary event—selected because of its meaningful behaviour—from

29. August 2002 to 03. September 2002: (a) independently of the catchment size and elevation, the precipitation varies most significantly on the third day, the day of the precipitation peak; (b) for the simulated runoff, in contrast, the ensemble runs differ the most on day 4; (c) this example clearly shows how variability of runoff and precipitation is dependent on intensity.

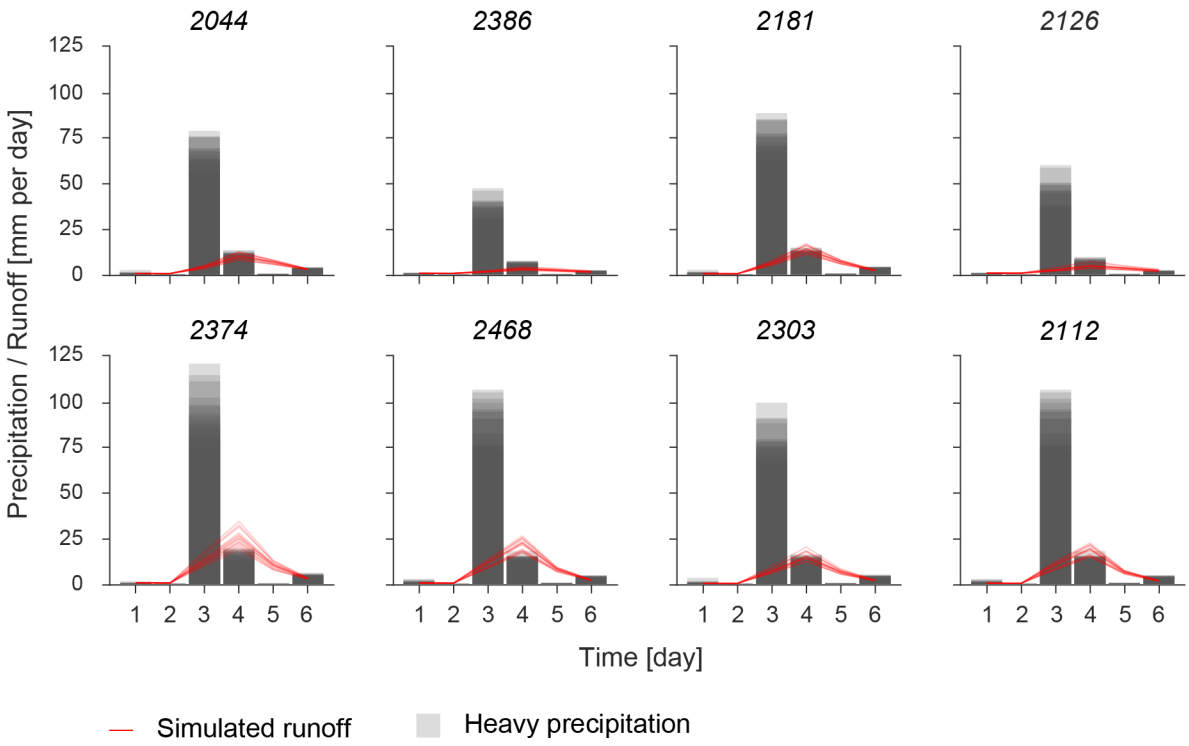

Figure 57: Behaviour of ensemble runs of precipitation and simulated runoff during a heavy stratiform precipitation event per MSC. *Two days prior and three days posterior to a precipitation peak are considered. The highest variability of the ensemble runs of precipitation is recorded on peak day (day 3) whereas the runoff varies the most one day after the precipitation peak (day 4).*

The general behaviour of runoff and precipitation during stratiform heavy precipitation events is shown using the probabilistic data set mean of 50 randomly selected events in Figure 58. The observation window of runoff behaviour is based on the precipitation peak (see chapter *5.3.1 Precipitation Event and Period*), wherefore the precipitation amount is highest on day 3. A typical runoff change during heavy precipitation events starts rising on day 3 but reaches its maximum on day 4, whereas the amplitude differs from event to event but not significantly within the various *MSCs*. In most of the events, the water level settles down to an average level after three to four days of post peak precipitation.

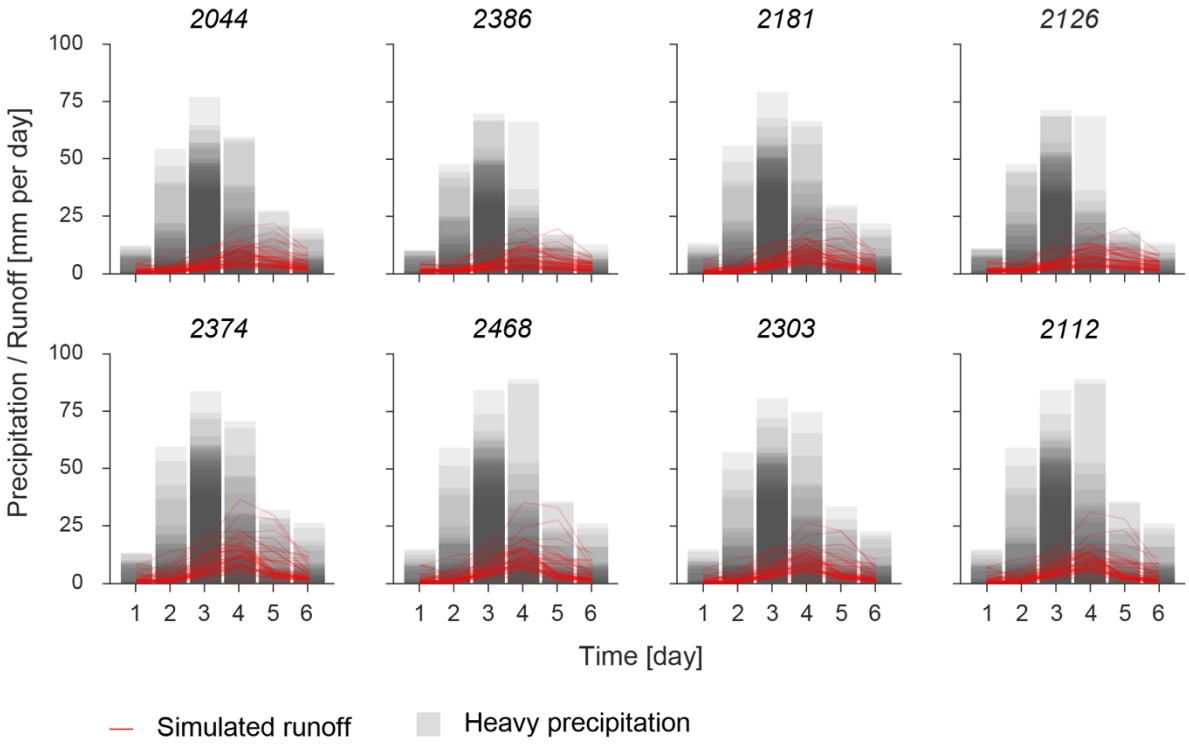

Figure 58: Behaviour of probabilistic data set mean of precipitation and simulated runoff during 50 randomly selected heavy precipitation event per MSC. *Two days prior and three days posterior to a precipitation peak are considered. The highest variability of precipitation is recorded the day prior and after the precipitation peak (day 3) whereas the runoff varies the most the two days after the precipitation peak (day 4 and 5).*

The mathematical variability analysis of the absolute simulated runoff spread on each day over the entire validation period underlines the visual perception (Figure 59). Not only does the amplitude of runoff peak vary the most on day 4, but the absolute ensemble spread positively correlates with higher runoff values. In all *MSCs*, the median runoff spread rises from around 0.04 mm per day on day 1 up to on average 0.45 mm per day on day 4, where the increase is highest for *MSC 2374* with on average 0.7 mm per day. It is also *MSC 2374* together with *MSC 2468* and *2112*, for which the highest ensemble spreads are recorded. This clustering indicates a spatial relationship of runoff simulation uncertainty and mean elevation during heavy precipitation events.

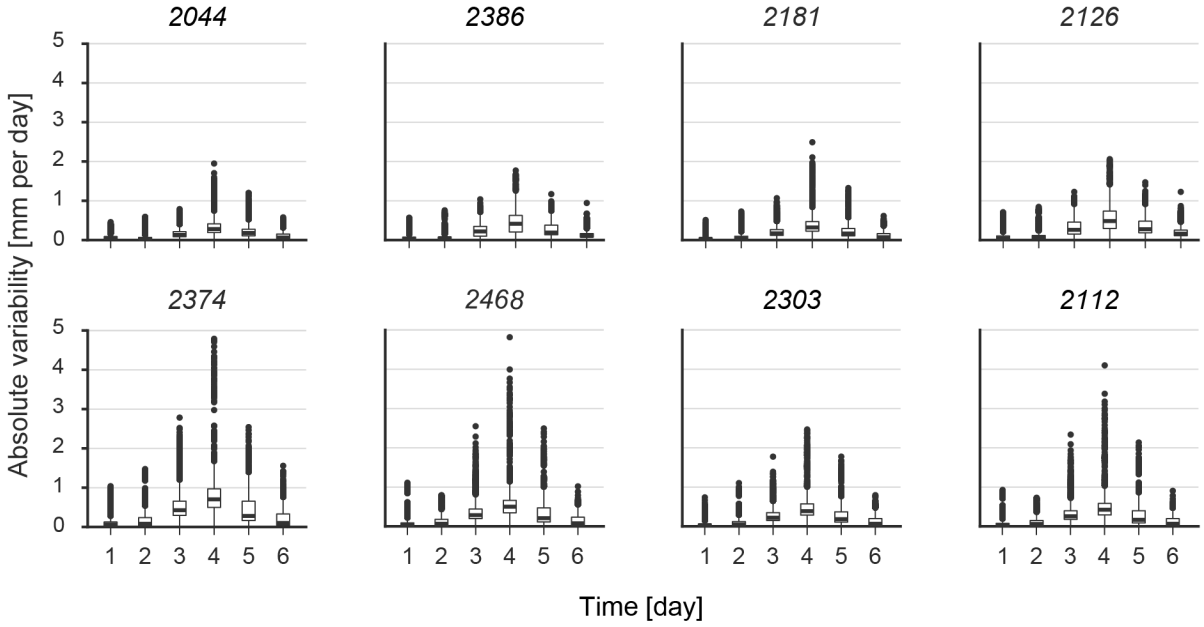

Figure 59: Absolute variability of runoff values during heavy precipitation events per MSC. *Two days prior and three days posterior to a precipitation peak are considered. As already indicated in Figure 57, the runoff ensemble spread is highest on day 4 with a time lag of one day to the precipitation peak. The higher-lying MSC 2374, 2468 and 2112 show the highest variability.*

Girons & Seibert (2016) and Girons et al. (2017) warn of severe natural hazards triggered by rapid discharge generation in Swiss Alpine regions. Figure 59 shows that such risks are most likely to occur on day 4 of the considered periods, the day after the precipitation peak and most likely with the highest runoff increase. As already stated, the simulations are almost always below the observed runoff. Thus, the question that arises is if there is a difference between the deterministic and the probabilistic simulations during these heavy events. In general, it can be stated that the probabilistic data set mean shows nearly no deviation from the deterministic simulation. However, the probabilistic simulation values above the median value—which was chosen as a threshold in order to exclude the very low values but also include some with moderate intensity—of all runoff values during heavy precipitation events tend to be above the deterministic simulated and closer to the observed runoff value. The deterministic data has an average deviation of 5.71 mm per day whereas the probabilistic data differs at 5.61 mm per day. Nevertheless, these differences are on a very small range, which is why the probabilistic approach could only slightly improve the simulations.

6.3.5 Differences of *RhiresD* and *RhydchprobD* Ensemble Mean Simulations

As in the meteorological part, the performance of the deterministic and probabilistic data set mean is examined for the simulation uncertainty. The histograms in Figure 60 illustrate the deviation of Q_{sim} and Q_{obs}, where overperformed probabilistic (*RhydchprobD data set mean*) compared to deterministic values (*RhiresD)* are negative and underperformed are positive. To simplify the interpretation, only deviations below the 25th percentile as well as above the 75th percentile are shown (reduced to 50% of the data points). Half of the runoff values show a deviation of Q_{sim} and Q_{obs} between −0.5 and 1 mm per day (25th to 75th percentile), which indicates together with the symmetric distribution that the data sets are almost identical. By extracting the 50% of all events

with larger deviation values from the simulated to the observed values, spatial patterns can be made visible. The excluded half of the data set has a very similar distribution in all *MSCs*. The distribution of deviation values in the positive and negative areas is almost symmetrical for all *MSCs*. In contrast, the number of runoff events with large deviation correlates positively with increasing mean elevation. The fewest events are recorded in *MSC 2386*, the most in *MSC 2112*.

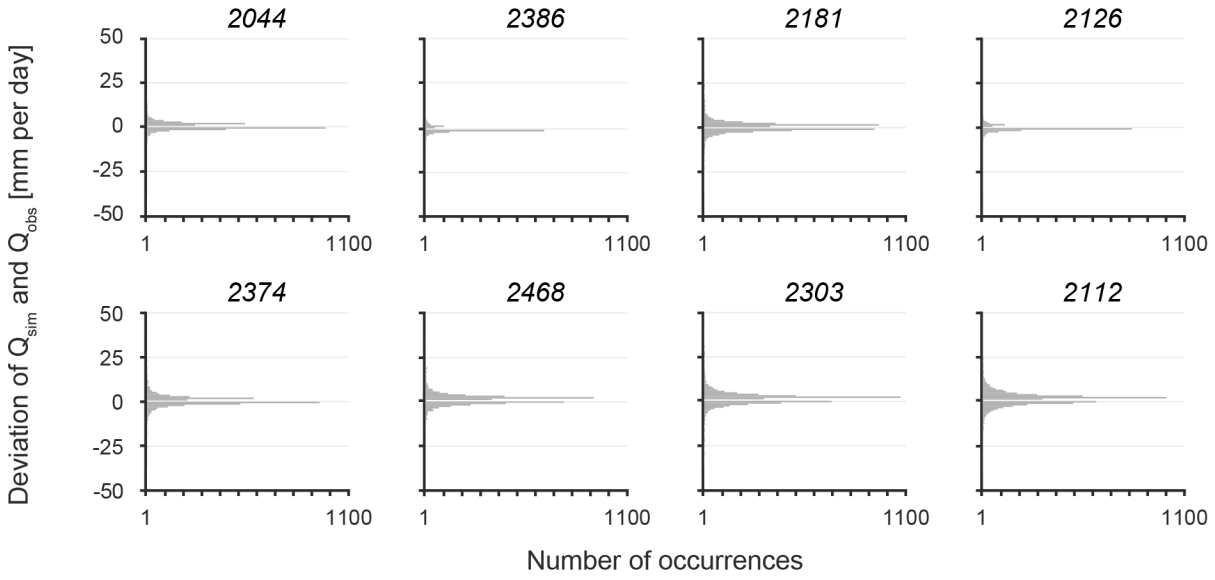

Figure 60: Deviation of simulated and observed runoff per MSC for half of the data set with major deviations (below 25th percentile and above 75th percentile). *The deviation of the deterministic (RhiresD) and probabilistic (RhydchprobD data set mean) from the observed runoff is calculated. The data set with the smaller of the two deviations is considered the better simulation. Negative deviations result from overperforming probabilistic (RhydchprobD ensemble mean) compared to deterministic values (RhiresD) and positive from underperforming values. The figure shows that most of the deviations are below 10 mm per day and the deterministic and probabilistic perform equally well.*

The values in Figure 60 show that the distribution of deviations is relatively narrow. In 29 029 daily runoff simulations the *RhiresD* data sets is closer to the observed runoff whereas in 23 571 runoff events the *RhydchprobD* data set corresponds more to reality. The same can be observed in the five-day period prior to a runoff peak, the ensemble data set mean cannot predominantly achieve a better performance. In 7 102 runoff simulations *RhiresD* performs with an average deviation of 0.08 mm per day better than *RhydchprobD* ensemble mean whereas in 5 150 runoff simulations *RhydchprobD* is closer to the observation with an average deviation of 0.07 mm per day. These values suggest that the deterministic data set *RhiresD* slightly overperforms the probabilistic data set *RhydchprobD*. The visual analysis (Figure 61) additionally shows that performance does not depend on seasonality or on the intensity of precipitation and runoff volume. It is evident that also in this respect the topography and the associated natural precipitation occurrence are responsible for higher, although not regular deviations.

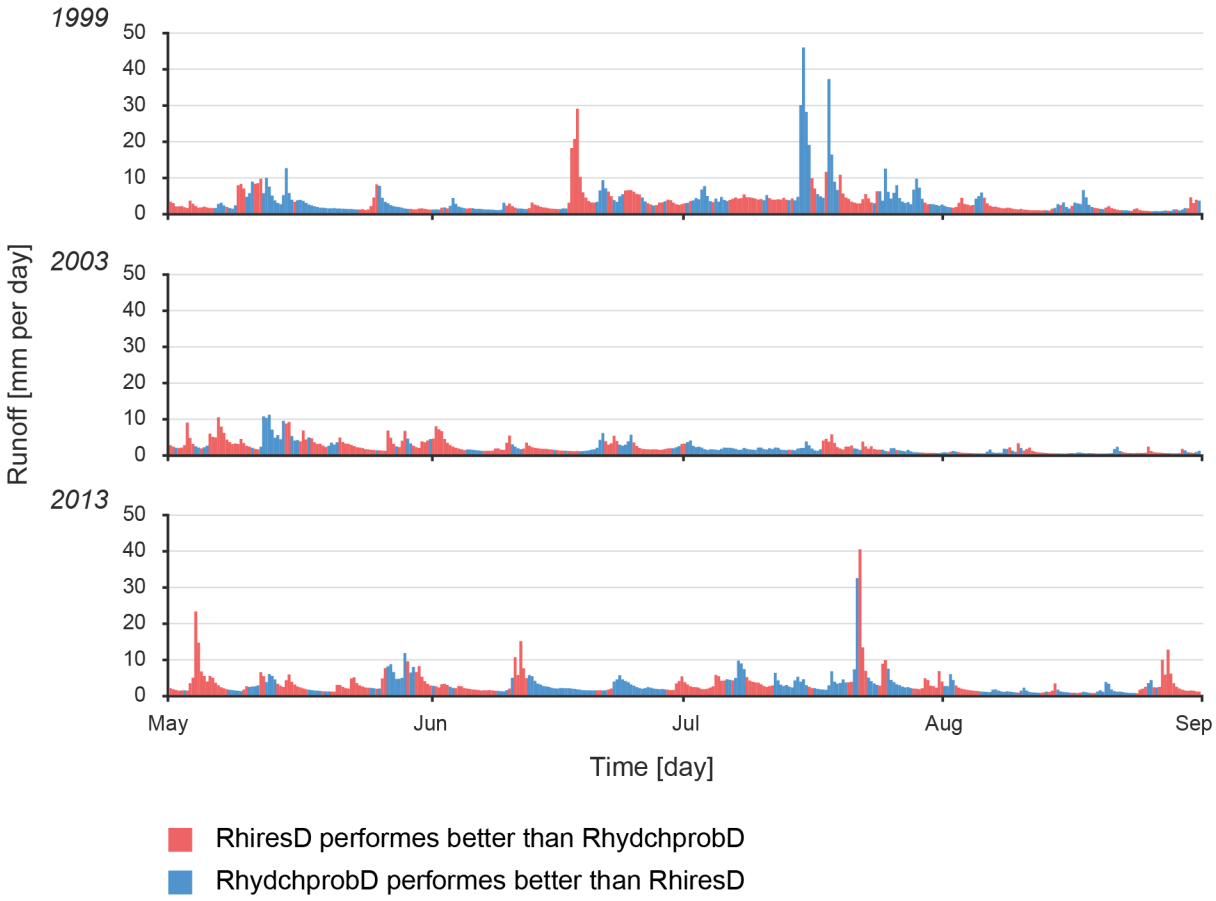

Figure 61: Runoff behaviour during the hydrological years 1999, 2003 and 2013 coloured in the better performing data set. *The outperformance of the deterministic (RhiresD) and the probabilistic (RhydchprobD data set mean) is independent of seasonality and runoff volume. If the simulated runoff with the deterministic data set is closer to the observed runoff, the runoff event is coloured in red. Vice versa, if the deviation of the probabilistic runoff value from the observed runoff is smaller than the deterministic one, the runoff event is coloured in blue.*

7 Discussion

The previous section introduced the results based on the earlier outlined methodology in chapter *5 Methods*. The data analysis revealed several spatio-temporal patterns in precipitation estimations and runoff simulations. The intention of this section is to discuss the research objectives outlined in chapter *1.2 Research Objectives* by placing the findings into the scientific context introduced in chapter *2 Scientific Background*. The present chapter is structured analogue to previous chapters and builds on the following three main parts: meteorology (*7.1 Meteorological Data Analysis*), model (*7.2 Model Variability*) and hydrology (*7.3 Hydrological Data Analysis*). All variabilities can be ascribed to two different sources of origin, natural patterns in the precipitation and runoff occurrence (*natural variability*) as well as methodological uncertainties (*methodological variability*). *Natural variability* occurs due to natural influencing factors such as topography or seasonality, whereas the information on *methodological variability* is derived from the spread of the ensemble run values in the probabilistic data set *RhydchprobD*.

7.1 Meteorological Data Analysis

This section gives answers to the three research objectives by focusing on the variabilities found in the precipitation data sets. The research objective RO.1.1 aims to describe spatio-temporal precipitation patterns regarding their natural or methodological origin in the probabilistic data set. The patterns during heavy precipitation events, intended to separate from general patterns, are shown and discussed in RO.1.2 using an example event in the year 2013. Finally, the extent to which the deterministic and probabilistic data set coincide is investigated in research objective RO.1.3.

7.1.1 General Precipitation Variability

RO.1.1 What are the measurable spatio-temporal patterns in precipitation estimations within the probabilistic precipitation data set (RhydchprobD)?

To answer the research objective 1.1, the patterns are described using the four variability types *temporal*, *spatial*, *spatio-temporal* and *scaling*, combined with the different sources of origin.

Temporal Variability Patterns

In the following, the patterns that were found regarding the temporal variability in the probabilistic precipitation data set (*RhydchprobD*) are discussed along their variability class, which is either *natural variability* or *methodological variability*.

Natural Variability

Natural variability—defined as the natural deviation of the precipitation sums—describes the interannual pattern of precipitation occurrence. Four main temporal patterns could be detected through the data analysis. (1) A strong seasonal dependency with more frequent precipitation

events in spring and summer months can be observed. (2) The larger probability of precipitation events leads to the total precipitation sum being greatest in the summer months. (3) The precipitation sums per month and season show a higher variability for spring and summer months when compared over the full extent of the analysed time period (58 years; 1961–2019). (4) Precipitation generated through convective processes is less frequent in winter months, whereas stratiform precipitation occurs all year round. These findings of seasonal patterns in precipitation occurrence are widely supported by earlier studies focussing on the interannual precipitation cycle in alpine regions (e.g. Brönnimann et al. 2018; Bartolini et al. 2009). However, the data shows an increased occurrence of precipitation during the studied period, which is the opposite of the estimated decrease of summer precipitation occurrences (e.g. Bronnimann et al. 2018; Zierl & Bugmann 2005). Whether a (negative) trend can be observed or not lies outside the scope of this work. It is assumed that the reason for the contradicting findings is found in the considered time horizon and the applied methodology. Therefore, the *natural variability* patterns in the mountainous catchment area of *Andelfingen* differs from trend studies.

Methodological Variability

In general, the absolute interannually *methodological variability* of the probabilistic data set *RhydchprobD* follows the *natural precipitation variability* pattern. (1) An increase of both absolute and relative variability is observable during spring and summer months. (2) Regarding the absolute variability, the above-mentioned *temporal pattern* of higher precipitation sum on spring and summer days is not surprising due to the mathematical calculation of the absolute ensemble spread (standard deviation of all ensemble run values without normalisation by precipitation sum). (3) The temporal accumulation of relative variability during spring and summer months is linked to the previously mentioned natural precipitation variability. On the one hand, if a linear uncertainty probability is assumed, the *methodological variability* must be greater with more frequent precipitation occurrences. On the other hand, the precipitation generation type seems to affect the relative *methodological variability*. High relative variabilities are found for the more frequently occurring convective precipitation events during spring and summer days which are more uncertain to estimate because of their local occurrence. Although the relative variability calculation is not influenced by the precipitation sum, the greater variability correlates with stronger, mostly convective precipitation events. The increased variability—in this work used as an approximation of the estimation uncertainty—in relation with higher precipitation sum supports the findings of Frei & Isotta (2019). Based on these findings it can be concluded that within the probabilistic data set a higher *methodological variability* for moderate to heavy precipitation events during spring and summer months is found. The ability that the variability is translatable into estimation uncertainty underlines the advantage of applying a probabilistic data set in precipitation estimations (Buizza et al. 1999; Wu et al. 2011; Strauch et al. 2012; Yu et al. 2015; Frei & Isotta 2019).

Spatial Variability Patterns

In the same way as with the temporal variability patterns, the patterns that were found regarding the spatial variability in the probabilistic precipitation data set (*RhydchprobD*) are structured into the two variability classes: *natural variability* and *methodological variability*.

Natural Variability

Regarding natural spatial patterns, a positive precipitation rate for local, convective precipitation with increasing elevation is found. This *spatial pattern* agrees with previous studies (e.g. Sikorska & Seibert 2018; Hendriks 2010; Yu et al. 2015). Compared to large-scale stratiform fronts, convective precipitation occurs more often in the higher-lying areas in the southeast of the catchment *Andelfingen*. Various studies have shown that large spatial topological heterogeneity leads to higher precipitation variability and to more diverse precipitation formation processes in catchments (Isotta et al. 2014; Sikorska & Seibert 2018; Thurai et al. 2016). Due to the existing topological diversity in the study area, these findings can be applied to the present research. Therefore, it is concluded that the above-mentioned temporal (chapter *7.1.1 Natural variability*) as well as spatial heterogeneous precipitation variabilities occur in the catchment *Andelfingen* due to seasonality of natural processes and their spatial characteristics.

Methodological Variability

Greater precipitation estimation uncertainty positively correlates with the mean elevation. The *natural spatial variability* of precipitation together with the density of the measurement station network leads to this spatial pattern in the *methodological variability*. The spatial pattern of precipitation variability supports the general uncertainty of precipitation estimates in the mountains (Huizman et al. 2009; Girons et al. 2015; Sikorska & Seibert 2018; Frei & Isotta 2019). Nevertheless, *methodological variability* is also observable in the flatlands. This weaker and less frequently occurring correlation is most likely due to the precipitation generation processes and the storage capacity of the soil.

Spatio-Temporal Variability Patterns

The discussion of the spatio-temporal patterns in the probabilistic precipitation data set (*RhydchprobD*) follows the above used structure, except that there are only novel contributions in respect of *natural variability*.

Natural Variability

Precipitation often occurs over a longer time period (>1 day), whereby the duration and intensity greatly depend on the precipitation generation type. The analysis showed an elongation of precipitation periods for May and June, regardless of the spatial location. This *spatio-temporal variability* goes along with the above discussed natural, temporal variability patterns (more frequent precipitation occurrence during spring and summer months). With a long-term average precipitation period of 10.4 days, the longest wet periods are observed in June. Due to the high saturation of soils during this stage, the potential to overload the runoff system and the associated risk of natural hazards is increased. Since a precipitation period is defined by a minimum of two days with no more than single dry days in between, it has a direct influence on the number of resulting precipitation periods. The single dry day is added due to the assumption that the runoff regime and soil cannot recover from exhaustion or complete saturation in less than 24 hours without precipitation. The aggregation of consecutive, convective events in mountainous areas leads to the regular spatial pattern of precipitation period duration.

Scale Variability Patterns

As shown in the previous sections, higher variability is generally found for the (a) *temporal*, (b) *spatial* and (c) *spatio-temporal scales*, which is in agreement with the findings of Girons et al. (2015) and Song et al. (2014). The *scale variability* discussed in this section should give an indication of the resolution needed to perceive such events of high variability or in other words, up to what resolution individual variable events remain noticeable. Because the *scale variability* is characterised by the ensemble spread in the probabilistic data set, only the *methodological variability* is discussed.

(a) *Temporal scale*: The *methodological variability* decreases with temporal aggregation. Nevertheless, precipitation events featuring high *methodological variability* remain noticeable up to a temporal aggregation window of seven days, even though they occur only locally. The empirical cumulative density functions (*ECDF*) of the various temporal aggregation windows visualise that higher precipitation occurrence in mountainous regions mitigates the temporal smoothing effect. The value range of the *methodological variability* for spatially aggregated data is greater in higher elevations than in the lowlands. (b) *Spatial scale:* A spatial aggregation results in more than a doubling of the *methodological variability*. The extent of the change is dependent on the topography and the related precipitation generation type. The spatial aggregation has a smoothening effect on local, convective precipitation events with high variability (small-scale variability) compared to stratiform events with high variability (large-scale variability). Such local precipitation is known to be typical for mountainous catchments (e.g. Sikorska & Seibert 2018; Girons et al. 2015; Yu et al. 2015). Nevertheless, the *methodological variability* remains observable up to the spatial resolution of the entire catchment *Andelfingen*. (c) *Spatio-temporal scale:* From spatio-temporal aggregations it becomes apparent that the *methodological variability* significantly decreases with coarser resolution.

With respect to the demand for high resolved precipitation data and thus accurate knowledge (Girons Lopez et al. 2015), it is concluded that both spatial and temporal resolution are relevant, whereas the exact resolution can be depending on the application. For spatially heterogeneous areas like the catchment *Andelfingen*, however, the spatial resolution is certainly more important than the temporal resolution. If an unsuitable data resolution is used, as Girons et al. (2015) pointed out, the risk of missing relevant local, high-intensity events in meteorological analysis increases with coarser resolutions. Song et al. (2014), in contrast, argue that the complexity of higher resolved data can decrease the model accuracy because models can only deal with limited spatio-temporal information. Therefore, it is a sensitive question of the optimal data resolution for the intended application. The optimal resolution does not necessarily have to be the highest possible. The results have shown that for the diversified catchment *Andelfingen,* the spatio-temporal resolution of the subcatchments *TEZGNR40* on daily basis is suitable to also have reliable information on local heavy precipitation. The variability patterns of such events are discussed in the next section.

7.1.2 Precipitation Variability during Heavy Precipitation Events

RO.1.2 What are the spatio-temporal patterns of the occurrence of heavy precipitation events and what is their influence on precipitation estimates?

The analysis of natural and methodological variability has indicated that the estimation uncertainty is likely to be higher for heavy precipitation events. Such events show— similar to the general

analysis—(a) *temporal* and (b) *spatial characteristics*. (a) Heavy precipitation events occur more frequently in summer months. The *methodological variability* follows the *temporal pattern* of the *natural variability* increase during this period. Since heavy precipitation events are, for example with respect to natural hazards (Girons & Seibert 2016; Girons et al. 2017; Sikorska & Seibert 2018), of particular interest, further positive coherences are being examined. The general comparison of the probabilistic data set mean to the deterministic value reveals the highest ensemble variabilities and precipitation sums for stratiform precipitation. Heavy precipitation events, however, occur more frequently in form of convective precipitation. Consequently, it can be concluded that the greatest ensemble variabilities are not detected for heavy precipitation events. (b) The classification of the precipitation occurrence type is accompanied by a spatial correlation of the estimation uncertainties. Convective precipitation and thus heavy precipitation events occur with a higher frequency in mountainous regions. This spatial cluster of higher variability in more mountainous regions aligns well with the results of Girons et al. (2015) and supports the application of ensemble weather data for forecasts in mountainous catchments as suggested by Yu et al. (2015).

To highlight the benefits of the application of probabilistic data to reveal estimation uncertainties during heavy precipitation events, the two measures *absolute precipitation variability* and the *precipitation range* are compared in general as well as for one specific flood event. The comparison of *absolute precipitation variability* and *precipitation range* shows a linear increase of the values. This relationship gives evidence that more than a single ensemble run is needed to find particularly low or high values. Otherwise only the *precipitation range* without the corresponding *absolute precipitation variability* would show a distinctive high value. Only a single deviating value is not sufficient for a high standard deviation. These circumstances are discussed by taking the example of the flood event on 1st June 2013. A depression over Eastern Europe active on 30th May 2013 and 2nd June 2013 was responsible for very intense, continuous precipitation (categorised as stratiform precipitation in Figure 62) with up to 180 mm per day on the north side of the Alps. Runoff values of a return period between 10 and 30 years were measured for the *Thur* which set a new record for June in the catchment *Andelfingen* (FOEN 2013). The following maximum daily values in the probabilistic data set show the high *methodological variability* during this heavy precipitation event: *ensemble mean precipitation* at 120 mm (*TEZGNR40* #40); *ensemble precipitation range* at 60.6 mm (*TEZGNR40* #32); and the *absolute precipitation variability* at 12.4 mm (*TEZGNR40* #36). It becomes obvious that the highest variabilities arise in the higher-lying subcatchments. The *spatio-temporal pattern* of the *absolute precipitation variability* and *precipitation range* (Figure 62) are almost congruent. This similarity can be explained with the distribution of the ensemble run values (Figure 63). The *precipitation range* of approximately 60 mm per day indicate a high variability of the precipitation estimation of the various ensemble runs. Because of the above-mentioned relationship, a simultaneously large *absolute precipitation variability* can only be achieved if several ensemble runs show noticeable deviations from the ensemble mean. The coincident occurrence of a large *precipitation range* and *absolute precipitation variability* is equivalent to a large estimation uncertainty of precipitation. This combination of high values mainly occurs in higher elevation areas (subcatchments *TEZGNR40* #19–40). Although for instance in subcatchment *TEZGNR40* #14 a *precipitation range* of 21.6 mm per day was calculated, the *absolute precipitation variability* only reaches a value of 4.33 mm per day because a few outliers cause the high *precipitation range* but do not have a greater influence on the *absolute precipitation variability*.

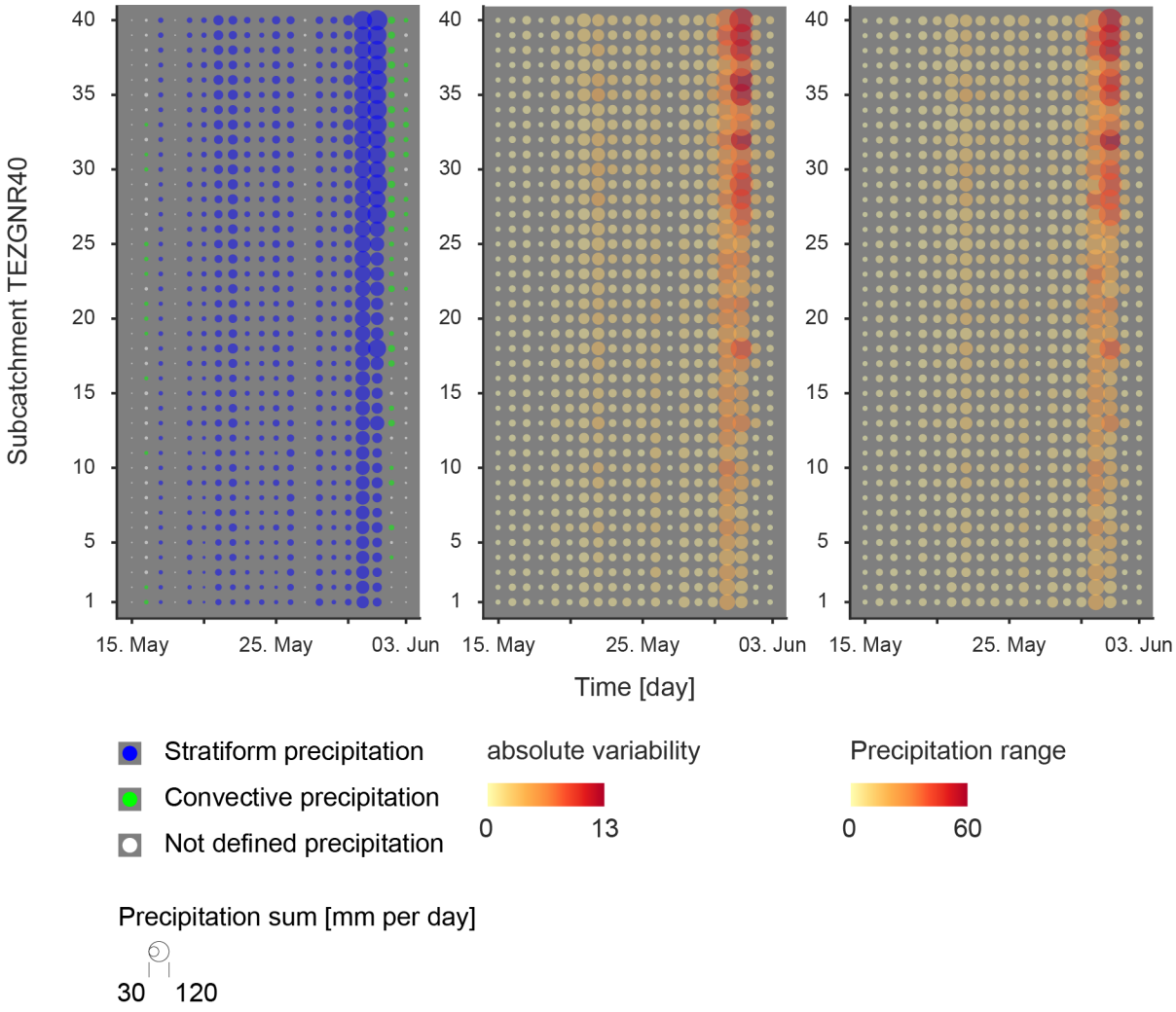

Figure 62: Characteristics of heavy precipitation event from 30th May 2013 until 2nd June 2013 over all subcatchments TEZGNR40. *The size of the precipitation event gives the information on the precipitation sum. Left: Classification of precipitation type. The example heavy precipitation event is classified as «stratiform period». Middle: The precipitation events are coloured according to their absolute variability of the probabilistic data set. Right: The precipitation events are coloured according to their precipitation value range within the probabilistic data set. It becomes visible, that the behaviour of absolute variability and precipitation range is almost identical.*

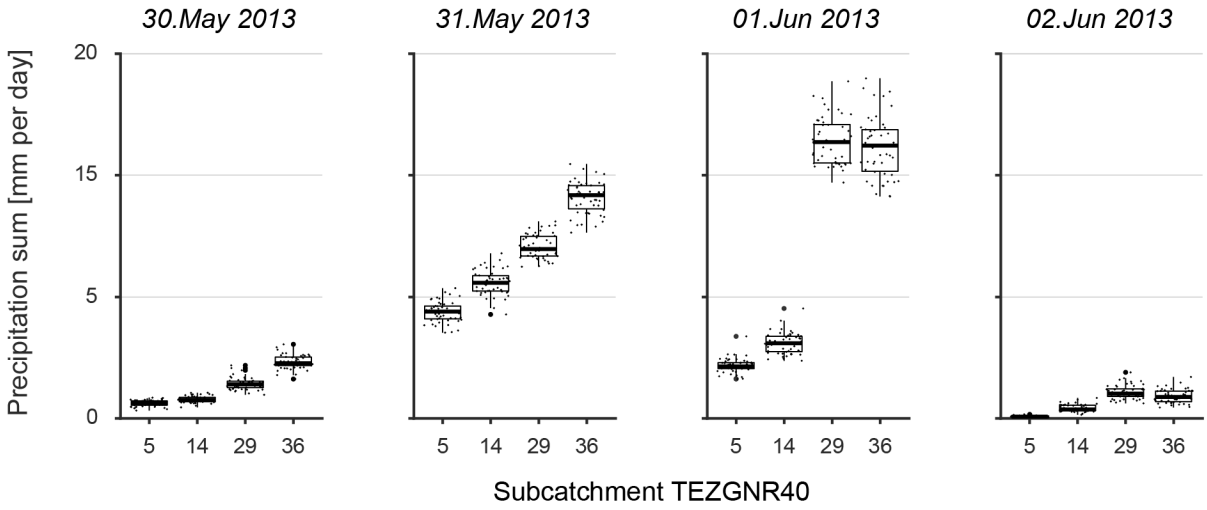

Figure 63: Distribution of the precipitation ensemble run values for the subcatchments TEZGNR40 #5, #14, #29 and #36. *During intense precipitation on 31th May 2013 and 1st June 2013, a spatial differentiation is recognisable. The ensemble spread in the lower-lying subcatchments TEZGNR40 #5 and #14 is conspicuously smaller than for the higher-lying subcatchments TEZGNR40 #29 and #36.*

The deviations of the deterministic values (*RhiresD*) compared to the probabilistic data set means (*RhydchprobD*) during the exemplary heavy precipitation events evenly fluctuate around 0. Neither on a daily nor on a precipitation period scale a clear spatial correlation between the performance and the data set becomes visible (Figure 64). Assuming that periods of heavy precipitation are generally underestimated, only the 5 ensemble runs (90th percentile of the data values per day and subcatchment *TEZGNR40*) with the highest precipitation values are tentatively averaged. If this new mean value is now compared with the deterministic value, the deviations show a clear pattern. Except for one value in the subcatchment *TEZGNR40* (#18 on 30th May 2013, a day with little precipitation), the probabilistic mean values of the data subset show higher values. Even when considering only the upper half of the ensemble run values (median = 20 values), for 87% of the data points a higher precipitation sum result compared to the deterministic values. If the assumption of a general underestimation of heavy precipitation events according to Girons et al. (2015) is now taken, the probabilistic data set for such events could be reduced to a limited number of ensemble runs with the highest precipitation calculations. Whether this approach is also valid for other heavy precipitation events, and should be further pursued, requires additional investigation.

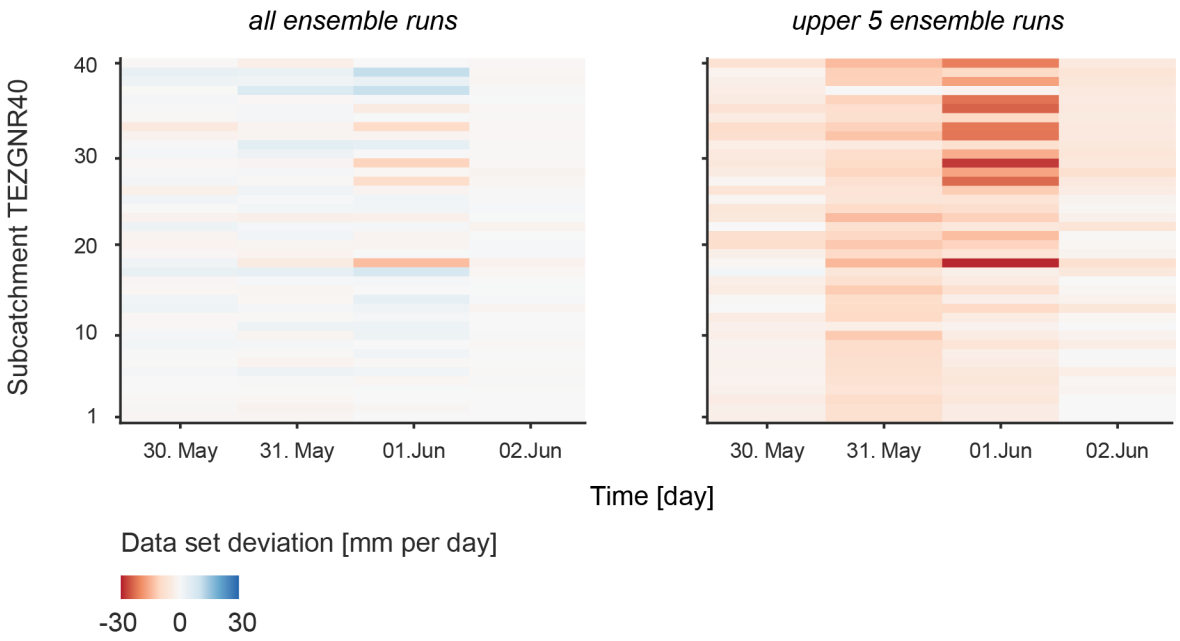

Figure 64: Data set deviation deterministic (RhiresD) to probabilistic (RhydchprobD data set mean) with all ensemble runs as well as a subset of the 5 runs with the highest precipitation values. *Positive deviations indicate higher deterministic precipitation values whereas negative deviations imply higher probabilistic values. Left: considering the RhydchprobD data set mean of all ensemble runs, the deviation of the two data sets is almost consistent. Right: if the RhydchprobD data set mean is calculated with a subset of the 5 runs with the highest precipitation values, the probabilistic data set shows higher precipitation values compared to the deterministic data set.*

7.1.3 Data Set Variability

RO.1.3 To what extent do the daily precipitation sums per subcatchment of the deterministic (RhiresD) and probabilistic data sets (RhydchprobD ensemble mean) coincide?

In general, the daily precipitation sums in the deterministic (*RhiresD*) and probabilistic data sets (*RhydchprobD ensemble mean*) show almost identical values. The maximum difference lies at 1 mm per day. This observation leads to the conclusion that the probabilistic data set mean greatly coincides with the deterministic data set. The differences that were found seem to be small enough to consider them negligible. Nevertheless, detailed analysis on these differences reveals three main patterns. (1) The found differences follow a spatial pattern of lower precipitation values for the lowlands towards higher values for the higher altitudes when comparing the probabilistic data set mean to the deterministic data set. (2) Positive differences are found for heavy precipitation events during spring and summer months. This temporal pattern correlates with the spatio-temporal relationship of a precipitation sum increase in high altitudes during summer as seen in chapter *7.1.1 General Precipitation Variability*. (3) In 90% of the precipitation estimations during winter months, the difference is positive independent of the precipitation sum and location. These spatio-temporal relationships if combined with the findings of Girons et al. (2015)—who concluded that the precipitation sum in the deterministic data set is generally underestimated/overestimated for heavy/low precipitation sums—support the usage of the probabilistic data sets for heavy precipitation events. Under these assumptions, it can thus be concluded that the probabilistic data

set mean is able to better capture heavy precipitation than the deterministic data set and that the little precipitation in the winter months might be overestimated.

7.2 Model Variability

RO.2 How does the probabilistic data set (RhydchprobD) influence the accuracy of hydrological simulations compared to the simulation based on the deterministic data set (RhiresD)?

The influence of the probabilistic data set on the model accuracy is investigated by applying three calibration-validation combinations, namely (A) the deterministic-probabilistic approach where the model is calibrated with *RhiresD* from 1977 to 1995 and validated with *RhydchprobD* as well as *RhiresD* from 1998 to 2015; (B) the inverted deterministic-probabilistic approach wehere the model is calibrated with *RhiresD* from 1998 to 2015 and validated with *RhydchprobD* as well as *RhiresD* from 1977 to 1995; and (C) the probabilistic-deterministic approach where the model is calibrated with *RhydchprobD* from 1977 to 1995 and validated with *RhiresD* from 1998 to 2015. The focus of the discussion is on the *Version A* that is finally used for the variability analysis in runoff simulations.

For all *MSCs*, no change in the general accuracy could be found using the probabilistic data set for the model validation. The model performance measures of *Version A* in the results (*6.2.1 HBV Model Calibration and Validation Version A*) has shown highly variable estimation accuracies for the various *MSCs*, independent of the data set. The influence of five factors to the accuracy, i.e. (a) initial model parameters, (b) catchment size, (c) topography, (d) vegetation zones and (e) human activity, are discussed in the following. (a) The initial model parameters from Seibert & Vis (2012) used in this research are well established in semi-distributed modelling of Swiss alpine catchments. Because the best performance parameter sets from the GAP do not exceed but span those default value ranges, they are considered suitable. Furthermore, the parameter values within the different parameter sets show an irregular distribution, which indicates that all components are interdependent. This means that, for example, no parameter set has conspicuous high or low parameter values. With the selection of model parameters in the automatic calibration step (*GAP*) together with the application of the equifinality concept, the prediction uncertainty is reduced to the best possible minimum (Gourley & Vieux 2005). Nevertheless, the anticipated advantage of ensemble data in runoff simulations remains limited at first impression. The model performance does not seem to improve. The simulation uncertainties can be attributed to various factors. (b) Larger catchments seem to perform generally poorer. A large catchment area has a higher variability of present processes such as runoff generation and soil storage capacity. Thus, an increased difficulty in simulating runoff must be assumed. A smaller catchment size does not necessarily minimize the number of dominant processes, but it does minimize their influence (Hendriks 2010; Häckel 2016). (c) The model performance is strongly dependent on topography. Intrinsically, relatively accurate runoff simulations for mountainous regions should be expected. In these areas almost all precipitation is discharged as surface water due to the steep flanks and shallow soil. However, previous studies provide insights that data inaccuracies for mountainous areas exist. Precipitation measurements due to windy conditions and small-scale weather variations in such areas lead to uncertain input data and timing errors (Beven 2012; Rafieeinasab et al. 2015). (d) In contrast to the elevation zones, only one vegetation zone was used for the runoff simulations

according to the recommendation of Seibert & Vis (2012). However, the results show a correlation between the inter-ensemble runoff variability and the soil storage capacity. The type of vegetation contributes significantly to the storage capacity of the soil (Kammer et al. 2013). Therefore, the implementation of different vegetation zones could give indication of its effect on the model accuracy. This uncertainty factor does not only apply to probabilistic data, but also to model simulations with deterministic inputs. (e) The human influence on water (e.g. irrigation, structures, consumption…) increases the simulation uncertainty in addition to the errors in the input data, model states, model parameters and structures (Rafieeinasab et al. 2015). This factor is not included in any of the analysis. Further research should address how such factors can be incorporated into the runoff simulation to decrease the estimation uncertainty.

Besides the discussed sources of error, some sources can also be excluded. On the one hand, the calibration and validation period of 17 years each is long enough for an accurate model performance. The longer the period, the less individual, conspicuous events are weighted. On the other hand, a systematic bias of the ensemble runs can, contrary to the results of Strauch et al. (2012), most likely be excluded. The precipitation variability analysis, performed before the data was used as the simulation input, gives no evidence that the ensemble precipitation data are depending on the ensemble run, catchment size or elevation. Additionally, the parameter analysis of the individual ensemble runs shows independent values. Even the most sensitive parameters PERC, CFR and CWH do not have a trend in the ensemble runs.

The analysis has shown that the model validation with probabilistic input data over the entire study period cannot achieve more accurate simulation values than with deterministic input data. In contrast to the findings of Buizza et al. (1999), Wu et al. (2011) and Yu et al. (2015), runoff simulations cannot benefit from the equifinality approach of the probabilistic data. Nevertheless, the statement of Frei & Isotta (2019) that the application of probabilistic data in meteorology improves the knowledge of spatial precipitation can be supported. In the more alpine subcatchments of *TEZGNR40*, the number of convective precipitation events increase due to the topological barriers. Together with the information on the uncertainty estimate, the precipitation values gain in significance. The amount of precipitation for events with low *methodological variability* are estimated relatively accurately, whereas the precipitation sums of events with high variability should be considered with caution. This improved spatial understanding of precipitation estimation can be used to improve reservoir management and early warning systems (Georgakakos et al. 2004; Yu et al. 2015). There is a tendency that the absolute ensemble spread of the runoff and the runoff peak range increase with higher precipitation sum prior to a runoff peak. Especially heavier events are of great importance for runoff-dependent processes like early warning systems due to their influence. The information of the simulation uncertainty can therefore be used as an indication for alert and readiness to act.

In contrast to the research approach in *Version A*, no noticeable improvements in model accuracy or in the individual measures *time to peak* or *number of runoff peak events* are found in *Versions B* and *C*. The fact that in *Version B*, in which the time periods for calibration and validation were swapped, no differences in respect of performance were found compared to *Version A*, is a desirable result. This proves that the model calibrates appropriately for the data regardless of the time period and is able to estimate the discharge with the same accuracy. In *Version C*, where the model is calibrated with the individual ensemble runs of the data set *RhydchprobD*, the averaging of the data sets of the

individual ensemble runs is most likely responsible for the circumstances that large variabilities in the runoff simulations remain invisible. In order to make better use of the advantage of the probabilistic data set of making the estimation uncertainty visible, an approach could be considered in which not all ensemble runs are included or not all ensemble runs are weighted equally in the averaging. Finally, in none of the *Versions A, B* and *C* a dependence of the value ranges of the individual model parameters and the model accuracy is found. This also suggests that the model was well calibrated and that the model parameters are unbiased.

7.3 Hydrological Data Analysis

Analogous to the discussion of temporal and spatial precipitation patterns, this section discusses the patterns of runoff variability in the context of their influencing factors of space and time as well as current scientific knowledge. In order to answer the first research objective, the patterns are once again subdivided into *temporal*, *spatial*, *spatio-temporal* and *scale variability*. Further, the patterns are assigned to their origin, which is either natural or simulative. The influence of heavy precipitation events on the runoff variability patterns is answered within the second research objective. Finally, the third research objective focusses on the coincidence of the deterministic *RhiresD* and the probabilistic *RhydchprobD* data sets.

7.3.1 General Runoff Variability

RO.3.1 What are the measurable spatio-temporal patterns in runoff estimations within the probabilistic precipitation data set (RhydchprobD)?

To answer the research objective 3.1, the patterns are described using the four variability types *temporal*, *spatial*, *spatio-temporal* and *scaling*, combined with the different sources of origin.

Temporal Variability Patterns

In the following, the patterns that were found regarding the temporal variability in the probabilistic runoff simulations (*RhydchprobD*) are discussed along their variability class, which is either natural variability or methodological variability.

Natural Variability

This section discusses the patterns of the natural variability in time. The model efficiency below 1 indicates that the runoff values are simulated with a certain degree of uncertainty. With model efficiencies between 0.36 and 0.79, the simulated runoff values deviate from the observed values by an average of 1.05 mm per day. The daily underestimation is intensified for summer months. As discussed in the previous section (chapter *7.1.1 General Precipitation Variability*), intense convective precipitation is more frequent during these months. The daily resolution of the runoff simulations has the consequence that spontaneously strong-changing runoff values get lost. These temporal patterns are consistent with the results of Hendriks (2010) and Yu et al (2015).

However, if runoff is not considered a daily event but a process occurring over a period of time identical to the precipitation analysis, the overall differences between observed and simulated runoff values decreases. The seasonal patterns of runoff periods are described through the

characteristics *time to runoff peak* and *time lag between the precipitation and runoff peak*. By looking at these characteristics, three main conclusions can be drawn about *seasonal, natural variability*. (1) Both the *time to runoff peak* and the *time lag between the precipitation and runoff peak* for the simulated and observed measured values show very similar patterns over the year. (2) The characteristic *time to runoff peak* elongates during the months May to October. This relationship is likely attributable to the saturation of soil. The soil is highly saturated in the winter months and the precipitation in form of rain contributes directly into the runoff, while this reservoir is filled up before the remaining water flows into the runoff from May onwards (Häckel 2016). Although the methodology used for event classification is based on the precipitation amount and not on the runoff peak, the influence of snow on the *time to runoff peak* is negligible. On the one hand, Figure 65 shows that the observed and simulated runoff reacts more or less immediately to precipitation events, even in the winter months. Furthermore, the thresholds in the precipitation period classification are set to include already small precipitation events for example in the form of snow. On the other hand, the highest measuring station (*MSC 2112 Appenzell*) is located at just 769 m a.s.l., where the snow line is not consistently lower (HYDROmaps 2020). (3) The characteristic *time lag between the precipitation and runoff peak* shows only small seasonal differences. This finding suggests that the subcatchments are only affected by snow during sporadic events. In case of a large influence of snow, the *time lag* in the winter months would be much greater than in the summer months, as the snow often remains first on the ground before it is injected into the runoff. Additionally, the small seasonal patterns in the *time lag* values indicate that the soil reservoir can compensate for a larger amount of precipitation in the summer months. Therefore, the *time lag* between the two peaks is not shortened. Instead, the storage capacity tends to slightly extend the *time lag*. From these observations, it can be concluded that the underestimation of simulated runoff values compared to observations gradually decreases when analysing precipitation and runoff periods.

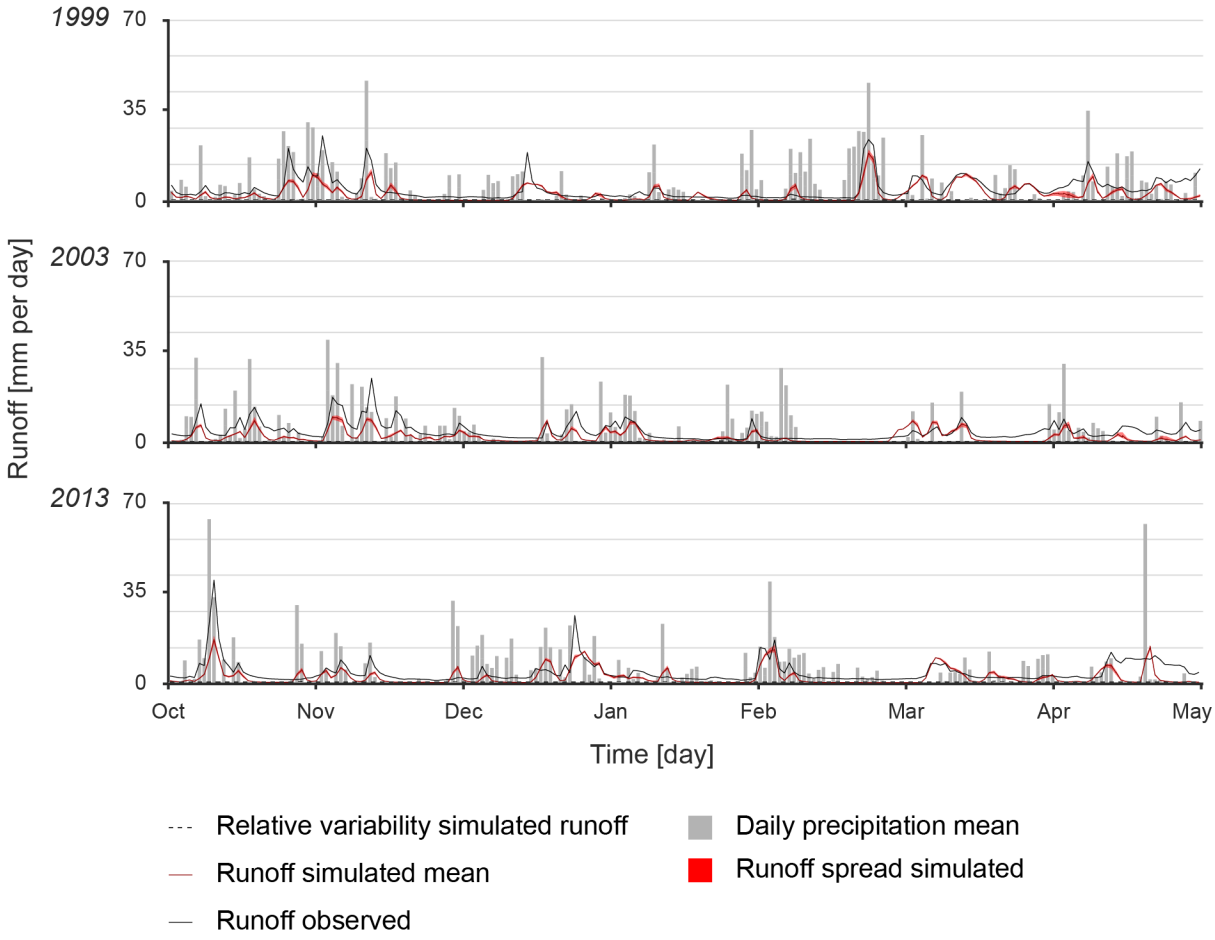

Figure 65: Daily precipitation and runoff during the hydrological years 1999, 2003 and 2013 for the MSC 2112 (Andelfingen). *The figure shows the reaction of the runoff to precipitation occurrences. The observed runoff (black) is generally higher than the mean simulated runoff (red). The red band gives indication to the value range of the simulated runoff values. The corresponding relative variability is very low (black dashed line).*

Methodological Variability

Compared to the temporal precipitation patterns of the ensemble variability, the runoff ensemble runs do not show clear seasonal characteristics. It is noticeable that despite the more frequent, often strong occurrence during the spring and summer months, not all major precipitation events show a large runoff simulation uncertainty. It could be assumed that high precipitation sum leads to a higher runoff value. The simulation uncertainty of those intense runoffs positively correlates with the amplitude level. The circumstance that not every major precipitation event leads to greater runoff simulation uncertainty is likely explainable with the soil's storage capacity because the history of the preceding days is important for the runoff regime (Häckel 2016). With regards to the storage capacity of soil, the four temporal patterns of *methodological variability* are observable. (1) In the spring and summer months, the absolute and relative runoff ensemble spread (*methodological variability*) varies more often compared to the fall and winter months. This correlation exists due to the similar intensification of evaporation and the decrease in soil moisture because of higher air temperatures and periods of no precipitation (Figure 4 in chapter *2.2 Precipitation and Runoff Generation*). The combination of those characteristics increases the soil storage capacity which minimizes the direct contribution of a precipitation event to the runoff. Such precipitation-runoff events record a moderate to major precipitation sum combined with large *absolute runoff variability* since the model

underestimates the storage capacity. (2) A large proportion of the precipitation is added directly to the runoff if the soil is already saturated because of no evaporation during winter months or by previous precipitation events. The soil storage capacity plays a minor role during the saturated periods; such events can be more accurately simulated by the model. Consequently, the absolute and relative runoff ensemble spreads (*methodological variability*) for those precipitation events are smaller. This correlation is supported by the negative correlation of the *relative runoff variability* and the runoff volume. The initial precipitation is partly stored in the soil, which explains the delayed increase in runoff. The model's underestimation of the soil storage capacity results in a higher *relative runoff variability* for low runoff values. After the reservoir is filled up, the runoff is generally simulated more accurately. (3) A large runoff change within five days prior to the runoff peak occurs with any precipitation sum from 25 mm per period. This observation underlines that the *methodological variability* does not clearly correlate with the seasonal increase of precipitation sum and occurrence probability. With a saturated soil, already small precipitation sum can lead to a large runoff change. (4) Finally, small precipitation sums throughout the whole year can be absorbed by the soil. Consequently, no high *methodological variability* is recorded for such precipitation events.

As a possible cause of *methodological variability* in runoff simulations, the influence of snowmelt can be reliably excluded. The combined analysis of precipitation and runoff variability show that an increased runoff ensemble spread (*methodological variability*) almost always follows a precipitation event with a high *methodological variability*. If snowmelt influenced the variability of runoff simulations, at least in spring and early summer higher runoff ensemble spread without a precipitation event should be visible. However, a correlation of a higher snow melt rate in the warmer months and a higher runoff ensemble spread is not found.

Spatial Variability Patterns

As before, the patterns that were found regarding the spatial variability in the probabilistic runoff simulations set (*RhydchprobD*) are structured into the two variability classes: natural variability or methodological variability.

Natural Variability

The amount of water in the streams and rivers (average runoff) naturally differs due to their size in the study area *Andelfingen*. The average runoff is smaller for mountainous streams in the south east compared to the runoff of the rivers in the flatlands in the north. However, the change in runoff at the measurement stations during stratiform precipitation events—which occur over the entire study area—show similar spatial patterns. That the developments are almost concurrent is most likely due to the fact that the simulation are based on subcatchments and not on rivers. Medium to large rivers are present in all *MSCs*. As a result, *natural variabilities* of smaller streams are lost in the measurements and simulations at the measurement stations.

Methodological Variability

The deviations of observed and simulated runoff values follow a clear spatial pattern. In general, the simulated values deviate more strongly from the observations as the mean catchment elevation increases. For the lower-lying *MSCs 2386* and *2126* the highest model accuracies are achieved, while the lowest model accuracies are recorded from the highest *MSCs 2303* and *2112*. The findings of increasing runoff variabilities with higher mean elevation agree with the results of

Girons et al. (2015) and are explained with the high spatio-temporal variability of precipitation occurrence in mountainous areas. However, similar to the temporal patterns in *methodological variability*, these spatial patterns disappear when the runoff characteristics (*time to peak* and *time lag precipitation to runoff peak*) rather than the daily values are compared.

Spatio-temporal variability patterns

The discussion of the spatio-temporal patterns in the probabilistic runoff simulations (*RhydchprobD*) follows the above used structure of *natural* and *methodological variability*.

Natural Variability

The results in chapter *6.3.1 Deviation of Observed and Simulated Runoff* indicate that *natural variability* of runoff is stronger influenced by seasonality than spatial factors such as *MSC* size and topography with their associated spatial distribution of precipitation. These findings contradict the results of Huss et al. (2008) and Farinotti et al. (2012) who found a higher spatial than temporal dependency of *natural variability*. Both Huss et al. (2008) and Farinotti et al. (2012) conducted research in catchments with glacial influence. Therefore, the absence of glaciers in the catchment *Andelfingen* might be responsible for the contradicting relationship.

Methodological Variability

Compared to the *methodological variability* of precipitation, the absolute and relative runoff ensemble spreads (*methodological variability* of runoff) show significantly lower values. Nevertheless, they should not be underestimated because the value ranges for runoff in general are much smaller than for precipitation. This circumstance implies that comparably small runoff variability can still have a great impact. The influence of (a) catchment size and (b) topography on the spatio-temporal patterns of runoff's *methodological variability* is discussed in the following. (a) Even though the *MSCs* are of very different sizes, the *methodological variability* shows no spatio-temporal correlation to the catchment size. (b) The *methodological variability* in *MSCs* with higher mean elevation is less volatile compared to lower-laying areas during spring and summer months because of the influence of the surface and soil on the runoff estimation uncertainty. This spatial pattern is an extension of the previously discussed temporal variability of the characteristic *time to peak* (7.3.1 Temporal variability). As already discussed, the soil storage capacity increases during spring and summer months and influences the simulation accuracy. Because the southern part of the catchment is mainly characterised by grass and loose rock as well as steep slopes, the soils are less deep compared to the agricultural characterised lowlands in the northern part. Consequently, the storage capacity is comparably lower in the higher *MSCs*. This relationship leads to less spatio-temporal variable patterns.

Attention has been drawn to the existence of only small *methodological variabilities* in runoff values compared to the one in precipitation values. A possible explanation draws from the processing of the simulation data sets. The model validation with the ten best parameter sets from the calibration results in ten simulation data sets for each ensemble run. These simulation data sets have considerable differences. But the ten data sets are averaged leaving one simulation data sets per ensemble run for the analysis. This processing step is responsible for the smoothing of the ensemble run values and the resulting reduced variability. For this reason, two methodologies for the data set processing should be pursued more closely. (1) An uncertainty coefficient, for example

calculated by the range of simulation data set values, could be used to characterise the averaging calculation. (2) Only a number of simulation data sets could be included to give more weight to conspicuous values. The general underestimation of the simulated runoff values would suggest that, for example, only the five highest simulation values out of the available ten are considered.

Scale variability patterns

In this part, *scale variability* is understood as a temporal restriction of the considered data which focuses the consideration on the runoff peaks. The *methodological variability* of the ensemble runs within 5 days prior to runoff peaks is discussed. The temporal subset of the data underlines the previously discussed spatio-temporal patterns. In particular, the influence of soil storage capacity as one of the major influencing factors on the simulation accuracy can be illustrated. One of the indications to storage capacity in the different *MSC* is the runoff coefficient. A majority of the runoff coefficients are smaller than 0.5, whereby a coefficient of 1 implies that the total precipitation amount is converted into runoff and 0 that none of the precipitation is transferred to runoff. For the coefficients, three spatio-temporal patterns are observable. (1) During winter months, the runoff coefficient is comparably higher in all *MSCs* because the soil is more saturated wherefore less precipitation can be stored and consequently becomes streamflow. It is therefore possible that a moderate precipitation sum of about 50 mm within five days can already increase the runoff up to 20 mm per day. Such precipitation sum and runoff volume combinations result in high runoff coefficients. (2) Occasionally, runoff coefficients above 1 are observed. Such events, where the precipitation sum is greater than the runoff, mainly occur in the higher *MSCs 2374, 2468, 2303* and *2112* from January to March. It is very likely that these observations are due to precipitation in the form of snow. The snow accumulates on the surface and does not affect the runoff during and shortly after the precipitation event. (3) Conversely, higher temperatures in summer months have a higher evaporation potential, which leads to a generally larger storage capacity and thus lower runoff coefficients. The lowest mean runoff coefficient, where most precipitation is absorbed by the soil, is observable in July. It is noticeable that the *MSC 2374* and *2468* have slightly higher average values than the other *MSC*. Steeper, rocky slopes on the north side of the *Säntis* have the consequences that the soil has a lower storage capacity as in other regions and therefore the runoff coefficients are comparably higher.

7.3.2 Runoff Variability During Heavy Precipitation Events

RO.3.2 What are the spatio-temporal patterns of the occurrence of heavy precipitation events and what is their influence on runoff estimates.

The runoff values and their *methodological variability* are very sensible to heavy precipitation events. Previously discussed spatio-temporal patterns in section *7.1 Meteorological data analysis* are also applicable. Five of those patterns are more clearly observable for the periods of heavy precipitation. (1) The *time lag between the precipitation and runoff peak* of around 1 day is clearly shorter than the general *time lag* of 3 days. The immediate increase of the runoff indicates that the precipitation sum is aggregated within less than 24 hours with a high intensity rather than over a couple of days with moderate intensity. Unfortunately, the soil is not able to store water to this extent because the storage capacity is exhausted. The runoff is thus changing significantly. (2) In addition to the runoff peak, the absolute runoff ensemble spread also changes considerably during less than one day. Two

days prior to and three days after the precipitation peak, the runoff has on average an absolute ensemble spread of only 0.04 mm per day. This ensemble spread quadruples during the precipitation peak. Those findings support the assumption that the combination of high *methodological variability* in precipitation and the inaccurate estimation of soil storage capacity during heavy precipitation events lead to high simulation uncertainty equated to the runoff ensemble spread. (3) The absolute runoff ensemble spread (*methodological variability* of the ensemble runs) increases more strongly with mean elevation compared to the general dependency of *methodological variability* and elevation. (4) The high *methodological variability* and the rapid change in runoff in mountainous areas can be explained with the spatial characteristics. The *MSCs* with higher mean elevation are characterised by less permeable, rocky, steep surface and are subject to a larger number of less predictable, convective precipitation events. Rapid runoff changes are according to Girons & Seibert (2016) typical of mountainous headwater regions, which descriptions fits the characteristics of the *MSCs 2374* and *2468*. (5) The general underestimation of precipitation sums and runoffs is enhanced for heavy precipitation events. It is concluded that the *methodological variability* as a measure for uncertainty can help to improve the knowledge about spatio-temporal patterns of runoff changes during such periods. The improved uncertainty knowledge can help to reduce environmental risks which recommendation is in accordance with Georgakakos et al. (2004) and Yu et al. (2015).

7.3.3 Data Set Variability

RO.3.3 To what extent do the daily runoffs per subcatchment of the deterministic (RhiresD) and probabilistic data sets (RhydchprobD ensemble mean) coincide?

The results clearly show that none of the two data sets, i.e. the deterministic (*RhiresD*) and probabilistic data set mean (*RhydchprobD*), performs noticeably better than the other. However, the simulated runoff values for the deterministic data set slightly overperforms the probabilistic data set. From this fact it can be concluded that the advantage of a probabilistic data set is lost through the averaging process. The analysis could not find any correlation of the performance to either precipitation sum, runoff volume, catchment size or spatial patterns which is why the performance results are treated as coincidental.

8 Conclusion

This research work aimed to explore the application of a probabilistic data set for precipitation and runoff estimation. The approach of several equally likely realisations of natural processes intend to give information on the reliability of the interpolations and simulation values, measured by the ensemble spread of the daily values. With the availability of a probabilistic data set for Switzerland and the advanced computational capabilities, there is an ever-growing number of potential use cases for the inclusion of uncertainty measures. To describe the significance of this measure, the basic idea was to (a) describe the spatio-temporal patterns of precipitation and runoff variability; (b) quantify the influence of heavy precipitation events on the variability; (c) characterise the coincidence of the deterministic and probabilistic data sets; and (d) examine the influence of a probabilistic approach on the accuracy of hydrological simulations. The approach of using the same probabilistic data set for variability analysis in precipitation occurrence and runoff generation tried to close the unveiled research gap for Switzerland.

8.1 Insights

The main objective of this study was to quantify the spatio-temporal patterns of precipitation and runoff variability, ascribed to natural and interpolation/simulation origin. To achieve this objective, the study has been divided into the three parts meteorology, model and hydrology.

Meteorology

The topography of the study catchment *Andelfingen* is mainly responsible for natural precipitation variability. Convective as well as stratiform precipitation occurs more frequently and with greater intensity in the higher-lying alpine areas in the south-east of the region during the summer months. These spatio-temporal patterns influence the interpolation variability of precipitation values. A similar accumulation of the absolute and relative interpolation variability in the spring and summer months can be observed in the subcatchments with a higher mean elevation. The findings indicate that the interpolation uncertainty mainly depends on the precipitation generation processes and the associated precipitation intensities. Heavy precipitation events occur more often in the form of convective precipitation. Due to the described relationship between precipitation sum, formation process and estimation uncertainty, the interpolation uncertainty for such heavy precipitation events increases. The fact that the deterministic and probabilistic mean data sets coincide very well suggests that the advantage of the probabilistic data set does not lie in the generally improved estimation accuracy but much more in the important information of the estimation uncertainty.

Model

The variability of model performance is highly dependent on the catchment size and the topography. The results show that not enough attention has been paid to the history of precipitation events and therefore the soil storage capacity is sometimes underestimated in the simulations. This underestimation leads to smaller simulation than observation runoff values.

Hydrology
The meteorological data (first part) are used as model input to calculate runoff simulations (second part). The analysis of those runoff simulations in the third part shows that the *methodological variability* in the probabilistic data set increases during summer months. This temporal uncertainty pattern goes along with the natural increase of summer precipitation. The intensification of evaporation and the decrease in soil moisture, which increase the soil storage capacity, are very likely the drivers of the inaccurate runoff estimations during this period. The surface characteristics and the associated runoff simulation variability further positively correlate with the mean elevation. However, compared to the precipitation variability analysis, the runoffs' natural as well as the simulation uncertainty analysis are less spatially dependant. It is assumed that this observation is relatable to the placement of monitoring stations only on the larger rivers.

As an overarching conclusion, it remains crucial to question the possibilities with which the established information of spatio-temporal patterns in uncertainty estimations can be transferred into an advantage in various application fields, e.g. reservoir managements, early warning systems (Georgakakos et al. 2004; Yu et al. 2015). The existing interpolation and simulation variabilities can undoubtedly improve the knowledge of the natural processes in the catchment *Andelfingen*. Moreover, the influencing factors for precipitation generation and runoff changes need further investigations to gain more knowledge about it.

8.2 Outlook

Future work should be concerned with the implication of the variability information of precipitation and runoff. The application method was not part of this research. Firstly, a methodology could be considered in which information on reliability is provided in addition to the quantity of precipitation and runoff. Furthermore, training a suitable model could lead to the introduction of a correction factor depending on the estimation uncertainty. Secondly, more pronounced variabilities in the probabilistic data set are found for the precipitation estimation compared to the runoff simulations. This indicates that the naturally occurring smaller-scale fluctuations are additionally weakened by the calculation of the simulation data sets. A systematic underestimation of the runoff is found. For this reason, the findings suggest that not all ensemble runs are taken into account in the case of conspicuous runoff changes in further research. Lastly, the overcoming of the coarse resolution problem should be considered. On the one hand, higher temporal resolution allows to represent short, intense precipitation with greater probability that would be missed with the daily data resolution. It is precisely such heavy precipitation events that will increase and implicate greater local risk. On the other hand, other possible data sources to improve the resolution problem should be considered. Radar data and satellite images are possible data sources. Overall, an increase of the rain-gauge density is to be intended, especially in the mountainous areas. The above explained approaches can help to broaden the knowledge about the probabilistic data set application. This intends to better understand natural processes, to anticipate short-term but also long-lasting variabilities and to adapt to new circumstances.

9 Literature

Ahrens, Bodo & Jaun, Simon (2007): On evaluation of ensemble precipitation forecasts with observation-based ensembles. *In: Advances in Geosciences*, 10, 139–144.

Amiri, Mohammad Arab & Mesgari, Mohammad Saadi (2016): Spatial variability analysis of precipitation in northwest Iran. In: *Arabian Journal of Geosciences*, 9(11), 578.

Andréassian, Vazken; Perrin, Charles; Michel, Claude; Usart-Sanchez, Iolanda; Lavabre, Jacques (2001): Impact of imperfect rainfall knowledge on the efficiency and the parameters of watershed models. *In: Journal of Hydrology*, 250(1–4), 206–223.

Antolini, Gabriele; Auteri, Luca; Pavan, Valentina; Tomei, Fausto; Tomozeiu, Rodica; Marletto, Vittorio (2015): A daily high-resolution gridded climatic data set for Emilia-Romagna, Italy, during 1961–2010. *In: International Journal of Climatology*, 36(4), 1970–1986.

Bárdossy, Andras & Das, Tapash (2008): Influence of rainfall observation network on model calibration and application. *In: Hydrology and Earth System*, 12, 77–89.

Bartolini, Elisa; Claps, Pierluigi; D'Odorico, Paolo (2009), Interannual variability of winter precipitation in the European Alps: Relations with the North Atlantic oscillation. *In: Hydrology and Earth System Sciences*, 13(1), 17–25.

Benninghaus, Hans (2007): Deskriptive Statistik: Eine Einführung für Sozialwissenschaftler. Springer-Verlag.

Bergström, Sten (1976): Development and application of a conceptual runoff model for Scandinavian catchments. SMHI RHO 7, Norrköping, 134 pp.

Bergström, Sten (1990): Parametervärden för *HBV*-modellen i Sverige, Erfarenheter från modelkalibreringar under perioden 1975–1989 (Parametervalues for the *HBV* model in Sweden, in Swedish), SMHI Hydrologi 28, Norrköping, 35 pp.

Bergström, Sten (1992): The *HBV* model – its structure and applications. SMHI RH 4, Norrköping, 35 pp.

Beven, Keith (2012): Rainfall-Runoff Modelling: The Primer, 2nd Edition. John Wiley & Sons, Ltd. Chicester, 488pp.

Beven, Keith J. (2000): Uniqueness of place and process representations in hydrological modelling. *In: Hydrology and earth system sciences*, 4(2), 203–213.

Biggs, Eloise M. & Atkinson, Peter M. (2011): A comparison of gauge and radar precipitation data for simulating an extreme hydrological event in the Severn Uplands, UK. *In: Hydrological Processes*, 25(5), 795–810.

Bormann, Helge & Diekkrüger, Bernd (2003): Possibilities and limitations of regional hydrological models applied within an environmental change study in Benin (West Africa). *In: Physics and Chemistry of the Earth*, 28(33–36), 1323–1332.

Brönnimann, Stefan; Rajczak, Jan; Fischer, Erich M.; Raible, Christoph C.; Rohrer, Marco; Schär, Christoph (2018): Changing seasonality of moderate and extreme precipitation events in the Alps. In: *Natural Hazards and Earth System Sciences*, 18(7), 2047–2056.

Brown, James D.; Seo, Dong-jun; Du, J Jun (2012): Verification of precipitation forecasts from NCEP's short-range ensemble forecast (SREF) system with reference to ensemble streamflow prediction using lumped hydrologic models. *In: Journal of Hydrometeorology*, 13(3), 808–836.

Buizza, Roberto; Hollingsworth, Andrew D.; Lalaurette, François; Ghelli, Anna (1999): Probabilistic predictions of precipitation using the ECMWF Ensemble Prediction System. *In: Weather and Forecasting*, 14(2), 168–189.

Burn, Donald H.; Elnur, Mohamed A. H. (2002): Detection of hydrologic trends and variability. *In: Journal of hydrology*, 255(1–4), 107–122.

Chappell, Adrian; Renzullo, Luigi; Haylock, Malcolm (2012): Spatial uncertainty to determine reliable daily precipitation maps. *In: Journal of Geophysical Research*, 117(D17).

CLC 2018 (Corine Land Cover): CORINE Schweiz. <https://www.wsl.ch/de/projekte/corine-schweiz.html> [26.03.20].

Craig, George C.; Keil, Christian; Leuenberger, Daniel (2012): Constraints on the impact of radar rainfall data assimilation on forecasts of cumulus convection. *In: Quarterly Journal of the Royal Meteorological Society*, 138(663), 340–352.

Dawdy, David R. & Bergmann, James M. (1969): Effect of rainfall variability on streamflow simulation. *In: Water resources research*, 5(5), 958–966.

Deng, Xingxiu & Stull, Roland (2005): A mesoscale analysis method for surface potential temperature in mountainous and coastal terrain. *In: Monthly weather review*, 133(2), 389–408.

Duan, Qingyun; Ajami, Newsha K.; Gao, Xiaogang; Sorooshian, Soroosh (2007): Multi-model ensemble hydrologic prediction using Bayesian model averaging. *In: Advances in Water Resources*, 30(5), 1371–1386.

Duncan, Mike R.; Austin, B.; Fabry, Frédéric; Austin, Geoffrey L. (1993): The effect of gauge sampling density on the accuracy of streamflow prediction for rural catchments. *In: Journal of Hydrology*, 142(1–4), 445–476.

European Environment Agency (EEA) (2009): Regional climate change and adaptation. The Alps facing the challenge of changing water resources. EEA Technical Report, 143 pp.

Falkenmark, Malin; Rockstrom, Johan; Rockström, Johan (2004): Balancing water for humans and nature: The new approach in ecohydrology. Earthscan, London, 247pp.

Fantini, Adriano; Raffaele, Francesca; Torma, Csaba; Bacer, Sara; Coppola, Erika; Giorgi, Filippo; Ahrens, Bodo; Dubois, Clotilde; Sanchez, Enrique; Verdecchia, Marco (2018): Assessment of multiple daily precipitation statistics in ERA-Interim driven Med-CORDEX and EURO-CORDEX experiments against high resolution observations. *In: Climate Dynamics*, 51(3), 877–900.

Farinotti, Daniel; Usselmann, Stephanie; Huss, Matthias; Bauder, Andreas; Funk, Martin (2012): Runoff evolution in the Swiss Alps: Projections for selected high-alpine catchments based on ENSEMBLES scenarios. *In: Hydrological Processes*, 26(13), 1909–1924.

Faurès, Jean-Marc; Goodrich, David C.; Woolhiser, David A.; Sorooshian, Soroosh (1995): Impact of small-scale spatial rainfall variability on runoff modeling. *In: Journal of Hydrology*, 173(1–4), 309–326.

Federal Office for the Environment *FOEN* (2013): Hochwasser auf der Alpennordseite vom 1. Bis 3. Juni 2013. < https://www.bafu.admin.ch/bafu/de/home/themen/wasser/dossiers/hochwasser-auf-der-alpennordseite-vom-1--bis-3--juni-2013.html> [01.11.20]

Federal Office for the Environment *FOEN* (2019): Einzugsgebietsgliederung Schweiz, EZGG-CH – Topographische Einzugsgebiete der Schweizer Gewässer. Produktdokumentation, Ausgabe 2015.

Federal Office for the Environment *FOEN* (2020): Abfluss Stundenmittel.

Federal Office for the Environment *FOEN* (2020): Hydrological data and forecasts Thur–Andelfingen (2044). <https://www.hydrodaten.admin.ch/en/2044.htm> [01.07.2020]

Frei, Christoph (2020): Email conversation with MeteoSwiss on 14th April 2020, <christoph.frei@meteoswiss.ch>.

Frei, Christoph & Isotta, Francesco A. (2019): Ensemble spatial precipitation analysis from rain gauge data: Methodology and application in the European Alps. In: *Journal of Geophysical Research: Atmospheres*, 124, 5757–5778.

Frei, Christoph & Schär, Christoph (1998): A precipitation climatology of the Alps from high-resolution rain-gauge observations. In: *International Journal of Climatology: A Journal of the Royal Meteorological Society*, 18(8), 873–900.

Frei, Christoph; Schöll, Regina; Fukutome, Sophie; Schmidli, Jürg; Vidale, Pier Luigi (2006): Future change of precipitation extremes in Europe: intercomparison of scenarios from regional climate models. *In: Journal of Geophysical Research: Atmospheres*, 111(D6).

Georgakakos, Konstantine P.; Seo, Dong-Jun; Gupta, Hoshin; Schaake, John; Butts, Michael B. (2004): Towards the characterization of streamflow simulation uncertainty through multimodel ensembles. *In: Journal of Hydrology*, 298(1–4), 222–241.

Germann, Urs; Berenguer, Marc; Sempere-Torres, Daniel; Zappa, Massimiliano (2009): REAL—Ensemble radar precipitation estimation for hydrology in a mountainous region. *In: Quarterly Journal of the Royal Meteorological Society*, 135(639), 445–456.

Girons Lopez, Marc & Seibert, Jan (2016): Influence of hydro-meteorological data spatial aggregation on streamflow modelling. *In: Journal of Hydrology*, 541, 1212–1220.

Girons Lopez, Marc; Di Baldassarre, Giuliano; Seibert, Jan (2017): Impact of social preparedness on flood early warning systems. *In: Water Resources Research*, 53, 522–534.

Girons Lopez, Marc; Wennerström, Hjalmar; Nordén, Lars-Åke; Seibert, Jan (2015): Location and density of rain gauges for the estimation of spatial varying precipitation. *In: Geografiska Annaler: Series A, Physical Geography*, 97(1), 167–179.

Gobiet, Andreas; Kotlarski, Sven; Beniston, Martin; Heinrich, Georg; Rajczak, Jan; Stoffel, Markus (2014): 21st century climate change in the European Alps—A review. *In: Science of the Total Environment*, 493, 1138–1151.

Gourley, Jonathan J.; Vieux, Baxter E. (2006): A method for identifying sources of model uncertainty in rainfall-runoff simulations. *In: Journal of Hydrology*, 327(1–2), 68–80.

Häckel, Hans (2016): Meteorologie (8. Auflage). UTB, Verlag Eugen Ulmer, Stuttgart, 473 pp.

Hamill, Thomas M.; Hagedorn, Renate; Whitaker, Jeffrey S. (2008): Probabilistic forecast calibration using ECMWF and GFS ensemble reforecast. Part II: precipitation. *In: Monthly Weather Review*, 136(7), 2620–2632.

Hendriks, Martin (2010): Introduction to physical Hydrology. Oxford University Press, 331 pp.

Hiebl, Johann; Frei, Christoph (2018): Daily precipitation grids for Austria since 1961—Development and evaluation of a spatial dataset for hydroclimatic monitoring and modelling. *In: Theoretical and Applied Climatology*, 132(1), 327–345.

Hijmans, Robert J.; Cameron, Susan E.; Parra, Juan L.; Jones, Peter G.; Jarvis, Andy (2005): Very high resolution interpolated climate surfaces for global land areas. *In: International Journal of Climatology*, 25(15), 1965–1978.

Hock, Regine (2005): Glacier melt: A review of processes and their modelling. *In: Progress in physical Geography*, 29(3), 362–391.

Hoffman, Ross N.; Boukabara, Sid-Ahmed; Kumar, V. Krishna; Garrett, Kevin; Atlas, Robert (2017): An Empirical Cumulative Density Function Approach to Defining Summary NWP Forecast Assessment Metrics. *In: Monthly Weather Review*, 145(4), 1427–1435.

Huizman, Johan A.; Breuer, Lutz; Bormann, Helge; Bronstert, Axel; Croke, Barry F.W.; Frede, Hans-Georg; Gräff, Thomas; Hubrechts, Lode; Jakeman, A.J.; Kite, Geoffrey; Lanini, Jordan; Leavesley, George H.; Lettenmaier, Dennis P.; Lindström, Goeran; Seibert, Jan; Sivapalan, Murugesu; Viney, Neil R.; Willems, Patrick (2009): Assessing the impact of land use change on hydrology by ensemble modelling (LUCHEM) III: Scenario analysis. *In: Advances in Water Resources*, 32(2), 159–170.

Huss, Matthias (2011): Present and future contribution of glacier storage change to runoff from macroscale drainage basins in Europe. *In: Water Resources Research*, 47(7).

Huss, Matthias; Farinotti, Daniel; Bauder, Andreas; Funk, Martin (2008): Modelling runoff from highly glacierized alpine drainage basins in a changing climate, *In: Hydrological Processes*, 22(19), 3888–3902.

Huza, Jessica; Teuling, Adriaan J.; Braud, Isabelle; Grazioli, Jacopo; Melsen, Lieke A.; Nord, Guillaume; Raupach, Timothy H.; Uijlenhoet, Remko (2014): Precipitation, soil moisture and runoff variability in a small river catchment (Ardèche, France) during HyMeX Special Observation Period 1. *In: Journal of Hydrology*, 516, 330–342.

Hydrolgical Atlas of Switzerland HADES (2015): <www.hydrologicalatlas.ch> [26.03.20].

HYDROmaps (Hydrologischer Atlas der Schweiz) (2020): Daten- und Analyseplattform. <www.hydromaps.ch> [26.03.20].

Isotta, Francesco A.; Frei, Christoph; Weilguni, Viktor; Perčec Tadić, Melita; Lassegues, Pierre; Rudolf, Bruno; Pavan, Valentina; Cacciamani, Carlo; Antolini, Gabriele; Ratto, Sara M.; Munari, Michela; Micheletti, Stefano; Bonati, Veronica; Lussana, Cristian; Ronchi, Christian; Panettieri, Elvio; Marigo, Gianna, Vertačnik, Gregor (2014): The climate of daily precipitation in the Alps: development and analysis of a high-resolution grid data set from pan-Alpine rain-gauge data. *In: International Journal of Climatology*, 34(5), 1657–1675.

Isotta, Francesco A.; Vogel, Raphaela; Frei, Christoph (2015): Evaluation of European regional reanalyses and downscalings for precipitation in the Alpine region. *In: Meteorologische Zeitschrift*, 24(1), 15–37.

Kammer, Peter M.; Schöb, Christian; Eberhard, Gabriel; Gallina, Renzo; Meyer, Remo; Tschanz, Christian (2013): The relationship between soil water storage capacity and plant species diversity in high alpine vegetation. In: *Plant Ecology & Diversity*, 6(3–4), 457–466.

Kling, Harald; Fuchs, Martin; Paulin, Maria (2012): Runoff conditions in the upper Danube basin under an ensemble of climate change scenarios. *In: Journal of Hydrology*, 424, 264–277.

Kusumastuti, Dyah Indriana; Jokowinarno, Dwi (2012): Time step issue in unit hydrograph for improving runoff prediction in small catchments. *In: Journal of Water Resource and Protection*, 4(8), 686–693.

Kuusela, Mikael & Stein, Michael L. (2018): Locally stationary spatio-temporal interpolation of Argo profiling float data. *In: Proceedings of the Royal Society A: Mathematical, Physical and Engineering Sciences*, 474(2220), 20180400.

Liechti, Katharina; Barben, Martin; Zappa, Massimiliano (2020): Wasserhaushalt der Schweiz 2019. In: Wasser Energie Luft, 2, 93–94.

Lobligeois, Florent; Andréassian, Vazken; Perrin, Charles; Tabary, Pierre; Loumagne, Cécile (2014): When does higher spatial resolution rainfall information improve streamflow simulation? An evaluation using 3620 flood events. *In: Hydrology and Earth System Science*, 18(2), 575–594.

Lopes, Vincent L. (1996): On the effect of uncertainty in spatial distribution of rainfall on catchment modelling. *In: Catena*, 28(1–2), 107–119.

Martín, Marisa L.; Santos-Muñoz, Daniel; Valero, Francisco; Morata, Alex (2010): Evaluation of an ensemble precipitation prediction system over the Western Mediterranean area. *In: Atmospheric Research*, 98(1), 163–175.

Massari, Christian; Brocca, Luca; Barbetta, Silvia; Papathanasiou, Chrysoula; Mimikou, Maria; Moramarco, Tommaso (2013): Using globally available soil moisture indicators for flood modelling in Mediterranean catchments. In: Hydrology & Earth System Sciences Discussions, 10(8), 10997–11033.

MeteoSwiss (2019): Manual precipitation monitoring network. <https://www.meteoswiss.admin.ch/home/measurement-and-forecasting-systems/land-based-stations/manual-precipitation-monitoring-network.html> [12.11.2020].

MeteoSwiss (2020a): Automatic monitoring network. <https://www.meteoswiss.admin.ch/home/measurement-and-forecasting-systems/land-based-stations/automatisches-messnetz.html> [12.11.2020].

MeteoSwiss (2020b): Daily Mean, Minimum and Maximum Temperature: TabsD, TminD, TmaxD.

MeteoSwiss (2020c): Daily Precipitation: RhiresD.

MeteoSwiss (2020d): Daily Precipitation Ensemble: RhydchprobD.

Nakicenovic, Nebojsa & Swart, Rob (2000): Special Report on Emission Scenarios (SRES) – A Special Report of Working Group III of the Intergovernmental Panel on Climate Change (IPCC), Cambridge Univercity Press, 570 pp.

Neff, Earl L. (1977): How much rain does a rain gage gage?. *In: Journal of Hydrology*, 35(3–4), 213–220.

Ochoa-Rodriguez, Susana; Wang, Li-Pen; Gires, Auguste; Pina, Rui D.; Reinoso-Rondinel, Ricardo; Bruni, Guendalina; Ichiba, Abdellah; Gaitan, Santiago; Cristiano, Elena; van Assel, Johan; Kroll, Stefan; Murlà-Tuyls, Damian; Tisserand, Bruno; Schertzer, Daniel; Tchiguirinskaia, Ioulia; Onof, Christian; Willems, Patrick; ten Veldhuis, Marie-Claire (2015): Impact of spatial and temporal resolution of rainfall inputs on urban hydrodynamic modelling outputs: A multi-catchment investigation. *In: Journal of Hydrology*, 531, 389–407.

On, Nuri; Kim, Hyun Mee; Kim, SeHyun (2018): Effects of Resolution, Cumulus Parameterization Scheme, and Probability Forecasting on Precipitation Forecasts in a High-Resolution Limited-Area Ensemble Prediction System. *In: Asia-Pacific Journal of Atmospheric Sciences*, 54(4), 623–637.

Osborne, Joe M.; Lambert, Hugo F.; Groenendijk, Margriet; Harper, Anna B.; Koven, Charles D.; Poulter, Benjamin; Pugh, Thimas A. M.; Sitch, Stephen; Stocker, Benjamin D.; Wltshire, Andy; Zaehle, Sönke (2015): Reconciling precipitation with runoff: Observed hydrological change in the midlatitudes. *In: Journal of Hydrometeorology*, 16(6), 2403–2420.

Oudin, Ludovic; Hervieu, Frédéric; Michel, Claude; Perrin, Charles; Andréassian, Vazken; Anctil, François; Loumagne, Cécile (2005): Which potential evapotranspiration input for a lumped rainfall–runoff model? Part 2—Towards a simple and efficient potential evapotranspiration model for rainfall–runoff modelling. In: *Journal of Hydrology*, 303(1–4), 290–306.

Partnershop for European Environmental Research PEER (2010): River *Thur* – Hydrological observatory description.

Peck, Eugene L. & Brown, Merle J. (1962): An approach to the development of isohyetal maps for mountainous areas. *In: Journal of Geophysical Research*, 67(2), 681–694.

PEER (2010): River Thur, Switzerland – Hydrological Observatory Description. Leipzig, Germany.

Rafieeinasab, Arezoo; Norouzi, Amir; Kim, Sunghee; Habibi, Hamideh; Nazari, Behzad; Seo, Dong-Jun; Lee, Haksu; Cosgrove, Brian; Cui, Zhengtao (2015): Toward high-resolution flash flood prediction in large urban areas–Analysis of sensitivity to spatiotemporal resolution of rainfall input and hydrologic modelling. *In: Journal of Hydrology*, 531, 370–388.

Rakovec, Oldrich; Hazenberg, Pieter; Torfs, Paul J. J. F.; Weerts, Albrecht; Uijlenhoet, Remko (2012): Generating spatial precipitation ensembles: impact of temporal correlation structure. *In: Hydrology and Earth System Sciences*, 16(9), 3419–3434.

Ratzlaff, John R. (1994): Mean Annual Precipitation, Runoff, and Runoff Ratio for Kansas , 1971–1990. *In: Transactions of the Kansas Academy of Science*, 1903, 94–101.

Rauthe, Monika; Steiner, Heiko; Riediger, Ulf; Mazurkiewicz, Alex; Gratzki, Annegret (2013): A Central European precipitation climatology – Part I: generation and validation of a high-resolution gridded daily data set (HYRAS). *In: Meteorologische Zeitschrift*, 22, 235–256.

Reiter, Andrea; Ruth Weidinger; Wolfram Mauser (2012): Recent climate change at the upper Danube—a temporal and spatial analysis of temperature and precipitation time series. *In: Climatic Change,* 111(3–4), 665–696.

Rivoire, Pauline; Tramblay, Yves; Neppel, Luc; Hertig, Elke; Vicente-Serrano, Sergio M. (2019): Impact of the dry-day definition on Mediterranean extreme dry-spell analysis. *In: Natural Hazards and Earth System Sciences*, 19(8), 1629–1638.

Schleiss, Marc; Jaffrain, Joel; Berne, Alexis (2012): Stochastic simulation of intermittent DSD fields in time. *In: Journal of Hydrometeorology*, 13(2), 621–637.

Schroeer, Katharina; Kirchengast, Gottfired; O, Sungmin (2018): Strong dependence of extreme convective precipitation intensities on gauge network density. *In: Geophysical Research Letters*, 45, 8253–8263.

Schwarb, Manfred; Daly, Christopher; Frei, Christoph; Schär, Christoph (2001), Mean annual and seasonal precipitation in the European Alps 1971– 1990. *In: Hydrological Atlas of Switzerland*, 2.6.

Seibert, Jan; Vis, Marc J. (2012): Teaching hydrological modeling with a user-friendly catchment-runoff-model software package. *In Hydrology and Earth System Sciences*, 16(9), 3315–3325.

Sevruk, Boris (1985): Systematischer Niederschlagsmessfehler in der Schweiz. *In: Der Niederschlag in der Schweiz*, 31, 65–75.

Sikorska, Anna E. & Seibert, Jan (2018): Value of different precipitation data for flood prediction in an alpine catchment: A Bayesian approach. *In: Journal of Hydrology*, 556, 961–971.

Song, Joon Jin; Kwon, Soohyun; Lee, GyuWon (2015): Incorporation of parameter uncertainty into spatial interpolation using Bayesian trans-Gaussian kriging. *In: Advances in Atmospheric Sciences*, 32(3), 413–423.

Stahel, Werner A. (2009): Statistische Datenanalyse: Eine Einführung für Naturwissenschaftler (%. Auflage). Vieweg + Teubner, Wiesbaden.

Stahl, Kerstin & Moore, Robert D. (2006), Influence of watershed glacier coverage on summer streamflow in British Columbia, Canada. *In: Water Resources Research*, 42(6), W06201.

Strauch, Michael; Bernhofer, Christian; Koide, Sérgio; Volk, Martin; Lorz, Carsten; Makeschin, Franz (2012): Using precipitation data ensemble for uncertainty analysis in SWAT streamflow simulation. *In: Journal of Hydrology*, 414, 413–424.

Swisstopo. Bundesamft für Landestopografie (2005): DHM25.

Swisstopo. Bundesamft für Landestopografie (2020): VECTOR25.

Ternynck, Camille; Ben Alaya, Mohamed A.; Chebana, Fateh; Dabo-Niang, Sophie; Ouarda, Taha B. M. J. (2016): Streamflow hydrograph classification using functional data analysis. *In: Journal of hydrometeorology*, 17(1), 327–344.

Thurai, Merhala; Gatlin, Patrick N.; Bringi, Viswanathan N. (2016): Separating stratiform and convective rain types based on the drop size distribution characteristics using 2D video disdrometer data. *In: Atmospheric Research*, 169, 416–423.

Tobler, Waldo R. (1970): A computer movie simulating urban growth in the Detroit region. *In: Economic Geography*, 46(sup1), 234–240.

Troutman, Brent M. (1983): Runoff prediction errors and bias in parameter estimation induced by spatial variability of precipitation. *In: Water Resources Research*, 19(3), 791–810.

Vaze, Jai; Post, David A.; Chiew, Francis H.S.; Perraud, Jean-Michel; Teng, Jin; Viney, Neil (2011): Conceptual rainfall–runoff model performance with different spatial rainfall inputs. In: Journal of Hydrometeorology, 12(5), 1100–1112.

Viviroli, Daniel; Archer, David R.; Buytaert, Wouter; Fowler, HayleyJ.; Greenwood, Gregory B.; Hamlet, A.F.; Huang, Y.; Koboltschnig, Gernot; Litaor, Micheal.I.; López-Moreno, J.I.; Lorentz, Simon; Schädler, Bruno; Schreier, Hans; Schwaiger, K.; Vuille, Mathias; Woods, Ross A. (2011): Climate change and mountain water resources: overview and recommendations for research, management and policy. *In: Hydrology and Earth System Science*, 15(2), 471–504.

Viviroli, Daniel; Weingartner, Rolf; Messerli, Bruno (2003): Assessing the hydrological significance of the world's mountains. *In: Mountain Research and Development*, 23(1), 32–40.

Viviroli, Daniel; Zappa, Massimiliano; Schwanbeck, Jan; Gurtz, Joachim; Weingartner, Rolf (2009): Continuous simulation for flood estimation in ungauged mesoscale catchments of Switzerland—Part I: Modelling framework and calibration results. *In: Journal of Hydrology*, 377(1−2), 191–207.

Widmann, Martin & Bretherton, Christopher S. (2000): Validation of mesoscale precipitation in the NCEP reanalysis using a new gridpoint data set for the northwestern US. In: *Journal of Climate*, 13(11), 1936–1950.

Winchell, Michael; Gupta, Hoshin Vijai; Sorooshian, Soroosh (1998): On the simulation of infiltration-and saturation-excess runoff using radar-based rainfall estimates: Effects of algorithm uncertainty and pixel aggregation. *In: Water Resources Research,* 34(10), 2655–2670.

Woosley, Sharon; Capelli, Florence; Gonser, Tom; Hoehn, Eduard; Hostmann, Markus; Junker, Berit; Paetzold, Achim; Roulier, Christian; Schweizer, Steffen; Tiegs, Scott D.; Tockner, Klement; Weber, Christine; Peter, Armin (2007): A strategy to assess river restoration success. *In: Freshwater Biology*, 52(4), 752–769.

World meteorological organization (WMO) (2008): Guide to meteorological instruments and methods of observation. WMO-No. 8, Seventh Edition, 681 pp.

Wu, Limin; Seo, Dong-Jun; Demargne, Julie; Brown, James D.; Cong, Shuzheng; Schaake, John (2011): Generation of ensemble precipitation forecast from single-valued quantitative precipitation forecast for hydrologic ensemble prediction. *In: Journal of Hydrology*, 399(3–4), 281–298.

Xie, Pingping; Chen, Mingyue; Yang, Song; Yatagai, Akiyo; Hayasaka, Tadahiro, Fukushima, Yoshihiro; Liu, Changming (2007): A gauge-based analysis of daily precipitation over East Asia. *In: Journal of Hydrometeorology*, 8(3), 607–626.

Xu, Chong-Yu; Singh, Vijay P. (2004): Review on regional water resources assessment models under stationary and changing climate. *In: Water Resources Management*, 18(6), 591–612.

Xu, Kehui; Milliman, John D.; Xu, Hui (2010): Temporal trend of precipitation and runoff in major Chinese rivers since 1951. *In: Global Planetary Change,* 73(3–4), 219–232.

Yang, Daqing; Elomaa, Esko; Tuominen, Asko; Aaltonen, Ari; Goodison, Barry; Gunther, Thilo; Golubev, Valentin; Sevruk, Boris; Madsen, Henning; Milkovic, Janja (1999): Wind-induced precipitation undercatch of the Hellmann gauges. In: Hydrology Research, 30(1), 57–80.

Yang, Jing; Reichert, Peter; Abbaspour, Karim C. (2007): Bayesian uncertainty analysis in distributed hydrologic modeling: A case study in the Thur River basin (Switzerland). *In: Water resources research*, 43(10).

Yu, Wansik; Nakakita, Eiichi; Kim, Sunmin; Yamaguchi, Kosei (2015): Improvement of rainfall and flood forecasts by blending ensemble NWP rainfall with radar prediction considering orographic rainfall. *In: Journal of Hydrology*, 531, 494–507.

Zierl, Bärbel; Bugmann, Harald (2005): Global change impacts on hydrological processes in Alpine catchments. *In: Water Resources Research*, 41(2).

10 Appendix

A.1 Additional Illustrations

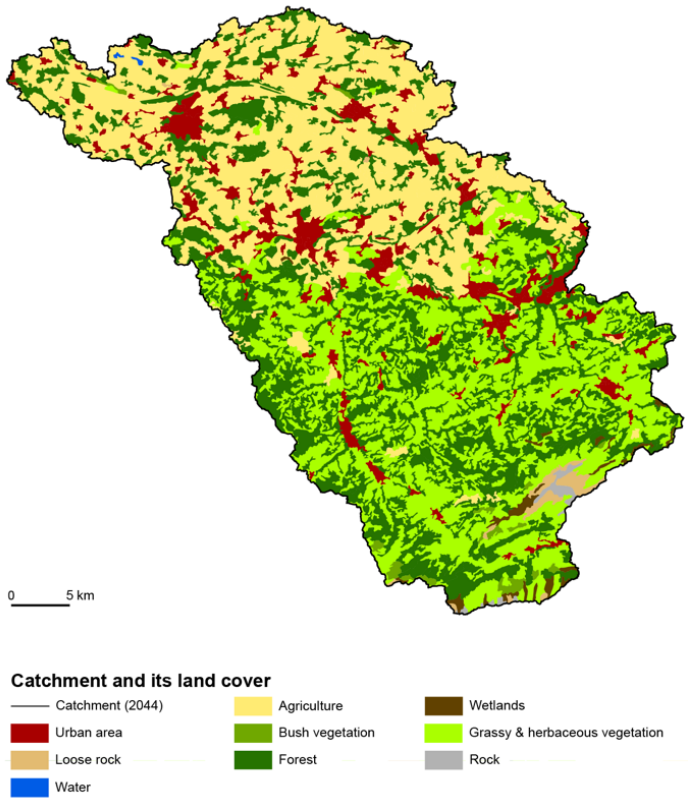

Figure 66: Land cover in the catchment Andelfingen. *(Corine Land Cover (2018): CLC Klassen; Federal Office of the Environment FOEN (2019): Einzugsgebiete Schweiz 40km).*

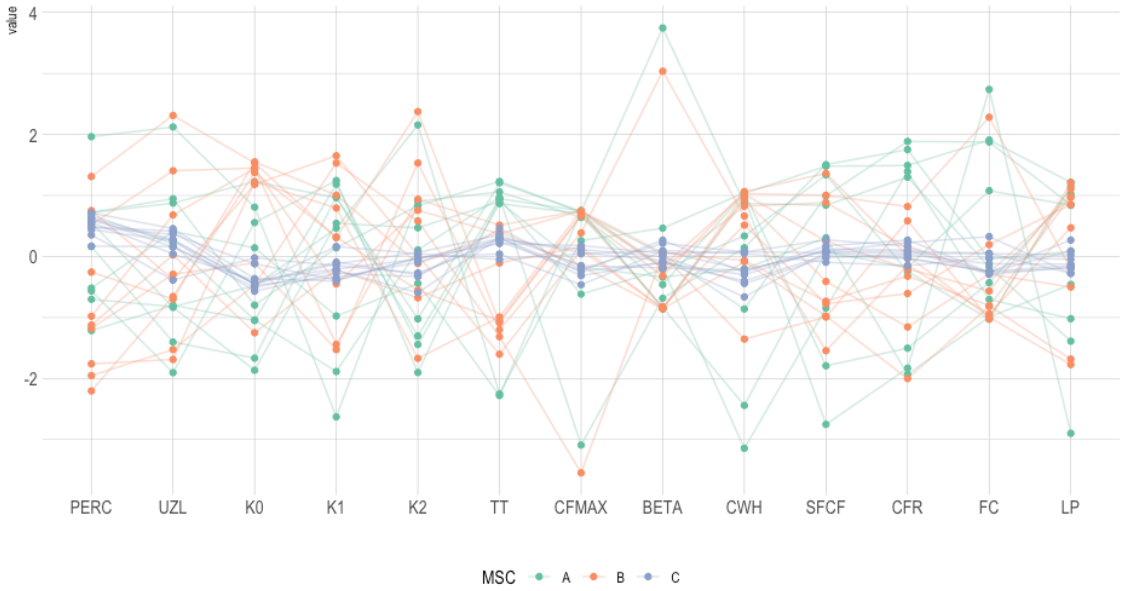

Figure 67: Comparison of model parameters for the different calibration-validation-versions.

A.2 Code

Chapter 5.2: Calculation of coefficient of variation for precipitation (relative variability):

```
CV = ifelse(Ensemble_precip_mean>1, Run_precip_sd/ Ensemble_precip_mean, 0)
```

Chapter 5.3.1: Calculation and definition of Precipitation event

```
threshold_event_count <- (50*0.8)
mutate(Run_relevance = (Precip >= 1),
        Event_relevance_80 = case_when(
                                    sum(Run_relevance)>=threshold_event_count~TRUE,
                                    TRUE~FALSE))

threshold_event_type_count <-  (0.8*40)
mutate(Event_type = case_when(
                            sum(Event_relevance_80) >= threshold_event_type_count~"stratiform",
                            sum(Event_relevance_80) < threshold_event_type_count &
                                  Event_relevance_80 == TRUE ~"convective",
                            TRUE~"no precipitation event"))
```

Chapter 5.3.1: Numbering of precipitation periods:

```
 number_groups <- function(input,include_first_false = F, include_trailing_na= F){
  if(all(c(include_first_false,include_trailing_na))){
    # warning("Strange things can happen if both 'include_first_false' and 'include_trailing_na' options
are set to TRUE")
  }
  if(include_trailing_na){
    trailing_na <- which(is.na(input) & !(dplyr::lag(input)))
    input[trailing_na] <- T
  }
  input <- ifelse(is.na(input),F,input) #turn all NAs to FALSE
  index_trues = which(input)+1  # get the indexes of the values after the TRUE Values
  #make sure the indexes are greater than 0 and
  index_trues = index_trues[index_trues <= length(input)]

  group = cumsum(!input)+1 # make groups by incrementing at FALSE values
  if(include_first_false){
    input[index_trues] <- TRUE # if first F should be included,
    group[index_trues] <- group[index_trues-1]
  }
  group <- ifelse(input,group,NA)
  newlabels <- 1:length(unique(group[!is.na(group)]))
  group <- factor(group,labels = newlabels)
  return(group)
```

Chapter 5.3.4: Definition of heavy precipitation event:

```
group_by(Date) %>%
mutate(Extreme_event_type = case_when(
     sum(Extreme_event_relevance_80) >= threshold_extreme_event_type_count~"stratiform",
     sum(Extreme_event_relevance_80) < threshold_extreme_event_type_count &
     Extreme_event_relevance_80 == TRUE ~"convective",
     TRUE~"no extreme precipitation event"))
```

Chapter 5.3.5: Calculation of temporal aggregation of precipitation data:

```
roll_windows <- c(2,3,7,14,30)

group_by(elev_class, EnsembleRun) %>%
mutate(Precip_roll = rollmean(Precip, k= roll_window, fill = NA, align = c("center")))

group_by(elev_class, Date) %>%
summarise(Run_precip_sd = sd(Precip_roll)) %>%
mutate(CV = ifelse(Precip_roll_mean >1, Run_precip_sd/Precip_roll_mean, 0))

roll_windows <- c(2,3,7,14,30)

stat_ecdf(aes(CV, color = roll_window), lwd = 0.1)
```

Chapter 5.4: Command line for HBV simulations:

```
# Specify paths:
catchmentNumber = "2044"
catchment = paste0("//service.geo.uzh.ch/private/lmarkwal/data/Documents/Masterarbeit/HBV/",
catchmentNumber)
# refer to the new .exe file!! (not on server)
HBVPath = "//service.geo.uzh.ch/private/lmarkwal/data/Documents/Masterarbeit/HBV/HBV-light/HBV-
light-CLI.exe";

# Run a GAP simulation
outputFolderGAP = "Results_GAP"
calibrationFile = paste0("Rhires_HBV_", catchmentNumber, ".txt")

old <- Sys.time()
command = paste0(HBVPath," Run ",catchment," GAPRun ",outputFolderGAP, " /ptq:", calibrationFile)
system(command,TRUE)
# print run time
new <- Sys.time() - old # calculate difference
print(new)

# Copy GAP_Parameter.xml file to Data folder
# get a list of all parameter files from GAP simulation
paramFiles = list.files(path = file.path(catchment, outputFolderGAP), pattern =
"(?i)GAP_Parameter.*\\.xml", full.names = FALSE, recursive = FALSE)

# copy all parameter files to Data folder
for (paramFile in paramFiles) {
  file.copy(file.path(catchment, outputFolderGAP, paramFile), file.path(catchment, "Data", paramFile),
overwrite = TRUE)
}

# List all files starting with "RhydchprobD" (case insensitive) and with extension ".txt" in the 'Data'
folder of the catchment
ptqFiles = list.files(path = file.path(catchment, "Data"), pattern = "(?i)RhydchprobD.*\\.txt", full.names =
FALSE, recursive = FALSE)

# REMARK: ptq filenames are NOT allowed to contain any spaces!
# creates an output folder

old <- Sys.time()
outFolder = "Results_SungleRun"
for(ptqFile in ptqFiles){

  # Extract name of ensemble from ptq filename
  ensembleName = sub("(?i)RhydchprobD_HBV_(.*)\\.txt", "\\1", ptqFile)
```

```
  print(ptqFile)
  # Run a single model run
  # /p: for different parameter set file name
  for (paramFile in paramFiles) {
    # get number of parameter set for file name
    paramName = sub("(?i)GAP_Parameter_(.*)\\.xml", "\\1", paramFile)
    # create file names
    resultFile = paste0("Result", ensembleName,"_param", paramName)
    summaryFile = paste0("Summary_",ensembleName, "param_", paramName,  ".txt")

  command = paste0(HBVPath," Run ",catchment," SingleRun ",outFolder," /ptq:",ptqFile, " /p:",
paramFile, " /results:", resultFile, " /summary:", summaryFile)
  system(command,TRUE)

  }

}
# print run time
new <- Sys.time() - old # calculate difference
print(new)
```

Chapter 5.5: Calculation and numbering of runoff peaks:

```
HBV_input_sim_RhydchprobD_runoff_peak <- HBV_input_sim_RhydchprobD %>%
  filter(EnsembleRun == 0) %>%
  group_by(Catchment) %>%
  mutate(is_runoff_peak = ifelse(lead(Qsim,1)<Qsim & lag(Qsim,1)< Qsim &
                                 lead(Qsim,2)<Qsim & lag(Qsim,2)< Qsim &
                                 lead(Qsim,3)<Qsim & lag(Qsim,3)< Qsim &
                                 lead(Qsim,4)<Qsim & lag(Qsim,4)< Qsim &
                                 lead(Qsim,5)<Qsim & lag(Qsim,5)< Qsim &
                                 lead(Qsim,6)<Qsim & lag(Qsim,6)< Qsim &
                                 (lag(Precip,3) > 1 | lag(Precip,2) >1) &
                                 Qsim >= 2.1725,
                               TRUE, FALSE)) %>%
  filter(Date >= "1998-10-01" & Date < "2016-09-30")

HBV_runoff_ratio_ensemble_mean <- HBV_runoff_peak_events %>%
  filter(EnsembleRun == 0 & !is.na(RunoffEventNumber)) %>%
  mutate(RunoffEventNumber = as.integer(RunoffEventNumber)) %>%
  group_by(Catchment, RunoffEventNumber) %>%
  summarise(Date_Start = first(Date),
            Date_End = last(Date),
            Precip_sum = sum(Precip),
            Qsim_sum = sum(Qsim),
            Runoff_ratio = ifelse(Precip_sum >= 1, Qsim_sum/Precip_sum, 0))
```

A.3 Software

R Programming Language and Environment

R	3.6.3	www.r-project.org/
R Studio	1.2.5033	rstudio.com/

R Packages	**Version**	**URL**
data.table	data.table_1.12.8	r-datatable.com
dplyr	dplyr_0.8.5	dplyr.tidyverse.org
forcast	forcats_0.5.0	forcats.tidyverse.org
GGally	GGally_2.0.0	github.com/ggobi/ggally
ggplot	ggplot2_3.3.0	ggplot2.tidyverse.org
gridExtra	gridExtra_2.3	–
hrbrthemes	hrbrthemes_0.8.0	github.com/hrbrmstr/hrbrthemes
lubridate	lubridate_1.7.4	lubridate.tidyverse.org
maptools	maptools_0.9-9	–
ncdf4	ncdf4_1.17	cirrus.ucsd.edu/~pierce/ncdf
plyr	plyr_1.8.6	github.com/hadley/plyr
purrr	purrr_0.3.3	purrr.tidyverse.org
raster	raster_3.0-12	rspatial.org/raster
RColorBrewer	RColorBrewer_1.1-2	–
readr	readr_1.3.1	readr.tidyverse.org
reshape2	reshape2_1.4.3	github.com/hadley/reshape
rgdal	rgdal_1.4-8	–
rgeos	rgeos_0.5-2	rgeos.r-forge.r-project.org/index.html
sf	sf_0.8-1	github.com/r-spatial/sf/
sp	sp_1.4-1	github.com/edzer/sp/
stringr	stringr_1.4.0	stringr.tidyverse.org
tibble	tibble_2.1.3	tibble.tidyverse.org
tidyr	tidyr_1.0.2	tidyr.tidyverse.org
tidyverse	tidyverse_1.3.0	tidyverse.tidyverse.org
viridis	viridis_0.5.1	github.com/sjmgarnier/viridis
viridisLite	viridisLite_0.3.0	github.com/sjmgarnier/viridisLite
XML	XML_3.99-0.3	omegahat.net/RSXML
xts	xts_0.12-0	github.com/joshuaulrich/xts
zoo	zoo_1.8-7	–

A.4 Icons

Icon	*URL*
Gear	flaticon.com/authors/freepik [01.05.2020]
Thermometer	flaticon.com/authors/Those [01.05.2020]

11 Personal Declaration

I hereby declare that the submitted thesis is the result of my own, independent work. All external sources are explicitly acknowledged in the thesis.

Laura Markwalder, 28.01.2021